Clinical Utility of Near-infrared Spectroscopy in Skeletal Muscle

A thesis presented in partial fulfillment of the requirements for the degree of Doctor of Philosophy (Sport and Exercise Science)

At Massey University, Wellington, New Zealand

Adam Alexander Lucero

2021

Abstract

Introduction: Near infrared spectroscopy (NIRS) provides for non-invasive assessment of resting skeletal muscle hemodynamic and respiratory responses. However, the interday reliability of skeletal muscle blood flow (mBF) and oxygen consumption ($m\dot{V}O_2$) responses to stressors such as exercise in both healthy and clinical populations has not been established. Moreover, direct comparison of differing NIRS technologies is absent. The purpose of this thesis is three-fold 1) establish a standard protocol for the assessment of resting and exercise skeletal muscle hemodynamics for healthy and clinical populations, 2) compare the reliability of NIRS outcomes in continuous wave (cw) NIRS to the more robust frequency domain (fd) NIRS technology, and 3) assess validity against *in-vitro* skeletal muscle metabolic parameters.

Methods: In the first study, a standard protocol developed to measure mBF, $m\dot{V}O_2$, and perfusion ([tHb]) in the *vastus lateralis* (VL) at rest and up to 30% of maximum voluntary contraction and m$\dot{V}$O2 recovery rate constant (k) as an index of muscle oxidative capacity was conducted in twelve healthy adults and was repeated twice within 10 days to establish repeatability. The NIRS measures were conducted using a cw-NIRS device. Secondly, this protocol was repeated in 10, healthy males and 10 non-insulin dependent sedentary males with T2D for characterisation and comparison of outcomes derived from cw-NIRS versus fd-NIRS. Thirdly, cw-NIRS and whole-body oxygen consumption ($\dot{V}O_2$) were measured in 24 men with T2D while performing incremental ramp cycle exercise to volitional exhaustion; in addition, biopsies of the VL were collected.

Results: In study 1, mBF and $m\dot{V}O_2$ proportionally increased with intensity (0.55 to 7.68 ml·min-1·100ml-1 and 0.05 to 1.86 mlO2·min-1·100g-1, respectively) up to 25% MVC where it began to plateau at 30% MVC. For studies 1 and 2, a mBF/$m\dot{V}O_2$ ratio of ~5 was consistent for all exercise stages. For both Healthy and T2D groups, patterns of change and values for mBF and $m\dot{V}O_2$ during exercise were not substantially different

between devices and were moderate to highly reproducible (ICC: 0.72-0.98). The mean typical error for exercise mBF and mV̇O2 with 90% Confidence Intervals was 0.41 (0.31-0.59) and 0.38 (0.29-0.55) for ND and T2D, respectively. Substantial differences were seen in ND and T2D, respectively, between CW- and FD-NIRS values for perfusion. Thirdly, the [HHb] primary phase during dynamic exercise was substantially correlated to $\dot{V}O_2$peak while the secondary phase was substantially correlated to measures of mitochondrial function.

Conclusion: NIRS can reliably assess mBF and $m\dot{V}O_2$ responses at rest and during low-moderate exercise. The popular cw-NIRS device performed comparably to the more robust fd-NIRS when assessing mBF and mVO2 in both healthy and T2D populations, but cw-NIRS tended to overestimate perfusion, likely due to assumptions of constant scattering. Finally, combining NIRS with external respiration during continuous exercise has potential in investigating barriers to glucose disposal and exercise tolerance in T2D. Taken together, NIRS is a valid tool for applications in research, clinical diagnosis, and therapeutic assessment of skeletal muscle hemodynamics, microvascular, and respiratory plasticity.

Acknowledgments

It takes a village to raise a child, and an army to graduate a PhD candidate. I have met so many wonderful people along my journey through graduate school, many of which played pivotal roles in encouraging me to keep going and pushing me forward with all their might, not only within the University but outside of it as well.

I would like to thank my Supervisors David Rowlands, Lee Stoner, and James Faulkner for continually supporting and being patient even as the years dragged on. Each of them imparted their career, research, and life advice guiding me through my growing pains. Outside of my supervisors, help and advice from other professors in the building Sarah Schultz, Sally Lark, Michelle Thunders, Jim Jones, Rachel Page, Jim Clark, to name just a few, helped round my perspective and skills. Beyond Massey University professors like Mike Hamlin, Peter Wagner, Robert Ternansky, John Stanskas, Sheri Lillard, Diana Avila all inspired me with their passion for science and research embedding within me a want to discover.

I am very thankful for all the help and support from lab technicians, research assistants, fellow graduate students, and study participants. We spent many many hours in lab together and I will always revere those times and one of the best chapters of my life. Special thanks to Chris Harris, Glen Bell, Terrance Ryan, and Osvaldo Enriquez for your contributions to the custom equipment and analysis software I had to build for this thesis.

Finally I would like to thank my awesome, awesome friends and family for their constant love and support. To my friends for celebrating with me when the results were good, and joining my pity parties when p was in a galaxy far far away from 0.05. To my parents Adan and Roxanna Lucero for teaching me the importance of education from day 1, and sacrificing themselves to help me through to the end. And to my husband Logan Smith for carrying me to the finish line.

Publications

Publications arising from This Thesis

1. **Lucero, A. A.**, Addae, G., Lawrence, W., Neway, B., Credeur, D. P., Faulkner, J., ... & Stoner, L. (2018). Reliability of muscle blood flow and oxygen consumption response from exercise using near-infrared spectroscopy. Experimental physiology, 103(1), 90-100.

Other Publications During Thesis

1. **Lucero, A. A.,** Lambrick, D. M., Faulkner, J. A., Fryer, S., Tarrant, M. A., Poudevigne, M., ... & Stoner, L. (2014). Modifiable cardiovascular disease risk factors among indigenous populations. Advances in Preventive Medicine, 2014..
2. Gaffney K, **Lucero AA,** Macartney-Coxson D, Clapham J, Whitfield P, Palmer B, Wakefield S, Faulkner J, Stoner L, Rowlands DS. Effects of Whey Protein on Skeletal Muscle Microvascular and Mitochondrial Plasticity Following 10-Weeks of Exercise Training in Men with Type-2 Diabetes. Applied Physiology, Nutrition, and Metabolism. 2021 Feb 16(ja).
3. Trexler ET, Keith DS, **Lucero AA**, Stoner L, Schwartz TA, Persky AM, Ryan ED, Smith-Ryan AE. Effects of citrulline malate and beetroot juice supplementation on energy metabolism and blood flow during submaximal resistance exercise. Journal of dietary supplements. 2020 Nov 1;17(6):698-717.
4. Black MJ, **Lucero AA**, Fink PW, Stoner L, Shultz SP, Lark SD, Rowlands DS. The effects of uniquely-processed titanium on balance and walking performance in healthy older adults. Journal of functional biomaterials. 2018 Jun;9(2):39.
5. Gaffney KA, **Lucero AA**, Stoner L, Faulkner J, Whitfield P, Krebs J, Rowlands DS. Nil Whey Protein Effect on Glycemic Control after Intense Mixed-Mode

Training in Type 2 Diabetes. Medicine and science in sports and exercise. 2018 Jan 1;50(1):11-7.

6. Gaffney KA, **Lucero AA**, Stoner L, Faulkner J, Whitfield P, Krebs J & Rowlands DS (2018). Nil Whey Protein Effect on Glycemic Control after Intense Mixed-Mode Training in Type 2 Diabetes. Medicine and science in sports and exercise 50, 11-17.

7. Lizamore CA, Stoner L, Lucas S, **Lucero AA** & Hamlin MJ (2015). Does arterial health affect VO2peak and muscle oxygenation in a sedentary cohort? Medicine and science in sports and exercise 47, 272-279.

8. Witter T, Poudevigne M, Lambrick DM, Faulkner J, **Lucero AA**, Page R, Perry III LG, Tarrant MA & Stoner L (2015). A conceptual framework for managing modifiable risk factors for cardiovascular diseases in Fiji. Perspectives in public health 135, 75-84.

9. Fryer S, Stoner L, **Lucero AA**, Witter T, Scarrott C, Dickson T, Cole M & Draper N (2015). Haemodynamic kinetics and intermittent finger flexor performance in rock climbers. International journal of sports medicine 36, 137-142.

10. Fryer S, Stoner L, Scarrott C, **Lucero AA**, Witter T, Love R, Dickson T & Draper N (2015). Forearm oxygenation and blood flow kinetics during a sustained contraction in multiple ability groups of rock climbers. Journal of sports sciences 33, 518-526.

11. Fryer S, Stoner L, Scarrott C, **Lucero AA**, Witter T, Love R & Draper N (2014). Oxygen Uptake Or Delivery, Which Is The Limiting Factor For Intermittent Forearm Contractions In Rock-climbers? In Medicine and science in sports and exercise, vol. 46, pp. 756-757.

12. Gaffney K, **Lucero AA** & Stoner L (2014). Obesity is driving the cardiovascular disease epidemic: however, should obesity be classified as a disease? Journal of atherosclerosis and thrombosis 21, 77-78.

13. Stoner L, **Lucero AA**, Palmer BR, Jones LM, Young JM & Faulkner J (2013). Inflammatory biomarkers for predicting cardiovascular disease. Clinical biochemistry 46, 1353-1371.

Refereed Conference Presentations

1. Non-invasive interest group poster award for ACSM conference (USA 2016)
2. Best poster award at SESNZ/MedSci conference (NZ 2015)
3. Co-lead NIRS muscle measures symposium at SESNZ conference, Wellington NZ (2014)

Table of Contents

Table of Contents

List of Figures

List of Tables

List of Abbreviations

Abbreviation	Definition
AC	Amplitude of Intensity Oscillations
AO	Arterial Occlusion
ATT	Adipose Tissue Thickness
BFI	Blood Flow Index
BMI	Body Mass Index
CL	Confidence Limits
COX	Cytochrome Oxidase
CS	Citrate Synthetase
CV	Coefficient of Variation
Cw-NIRS	continuous wave NIRS
DC	Average Light Intensity
DO2	Delivery of Oxygen
DPF	Differential Path-length Factor
ECG	Electrocardiogram
EMG	Electromyography
FBG	Fasting Blood-Glucose
Fd-NIRS	frequency domain NIRS

Hb	Hemoglobin
HBDif	Hemoglobin Difference
HHB	Deoxygenated Hemoglobin
HR	Heart Rate
ICC	Intra-Class Correlation Coefficient
ICG	Indocyanine Green
LT	Lactate Threshold
MB	Myoglobin
mBF	Skeletal Muscle Blood Flow
MORC	Skeletal Muscle Oxygen Recovery Capacity
MRT	Mean Response Time
MVC	Maximum Voluntary Contraction
$m\dot{V}O_2$	Skeletal Muscle Blood Flow
NIRS	Near-infrared Spectroscopy
O_2Hb	Oxygenated Hemoglobin
O_2MB	Oxygenated Myoglobin
PAD	Peripheral Arterial Disease
PP	Peak Power
Qcap	Capillary Blood Flow
RF	Rectus Femoris
ROI	Region of Interest

SD	Standard Deviation
STE	Standardized Typical Error
StO_2	Tissue Oxygen Saturation
T2D	Type 2 Diabetes
tc	Time Constant
TD	Time Delay
tHb	Total Hemoglobin
TOF	Time of Flight
TSI	Tissue Saturation Index
VL	Vastus Lateralis
VM	Vastus Medialis
VO	Venous Occlusion
$\dot{V}O_2$	Systemic/Whole Body Oxygen Consumption
$\dot{V}O_2max$	Maximal Whole-body Oxygen Consumption

1- Introduction

Theoretical background

Skeletal muscles constitute 40-50% of total body weight enabling individuals to move, breathe, and do work. With respect to exercise, skeletal muscle must cope with a large range of activities from postural stability and basic locomotion to immediate explosive movements in response to unexpected environmental perturbation. Maintaining skeletal muscle function requires the integration of multiple protein, transporter, and organelle systems for dynamic control of energy metabolism. The energy systems are ultimately reliant upon oxygen-dependent respiration within the mitochondria, which adapt to providing energy for long periods of time at low to moderate output rates, to instantaneously increasing energy production more than 100-fold in response to explosive contractions (Westerblad et al., 2010). Skeletal muscle is also a primary tissue for nutrient disposal and utilization, coupled to its energy-strong role in locomotion and posture. Sustaining physical activity in skeletal muscle tissue is dependent upon the oxygen cascade system of processes including pulmonary ventilation, cardiac output, circulation, capillary microperfusion, uptake, transfer and respiratory energy production. Dynamic regulation of these processes is critical in upholding the physiological integrity of the body during sustained activity and fulfilling requirements of daily living. Dysregulation of several of the circulatory, capillary endothelial and basement membrane, and metabolic properties within skeletal muscle have been associated with metabolic diseases including type II diabetes (Bauer et al., 2007a; Hayden et al., 2005), generally attributed to the adverse effects of hyperglycemia and oxidative stress on vascular biology (Avogaro et al., 2011).

Near-Infrared Spectroscopy (NIRS) has been used to non-invasively investigate local muscle oxidative metabolism at rest, and recently during exercise (M. Ferrari et al., 2011; M. Van Beekvelt et al., 2002). With high temporal resolution and non-invasive properties, NIRS can be used within a wider range of exercise modalities than invasive

counterparts. Much research using NIRS has been focused on brain microperfusion, however there is growing popularity of NIRS research on skeletal muscle. Coupling NIRS with rapid arterial and venous occlusions has permitted the easy measurement of skeletal muscle blood flow (mBF) and oxygen consumption ($m\dot{V}O_2$) (Cross & Sabapathy, 2017a; T. Ryan et al., 2012; M. van Beekvelt et al., 2001). By conducting a set number of rapid arterial occasions after a brief bout of exercise, the resultant $m\dot{V}O_2$ over time can be plotted resulting in a curve showing the post exercise $m\dot{V}O_2$ recovery rate. This method provides an assay of the muscle oxygen respiratory capacity (MORC), which is a hybrid index incorporating delivery, deoxygenation, and mitochondrial respiratory functional kinetics (T. Ryan et al., 2012). These measures can be combined with perfusion and saturation of oxygen (SaO_2) derived from the NIRS signal to obtain an integrated picture of the combined systems maintaining skeletal muscle microvascular function. In a novel approach described in this thesis, I compared resting measures to measures taken at incremental levels of exercise intensity for investigation of the dynamic coupling of O_2 delivery to O_2 uptake adapting from rest to exercise. I show that NIRS can be used to investigate skeletal muscle health in metabolically diseased populations at rest, in association with insulin stimulation, and during controlled muscle contraction, and guide in treatment and intervention options.

Since the pioneering work of Jobsis in the 1980s (Jobsis, 1977), various NIRS technologies have been developed to measure the concentration of oxygenated and deoxygenated hemoglobin (O_2Hb and HHb) in skeletal muscle and brain tissue. Continuous-wave NIRS (cw-NIRS) has emerged as one of the preferred technologies due to its ease of use, affordability, and portability. However, cw-NIRS utilizes assumptions that may not hold under certain situations or for specific populations. Frequency-domain NIRS utilizes more advanced methods to determine hemoglobin concentrations, however it is more complex, more expensive, and less portable than cw-NIRS. Comparing and contrasting metrics derived with fd-NIRS to those of cw-NIRS will further our understanding of the assumptions of cw-NIRS allowing for confidence in its use under various modalities for differing cohorts.

Purpose statement & research significance

The purpose of the current thesis is to evaluate the reproducibility and clinical utility of cw-NIRS for the purposes of evaluating skeletal muscle performance in health and metabolic disease tissue (type-2 diabetes, T2DM). I achieved this by:

1) Designing a comprehensive test to evaluate mBF, mVO_2, perfusion, saturation, and MORC at rest and during exercise and establish the day-to-day reliability of this test in healthy individuals and compare and contrast the NIRS derived parameters to the same parameters derived from other methodologies in the literature.

2) Repeat this protocol in T2D individuals with the addition of a benchmark NIRS technology frequency-domain NIRS to test if the assumptions made in cw-NIRS are valid at exercise, and if they are affected by the diseased state of the muscle.

3) Investigate combining NIRS with systemic oxygen uptake to further examine the coupling of O_2 delivery and consumption in T2Ds during incremental ramp cycle exercise and correlate the modeled profile to metrics derived from *in vitro* skeletal muscle biopsy to help explain the increases from rest to exercise.

Skeletal muscle is the largest insulin sensitive tissue in the human body and is an important site for glucose handling and disposal. In T2D, skeletal muscle is characterised by decreased muscle mass (Guerrero et al., 2016), decreased blood flow, particularly at the microvascular level (L.S et al., 2008), and decreased mitochondrial respiratory capacity (Kelley et al., 2002). Chronic exercise has been shown to improve these abnormalities in skeletal muscle and improve metabolic function in T2D (Colberg et al., 2002)(Stanford et al., 2014). However, there is currently no consensus on a critical point of impairment or restoration in insulin resistant muscle. A comprehensive exploration of skeletal muscle adaptation in response to exercise therapy is required to establish important targets for rehabilitation. This thesis will investigate the ability of NIRS to meet this need, at least from the perspective of microvascular haemodynamics.

Thesis organization

This thesis comprises 7 chapters with four primary sections. Chapters 4-6 are written as stand-alone chapters that incorporate standard paper format (abstract, introduction, methodology, results, discussion) and are specific to the aims of that chapter. The thesis is organized according to the flowcharts below (Figures 1.1 and 1.2). The Thesis is introduced in chapter 1 with chapters 2 and 3 providing a review of NIRS use in skeletal muscle and methodological considerations. The primary research studies are described in chapters 4-6. The study described in chapter 4 describes the reliability of muscle blood flow and oxygen consumption response from exercise using NIRS and has been published in the Journal of Experimental Physiology. The study described in chapter 5 provides a novel and important description of the comparative reproducibility and utility of cw-NIRS validated against fd-NIRS in healthy and T2Ds. This study is currently under review in the Journal of Applied Physiology. Finally, the study described in chapter 6 provides a novel characterization of the temporal profile of [HHb] during incremental ramp cycle exercise in T2Ds and a comparison of modeling kinetic parameters to skeletal muscle biopsied tissue, affirming interpretations of previous research of modeling the dynamic coupling of O_2 delivery, [HHb] deflection thresholds, and utilization during incremental exercise to exhaustion.

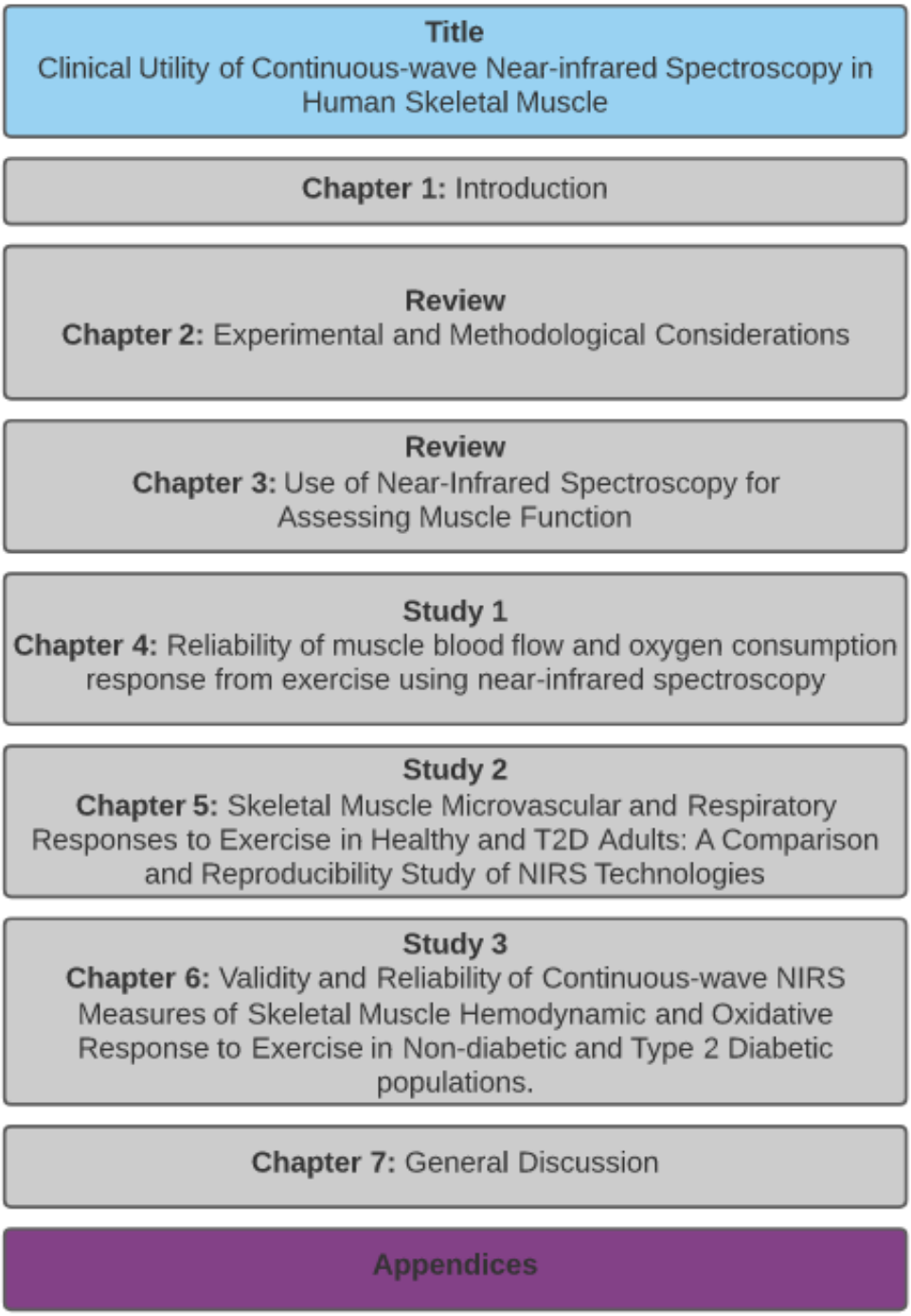

Figure 1.1. Organization of the thesis.

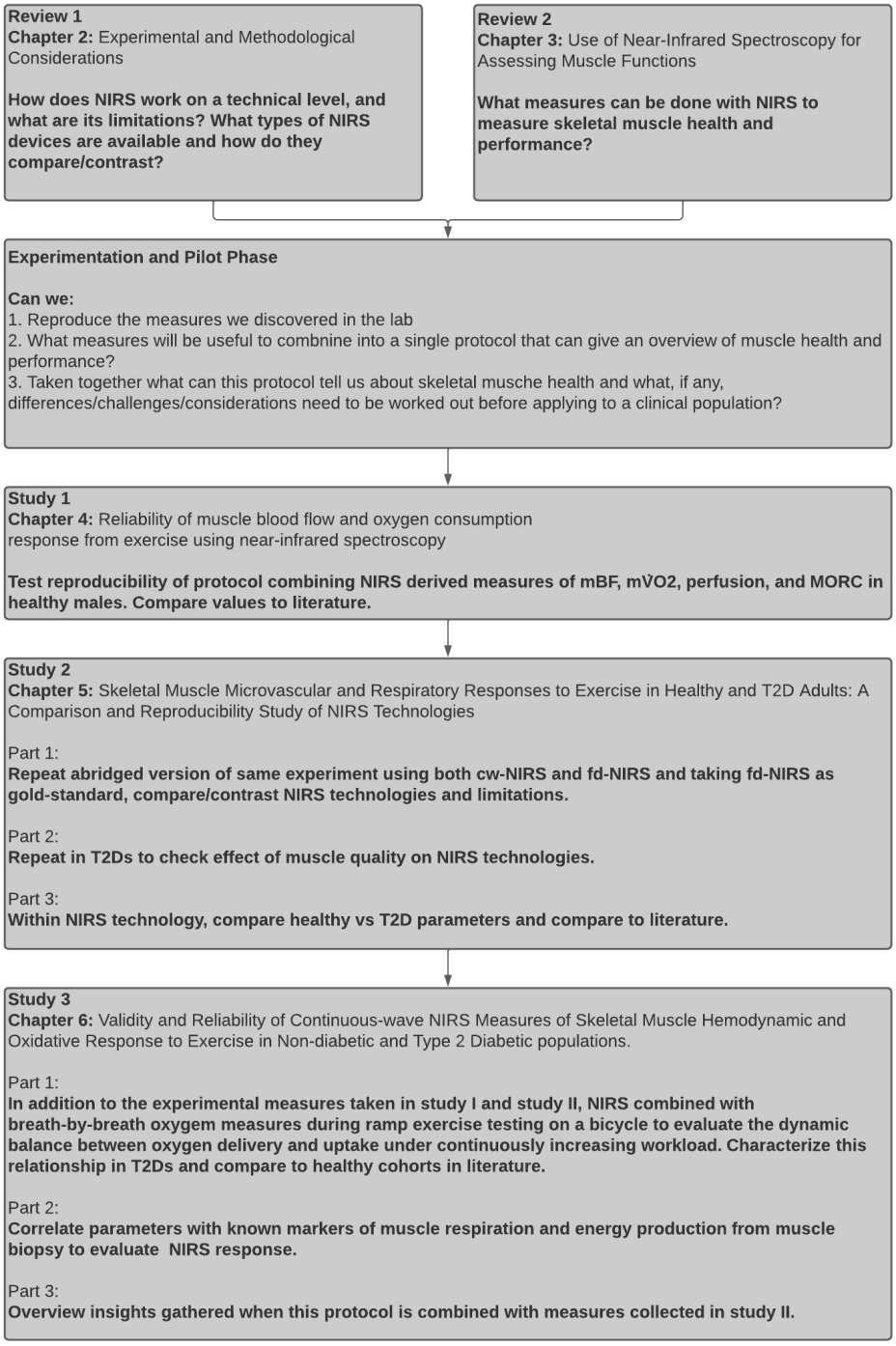

Figure 1.2. Progression of thesis.

References

Avogaro, A., Albiero, M., Menegazzo, L., Kreutzenberg, S. de, & Fadini, G. P. (2011). Endothelial Dysfunction in Diabetes. *Diabetes Care*, *34*(Supplement 2), S285–S290. https://doi.org/10.2337/DC11-S239

Bauer, T. A., Reusch, J. E. B., Levi, M., & Regensteiner, J. G. (2007). Skeletal Muscle Deoxygenation After the Onset of Moderate Exercise Suggests Slowed Microvascular Blood Flow Kinetics in Type 2 Diabetes. *Diabetes Care*, *30*(11), 2880–2885. https://doi.org/10.2337/dc07-0843

Colberg, S. R., Stansberry, K. B., McNitt, P. M., & Vinik, A. I. (2002). Chronic exercise is associated with enhanced cutaneous blood flow in Type 2 diabetes. *Journal of Diabetes and Its Complications*, *16*(2), 139–145. https://doi.org/10.1016/S1056-8727(01)00222-7

Cross, T. J., & Sabapathy, S. (2017). The impact of venous occlusion per se on forearm muscle blood flow: implications for the near-infrared spectroscopy venous occlusion technique. *Clinical Physiology and Functional Imaging*, *37*(3), 293–298. https://doi.org/10.1111/cpf.12301

Ferrari, M., Muthalib, M., & Quaresima, V. (2011). The use of near-infrared spectroscopy in understanding skeletal muscle physiology: recent developments. *Philosophical Transactions of the Royal Society A: Mathematical, Physical and Engineering Sciences*, *369*(1955), 4577–4590. https://doi.org/10.1098/rsta.2011.0230

Guerrero, N., Bunout, D., Hirsch, S., Barrera, G., Leiva, L., Henríquez, S., & De la Maza, M. P. (2016). Premature loss of muscle mass and function in type 2 diabetes. *Diabetes Research and Clinical Practice*, *117*, 32–38. https://doi.org/10.1016/J.DIABRES.2016.04.011

Hayden, M. R., Sowers, J. R., & Tyagi, S. C. (2005). The central role of vascular extracellular matrix and basement membrane remodeling in metabolic syndrome and type 2 diabetes: the matrix preloaded. *Cardiovascular Diabetology 2005 4:1*, *4*(1), 1–20. https://doi.org/10.1186/1475-2840-4-9

Jobsis, F. (1977). Noninvasive, infrared monitoring of cerebral and myocardial oxygen sufficiency and circulatory parameters. *Science*, *198*(4323), 1264–1267. https://doi.org/10.1126/SCIENCE.929199

Kelley, D. E., He, J., Menshikova, E. V., & Ritov, V. B. (2002). Dysfunction of Mitochondria in Human Skeletal Muscle in Type 2 Diabetes. *Diabetes*, *51*(10), 2944–2950. https://doi.org/10.2337/DIABETES.51.10.2944

Ryan, T. E., Erickson, M. L., Brizendine, J. T., Young, H.-J., & McCully, K. K. (2012). Noninvasive evaluation of skeletal muscle mitochondrial capacity with near-infrared spectroscopy: correcting for blood volume changes. *Journal of Applied Physiology*, *113*(2), 175–183. https://doi.org/10.1152/japplphysiol.00319.2012

S, L., S, G., PL, H., & JC, B. (2008). Reduced leg blood flow during submaximal exercise in type 2 diabetes. *Medicine and Science in Sports and Exercise*, *40*(4), 612–617. https://doi.org/10.1249/MSS.0B013E318161AA99

Stanford, K. I., & Goodyear, L. J. (2014). Exercise and type 2 diabetes: molecular mechanisms regulating glucose uptake in skeletal muscle. *Https://Doi.Org/10.1152/Advan.00080.2014*, *38*(4), 308–314. https://doi.org/10.1152/ADVAN.00080.2014

Van Beekvelt, M. C. P., Van Engelen, B. G. M., Wevers, R. A., & Colier, W. N. J. M. (2002). In vivo quantitative near-infrared spectroscopy in skeletal muscle during incremental isometric handgrip exercise. *Clinical Physiology and Functional Imaging*, *22*(3), 210–217. https://doi.org/10.1046/j.1475-097X.2002.00420.x

van Beekvelt, M., Colier, W. N. J. M., Wevers, R. O. N. A., Engelen, B. G. M. V. A. N., Wevers, R. A., & Perfor-, B. G. M. V. E. (2001). *Performance of near-infrared spectroscopy in measuring local O 2 consumption and blood flow in skeletal muscle*. 511–519.

Westerblad, H., Bruton, J. D., & Katz, A. (2010). Skeletal muscle: Energy metabolism, fiber types, fatigue and adaptability. *Experimental Cell Research*, *316*(18), 3093–3099. https://doi.org/10.1016/J.YEXCR.2010.05.019

2 - Experimental and Methodological Considerations

Introduction to topic

Since its inception in 1980 by Jobsis (Jobsis, 1977), near-infrared spectroscopy (NIRS) has exponentially increasing in its ability to non-invasively determine concentrations of oxygenated and deoxygenated hemoglobin in tissues 2-4 cm under the skin. While the majority of the research and strides have been made in neural monitoring (Cour et al., 2018), much work has been done on NIRS use in skeletal muscle at rest and during exercise (Grassi & Quaresima, 2016a). Although NIRS has much potential and promise in clinical applications, there exists many obstacles and limitations in experimental standardizations, signal processing equation coefficients, analysis parameters and processes, and interpretation of results. Before NIRS can be beneficial clinically more understanding and research is needed to more thoroughly develop our light transport models in biological tissue and characterize NIRS signals in various populations of all ages.

There exist three main considerations to NIRS that affect confidence in the accuracy of NIRS derived concentrations of oxy and deoxy haemoglobin:

1. External influences on NIRS signal
2. Internal influences on NIRS signal
3. Signal processing and analysis

An example NIRS output is given in figure 2.1. For NIRS devices that can calculate absolute [Hb] these values can be reported as an average for a given period. For other devices where the [Hb] is arbitrary, an average value from a resting baseline is obtained and other measures are reported as a change from that baseline. For measures such as blood flow and oxygen consumption, they are calculated from the slope of the NIRS signal giving a rate of change. Each of the three points mentioned above can contribute substantially to the outputted NIRS signal, leading to inaccurate results. Thorough and detailed understanding of how each of these points affects the accuracy of NIRS derived measures under differing experimental conditions and populations is the ultimate goal of the current thesis.

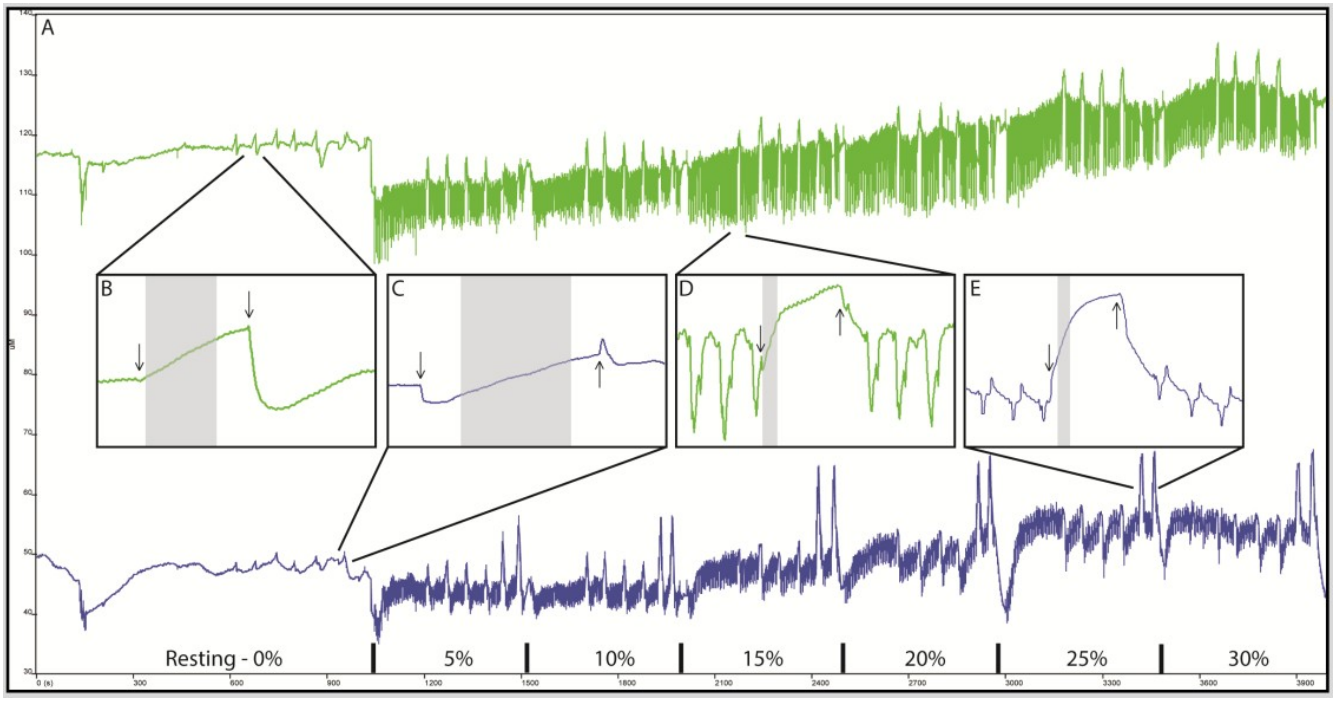

Figure 2.1. Panel A shows a representative example of NIRS signals (µM) collected during experiments showing the raw t[Hb] (green) and [HHb] (blue) traces. The y-axis denotes relative [Hb] (uM) and the x-axis showing time (s). Values obtained from averaging the NIRS signal or collecting the rate of change during an occlusion event from the resting period (seconds 300-900) are defined as baseline and other values are evaluated as a change from rest. Zoom panels B and C show t[Hb] and [Hhb] signals under occlusion events during rest. Zoom panels D and E show t[Hb] and [HHb] signals

occlusion events during exercise with three knee extensions on either side of occlusion. Black arrows denote the inflation and deflation of occlusion and the shaded grey area denotes the linear increase used to calculate rate of change. Experimental conditions must be tightly controlled so that changes seen in the NIRS signal traces can be said to confidently reflect haemodynamic changes in the tissue being measured.

External influences on NIRS signal

Probe preparation

Regardless of technology used, NIRS probes all have a light source that emits the near-infrared light that passes through the tissue to be detected by a sensor placed 2-5 cm linearly from the light source. Environmental light can also be detected by the sensor, and for this reason it is recommended that the probe be taped directly to the skin so as to have no gap between probe and skin, and no movement in position during the experiment. In addition, a dark bandage or wrapping is commonly placed over the NIRS probe to prevent ambient light from hitting the probe. During pilot trials I identified that the wrapping was pushing the NIRS probe into the skin during contraction movements changing the region of tissue being measured and therefore the NIRS signals being output (T. Hamaoka et al., 2011). For this reason I made a custom ‘photon shield’ that encapsulated the probe allowing it to move freely with the skin during contractions while blocking out all ambient light. Figure 2.2 shows how the probe location was marked, attaching the probe to the skin with double sided tape and securely adhering the edges using strips of cross and lengthwise tape. Finally the photon shield was placed over the probe leaving room on all sides. This process yielded the lowest signal-to-noise ratio during pilot testing.

Finally, a rapid-inflation cuff (Hokanson SC 10D, D. E. Hokanson, Inc., Bellevue, WA) used with a custom-built rapid inflation device was used to manipulate blood flow for mBF and mVO_2 measures. This cuff was placed upstream of the NIRS probe as high as possible putting as much space as possible between the cuff and probe because in some participants the act of cuff inflation could swell the thigh artificially moving the probe and changing the area being measured. The participant was

familiarized with the occlusions at each session to prevent involuntary jerking motions caused by the shock of the inflation.

Figure 2.2. Process of attaching NIRS probe to *vastus lateralis*. Panel A shows the marked probe location, B shows how the probe was securely taped to skin preventing any side to side or lifting movements during experiment, and C shows the photon shield cover placed over the probe. The blue rapid inflation cuff can be seen upstream of the NIRS probe as high as possible so as to prevent artefact motion from cuff inflation.

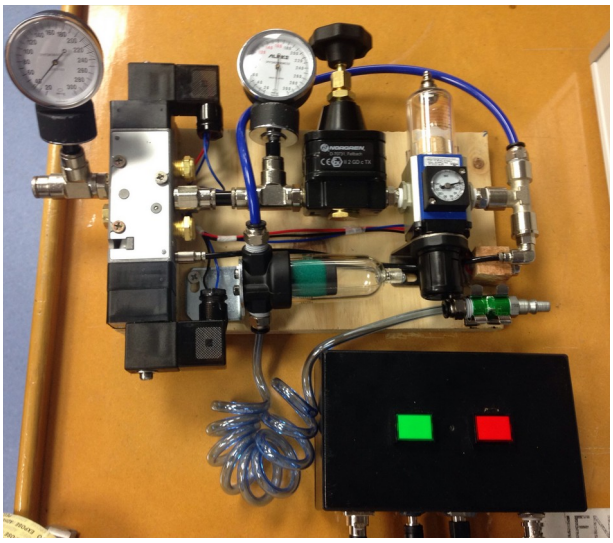

Figure 2.3. Custom built rapid occlusion device (Cuffinator). Compressed air would enter from the right and be regulated to occlusion pressure, which would rapidly inflate and deflate using green and red buttons, respectively.

Experimental set-up

Other external influences including seating position, height, angle of motion and workload needed to be standardized so as to keep the same conditions day to day. Studies using NIRS to assess m$\dot{V}O_2$ in response to exercise have shown that using resistance

bands or electrical stimulation yielded consistent results (Terence E Ryan et al., 2013). However, in the current study we measured blood flow in addition to $m\dot{V}O_2$ and found that mBF measures were much more sensitive. In order to ensure reliable results we needed to tightly control seating position and workload. Participants were seated on an isokinetic dynamometer in the same experimental position (Biodex Medical Systems, Inc. Shirly, NY, USA) reclined to 70° to obtain a 110° hip angle and a 90˚ knee extension angle, which was optimal for experimental measures (Grassi & Quaresima, 2016a). The settings were adjusted so that the axial portion of the knee aligned with the axis of rotation on the dynamometer. The non-working leg was suspended in a 150º knee-joint angle throughout to limit changes in blood distribution between legs. Isotonic knee extension exercise was chosen as the resistance arm applied a specific force (N·m) only at the 90º angle then released once the force was reach allowing the participant to freely swing their leg up the rest of the way standardizing the amount and duration force was applied on the working muscle. Other modes of exercise allowed participants to vary how much force they applied, changing the outcome variables. Figure 2.4 shows an example set-up.

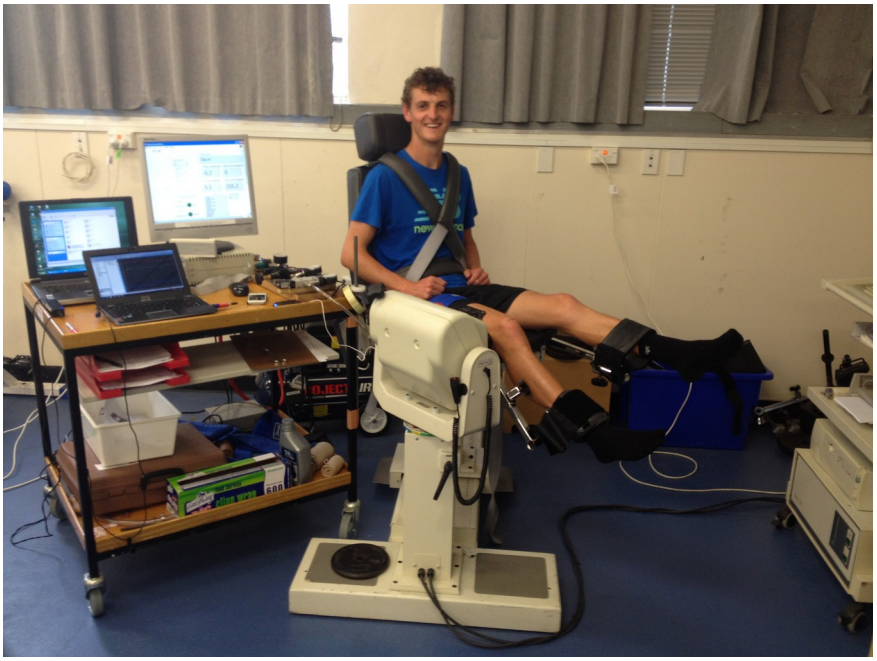

Figure 2.4. Example experimental set up depicting the participant seated in the Biodex alowing for tight control of seating position and workload.

Internal influences on NIRS signal

Internal influences on NIRS signal include adipose tissue, skin temperature, skin blood flow, and probe placement limiting muscle cross talk. Skeletal muscle tissue makeup can change the measured [Hb] concentrations using NIRS, and it is a goal of this thesis to identify if skeletal muscle differences in healthy and T2D show any changes in measured NIRS parameters, therefore all other influences must be minimized. Adipose tissue thickness (ATT) is known to alter optical properties of NIRS (Pirovano et al., 2021), and in the current thesis all participants ATT was measured using B-mode ultrasound and participants were excluded if ATT exceeded 2 cm since this is greater than the penetration of the NIRS light. Monte-Carlo simulations and models have been suggested to correct NIRS signals for ATT (Soller et al., 2005), however this was not applied to the current study as we did not measure significant changes in ATT day-to-day and used ischaemic calibration to correct NIRS signals where applicable. It is known that skin blood flow increases which can be brought on by an increase in skin temperature can significantly contribute to the O_2Hb signal, mainly affecting blood flow measures (Buono et al., 2005). To minimize this, The temperature in the lab was constantly maintained at

20.5 ˚C, SD 0.8, and the experiment was designed so that the mBF measures were done prior to the more intensive and fatigue inducing m$\dot{V}O_2$ and MORC measures, saving the incremental cycling for last since this measure only used the HHb signal which is not significantly altered by changes in skin blood flow. Finally, it was imperative that a standard way of marking the probe placement on each individual was employed so that the NIRS was placed over the belly of *vastus lateralis* (VL) muscle, maximizing signal response and minimizing cross talk between muscle groups, especially during contractions (Iwasaki & Okada, 2004). In addition, the same spot needed to be located day-to-day, even weeks later from the initial test as changing the NIRS probe position changes the underlying tissue being measured which will introduce changes in the NIRS signals not related to the experiment. A standard method to locate the belly of the VL on individuals for use in electromyography was employed, accompanied with a custom template that allowed for ventral or dorsal changes in probe placement so that the probe could be placed on the flattest portion of the VL belly during isometric contraction limiting probe movement during contraction.

Signal Processing and Analysis

In the case of both NIRS devices, continuous wave (cw-) and frequency domain (fd-) NIRS, the raw data received from the detector can be processed using various equations and constants. How each approach affects the [Hb] measures and when to apply what method is still not fully understood. For cw-NIRS we followed recommendations in the literature for choosing default parameters. In the case of the fd-NIRS I wrote custom analysis software processing the signals using many different combinations of input variables following the literature for recommendations (see figure 2.5). Developing custom analysis software in python was critical to determining the optimal approach for calculation of [Hb], apart from how to incorporate real-time measures of scattering. . Figure 3.11 shows that the scattering changes abruptly during occlusion and applying real time scattering seemed to affect the NIRS derived [Hb] because the sharp decrease in scattering was altering the concentration. Two methods of

applying scattering were trialed, the first was to calculate the degree of scattering in the individual after a period of rest and hold it constant throughout the experiment, or apply a scattering value measured during occlusion to each measure. Ultimately, I decided to apply a resting scattering value to the whole experiment as this would allow us to evaluate the effect of assuming literature-based scattering coefficient for a cohort vs calculating a scattering coefficient for each individual in an experiment.

To determine reliability and reproducibility of the NIRS derived measures, methods developed by Will Hopkins were employed as they were developed specifically for exercise performance testing and accounted for the effects of habituation (such as familiarization, practice, motivation, fatigue, or even the training effect of a single test) and allowing for the determination of the smallest important mechanistic difference in measures. This was important to determine the acceptable variance between measures and between NIRS technologies so as to be confident that NIRS outcomes can be attributed to muscle mechanics and not measurement variability.

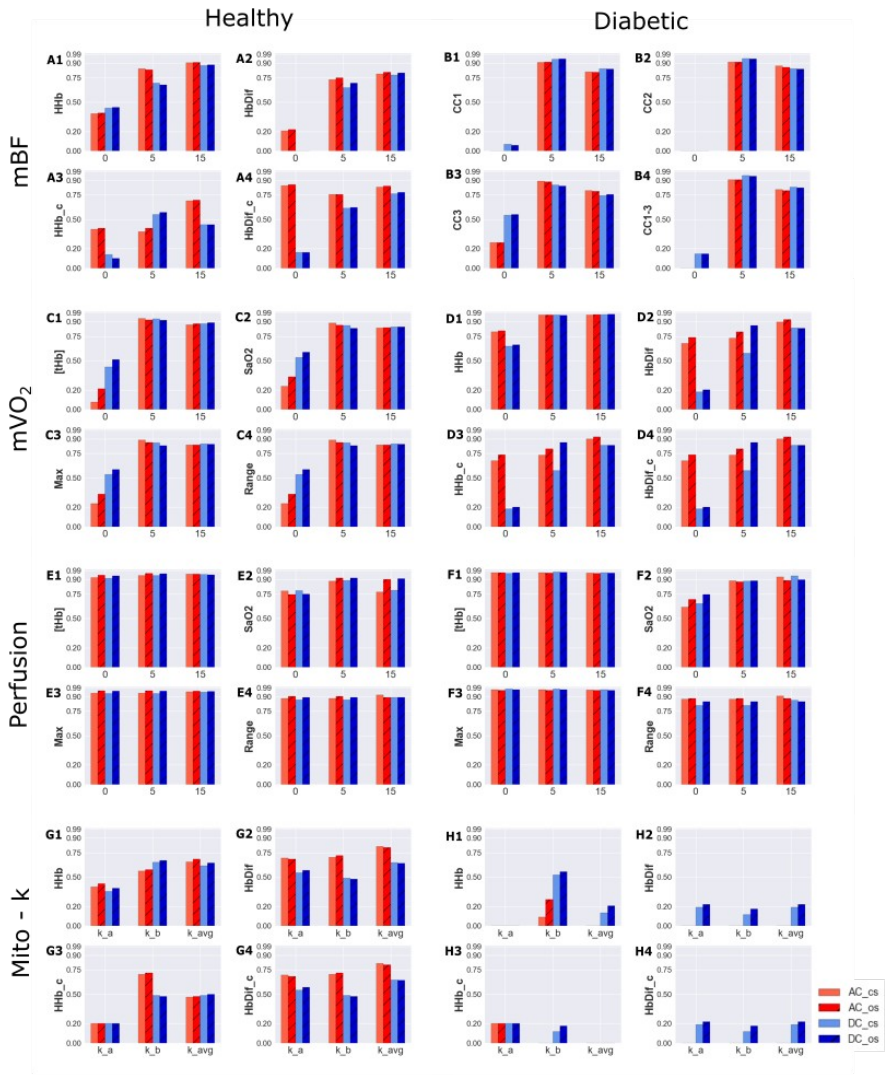

Figure 2.5. Example graph showing the ICC results obtained from processing the same NIRS data using the AC (red) or DC (blue) signal and if constant scattering (cs, solid) or occlusion scattering (os, hatched) affected the AC or DC signal for all NIRS parameters.

Conclusion

Due to the sensitive and experimental nature of NIRS, significant work went into piloting different aspects of the experimental design in order to develop a standardized protocol that could be built upon to enhance the ability of NIRS to non-invasively investigate skeletal muscle hemodynamic function. Achieving day-to-day reliability and correcting for external factors are critical steps in the development of NIRS for practical use in exercise and clinical physiology. It is my hope that this thesis contributes to the overall goal of development of non-invasive methodologies for clinical utility.

References

Buono, M. J., Miller, P. W., Hom, C., Pozos, R. S., & Kolkhorst, F. W. (2005). Skin Blood Flow Affects In Vivo Near-Infrared Spectroscopy Measurements in Human Skeletal Muscle. *The Japanese Journal of Physiology*, *55*(4), 241–244. https://doi.org/10.2170/jjphysiol.T649

Cour, A. la, Greisen, G., & Hyttel-Sørensen, S. (2018). In vivo validation of cerebral near-infrared spectroscopy: a review. *Neurophotonics*, *5*(4), 040901. https://doi.org/10.1117/1.NPH.5.4.040901

Grassi, B., & Quaresima, V. (2016). Near-infrared spectroscopy and skeletal muscle oxidative function in vivo in health and disease: a review from an exercise physiology perspective. *Journal of Biomedical Optics*, *21*(9), 91313.

Hamaoka, T., McCully, K. K., Niwayama, M., & Chance, B. (2011). The use of muscle near-infrared spectroscopy in sport, health and medical sciences: recent developments. *Philosophical Transactions of the Royal Society A: Mathematical, Physical and Engineering Sciences*, *369*(1955), 4591–4604. https://doi.org/10.1098/rsta.2011.0298

Iwasaki, A., & Okada, E. (2004). Influence of cross talk on near-infrared oxygenation monitoring of muscle. *Second Asian and Pacific Rim Symposium on Biophotonics - Proceedings, APBP 2004*, 159–160. https://doi.org/10.1109/apbp.2004.1412330

Jobsis, F. (1977). Noninvasive, infrared monitoring of cerebral and myocardial oxygen sufficiency and circulatory parameters. *Science*, *198*(4323), 1264–1267. https://doi.org/10.1126/SCIENCE.929199

Pirovano, I., Porcelli, S., Re, R., Spinelli, L., Contini, D., Marzorati, M., & Torricelli, A. (2021). Effect of adipose tissue thickness and tissue optical properties on the differential pathlength factor estimation for NIRS studies on human skeletal muscle. *Biomedical Optics Express*, *12*(1), 571. https://doi.org/10.1364/boe.412447

Ryan, T. E., Southern, W. M., Reynolds, M. A., & McCully, K. K. (2013). A cross-validation of near-infrared spectroscopy measurements of skeletal muscle oxidative capacity with phosphorus magnetic resonance spectroscopy. *Journal of Applied Physiology*, *115*(12), 1757–1766. https://doi.org/10.1152/japplphysiol.00835.2013

Soller, B. R., Landry, M. R., Soyemi, O. O., & Yang, Y. (2005). Influence of a fat layer on the near infrared spectra of human muscle: quantitative analysis based on two-layered Monte Carlo simulations and phantom experiments. *Optics Express, Vol. 13, Issue 5, Pp. 1570-1579*, *13*(5), 1570–1579. https://doi.org/10.1364/OPEX.13.001573

3 - Technical Review

Introduction

The purpose of this review is to highlight technical considerations of Near infrared spectroscopy (NIRS) to assess skeletal muscle hemodynamic parameters. This technology utilizes the oxygen dependent absorption characteristics of infrared light in the 600 – 900 nm range to provide information about the changes in tissue oxygenation. A major benefit of NIRS is that its non-invasive allowing for use during exercise, and can be used outside of the laboratory for unprecedented investigation of matching oxygen delivery (DO_2) to oxygen utilization (mVO_2) at rest or during exercise. This tool has the potential to further our understanding of perfusion, blood flow, and skeletal muscle respiratory dynamics, in both health and pathophysiology. By the end of this review it is hoped that the reader will be familiar with the background and operation of NIRS, be aware of its current limitations from the perspective of skeletal muscle, and understand the gaps in knowledge that need to be characterized so NIRS can be utilized in a clinical setting. The ability of NIRS to differentiate between and measure concentrations of the oxygenated and deoxygenated forms of hemoglobin and myoglobin (O_2Hb/Mb and HHb/Mb, respectively), which added together yields total hemoglobin concentration (tHb/Mb = O2Hb/Mb + Hhb/Mb) allows for measure of skeletal muscle blood flow (De Blasi et al., 1994; Nioka et al., 2006), muscle oxygenation, and muscle oxygen consumption (Takafumi Hamaoka et al., 1996; Malagoni et al., 2010; Takayuki Sako et al., 2001; M. van Beekvelt et al., 2001). More recently, repeated arterial occlusions have been used after exercise to assess the recovery of muscle oxygen consumption (mVO_2) as an index of mitochondrial function (Motobe et al., 2004; T.E. Ryan et al., 2012). Finally, the profile of HHb during ramp incremental exercise is said to reflect the dynamic balance between oxygen delivery and utilization (Boone et al., 2009; Spencer et al., 2012).

Taken together NIRS is a powerful, non-invasive tool for investigating skeletal muscle hemodynamics at rest, transition to, and during exercise. However, NIRS research is complicated by multiple technologies, devices withing technologies with slight variations in function, tissue makeup changing contribution of skeletal muscle to NIRS signal individual to individual and even measurement to measurement within an

individual (e.g., adipose tissue thickness, skin blood flow, melanin), and differing techniques for probe placement and experimental design make interpreting NIRS results within a study and comparing studies to one another difficult. This review will briefly cover NIRS theory, discuss different NIRS technologies and how they are employed, introduce common NIRS experimental methods, technical limitations to these methods, and finally the use of NIRS in clinical studies.

Theory

Principles of Spectroscopy

The principles of NIRS are based on the principles of traditional spectroscopy, modified to work for biological tissue. Spectroscopy is a technique for measuring concentration of a molecular compound suspended in a homogenous solution. It is based on the Beer-Lambert law which expresses the linear relationship between the absorbance and concentration of a compound at a fixed wavelength, given by:

Eq 3.1: $OD\lambda = \log(Io/I) = e\lambda * c * l$

Where $OD\lambda$ is a dimensionless factor known as the optical density of the medium, Io is the initial light intensity, I is the measured light intensity at the detector, $e\lambda$ the extinction coefficient of the chromophore (mM-1*cm-1), c is the concentration of the compound, and l is the distance between the point of light emission (source) and final measurement (detector).

As light is emitted from the source and travels through solution, some of the light will be absorbed by the chromophore in the molecular compound. The more molecular compound in solution the more of the emitted light that is absorbed and the less light that makes it to the detector. Therefore, by knowing the incident light (Io), detected light (I), source-detector distance (l) and optical properties of the light and molecular compound of interest, the molecular concentration can be calculated. This method has some requirements, namely that the molecular compound of interest has a light absorbing

chromophore, the emitted light wavelength is specific for that chromophore, there are no other molecules in solution that have chromophores absorbing light at the same wavelength, and that the light is traveling linearly and through a homogenous, non scattering medium so that the difference in the light intensity from source to detector is completely due to absorption by the molecular compound of interest.

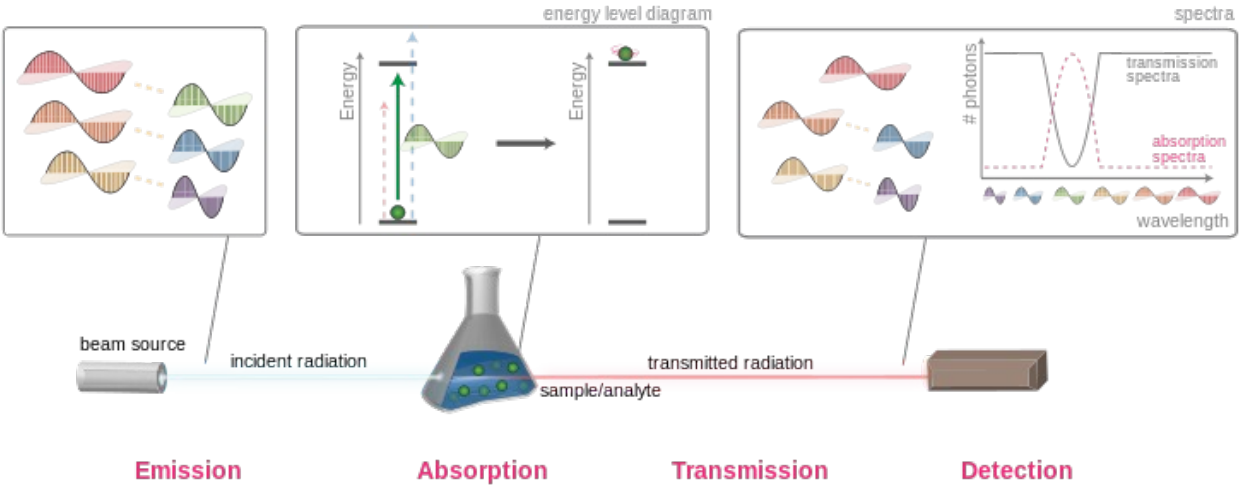

Figure 3.1. An overview of electromagnetic radiation absorption. Light is emitted form a source and passes through a solution. Upon striking the solution, photons matching the energy gap of molecules suspended within are absorbed resulting in an excitation for the molecule. By comparing the attenuation in the intensity of the transmitted light with its emitted intensity yields the molecular concentration. Figure borrowed from Wikimedia commons.

Spectroscopy in Tissue

Biological tissue presents many challenges for traditional spectroscopy. The wavelength of light used must be able to penetrate several centimeters of epidermal, adipose, and skeletal muscle tissue while being specific to a molecular compound of interest within the tissue. Wavelengths of light below 300 nm and above 1000 nm are completely absorbed by water molecules and not usable. From 450 nm - 650 nm (visible spectrum) light is also completely absorbed by hemoglobin and other chromophores. In the near-infrared spectrum, specifically between 700-1000 nm absorption of light is sufficiently low enough for light to be detected across many centimeters of tissue, and

within range of absorption spectra peaks for oxygenated and deoxygenated forms of hemoglobin, the main oxygen transporter in the blood. Moreover, it is thought that the [Hb] measured by NIRS comes mainly from blood vessels <1mm in diameter as vessels larger than this completely absorb the NIR light (Experimental study of migration depth for the photons measured at sample surface). Apart from wavelength of light used, spectroscopic techniques in biological tissue present many challenges, including multiple absorbing chromophores in the solution being measured, non-linear light travel, and that it is a non-homogenous scattering medium. The attenuation of light from source to detector is not only due to absorption by molecule of interest, but also absorption from chromophores of fixed concentration, absorption from chromophores of variable concentration, and light scattering. Differing NIRS technologies and apparatuses have been developed to account for these challenges, which adds complexity in accuracy and interpretation of results. This review will discuss these challenges with respect to three of the more popular NIRS technologies.

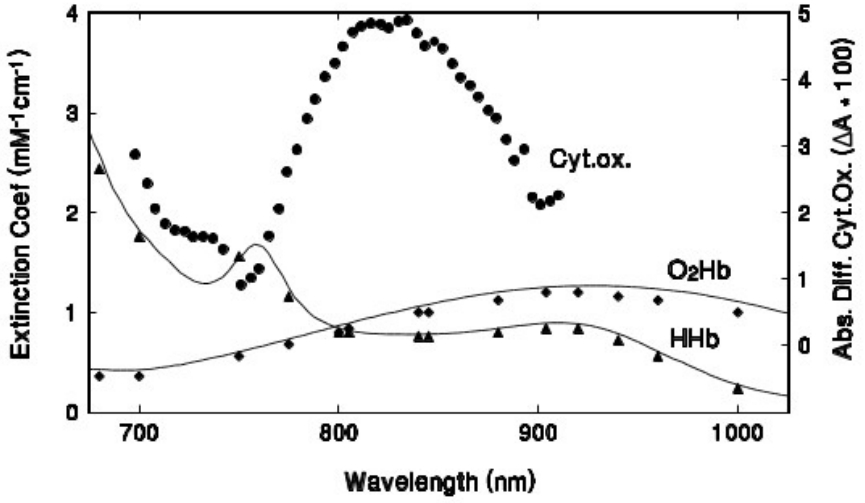

Figure 3.2. Absorption spectra of O_2Hb, HHb, and cytochrome oxidase (COX). Image borrowed from (M. van Beekvelt et al., 2001)

Multiple Chromophores in Tissue

In the near-infrared region there are three main absorbing oxygen dependent chromophores, hemoglobin, myoglobin, and cytochrome oxidase. Due to different absorption spectra, the concentration of the oxygenated form of hemoglobin (O_2Hb) can be measured separately from the deoxygenated form (HHb) by using wavelengths ~830 and ~750 nm, respectively. The degree of contribution to the calculated concentration by Mb and Cyt Ox is still being researched, but cyt Ox is thought to contribute negligible amounts of absorption while Mb is thought to vary between 10-50% (Davis & Barstow, 2013). The contribution of Mb to the NIRS light attenuation is controversial, but is thought to be constant and therefore any change in concentration can be attributed to changes in O_2Hb and HHb.

Non-Linear Light Travel

In traditional spectroscopy the solution is placed in a direct line between light emitter and detector. With NIRS this is not possible as the light would be completely absorbed by tissue and bone leaving no light to measure at the detector on the other side. Instead, the light emitting probe and detector are both facing downward securely attached to the skin 2-4.5 cm apart from each other (see figure 3.3). In this way, the light is emitted in all directions, and a percentage makes its way to the detector in a ‘banana’ shape that penetrates ½ the source-detector distance with light intensity extending on either side (Marco Ferrari et al., 2004).

Figure 3.3. Representation of path of NIRS light travel from source to detector. Image borrowed from (Marco Ferrari et al., 2004)

Non-Homogenous Medium

In addition to added travel distance due to *banana* shape, the differing refractive index of skin, adipose, tendon, and skeletal muscle tissue and their membranes and organelles means that the incident light does not travel in a perfect arch from source to detector but rather is *scattered* as it is forced to change direction and bounce off of obstacles as it travels through the cellular membrane structures of differing refractive indices. In the absence of scatter the total light absorption in the medium is a linear sum of each chromophore concentration, but in a scattering medium this linear summation is distorted by the differing optical pathlength of light travel, which may differ by wavelength and tissue makeup. The distance or length of light travel must be known to calculate molecular concentration and since the travel is non-linear and scattered, this distance must be calculated using a complex function of the tissue absorption and scattering coefficients (μs and μa), scattering phase function, and tissue measurement geometry. Measuring changes in concentration of O_2Hb and HHb became possible with the development of techniques to measure optical pathlength in tissue, and combined with literature based or individually sampled hemoglobin concentration from blood samples allowed for estimates of absolute concentration.

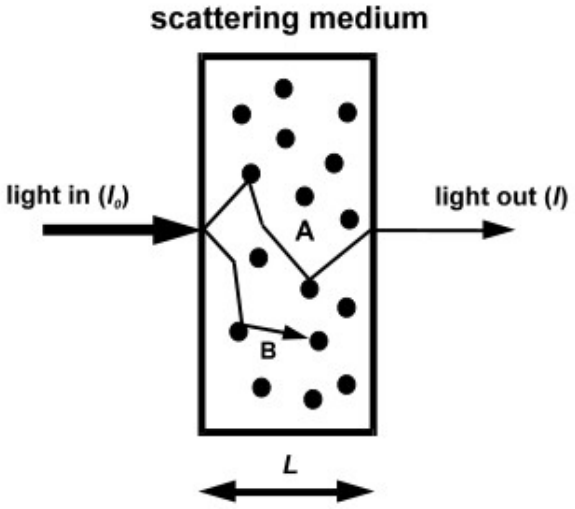

Figure 3.4. A scattering medium where the incident light (I_o) is scattered on cellular structures and organelles (represented by black dots). Light ray A is scattered traveling the pathlength correction factor times length (L). Light ray B is absorbed completely. Image borrowed from (M. van Beekvelt et al., 2001).

Instrumentation

To obtain an accurate high-resolution absolute [O2Hb] and [HHb] at rest and in response to exercise requires measuring more than just light attenuation at the tissue surface. Clever manipulations of light combined with highly sensitive light emitting and detecting equipment have allowed researchers to develop methods to quantify the degree of absorption and scattering of light (μs and μa) in the tissue being measured in real time. The three main technologies used to measure skeletal muscle oxygenation are continuous-wave (cw), time-resolved (TRS), and frequency-domain (fd; phase-modulated) NIRS (see figure 3.5). These technologies include utilization of a literature based correction factor as in continuous-wave NIRS, measuring the temporal dispersion of light from an ultrashort input light pulse, as in time-of-flight NIRS, or phase and modulation depth changes of light, as in frequency-domain NIRS. While these approaches have been successful in accurately determining hemoglobin concentrations and skeletal muscle optical properties, they are limited by the accuracy of the light transport models in inhomogeneous media, which is further complicated by sampling during exercise since the contraction of the skeletal muscle changes the volume and makeup of tissue being measured (Thomas J. Barstow, 2019).

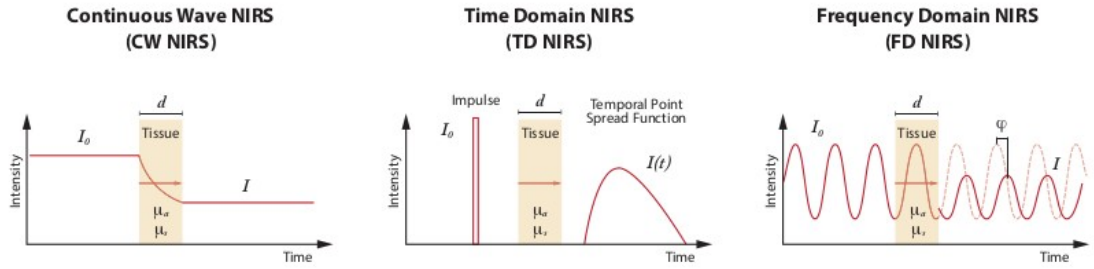

Figure 3.5. Schematic showing the three main types of NIRS instruments. d, source-detector separation (ρ in equations). Phase shift (ϕ) used to determine μa and μ's. Borrowed from (Thomas J. Barstow, 2019)

Continuous-wave

The most common, simplest to understand, easiest to use, and most portable NIRS technology is cw spatially resolved spectroscopy. The main advantages of cw-NIRS over the other two technologies affecting cost and ease of use are the ability to use LEDs vs laser diodes and no need for regular calibration. This technology utilizes a modified version of the Beer-Lambert law:

eq 3.1: $OD\lambda = \log(Io/I) = e\lambda * c * l * DPF$

Where DPF is a dimensionless factor that accounts for the light attenuation contributions of absorption and scattering so that heme concentrations can be calculated. The DPF literature values at a given wavelength were obtained by *time-of-flight* measurements, which uses an ultra-short laser pulse fired into the tissue that is detected by an ultrafast camera to track the time from light pulse emission to detection giving the time to travel through tissue. From this time travel measure, the distance traveled can be calculated using the speed of light. Dividing the distance travelled by the source-detector separation distance (ρ) yields the DPF (eq. 3.2). In addition, while the underlying theory is different, the DPF for a given wavelength can also be approximated as a function of ρ, μs and μa (eq. 3.3).

eq 3.2: $DPF(\boldsymbol{\lambda}) \cong d\rho = c * t(\boldsymbol{\lambda})n(\boldsymbol{\lambda})$

eq 3.3: $DPF(\boldsymbol{\lambda}) \approx \sqrt{3}\mu's / 2\sqrt{\mu a}$

Where c is the speed of light in a vacuum, $n(\boldsymbol{\lambda})$ is the tissue refractive index at wavelength, and $t(\lambda)$ is the photon mean time-of-flight (Essenpreis et al., 1993).

Assuming a constant DPF and optical properties of tissue allows for cheaper technology that is more portable and user friendly, however the main caveat is that absolute heme concentrations cannot be calculated, only changes. Moreover, the DPF is wavelength specific, affected by differing thicknesses and changing optical properties of the ATT and skeletal muscle layers, and has been shown to change under occlusion and skeletal muscle contraction (Marco Ferrari et al., 1992). Because cw-NIRS devices assume constant optical properties, they are limited to only measuring relative [Hb], and

can potentially introduce confounding results for interindividual analyses and in circumstances where the DPF value has changed, for example, change in adipose thickness or exercise (Pirovano et al., 2021).

Spatially-resolved (SRS) NIRS is an expansion of cw-NIRS that uses multiple light emitters at set distances from the detector (Figure 3.6). The intensity of the light emitted from the transmitters is measured as a function of the source-detector distance. The shape of this function is related to μa, from which the absolute heme concentrations and the tissue saturation index (TSI%), a surrogate of StO_2, can be calculated.

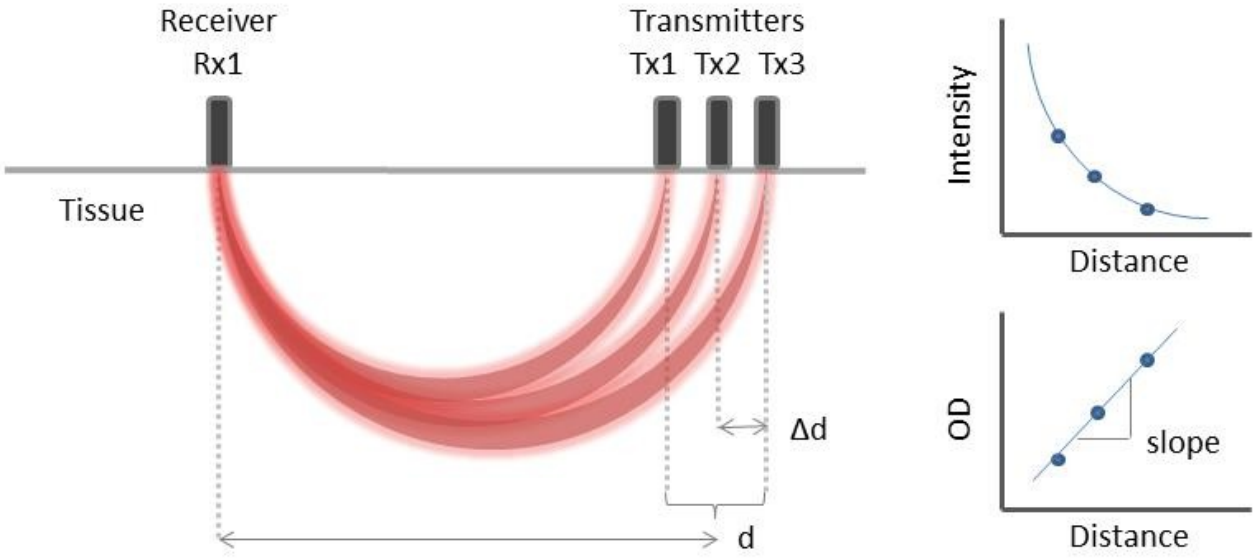

Figure 3.6. Schematic view of a TSI measurement. Light through tissue with three transmitters. Image borrowed from Artinis Manual.

Time-Resolved NIRS

As mentioned earlier, TRS was used in *time-of-fight* experiments to determine common DPF values in various muscle groups of men and women of varying ages (Duncan et al., 1995). In TRS, temporal changes in the reflected light intensity are measured after irradiation of an ultra-fast picosecond pulse, yielding a distribution of the total pathlength

of a photon traveling in the scattering medium. This technology allows for determination of relative light intensity, mean optical path length, and the optical properties of tissue μs an μa.

Figure 3.7. Phase shift between the incident light (dashed line) and scattered light through tissues (solid lines) at 70 MHz of modulation frequency. Image borrowed from (Yamashita et al., 2013).

Frequency-Domain NIRS

Phase-modulated or fd-NIRS is based on amplitude-modulated light sources (at a frequency of the order of 100 MHz or larger). The time delay is related to light scattering and absorption, including biological signals. By utilizing multiple light emitters, frequency-domain multi-distance spectroscopy yields the average value (DC), amplitude (AC) and phase (ϕ) of the modulated light intensity at several source-detector distances, which by using equations derived from diffusion theory allows for continuous measurement of μs an μa and thus absolute heme concentrations and StO2 (Fantini, S. Franceschini, 2002).

Multi-Channel Devices

Conventional NIRS devices offer a single channel spectrophotometer, which provides a limited (~3 cm^3) sample volume. This raises the question whether the measured value is representative for the whole muscle, especially in large muscles like the quadriceps or gastrocnemius muscle. Recent advances in NIRS technology have included the addition of multiple-source detector pairs to image skeletal muscle. This has been done to take advantage of classical studies that have shown regional differences in skeletal muscle oxygenation and metabolism in different locations within a muscle (Laughlin & Armstrong, 1982). By simultaneously collecting data from multiple skeletal muscle regions, these devices avoid the variability caused by position dependent differences in muscle oxygenation that plague all single location measurements. Imaging devices also allow the study of regional differences in how skeletal muscle responds to exercise. The challenge of NIR imaging systems is how to evaluate the much greater amounts of information that are collected. Kime et al (Kime et al., 2005) evaluated heterogeneity of muscle O_2 dynamics in a single muscle (VL) during bicycle exercise using an eight-channel NIRS mapping system. The half-time recovery (see above) was progressively delayed from distal sites to proximal sites of VL. On the other hand, there were no differences between medial and lateral sides at the same transverse level. Takagi et al (Takagi et al., 2013) examined O_2 saturation in several leg muscles with progressive intensity exercise. Twelve healthy young males performed 20 W/min ramp bicycle exercise until exhaustion. Muscle O_2 saturation was monitored continuously at the belly of the VL, rectus femoris, vastus medialis, biceps femoris, gastrocnemius lateralis, gastrocnemius medialis, and tibialis anterior by NIRS. Deoxygenation patterns were considerably different between muscles during ramp cycling exercise. Multiple channel NIRS devices have the potential to evaluate regional differences in oxygen status and could play an important role in monitoring exercise prescription and clinical uses (e.g. application of multiple NIRS imaging device to the exercising muscle metabolism).

NIRS Metrics and Methodology

Adequate delivery of oxygen (DO_2) to meet metabolic demand ($\dot{V}O_2$) is critical for all skeletal muscle, at rest and during exercise. At the microvascular level, DO_2 is represented by microvascular blood flow (mBF) and $\dot{V}O_2$ by skeletal muscle oxygen consumption ($m\dot{V}O_2$). Delivery of O_2 to the terminal cytochrome oxidase can be described by integration of the percussive (equation 3.4) and diffusive (equation .5) equations of Fick's Law:

eq 3.4: $\dot{V}O_2 = Q * (Ca - Cv)\ O_2$

eq 3.5: $\dot{V}O_2 = DO_2 * (PmvO_2 - pmitoO_2)$

Where Q is blood flow, Ca and Cv are concentrations in arterial and venous blood, respectively, DO_2 is the diffusivity of O_2, and $PmvO_2$ and $PmitoO_2$ are the partial pressures of O_2 in the microvasculature and mitochondria, respectively. The power of NIRS lies in its ability to non-invasively determine [HbO_2] and [HHb], which combined with clever methodology can provide insight into the relative balance of mBF and mVO_2 under given circumstances.

Tissue Oxygen Saturation and Perfusion

Early detection of inadequate tissue perfusion and oxygenation is critical in hemodynamic monitoring of oxygen saturation in tissue. Pulse Oximetry is the most common technology used to continuously measure tissue oxygenation but is limited in where it can be used (earlobe, finger, toe). Using similar technology, NIRS has greater tissue penetration than pulse oximetry, can be used to measure oxygenation up to 3 inches in depth all over the body, and provides a global assessment of oxygenation in all vascular compartments (arterial, venous, and capillary) (Lima & Bakker, 2006). From the calculated [O_2Hb] and [HHb], tissue oxygen saturation (StO_2) has been widely used to assess skeletal muscle oxygen saturation. StO_2 can be calculated from the ratio of increase in O_2Hb to tHb (O_2Hb + HHb).

Unlike fd-NIRS which can calculate absolute [O_2Hb] and [HHb], cw-NIRS is limited to relative changes in [O_2Hb] and [HHb] and cannot calculate absolute concentrations it cannot calculate StO_2 in a traditional sense but can calculate an Index of saturation known as the Tissue Saturation Index (TSI). This relies on the use of two or more light emitters to estimate absolute [Hb] values using principles of spatially resolved spectroscopy, and therefore the TSI is an estimation of StO_2 percentage.

Perfusion can be assessed as the average [tHb] ([O2Hb] + [HHb]) for a given period, and changes in [tHb] from a baseline are indicative of perfusion changes in the tissue being measured. A study using cw-NIRS looking at the perfusion changes in the calf muscles of patients with T2D, PAD, or both T2D + PAD before and after plantar-flexion exercise (Mohler et al., 2006)found reduced capillary volume expansion in T2D patients with or without PAD, concluding that it may be due to impaired vasodilation secondary to endothelial dysfunction.

Skeletal Muscle Blood Flow

Indocyanine Green Method using NIRS

Near-infrared spectroscopy (NIRS) emitting a wavelength specific to the tracer indocyanine green (ICG) has been validated for measurement of regional MBF during exercise (Bonde-Petersen et al., 1975). The passage of ICG through the tissue is monitored noninvasively by NIRS probes taped to the skin overlying the muscles of interest. The most commonly used algorithm to analyze the tracer requires simultaneous recording of the ICG concentration curve in arterial blood as the input function (Bonde-Petersen et al., 1975). Thus, although NIRS itself is noninvasive, the measurement requires arterial catheterisation and continuous withdrawal of blood through a photodensitometer for several seconds after injection. Blood flow to the gastrocnemius measured by NIRS-ICG provides comparable values to dye dilution in combination with MRI (Boushel et al., 2000).

Given the invasive nature of catheterisation, an alternative algorithm has been proposed to calculate tissue perfusion from the NIRS data, namely the blood flow index (BFI). This index is calculated by dividing the ICG peak concentration by the time for ICG to reach peak concentration. Kuebler et al. (Kuebler et al., 1998) validated the BFI for determining cerebral perfusion in pigs against simultaneously measured regional blood flow derived from the radioactive microsphere technique. Although the BFI does not provide absolute blood flow values, it has been shown to sensitively detect perfusion differences between cerebral hemispheres after an acute ischemic stroke (Kuebler et al., 1998), to be well reproducible, and to be suited to detect intra-individual changes in brain blood flow (Kuebler, 2008; Wagner et al., 2003). The approach has been validated against the standard NIRS-ICG (described above), which relies on the Fick principle, for the measurement of skeletal muscle blood flow during exercise (r = 0.98) (Habazettl et al., 2010). Moreover, the inter-observer variability, analysed by Bland-Altman plots, was considerably lower for BFI compared to arterial catheterisation.

Venous Occlusion Method using NIRS

The venous occlusion method has the distinct advantage over the ICG method in that it can be used non-invasively to determine muscle blood flow (mBF) by applying a similar occlusion technique as used in conventional venous strain-gauge plethysmography (De Blasi et al., 1994; M. van Beekvelt et al., 2001). NIRS-determined mBF by the venous occlusion method has been shown to agree with traditional measurements using plethysmographyand the Fick method (De Blasi et al., 1994; M. van Beekvelt et al., 2001). Whereas strain-gauge plethysmography cannot distinguish between the various tissues of the limb, NIRS measures blood volume changes directly in the muscle of interest. The reproducibility of forearm blood flow at rest using the venous occlusion method was reasonable reliability (CVs 20.4%, 30.3%) (M. van Beekvelt et al., 2001).

This method works by using rapid occlusions (~0.5 s) to manipulate blood flow so that microvascular blood flow can be measured. Rapidly inflating a tourniquet upstream

of the NIRS probe to a sub-systolic pressure (60-80 mmHg), known as a venous occlusion (VO), which occludes venous outflow without impeding arterial inflow, thus, the subsequent increase in venous volume is proportional to arterial inflow (Van Beekvelt et al. 2001b). The slope of the [tHb] signal after venous occlusion (See figure 6) can be converted into a mBF measure of units of mL per min per 100 mL of blood (mBF (mL·min-1·100 mL-1) = [(Δt[Hb]·60)/ (([Hb]·1000)/4)·1000]/10) using a total hemoglobin count of 7.5 and 8.5 mmol·l-1for female and male participants, respectively (M. van Beekvelt et al., 2001). For more accurate calculation of mBF, the literature values can be replaced with actual individual [Hb] determined from a blood sample. After cuff inflation, there is a rapid, progressive fall in mBF (especially during exercise), likely due to an increase in venous backpressure, diminishing the arteriovenous pressure gradient and stimulating the venoarterial reflex causing vasoconstriction of precapillary vessels (Rathbun et al., 2008). As a consequence, inclusion of more than one cardiac beat has been shown to underestimate mBF (Cross & Sabapathy, 2017a).

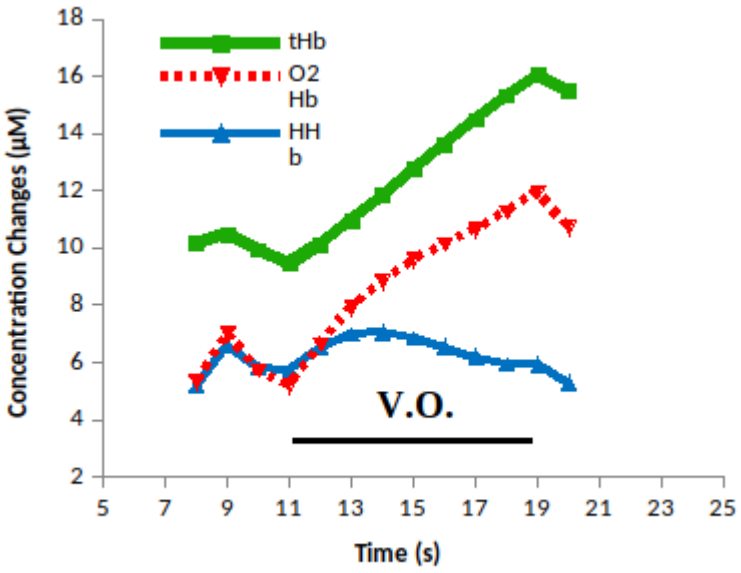

Figure 3.8. Example trace of NIRS [tHb] (green), [O_2Hb] (red), and [HHb] (blue) in response to venous occlusion (VO).

Skeletal Muscle Oxygen Consumption

The venous occlusion method can be used to determine $m\dot{V}O_2$ and mBF by applying the same technique used in conventional venous plethysmography (M. van Beekvelt et al., 2001). Since venous outflow is blocked and the increase in HHb is thought to be solely due to the O2 consumed. Venous occlusion is less inconvenient for the subject and can be repeated at short time intervals (Homma et al., 1996). However, venous occlusion is also more prone to variations in flow within the arm due to changes in blood pressure and local vasoreactivity, whereas these influences are negligible during arterial occlusion because of the closed compartment, temporarily cut off from centrally mediated variations. Van Beekvelt et al reported that $m\dot{V}O_2$ from venous occlusion appeared unreliable when repeated several times within one session (M. van Beekvelt et al., 2001). In another study, the same group we found a coefficient of variation of 30.4% (Van Beekvelt et al., 2001) for resting $m\dot{V}O_2$ during venous occlusion while the coefficient of variation was much lower (16.2%) for an arterial occlusion method.

Increasing the inflation pressure from sub-systolic to supra-systolic (250-300 mmHg), known as an arterial occlusion (AO), which restricts both venous outflow and arterial inflow, effectively arresting blood flow, is the more reliable and preferred method to measure $m\dot{V}O_2$. Under this method, tHb stays constant, and an increase of [HHb] and simultaneous decrease in [O_2Hb] as oxygen is released from hemoglobin and diffused into the surrounding muscle tissue (see figure 3.9) (M. van Beekvelt et al., 2001). Since the rate of increase in [HHb] is directly proportional to the rate of increase in [HHb] and the concentration of each is obtained independently, the signals are often subtracted from each other to get a hemoglobin difference [HbDiff] which increases signal-to-noise. The slope of the [HbDif] can then be converted into milliliters of O2 per min per 100 grams of tissue ($m\dot{V}O_2$ (mlO_2·min-1·100g-1) = abs[(Δ[HbDif/2]·60)/ (10 ·1.04) ·4] · 22.4/1000), assuming 22.4 L for the volume of gas (STPD) and 1.04 kg·L-1 for muscle density (M. van Beekvelt et al., 2001).

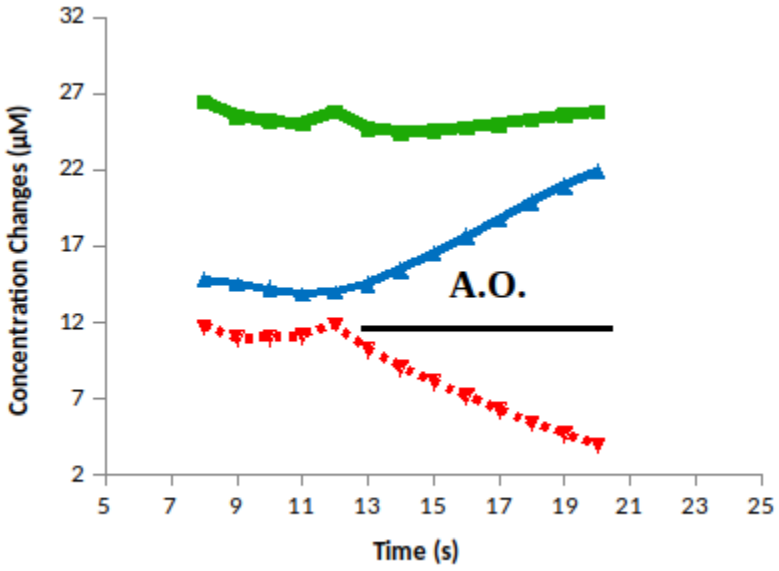

Figure 3.9. Example trace of NIRS [tHb] (green), [O2Hb] (red), and [HHb] (blue) in response to arterial occlusion (A.O.).

Arterial occlusion derived m$\dot{V}O_2$ values have been found to agree with the conventional Fick method (M. van Beekvelt et al., 2001; M. C. P. Van Beekvelt et al., 2002) and MRS (Takafumi Hamaoka et al., 1996; T Sako et al., 2001), which measures m$\dot{V}O_2$ indirectly from PCr kinetics. Van Beekvelt et al (M. Van Beekvelt et al., 2002) calculated CVs for mVO2 in the human flexor digitorum superficialis at rest and during rhythmic isometric exercise, and reported a CV of 17.6% at rest and 16.3% - 23.3% during the different intensities of exercise. Recently, Ryan et al (T.E. Ryan et al., 2012) validated a blood volume corrected technique for mVO2 (see below) measured at rest on the medial gastrocnemius and vastus lateralis. The between-day CV for mVO2 improved from 31.4% for uncorrected measurements to 2.4% for corrected measurements versus.

Ischaemic Calibration

Since cw-NIRS cannot measure absolute concentration of Hb, an ischaemic calibration must be performed to normalize the slope of the tHb signal to account for any differences in [tHb]. A simple and common method of calibrating the NIRS signal is to

use the range of muscle oxygenation caused by arterial occlusion followed by reactive hyperemia (B. Chance et al., 1992). The arterial occlusion method is based on the assumptions that an adequate duration of ischemia will result in the complete disappearance of O_2Hb, and that the reactive hyperemia after occlusion will almost completely eliminate HHb. So while O_2Hb and HHb in arbitrary units may vary between measurement sites and individuals, the occlusion calibration will account for these changes (Takafumi Hamaoka et al., 2007). Ischaemic calibrations are not required for frequency-domain or time-of-flight NIRS.

Correction for Blood-Volume Change

A number of researchers have suggested that during occlusions there is a blood volume change that could confound the slope measurements for oxygen consumption (M. van Beekvelt et al., 2001). Blood volume changes during occlusions can mask changes in the NIRS signals due to oxygen consumption. In order for the arterial occlusion method of measuring $m\dot{V}O_2$ to be valid, the NIRS signal should reflect a symmetrical change in O_2Hb and HHb, and therefore no change in tHb (tHb = O_2Hb + HHb) (T. E. Ryan et al., 2012). The dissociation of oxygen molecules from oxyhemoglobin/myoglobin, which supplies the oxygen required for oxidative phosphorylation, should be reflected in equal and opposite changes in the NIRS signals for O_2Hb and HHb.

The calculation of a blood volume correction factor (ß) is based on the assumption that during an arterial occlusion, changes in O_2Hb and HHb occur with a 1:1 ratio that represents mitochondrial oxygen consumption only (no arterial oxygen delivery or venous return of deoxygenated blood). The change in NIRS signals (both HHb and O_2Hb) during an arterial occlusion occurs due to a metabolic consumption of oxygen and a blood volume flux from the redistribution of heme between high pressure arteries/arterioles and low-pressure veins/venules. Therefore, accurate quantification of $m\dot{V}O_2$ requires either *1*) no change in blood volume, or *2*) the removal of blood volume change from the NIRS signal (i.e., $m\dot{V}O_2$ = ΔNIRS Signal - Δblood volume). To correct NIRS signals for changes in blood volume, the blood change must be proportioned into

oxygenated and deoxygenated sources. The equation below describes the calculation for this correction factor:

eq 3.6: $\beta(t)=|O_2Hb(t)| / (|O_2Hb(t)|+ |HHb(t)|$

Where β is the blood volume correction factor, *t* represents time, O2Hb is the oxygenated hemoglobin/myoglobin signal, and HHb is the deoxygenated hemoglobin/myoglobin signal. β is a nondirectional factor that represents the proportionality of the blood volume change (values range from 0 to 1).

Mitochondrial Oxidative Respiratory Capacity

Motobe and colleagues (Motobe et al., 2004) first described a method for measuring mitochondrial capacity using transient arterial occlusions following a bout of skeletal muscle contraction to deplete the ATP so the subsequent recovery curve can be measured. Electrical stimulation and voluntary exercise can be used as the bout of contraction, both methods have been shown to provide comparable results (Ryan et al., 2013), and the recovery curve not influenced by exercise intensity (Ryan et al., 2013). The signal should be corrected using ischemic calibration if a cw-NIRS device is used, (see above), and corrected for changes in blood volume (see above). Ryan et al (T. E. Ryan et al., 2012) did not find a significant influence of optode distance (sample depth) on muscle metabolic measurements, suggesting that the measurements of mitochondrial function can be compared between people with different ATT thicknesses and intramuscular fat percentages, as long as an ischemic calibration is performed. Ryan et al (T.E. Ryan et al., 2012) reported a mean CV of 21.0% for the time constant for the recovery of $m\dot{V}O_2$, improving to 10.6% when correcting for blood volume changes (see above) (T. E. Ryan et al., 2012).

Briefly, this method plots the $m\dot{V}O_2$ from using a series of 10-18 brief (5-10 seconds) arterial occlusions following exercise. The repeated arterial occlusions are fit to a mono-exponential curve and the time constant was calculated as an index of muscle

mitochondrial function, assuming the increase in O_2 consumption is due to mitochondria to replenish used ATP stores. To maximize the ability to measure the recovery of $m\dot{V}O_2$ while minimizing the discomfort to participants, the duration between arterial occlusions should begin at 5 s and extends to 20 s by the end of the repeated occlusions (i.e., 5 s for *cuffs 1–5*, 10 s for *cuffs 6–10*, 15–20 s for *cuffs 11–15*) (T. E. Ryan et al., 2012).

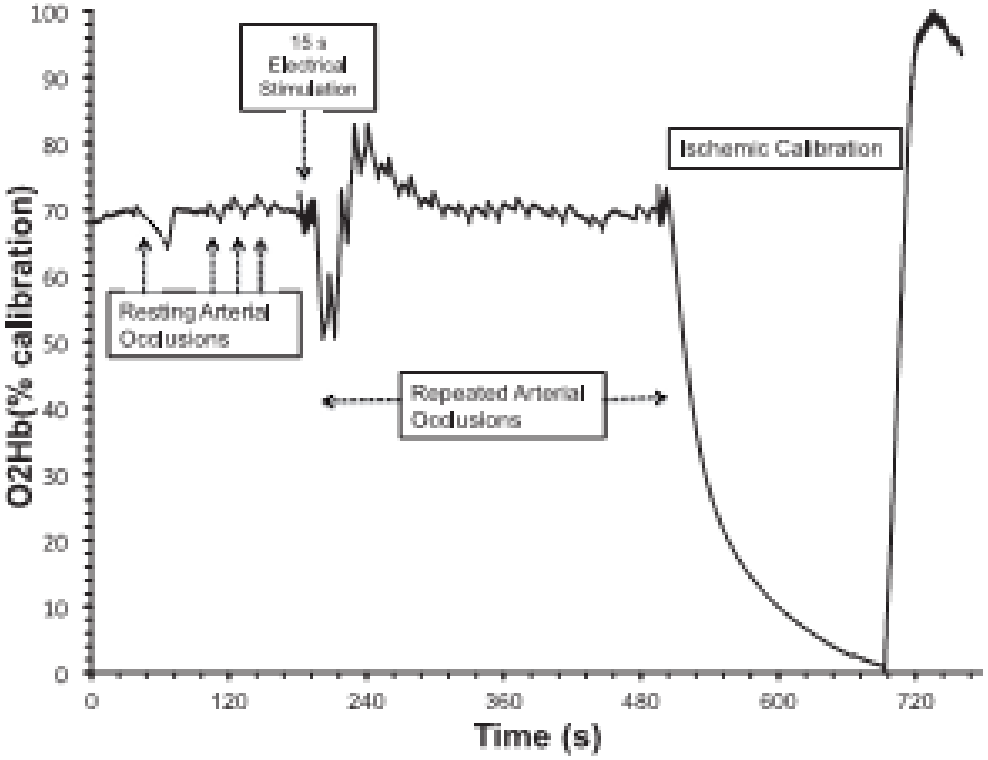

Figure 3.10. Muscle oxygenated hemoglobin/myoglobin (O_2Hb; as a percentage of the ischemic calibration) during rest, resting arterial occlusions, and a 15-s electrical stimulation exercise followed by a series of transient arterial occlusions after exercise. The final 3–5 min are an ischemic calibration used to determine a relative concentration.

Reoxygenation Rate

Another variable that can be calculated in relation to recovery from arterial occlusion or exercise is the rate of O_2Hb reoxygenation. The reoxygenation rate (ΔO_2Hb in μM·s-1) is calculated as the rate of increase in O_2Hb during the initial 3 s after cessation of occlusion and/or exercise. This variable reflects the initial inflow of O_2Hb

over a fixed time period and is, therefore, not influenced by the presence or absence of a hyperaemic response. Whereas the recovery time (or half-recovery time) includes all processes for total recovery of vascular O_2Hb, muscular O_2Mb as well as the continued oxygen consumption during recovery, the reoxygenation rate is thought to reflect the fast initial recovery rate at which primarily vascular components are restored, and is, therefore, directly related to microvascular function (M. van Beekvelt et al., 2001).

Oxygn delivery to utilization during exercise

Using whole-body oxygen consumption ($\dot{V}O_2$) during incremental exercise as a surrogate for $m\dot{V}O_2$ and skeletal muscle NIRS, the temporal change in the [HHB] (surrogate for tissue O_2 extraction) from warm-up to maximal exertion is thought to reflect the dynamic balance (expressed as a ratio to provide an index of extraction efficiency) in oxygen delivery to the perfused muscle mass (Qcap) and oxygen utilisation ($m\dot{V}O_2$) (Spencer et al., 2012).

Ferreira et al (Leonardo F. Ferreira, Townsend, et al., 2005) have proposed that the mBF response to exercise can be derived from the kinetics of whole-body oxygen uptake (VO_2) and HHb. The estimation is based on the fact that 1) during constant work rate exercise $\dot{V}O_2$ has been shown to approximate the $m\dot{V}O_2$ kinetics (T. J. Barstow et al., 1990; Rossiter et al., 1999), and 2) HHb measured by NIRS is proportional to O_2 extraction $(a\text{-}v)O_2$ (DeLorey et al., 2004; Grassi et al., 2003). By rearranging the Fick equation, the temporal characteristic of Qcap can be estimated using the formula:

eq 3.11: $Qcap(t) = m\dot{V}O_2(t) * a\text{-}vO_2(t) \propto \dot{V}O_{2p}\,(phase\ 2)(t) * [HHb](t)$

The temporal characteristics of the Qcap response is described using a three component exponential equation:

eq 3.12. $VO_2(t) = VO_2(b) + AI \cdot (1 - e^{-(t-TDI)/\tau I})$ (Phase 1)(Initial component)

$+ AP \cdot (1 - e^{-(t-TDp)/\tau p})$ (Phase 2)(Primary component)

$+ AP \cdot (1 - e^{-(t-TDp)/\tau p})$ (Phase 3)(slow component)

Where the subscripts b, I and P refer to baseline, the initial component and the primary component, respectively; *A* represents the amplitude, TD the time delay and *τ* the time constant of each exponential response and the subscript S represents the slow component.

The first 90s of HHb are modeled using an exponential function to determine the time course of muscle deoxygenation. Only minor changes in HHb after 90s, therefore, including data beyond this duration would likely lead to distortion of the initial TD and the time constant of the early, primary response of interest (Leonardo F. Ferreira, Lutjemeier, et al., 2005). Because the precise proportional contribution of arterial and venous blood to the HHb signal is unknown for skeletal muscle, the amplitude of Qcap is quantitatively uncertain. Nevertheless, the temporal characteristic of HHb, and thus Qcap, is likely to be preserved.

For direct comparison between $\dot{V}O_2$ and Qcap, the mean response time (MRT), time to approximately 63% of the primary response for Qcap is determined. For $\dot{V}O_2$ there is no time delay, so τ is used as MRT. The same procedures can be used to calculate kinetics, and MRT for direct comparison, for HHb and conduit blood flow.

Ferreira et al (Leonardo F. Ferreira, Lutjemeier, et al., 2005) compared $\dot{V}O_2$ and Qcap kinetics in response to two intensities of constant-rate cycling exercise (above and below lactate threshold (LT)). There was no significant difference between MRT (63% of the response) of Qcap and the time constant of $\dot{V}O_2$ for both intensities ($P = 0.99$), and these parameters were significantly correlated. Bucheit et al (Buchheit et al., 2009) investigated the effects of prior exercise on $\dot{V}O_2$ and Qcap kinetics during

moderate-intensity, field-based running in 14 moderately trained men, presenting with either moderately fast (16 s <TVO_2 < 30 s; MFK) or very fast $\dot{V}O_2$ kinetics (TVO_2 < 16 s; VFK) Participants completed a square-wave protocol involving two bouts of running at 90–95% LT (referred to as Mod1 and Mod2), separated by 2 min of repeated supramaximal sprinting. Findings suggest that local O_2 delivery (i.e., Qm) may be a factor contributing to the $\dot{V}O_2$ kinetic during the onset of moderate-intensity, field-based running exercise, at least in subjects exhibiting moderately fast VO_2 kinetics.

Harper et al (Harper et al., 2006) compared the kinetics of Qcap to those of femoral artery blood flow QFA and $m\dot{V}O_2$. Nine healthy subjects (6M/3F) performed 6 min bouts of two-legged knee extension exercise at @ 80%LT. Qm and $m\dot{V}O_2$ were estimated using NIRS. The overall kinetics of QFA (mean response time, MRT, 13.7±7.0 s), mVO_2 (τ, 27.8±9.0 s) and Qm (MRT, 41.4±19.0 s) were significantly (P <0.05) different from each other, suggesting that blood flow may be controlled differently at the conduit artery level than in the microcirculation. In a subsequent study (Harper et al., 2008) the same group investigated whether conduit artery blood flow during recovery from exercise provides an accurate representation of flow to the muscle capillaries. To investigate this, they: (a) examined the kinetic responses of QFA, Qcap and $m\dot{V}O_2$ following cessation of exercise two-leg dynamic knee-extension exercise at 80%LT in 9 (6M / 3F) subjects. Qcap and $m\dot{V}O_2$ were estimated using NIRS. There were no significant differences among the overall kinetics of the three parameters, suggesting the conduit artery and microcirculation blood flow become re-coupled during recovery.

Technical Limitations

Differential Pathlength Factor

Quantification of changes in [O_2Hb] and [HHb] using cw-NIRS requires incorporation of the DPF to account for scattering of the light within the tissue, which is assumed to be constant during the period of measurement. However, as mentioned earlier, since the DPF is a function of the optical properties μa and μs which have been shown to change with many factors, the DPF also is not constant. The DPF value has been shown

to change due to wavelength of light, adipose tissue thickness, skeletal muscle make-up, changing [Hb], external temperature, skin blood flow, muscular contraction, and occlusion (Koga et al., 2014; Pirovano et al., 2021). The degree to which assuming a constant DPF affects the end measures is unknown and future research needs to investigate how various factors play into a changing DPF.

In our pilot experiments using fd-NIRS conducted within this thesis (chapter 2), we found variation in μs from rest to exercise and under occlusions (figure 3.11) for both wavelengths of 690 nm and 830 nm. From resting to exercise and under arterial and venous occlusions, scattering varied by about one unit (figure 3.12), which ultimately affected the slope of the NIRS signal under both arterial and venous occlusions taken during exercise, however resting values seemed less affected (figure 3.13). Whether or not this variation affects the calculated mBF and m$\dot{V}O_2$ values significantly remains to be determined. Comparing signal responses with continuous wave NIRS devices to other NIRS technologies, as well as in vivo and in vitro methodologies, will further our understanding of the advantages and limitations of this technology.

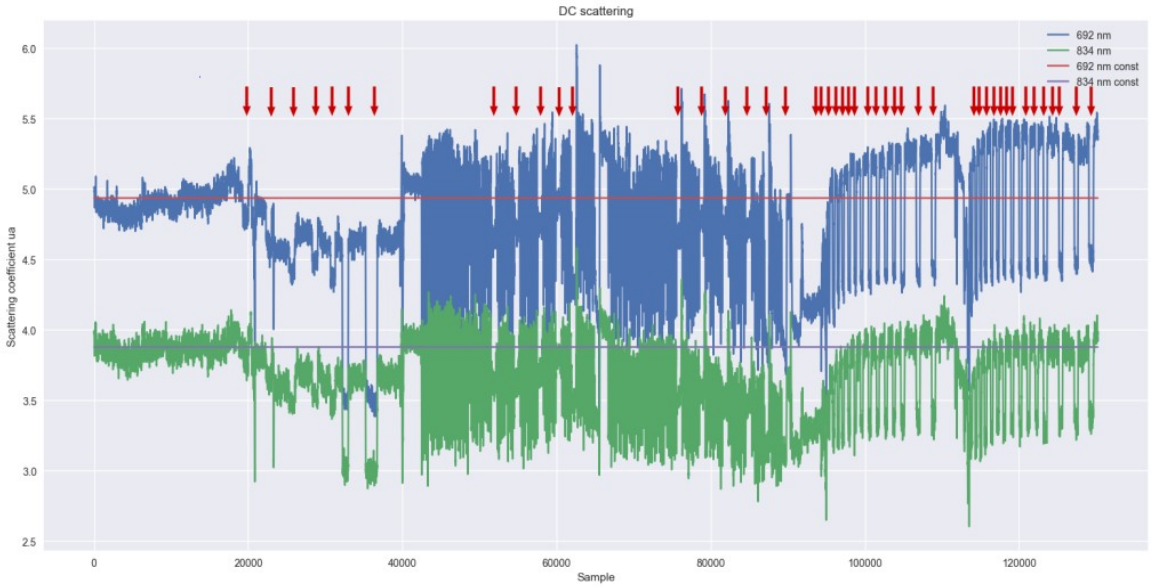

Figure 3.11. Scattering calculated from the DC signal of a fd-NIRS device for 692 and 834 nm over an entire experiment (see chapter 5). Assumed constant scattering is overlaid on the calculated scattering signal. Red arrows indicate where occlusions are occurring.

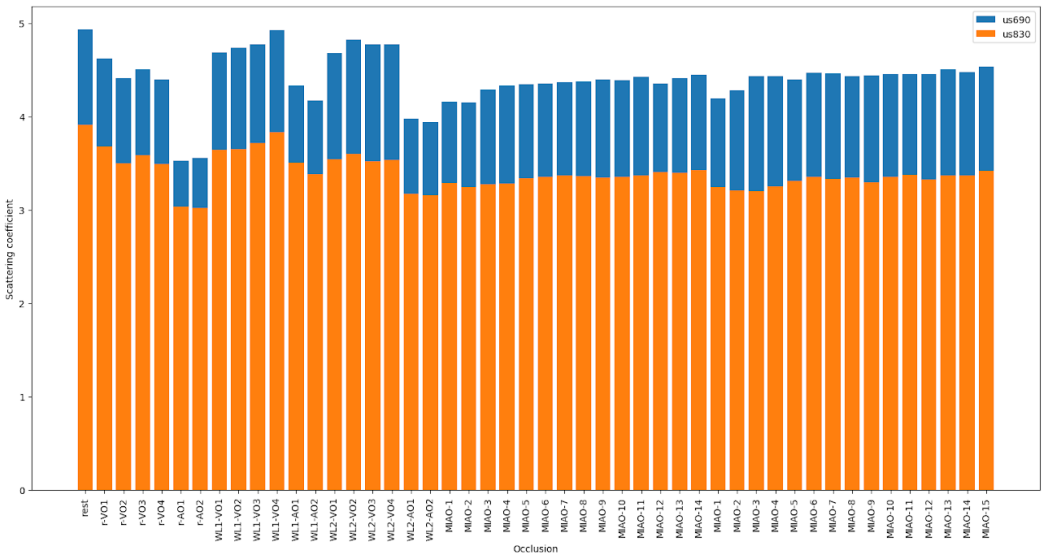

Figure 3.12. Average scattering values for 692 (blue) and 834 (orange) nm under each occlusion during experiment.

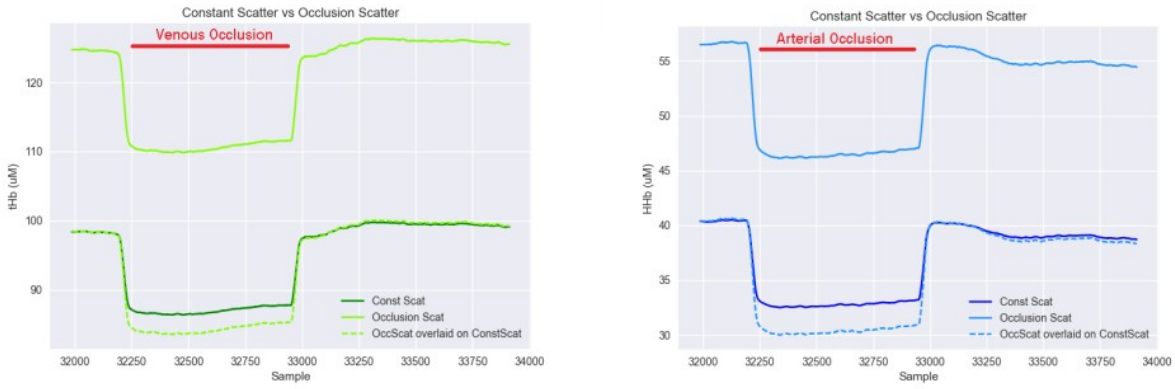

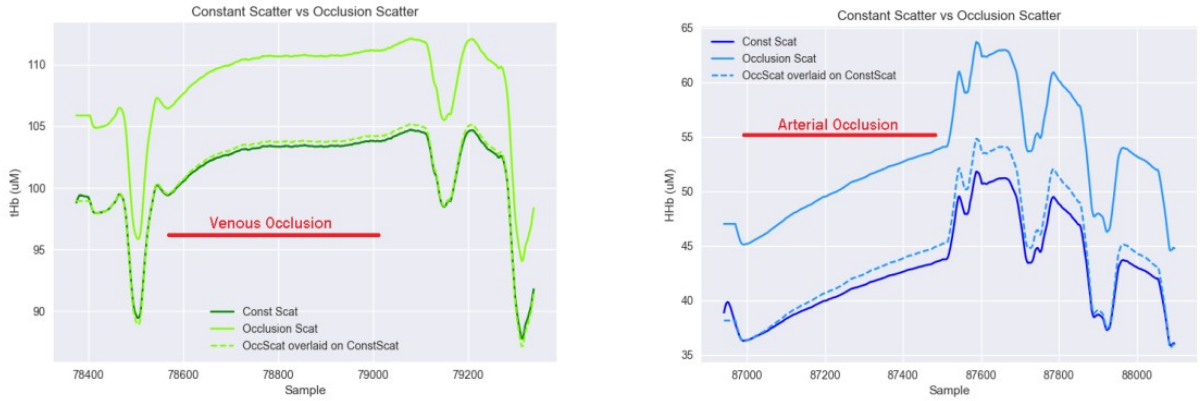

Figure 3.13. Hb parameters calculated under held-constant scattering (darker line) and occlusion specific scattering (lighter line) for venous and arterial occlusion during resting (A, B) and exercise 1 (C, D). The dashed line indicates the occlusion specific scattering overlaid over the constant scattering.

Haemoglobin vs. Myoglobin

Due to identical absorption spectra of Hb and Mb, NIRS is unable to distinguish between changes in [O_2Hb] and [O_2Mb] or in [HHb] and [HMb]. Recent studies have concluded that [Mb] contributes 60-90% to the NIRS signals coming from skeletal muscle (Davis & Barstow, 2013), however it is thought that this contribution remains constant and any changes in NIRS signals reflect changes in [Hb].

Skeletal mBF and m$\dot{V}O_2$

There are three main considerations when using NIRS to measure mBF and m$\dot{V}O_2$ at rest and during exercise:

i) The timing and magnitude of cuff inflation

ii) The need for objective and standardized analysis

iii) The assumptions and limitations of technology used.

With respect to i), specifically during exercise, VO’s can only be inflated between contractions, and therefore reflect post-exercise values and not exercise per se (Rådegran, 2017). However, immediate post-exercise mBF has been shown to increase in proportion to exercise intensity (Kagaya & Homma, 1997) and can show the mBF response to exercise (Marco Ferrari et al., 2004). That being said, to permit the recording of mBF responses that represent true exercise, and not recovery from exercise, the low-pressure occlusion must be rapid (~0.5 s) and inflate immediately upon cessation of exercise. To achieve this, a custom-built cuff inflation device was developed for the current thesis, providing robust and reliable mBF measurements (chapter 4).

With respect to ii) after cuff inflation, there is a window of linear increase in the t[Hb] signal followed by a slowing of the signal before it eventually plateaus. This is likely the result of back pressure due to blood pooling due to venous outflow occlusion while arterial inflow continues unimpeded (Cross & Sabapathy, 2017b). The higher the rate of mBF, the quicker the signal begins to plateau. A recent study by Cross et al. (Cross & Sabapathy, 2017b) suggests that measuring mBF over more than one cardiac cycle may underestimate mBF. Future work should investigate if a systematic mathematical data modeling approach could further improve the accuracy and reliability of mBF estimates at the analytical step.

With respect to iii) the technology used in cw-NIRS devices allow for simple, cost effective, portability. However, it is imperative to have a thorough understanding of the assumptions and limitations made, and how they affect signal responses under different conditions and populations. Researchers have shown cw-NIRS devices to be affected by adipose tissue thickness (Pirovano et al., 2021), skin blood flow, and contact pressure between NIRS probe and skin (T. Hamaoka et al., 2011). Correction models based on MonteCarlo simulations have been proposed to account for ATT with some success (Niwayama et al., 2000), however processing NIRS data using these models is not commonplace in NIRS studies. Careful consideration of limitations is required for standardizing conditions and achieving reliable, accurate estimates and avoiding mis-interpretation of outcomes.

NIRS in Clinical Research

There are several significant advantages NIRS offers over existing apparatuses and techniques, namely its non-invasive nature, ability to conduct measures in vivo and in real time, and its non-ionizing nature eliminating any risk of x-ray exposure. Similarly, NIRS does not produce excessive heat, unlike ultrasound, which can be a significant hazard (Fryback & Thornbury, 1991). Measuring oxygenation in human tissues can be accomplished with NIRS without the use of radioisotopes or other contrasting agents. Therefore, using NIRS as a diagnostic tool can bring about many benefits. The ability of NIRS to dynamically assess skeletal muscle hemodynamic and metabolic parameters at rest and during exercise makes it very useful for non-invasive research in clinical cohorts. NIRS has been used in experimental and clinical trials involving patients with congestive heart failure, chronic-obstructive pulmonary disorder, neuromuscular disorders, peripheral arterial disease, peripheral vascular disease, spinal cord injury, end-stage renal disease, and type 2 Diabetes Mellitus (T2D) (T. Hamaoka et al., 2011; Yamashita et al., 2013). The application of NIRS in metabolic and mitochondrial myopathies was pioneered by Bank & Chance in 1994 (Bank & Chance, 1994) who found an abnormal oxygenation during treadmill exercise in 6 patients with various metabolic myopathies and 1 patient with mitochondrial myopathy. This was followed by two other studies using NIRS in mitochondrial myopathies (Abe et al., 1997; Gellerich et al., 1998). Specifically, The half-recovery time method has been used to evaluate impaired oxidative capacity in a range of clinical populations (B. Chance et al., 1992; McCully et al., 1994, 1997, 2004; Pedersen et al., 2009).

The NIRS method offers a strong supplementary tool in cancer detection (N. S & B, 2005; Yu, 2012). Differences in the NIRS derived measures between tissues are phenomena of multiple physiological changes, which are in turn associated with such factors as vascularization, cellularity, oxygen consumption, or remodeling. Diagnostically significant results in terms of sensitivity and specificity have been seen for breast, colorectal, skin, and pancreatic cancers. An accuracy range of 72-97% has been achieved

for the various types of tumors studied (Kondepati et al., 2008). More recently NIRS has been used to detect age-related changes in skeletal muscle oxidative function using the MORC test (Susie Chung et al., 2018) and microvascular function (Rosenberry et al., 2018), with the authors claiming NIRS to be a ‘one stop shop’for assessing reactive hyperemia, neurovascular coupling, and skeletal muscle oxidative capacity.

Finally, NIRS use in brain oximetry continues to be a rapidly developing field (Marco Ferrari et al., 2004; Kuebler et al., 2016; Rooks et al., 2010). NIRS monitors have been continuously and safely employed on the many neonates who suffer from dysfunction in brain oxygenation. In addition, monitoring brain oxygenation under various activities has been used in studies of brain activation and blood flow. Unlike the gold standard functional MRI, NIRS measures [O_2Hb] and [HHb] separately, allowing for a better resolution and definition of initial hemodynamic response in neurovascular coupling measures (Chen et al., 2020). Using NIRS, researchers have made advancements in Language Mapping (Wroblewski et al., 2017), Epilepsy (Kadamati et al., 2018), and migraine research (Pourshoghi et al., 2015).

Improvements in NIRS technologies and apparatuses in the last 80 years have matured to the point where it is now a viable and effective tool in a wide range of applications. However, the vast majority of NIRS research to date are feasibility studies. Much more research, standardization, and understanding of NIRS limitations and interpretation are needed in order to become a major part of a monitoring system. Characterization of NIRS signal profiles under a wide range of males and females with varying ages, body types, and clinical conditions are necessary to understand problems associated with this technique, and to confirm its efficacy. These large-scale clinical trials are likely to occur in the coming years, and will have a large impact on research and monitoring for clinical and performance settings.

References

Abe, K., Matsuo, Y., Kadekawa, J., Inoue, S., & Yanagihara, T. (1997). Measurement of tissue oxygen consumption in patients with mitochondrial myopathy by noninvasive tissue oximetry. *Neurology*, *49*(3), 837–841. https://doi.org/10.1212/WNL.49.3.837

Bank, W., & Chance, B. (1994). An oxidative defect in metabolic myopathies: Diagnosis by noninvasive tissue oximetry. *Annals of Neurology*, *36*(6), 830–837. https://doi.org/10.1002/ana.410360606

Barstow, T. J., Lamarra, N., & Whipp, B. J. (1990). Modulation of muscle and pulmonary O2 uptakes by circulatory dynamics during exercise. *Journal of Applied Physiology*, *68*(3), 979–989. https://doi.org/10.1152/jappl.1990.68.3.979

Barstow, Thomas J. (2019). Understanding near infrared spectroscopy and its application to skeletal muscle research. In *Journal of Applied Physiology* (Vol. 126, Issue 5, pp. 1360–1376). American Physiological Society Bethesda, MD. https://doi.org/10.1152/japplphysiol.00166.2018

Bonde-Petersen, F., Henriksson, J., & Lundin, B. (1975). Blood flow in thigh muscle during bicycling exercise at varying work rates. *European Journal of Applied Physiology and Occupational Physiology 1975 34:1*, *34*(1), 191–197. https://doi.org/10.1007/BF00999932

Boone, J., Koppo, K., Barstow, T. J., & Bouckaert, J. (2009). Pattern of deoxy[Hb + Mb] during ramp cycle exercise: influence of aerobic fitness status. *European Journal of Applied Physiology*, *105*(6), 851–859. https://doi.org/10.1007/s00421-008-0969-2

Boushel, R., Langberg, H., Olesen, J., Nowak, M., Simonsen, L., Bulow, J., & Kjaer, M. (2000). Regional blood flow during exercise in humans measured by near-infrared spectroscopy and indocyanine green. *Journal of Applied Physiology*, *89*(5), 1868–1878. https://doi.org/10.1152/jappl.2000.89.5.1868

Buchheit, M., Laursen, P. B., & Ahmaidi, S. (2009). Effect of prior exercise on pulmonary O2 uptake and estimated muscle capillary blood flow kinetics during moderate-intensity field running in men. *Journal of Applied Physiology*, *107*(2), 460–470. https://doi.org/10.1152/japplphysiol.91625.2008

Chance, B., Dait, M. T., Zhang, C., Hamaoka, T., & Hagerman, F. (1992). Recovery from exercise-induced desaturation in the quadriceps muscles of elite competitive rowers.

American Journal of Physiology - Cell Physiology, *262*(3 31-3), C766–C775. https://doi.org/10.1152/ajpcell.1992.262.3.c766

Chen, W. L., Wagner, J., Heugel, N., Sugar, J., Lee, Y. W., Conant, L., ... & Whelan, H. T. (2020). Functional near-infrared spectroscopy and its clinical application in the field of neuroscience: advances and future directions. *Frontiers in Neuroscience*, *14*, 724.

Chung, Susie, et al. Near-infrared spectroscopy detects age-related differences in skeletal muscle oxidative function: promising implications for geroscience. *Physiological Reports* 6.3 (2018): e13588.

Cross, T. J., & Sabapathy, S. (2017a). The impact of venous occlusion per se on forearm muscle blood flow: implications for the near-infrared spectroscopy venous occlusion technique. *Clinical Physiology and Functional Imaging*, *37*(3), 293–298. https://doi.org/10.1111/cpf.12301

Cross, T. J., & Sabapathy, S. (2017b). The impact of venous occlusion per se on forearm muscle blood flow: implications for the near-infrared spectroscopy venous occlusion technique. *Clinical Physiology and Functional Imaging*, *37*(3), 293–298. https://doi.org/10.1111/cpf.12301

Davis, M. L., & Barstow, T. J. (2013). Estimated contribution of hemoglobin and myoglobin to near infrared spectroscopy. *Respiratory Physiology and Neurobiology*, *186*(2), 180–187. https://doi.org/10.1016/j.resp.2013.01.012

De Blasi, R. A., Ferrari, M., Natali, A., Conti, G., Mega, A., & Gasparetto, A. (1994). Noninvasive measurement of forearm blood flow and oxygen consumption by near-infrared spectroscopy. *Journal of Applied Physiology*, *76*(3), 1388–1393. https://doi.org/10.1152/jappl.1994.76.3.1388

DeLorey, D. S., Kowalchuk, J. M., & Paterson, D. H. (2004). Effects of prior heavy-intensity exercise on pulmonary O2 uptake and muscle deoxygenation kinetics in young and older adult humans. *Journal of Applied Physiology*, *97*(3), 998–1005. https://doi.org/10.1152/japplphysiol.01280.2003

Duncan, A., Meek, J. H., Clemence, M., Elwell, C. E., Tyszczuk, L., Cope, M., & Delpy, D. (1995). Optical pathlength measurements on adult head, calf and forearm and the head of the newborn infant using phase resolved optical spectroscopy. *Physics in Medicine and Biology*, *40*(2), 295–304. https://doi.org/10.1088/0031-9155/40/2/007

Essenpreis, M., Cope, M., Elwell, C. E., Arridge, S. R., Van der Zee, P., & Delpy, D. T. (1993). Wavelength dependence of the differential pathlength factor and the log slope in time-resolved tissue spectroscopy. In *Advances in Experimental Medicine and Biology* (Vol. 333, pp. 9–20). Springer, Boston, MA. https://doi.org/10.1007/978-1-4899-2468-1_2

Fantini, S. Franceschini, M. A. (2002). Frequency-domain techniques for tissue spectroscopy and imaging. In *Handbook of Optical Biomedical Diagnostics* (Vol. 1). SPIE Press.

Ferrari, M., Mottola, L., & Quaresima, V. (2004). Principles, techniques, and limitations of near infrared spectroscopy. *Canadian Journal of Applied Physiology = Revue Canadienne de Physiologie Appliquée*, *29*(4), 463–487. https://doi.org/10.1139/h04-031

Ferrari, M., Wei, Q., Carraresi, L., De Blasi, R. A., & Zaccanti, G. (1992). Time-resolved spectroscopy of the human forearm. *Journal of Photochemistry and Photobiology, B: Biology*, *16*(2), 141–153. https://doi.org/10.1016/1011-1344(92)80005-G

Ferreira, L. F., Lutjemeier, B. J., Townsend, D. K., & Barstow, T. J. (2005). Dynamics of skeletal muscle oxygenation during sequential bouts of moderate exercise. *Experimental Physiology*, *90*(3), 393–401. https://doi.org/10.1113/expphysiol.2004.029595

Ferreira, L. F., Townsend, D. K., Lutjemeier, B. J., & Barstow, T. J. (2005). Muscle capillary blood flow kinetics estimated from pulmonary O2 uptake and near-infrared spectroscopy. *Journal of Applied Physiology*, *98*(5), 1820–1828. https://doi.org/10.1152/japplphysiol.00907.2004

Fryback, D. G., & Thornbury, J. R. (1991). The efficacy of diagnostic imaging. *Medical Decision Making*, *11*(2), 88–94. https://doi.org/10.1177/0272989X9101100203

Gellerich, F. N., Mueller, T., Nioka, S., Hertel, K., Schulte-Mattler, W. J., Zierz, S., & Chance, B. (1998). NIR spectroscopic investigation of m. vastus lateralis in patients with mitochondrial myopathies as detected by respirometric investigation of mitochondrial function in skinned fibers. *Photon Propagation in Tissues III*, *3194*, 121–132. https://doi.org/10.1117/12.301043

Grassi, B., Pogliaghi, S., Rampichini, S., Quaresima, V., Ferrari, M., Marconi, C., & Cerretelli, P. (2003). Muscle oxygenation and pulmonary gas exchange kinetics

during cycling exercise on-transitions in humans. *Journal of Applied Physiology*, *95*(1), 149–158. https://doi.org/10.1152/japplphysiol.00695.2002

Habazettl, H., Athanasopoulos, D., Kuebler, W. M., Wagner, H., Roussos, C., Wagner, P. D., Ungruhe, J., Zakynthinos, S., & Vogiatzis, I. (2010). Near-infrared spectroscopy and indocyanine green derived blood flow index for noninvasive measurement of muscle perfusion during exercise. *Journal of Applied Physiology*, *108*(4), 962–967. https://doi.org/10.1152/japplphysiol.01269.2009

Hamaoka, T., McCully, K. K., Niwayama, M., & Chance, B. (2011). The use of muscle near-infrared spectroscopy in sport, health and medical sciences: recent developments. *Philosophical Transactions of the Royal Society A: Mathematical, Physical and Engineering Sciences*, *369*(1955), 4591–4604. https://doi.org/10.1098/rsta.2011.0298

Hamaoka, Takafumi, Iwane, H., Shimomitsu, T., Katsumura, T., Murase, N., Nishio, S., Osada, T., Kurosawa, Y., & Chance, B. (1996). Noninvasive measures of oxidative metabolism on working human muscles by near-infrared spectroscopy. *Journal of Applied Physiology*, *81*(3), 1410–1417. https://doi.org/10.1152/jappl.1996.81.3.1410

Hamaoka, Takafumi, McCully, K. K., Quaresima, V., Yamamoto, K., & Chance, B. (2007). Near-infrared spectroscopy/imaging for monitoring muscle oxygenation and oxidative metabolism in healthy and diseased humans. *Journal of Biomedical Optics*, *12*(6), 062105. https://doi.org/10.1117/1.2805437

Harper, A. J., Ferreira, L. F., Lutjemeier, B. J., Townsend, D. K., & Barstow, T. J. (2006). Human femoral artery and estimated muscle capillary blood flow kinetics following the onset of exercise. *Experimental Physiology*, *91*(4), 661–671. https://doi.org/10.1113/EXPPHYSIOL.2005.032904

Harper, A. J., Ferreira, L. F., Lutjemeier, B. J., Townsend, D. K., & Barstow, T. J. (2008). Matching of blood flow to metabolic rate during recovery from moderate exercise in humans. *Experimental Physiology*, *93*(10), 1118–1125. https://doi.org/10.1113/expphysiol.2008.042895

Homma, S., Eda, H., Ogasawara, S., & Kagaya, A. (1996). Near-infrared estimation of O2 supply and consumption in forearm muscles working at varying intensity. *Journal of Applied Physiology*, *80*(4), 1279–1284. https://doi.org/10.1152/jappl.1996.80.4.1279

Kadamati, J., Sugar, M. R., Sannagowdara, K., Malloy, M., Chen, W., Quirk, B., et al. (2018). Cerebral oxygen saturation and cytochrome oxidase redox state in children with epilepsy: a pilot study -MULTICHANNEL NIRS for epilepsy seizure detection, in *Proceedings of the International Congress of Clinical Neurophysiology*, Washington, DC.

Kagaya, A., & Homma, S. (1997). Brachial arterial blood flow during static handgrip exercise of short duration at varying intensities studied by a Doppler ultrasound method. *Acta Physiologica Scandinavica*, *160*(3), 257–265. https://doi.org/10.1046/j.1365-201X.1997.00158.x

Kime, R., Im, J., Moser, D., Lin, Y., Nioka, S., Katsumura, T., & Chance, B. (2005). Reduced heterogeneity of muscle deoxygenation during heavy bicycle exercise. *Medicine and Science in Sports and Exercise*, *37*(3), 412–417. https://doi.org/10.1249/01.MSS.0000155401.81284.76

Koga, S., Poole, D. C., Kondo, N., Oue, A., Ohmae, E., & Barstow, T. J. (2014). Effects of increased skin blood flow on muscle oxygenation/deoxygenation: comparison of time-resolved and continuous-wave near-infrared spectroscopy signals. *European Journal of Applied Physiology*, *115*(2), 335–343. https://doi.org/10.1007/s00421-014-3019-2

Kondepati, V. R., Heise, H. M., & Backhaus, J. (2008). Recent applications of near-infrared spectroscopy in cancer diagnosis and therapy. In *Analytical and Bioanalytical Chemistry* (Vol. 390, Issue 1, pp. 125–139). Springer. https://doi.org/10.1007/s00216-007-1651-y

Kuebler, W. M. (2008). How NIR is the future in blood flow monitoring? In *Journal of Applied Physiology* (Vol. 104, Issue 4, pp. 905–906). American Physiological Society. https://doi.org/10.1152/japplphysiol.00106.2008

Kuebler, W. M., Sckell, A., Habler, O., Kleen, M., Kuhnle, G. E. H., Welte, M., Messmer, K., & Goetz, A. E. (1998). Noninvasive Measurement of Regional Cerebral Blood Flow by Near-Infrared Spectroscopy and Indocyanine Green. *Journal of Cerebral Blood Flow & Metabolism*, *18*(4), 445–456. https://doi.org/10.1097/00004647-199804000-00013

Kuebler, W. M., Sckell, A., Habler, O., Kleen, M., Kuhnle, G. E. H., Welte, M., Messmer, K., & Goetz, A. E. (2016). Noninvasive Measurement of Regional Cerebral Blood Flow by Near-Infrared Spectroscopy and Indocyanine Green:

Http://Dx.Doi.Org/10.1097/00004647-199804000-00013, *18*(4), 445–456. https://doi.org/10.1097/00004647-199804000-00013

Laughlin, M. H., & Armstrong, R. B. (1982). Muscular blood flow distribution patterns as a function of running speed in rats. *American Journal of Physiology - Heart and Circulatory Physiology*, *12*(2). https://doi.org/10.1152/ajpheart.1982.243.2.h296

Lima, A., & Bakker, J. (2006). Noninvasive monitoring of peripheral perfusion. In *Applied Physiology in Intensive Care Medicine* (pp. 131–141). Springer, Berlin, Heidelberg. https://doi.org/10.1007/3-540-37363-2_26

Malagoni, A. M., Felisatti, M., Mandini, S., Mascoli, F., Manfredini, R., Basaglia, N., Zamboni, P., & Manfredini, F. (2010). Resting muscle oxygen consumption by near-infrared spectroscopy in peripheral arterial disease: A parameter to be considered in a clinical setting? *Angiology*, *61*(6), 530–536. https://doi.org/10.1177/0003319710362975

McCully, K. K., Halber, C., & Posner, J. D. (1994). Exercise-induced changes in oxygen saturation in the calf muscles of elderly subjects with peripheral vascular disease. *Journals of Gerontology*, *49*(3), B128–B134. https://doi.org/10.1093/geronj/49.3.B128

McCully, K. K., Landsberg, L., Suarez, M., Hofmann, M., & Posner, J. D. (1997). Identification of peripheral vascular disease in elderly subjects using optical spectroscopy. *Journals of Gerontology - Series A Biological Sciences and Medical Sciences*, *52*(3), B159–B165. https://doi.org/10.1093/gerona/52A.3.B159

McCully, K. K., Smith, S., Rajaei, S., Leigh, J. S., & Natelson, B. H. (2004). Muscle metabolism with blood flow restriction in chronic fatigue syndrome. *Journal of Applied Physiology*, *96*(3), 871–878. https://doi.org/10.1152/japplphysiol.00141.2003

Mohler, E. R., Lech, G., Supple, G. E., Wang, H., & Chance, B. (2006). Impaired exercise-induced blood volume in type 2 diabetes with or without peripheral arterial disease measured by continuous-wave near-infrared spectroscopy. *Diabetes Care*, *29*(8), 1856–1859. https://doi.org/10.2337/dc06-0182

Motobe, M., Murase, N., Osada, T., Homma, T., Ueda, C., Nagasawa, T., Kitahara, A., Ichimura, S., Kurosawa, Y., Katsumura, T., Hoshika, A., & Hamaoka, T. (2004). Noninvasive monitoring of deterioration in skeletal muscle function with forearm

cast immobilization and the prevention of deterioration. *Dynamic Medicine 2004 3:1*, *3*(1), 1–11. https://doi.org/10.1186/1476-5918-3-2

Nioka, S., Kime, R., Sunar, U., Im, J., Izzetoglu, M., Zhang, J., Alacam, B., & Chance, B. (2006). A novel method to measure regional muscle blood flow continuously using NIRS kinetics information. *Dynamic Medicine*, *5*(1), 1–13. https://doi.org/10.1186/1476-5918-5-5

Niwayama, M., Lin, L., Shao, J., Kudo, N., & Yamamoto, K. (2000). Quantitative measurement of muscle hemoglobin oxygenation using near-infrared spectroscopy with correction for the influence of a subcutaneous fat layer. *Review of Scientific Instruments*, *71*(12), 4571–4575. https://doi.org/10.1063/1.1322578

Pedersen, B. L., Bækgaard, N., & Quistorff, B. (2009). Muscle Mitochondrial Function in Patients with Type 2 Diabetes Mellitus and Peripheral Arterial Disease: Implications in Vascular Surgery. In *European Journal of Vascular and Endovascular Surgery* (Vol. 38, Issue 3, pp. 356–364). W.B. Saunders. https://doi.org/10.1016/j.ejvs.2009.04.014

Pirovano, I., Porcelli, S., Re, R., Spinelli, L., Contini, D., Marzorati, M., & Torricelli, A. (2021). Effect of adipose tissue thickness and tissue optical properties on the differential pathlength factor estimation for NIRS studies on human skeletal muscle. *Biomedical Optics Express*, *12*(1), 571. https://doi.org/10.1364/boe.412447

Pourshoghi, A., Danesh, A., Tabby, D. S., Grothusen, J., and Pourrezaei, K. (2015). Cerebral reactivity in migraine patients measured with functional near-infrared spectroscopy. *Eur. J. Med. Res.* 20:96. doi: 10.1186/s40001-015-0190-9

Rådegran, G. (2017). Limb and skeletal muscle blood flow measurements at rest and during exercise in human subjects. *Proceedings of the Nutrition Society*, *58*, 887–898. https://doi.org/10.1017/S0029665199001196

Rathbun, S., Heath, P. J., & Whitsett, T. (2008). The venoarterial reflex. In *Vascular Medicine (United Kingdom)* (Vol. 13, Issue 4, pp. 315–316). https://doi.org/10.1177/1358863X08092101

Rooks, C. R., Thom, N. J., McCully, K. K., & Dishman, R. K. (2010). Effects of incremental exercise on cerebral oxygenation measured by near-infrared spectroscopy: A systematic review. *Progress in Neurobiology*, *92*(2), 134–150. https://doi.org/10.1016/j.pneurobio.2010.06.002

Rosenberry, Ryan, Susie Chung, and Michael D. Nelson. Skeletal muscle neurovascular coupling, oxidative capacity, and microvascular function with'one stop shop'near-infrared spectroscopy. *JoVE (Journal of Visualized Experiments)* 132 (2018): e57317.

Rossiter, H. B., Ward, S. A., Doyle, V. L., Howe, F. A., Griffiths, J. R., & Whipp, B. J. (1999). Inferences from pulmonary O2 uptake with respect to intramuscular [phosphocreatine] kinetics during moderate exercise in humans. *Journal of Physiology*, *518*(3), 921–932. https://doi.org/10.1111/j.1469-7793.1999.0921p.x

Ryan, T. E., Erickson, M. L., Brizendine, J. T., Young, H.-J., & McCully, K. K. (2012). Noninvasive evaluation of skeletal muscle mitochondrial capacity with near-infrared spectroscopy: correcting for blood volume changes. *Journal of Applied Physiology*, *113*(2), 175–183. https://doi.org/10.1152/japplphysiol.00319.2012

S, N., & B, C. (2005). NIR spectroscopic detection of breast cancer. *Technology in Cancer Research & Treatment*, *4*(5), 497–512. https://doi.org/10.1177/153303460500400504

Sako, T, Hamaoka, T., Higuchi, H., Kurosawa, Y., & Katsumura, T. (2001). Validity of NIR spectroscopy for quantitatively measuring muscle oxidative metabolic rate in exercise. *Journal of Applied Physiology (Bethesda, Md. : 1985)*, *90*(1), 338–344. http://jap.physiology.org/content/90/1/338.abstract

Sako, Takayuki, Hamaoka, T., Higuchi, H., Kurosawa, Y., & Katsumura, T. (2001). Validity of NIR spectroscopy for quantitatively measuring muscle oxidative metabolic rate in exercise. *Journal of Applied Physiology*, *90*(1), 338–344. https://doi.org/10.1152/jappl.2001.90.1.338

Spencer, M. D., Murias, J. M., & Paterson, D. H. (2012). Characterizing the profile of muscle deoxygenation during ramp incremental exercise in young men. *European Journal of Applied Physiology*, *112*(9), 3349–3360. https://doi.org/10.1007/s00421-012-2323-y

Takagi, S., Kime, R., Niwayama, M., Murase, N., & Katsumura, T. (2013). Muscle oxygen saturation heterogeneity among leg muscles during ramp exercise. *Advances in Experimental Medicine and Biology*, *765*, 273–278. https://doi.org/10.1007/978-1-4614-4989-8_38

Van Beekvelt, Borghuis, M. S., Van Engelen, B. G. M., Wevers, R. A., & Colier, W. N. J. M. (2001). Adipose tissue thickness affects in vivo quantitative near-IR

spectroscopy in human skeletal muscle. *Clinical Science*, *101*, 21–28. https://pdfs.semanticscholar.org/245c/3c015e19b98384ca48a671593e9a5d0552b5.pdf

Van Beekvelt, M. C. P., Van Engelen, B. G. M., Wevers, R. A., & Colier, W. N. J. M. (2002). In vivo quantitative near-infrared spectroscopy in skeletal muscle during incremental isometric handgrip exercise. *Clinical Physiology and Functional Imaging*, *22*(3), 210–217. https://doi.org/10.1046/j.1475-097X.2002.00420.x

van Beekvelt, M., Colier, W. N. J. M., Wevers, R. O. N. A., Engelen, B. G. M. V. A. N., Wevers, R. A., & Perfor-, B. G. M. V. E. (2001). *Performance of near-infrared spectroscopy in measuring local O 2 consumption and blood flow in skeletal muscle*. 511–519.

Wagner, B. P., Gertsch, S., Ammann, R. A., & Pfenninger, J. (2003). Reproducibility of the blood flow index as noninvasive, bedside estimation of cerebral blood flow. *Intensive Care Medicine*, *29*(2), 196–200. https://doi.org/10.1007/s00134-002-1592-z

Wroblewski, G. J., Matsuo, K., Hirata, K., Matsubara, T., Harada, K., Watanabe, Y., et al. (2017). Effects of task language and second-language proficiency on the neural correlates of phonemic fluency in native Japanese speakers: a functional near-infrared spectroscopy study. *Neuroreport* 28, 884–889. doi: 10.1097/WNR.0000000000000852

Yamashita, Y., Niwayama, M., Absorption, L., & Scattering, L. (2013). *Application of Near Infrared Spectroscopy in Biomedicine*. https://doi.org/10.1007/978-1-4614-6252-1

Yu, G. (2012). Near-infrared diffuse correlation spectroscopy in cancer diagnosis and therapy monitoring. *Journal of Biomedical Optics*, *17*(1), 010901. https://doi.org/10.1117/1.jbo.17.1.010901

4 - Reliability of Muscle Blood Flow and Oxygen Consumption Response from Exercise Using Near-infrared Spectroscopy

Adam A. Lucero[1], Gifty Addae[2], Wayne Lawrence[2], Beemnet Neway[2], Daniel P. Credeur[3], James Faulkner[4], David Rowlands[1], Lee Stoner[1,5].

[1]School of Sport & Exercise, Massey University, Wellington, New Zealand, [2]School of Public Health, Harvard, Boston, MA, USA. [3]School of Kinesiology, University of Southern Mississippi, MS., USA, [4]Department of Sport and Exercise, University of Winchester, Winchester, United Kingdom. [5]Department of Exercise and Sport Science, University of North Carolina at Chapel Hill, NC, USA.

Running head: Local skeletal muscle blood flow and oxygen consumption assessment

Keywords: microvascular, hemodynamics, oxygen consumption

Subject Area: Human/environmental and exercise physiology

Correspondence:

Adam Lucero

School of Sport, Exercise, and Nutrition

Massey University

PO Box 756, Wellington

New Zealand

Adamluco1@gmail.com

ORCID: 0000-0002-2743-0209

New Findings

- What is the central question of this study?

Continuous wave near-infrared spectroscopy coupled with venous and arterial occlusions offers an economical, non-invasive alternative to measuring skeletal muscle blood flow and oxygen consumption, however its reliability during exercise has not been established.

- What is the main finding and its importance?

Continuous wave near-infrared spectroscopy devices can reliably assess local skeletal muscle blood flow and oxygen consumption from the vastus lateralis in healthy, physically active adults. The patterns of response exhibited during exercise of varying intensity agree with other published results using similar methodologies, meriting potential applications in clinical diagnosis and therapeutic assessment.

Abstract

Near-infrared spectroscopy (NIRS), coupled with rapid venous (VO) and arterial occlusions (AO) can be used to non-invasively estimate resting local skeletal muscle blood flow (mBF) and oxygen consumption ($m\dot{V}O_2$), respectively. However, the day-to-day reliability of mBF and $m\dot{V}O_2$ responses to stressors such as incremental dynamic exercise has not been established. *Purpose:* To determine the reliability of NIRS derived mBF and $m\dot{V}O_2$ response from incremental dynamic exercise. *Methods:* Measurements of mBF and $m\dot{V}O_2$ were collected in the *vastus lateralis* of twelve healthy, physically active adults [7 m and 5 f; 25 y (SD 6)] over 3 non-consecutive visits within 10 days. After 10 mins rest, participants performed 3 mins of rhythmic isotonic knee extension (1 extension/4 s) at 5, 10, 15, 20, 25, and 30% of maximal voluntary contraction (MVC), prior to 4 VOs and then 2 AOs. *Results:* mBF and $m\dot{V}O_2$ proportionally increased with intensity (0.55 to 7.68 $ml \cdot min^{-1} \cdot 100ml^{-1}$ and 0.05 to 1.86 $mlO_2 \cdot min^{-1} \cdot 100g^{-1}$, respectively) up to 25% MVC where it began to plateau at 30% MVC. Moreover, a mBF/$m\dot{V}O_2$ $m\dot{V}O$ratio of ~5 was consistent for all exercise stages. The intra-class coefficient (ICC) for mBF indicated high to very high reliability for 10-30% MVC (0.82-0.9). There was very high reliability for $m\dot{V}O_2$ across all exercise stages (ICC 0.91-0.96). *Conclusion:* NIRS can reliably assess muscle blood flow and oxygen consumption responses to low-moderate exercise, meriting potential applications in clinical diagnosis and therapeutic assessment.

Introduction

Advancements in apparatuses and methods have permitted measurement and enhanced understanding of *in vivo* local skeletal muscle blood flow (mBF) (Casey et al., 2008; Rådegran, 1999). Using techniques such as magnetic resonance imaging, contrast enhanced ultrasound, and intravascular tracer injection, the kinetics of flow through the microvasculature have been found to act differently of bulk flow through large conduit vessels (Vincent *et al.*, 2002, hence bulk flow may not accurately represent mBF (Harper et al., 2006), the site of gas exchange, nutrient, and hormone delivery. In addition, mBF can vary throughout a single muscle (Quaresima et al., 2004) and is tightly matched to metabolic demand (Joyner & Casey, 2015). Skeletal muscle oxygen consumption ($m\dot{V}O_2$) may be an important factor driving the regulation of mBF with previous evidence showing that $m\dot{V}O_2$/mBF ratio is maintained at a ratio of ~0.1 at rest and during exercise in healthy individuals (Vogiatzis et al., 2015).

Characterizing mBF and $m\dot{V}O_2$ at rest and during dynamic exercise has become an important component of skeletal muscle hemodynamic and metabolic assessment and is necessary to fully comprehend blood flow regulation and dysregulation in humans. However, assessment of mBF during exercise is limited due to apparatus design, cost, technical skill, invasiveness, and functionality with various populations (Andersen et al., 1985; Casey et al., 2008; Paunescu et al., 1999; Rådegran, 1999; Rudroff et al., 2014). There exists a need for a reliable, non-invasive, and affordable technique that can effectively investigate mBF and $m\dot{V}O_2$ kinetics in various populations and disease states under real-world exercise conditions.

Continuous wave near-infrared spectroscopy (NIRS) is an emerging, affordable, and portable technology which enables the assessment of skeletal muscle hemodynamics through relative concentrations of oxygenated and deoxygenated hemoglobin. Currently, NIRS cannot differentiate between hemoglobin and myoglobin, but its contribution to the NIR signal is suggested to be less than 20% at rest, with the main contributor being

hemoglobin (M. Ferrari et al., 2011). Given that NIRS only measures changes in vessels smaller than 1-2 mm in diameter, it is ideal for assessing local skeletal muscle microcirculation (Mancini et al., 1994). Combining NIRS with rapid venous (VO) and arterial (AO) occlusions to estimate mBF and $m\dot{V}O_2$, respectively, has been validated in the forearm (Cross & Sabapathy, 2017a; M. van Beekvelt et al., 2001), calf (Casavola et al., 2000), and VL (Quaresima et al., 2004). However, this technique has been limited to rest and maximal isometric exercise states and no protocol has been developed to reliably assess both mBF and $m\dot{V}O_2$ response to specific steady state exercise.

In pilot testing we sought to develop a protocol that would utilize these techniques to measure mBF and $m\dot{V}O_2$ at rest and during exercise at a specific intensities. Taking these measures at increasing levels of intensity would allow us to compare the pattern of increase in mBF, $m\dot{V}O_2$, and mBF/$m\dot{V}O_2$ from rest to increasing workload to the patterns seen in the literature (Joyner & Casey, 2015) to evaluate if NIRS and the occlusion technique is reflecting exercise response. Therefore the purpose of this study was to determine the reliability of continuous wave NIRS derived estimates of mBF and $m\dot{V}O_2$ in the *vastus lateralis* (VL) in response to incremental dynamic knee extension exercise.

Methods

Ethical Approval

Twelve healthy, (7 males and 5 females) physically active (>3 h of moderate intensity exercise per week) adults participated in this study (Table 1). Participants were excluded if they were smokers, reported any known cardio-metabolic disorders, or were taking medications known to affect cardiovascular function. This study was not designed to examine potential sex differences; thus, menstrual cycle status was not controlled for in female participants. Ethical approval was obtained from the institutional Human Ethics Committee (HEC: Southern A Application) and in accordance with the 1964 Helsinki declaration and its later amendments or comparable ethical standard, except for registration in a database. All participants were informed of any risks and discomfort associated with the experiments prior to providing written informed consent.

Table 4.1 Mean values and standard deviations for participant characteristics.

	Age	Height (m)	Weight (kg)	ATT (cm)	VL (cm)	VL Belly (cm)
Male	27.0	1.8	75.0	0.4	3.1	1.98
SD	7.0	0.0	9.6	0.2	0.41	0.31
Femal	21.0					
e	0	1.67	61.40	0.57	2.99	2.07
SD	4.00	0.05	0.42	0.16	0.47	0.26

Abbreviations: ATT, adipose tissue thickness; VL, vastus lateralis; VL Belly, distance from skin to the belly of the VL calculated as ATT + 1/2*VL

Experimental Procedures

Each participant was tested on four different days in a dimly-lit, temperature controlled room [(20.5 ˚C (SD 0.8)]. On visit 1, participants were familiarized with the testing protocol and their maximum voluntary contraction (MVC) for a 90˚ isometric knee extension was obtained and reported as the maximum of three trials using an isokinetic dynamometer (Biodex Medical Systems, Inc. Shirly, NY, USA). To determine the MVC, the participant was seated on the dynamometer reclined to 70° giving a 110° hip angle, and the settings were adjusted so that the axial portion of the knee aligned with the axis of rotation on the dynamometer. When assessing mBF and m$\dot{V}O_2$, the participant's dominant leg was suspended at a 'neutral' position during occlusion. The 'neutral' position consisted of a knee-joint angle of 150^0, which permitted a relaxed muscle length, thereby facilitating blood flow (Miura et al., 2004). The non-working leg was suspended in neutral position throughout.

The experimental protocol was conducted on visits 2-4. All experimental tests occurred between the hours of 7-10 am following an overnight fast, having consumed only water, refraining from caffeine and supplement intake that morning. Participants also avoided strenuous physical activity and alcohol for 24 hours prior to

experimentation. Using hemoglobin as an endogenous intravascular tracer, venous and arterial occlusions were used to estimate mBF and $m\dot{V}O_2$. Participants were seated on the dynamometer and while the NIRS probe was adhered to the skin and cuff was placed and tested for positioning and comfort. Following an additional 10 min of quiet seated rest, baseline measurements of mBF and $m\dot{V}O_2$ were assessed as the average of 4 VO and 2 AO measurements, respectively. Each occlusion was separated by 45 s of rest with VO durations of 15 s and AO durations of 15 and 30 s (Southern et al., 2014). The participant then completed 6 stages of progressive intensity (5, 10, 15, 20, 25, and 30% of MVC) 90˚ rhythmic isotonic knee extension exercise (1 extension/4 sec) on the dynamometer (Watanabe & Akima, 2011).

For each intensity, the participant exercised continuously for 3 min prior to occlusions. This time was chosen as a balance between the likelihood of achieving steady state physiology without causing fatigue. Steady state was determined through pilot trials by a stabilizing of whole body oxygen consumption. Participants were instructed to contract to full extension and then allow their leg to fall back to the starting position. Immediately after the contraction phase of the last knee extension for each measurement point, as the leg was falling, the dynamometer was locked to hold the leg in the neutral position simultaneously as the cuff was inflated for 10 s. This caused a brief pause in exercise during which the occlusion occurred. Exercise was then resumed for 45 s to maintain steady state before another measurement was collected. As with baseline measurements, mBF and $m\dot{V}O_2$ were assessed as the average of 4 VO and 2 AO measurements, respectively (see Fig. 1A). Complete occlusion during AO at rest and exercise was verified with Doppler ultrasound in the femoral artery during pilot trials and confirmed during testing by the cessation of the pulsatile motion in the tHb signal. An index of perfusion change and tissue saturation index were also assessed during each stage.

Near-infrared Spectroscopy

A continuous wave NIRS device (PortaLite, Artinis Medical Systems BV, the Netherlands) emitted wavelengths of 760 and 850 nm to detect relative changes in concentrations of oxygenated hemoglobin [HbO_2] and deoxygenated hemoglobin [HHb], respectively, as well as total blood volume ([tHb] = [O_2Hb] + [HHb]). Absolute hemoglobin concentrations can be estimated, however, in this study only relative changes are used in calculations. Wavelengths were emitted from LEDs with an inter-optode distances of 3.5 cm, allowing for theoretical penetration distances of 1.75 cm (B. Chance et al., 1992). A differential path-length factor of 4.0 was used to correct for photon scattering within the tissue, and data were collected at 10 Hz (Oxysoft, Artinis Medical Systems BV, the Netherlands). The NIRS probe was securely adhered to the skin parallel to the muscle fibers, about two-thirds from the top of the *vastus lateralis* over the muscle belly. A custom-made cover shielded the probe from ambient light while allowing it to move with the skin during contractions minimizing changes in contact pressure (T. Hamaoka et al., 2011). The thickness of the muscle at this location, along with adipose tissue thickness, was determined using B-mode ultrasound (Terason, United Medical Instruments Inc., San Jose, CA, USA).

Local Skeletal Muscle Blood Flow

Estimates of mBF were assessed as the [ΔtHb] signal during VO, analyzed using simple linear regression as previously described (Van Beekvelt *et al.*, 2001; Cross & Sabapathy, 2015). Briefly, a tourniquet (Hokanson SC 10D, D. E. Hokanson, Inc., Bellevue, WA, USA) was placed as high as possible around the proximal thigh, minimizing patient discomfort and avoiding artefact motion in the NIRS signal. The tourniquet was rapidly (~0.5 s) inflated to a subdiastolic pressure (60-80 mmHg) occluding venous outflow without impeding arterial inflow, thus, causing venous volume to increase at a rate proportional to arterial inflow (M. van Beekvelt et al., 2001). After cuff inflation, there is a rapid, progressive fall in the rate of [ΔtHb] (especially during exercise), likely due to an increase in venous backpressure, diminishing the arteriovenous pressure gradient and stimulating the venoarterial reflex causing vasoconstriction of

precapillary vessels (Rathbun et al., 2008). As a consequence, inclusion of more than one cardiac beat has been shown to underestimate mBF (Cross & Sabapathy, 2017a) (see Fig. 1B, C). Therefore, estimates of mBF were over the first cardiac cycle, defined using the pulsatile motion of the [tHb] signal. The slope of the [tHb] signal for each VO was averaged and converted into units of mL per min per 100 mL of blood (mBF ($mL \cdot min^{-1} \cdot 100\ mL^{-1}$) = $1/C \cdot [\Delta tHb]/\Delta t$) where $[\Delta tHb]/\Delta t$ is the average rate of tHb increase under VO (μM of $Hb \cdot s^{-1}$) and C is hemoglobin concentration in the blood, for which we assumed a value of 7.5 and 8.5 $mmol \cdot L^{-1}$for female and male participants, respectively (M. van Beekvelt et al., 2001). The molecular mass of hemoglobin (64.458 $g \cdot mol^{-1}$) and the ratio between hemoglobin and O_2 molecules (1:4) were accounted for.

Skeletal Muscle Oxygen Consumption

Estimates of $m\dot{V}O_2$ were calculated as the rate of change in the Hb difference signal ($[\Delta HbDif] = [\Delta HbO_2] - [\Delta HHb]$) during arterial occlusion (see Fig. 1D,E), analyzed using simple linear regression as previously described (T. E. Ryan et al., 2012). Briefly, the tourniquet was rapidly (~0.5 s) inflated to a supra-systolic pressure (250-300 mmHg) to occlude both venous outflow and arterial inflow, completely arresting blood flow, resulting in an increase of [HHb] and simultaneous decrease in [HbO2] as oxygen is released from hemoglobin and consumed by the surrounding muscle tissue (M. van Beekvelt et al., 2001). After correcting for blood-volume changes (T. E. Ryan et al., 2012), the slope of the [HbDif] signal for both AOs was averaged and converted into milliliters of O_2 per min per 100 grams of tissue ($m\dot{V}O_2$ ($mlO_2 \cdot min^{-1} \cdot 100g^{-1}$) = $abs[([\Delta HbDif/2] \cdot 60)/ (10 \cdot 1.04) \cdot 4] \cdot 22.4/1000$), assuming 22.4 L for the volume of gas (STPD) and 1.04 $kg \cdot L^{-1}$ for muscle density (M. van Beekvelt et al., 2001).

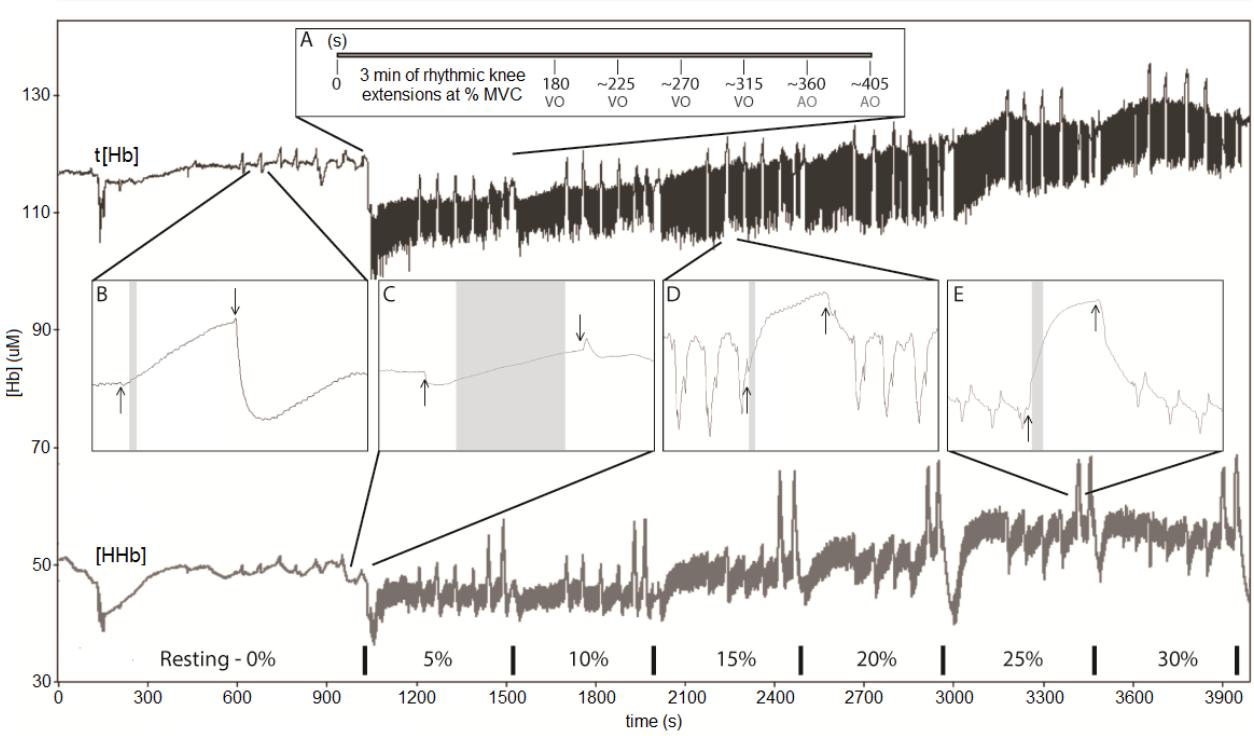

Figure 4.1. *Experimental Protocol.* Representative example of NIRS signals (µM) collected from visits 2-4 showing the raw [tHb] (dark grey) and [HHb] (light grey) traces. The horizontal black lines above the x-axis denote the start and end of each intensity level (%MVC). Panel A shows the timeline (s) for one exercise intensity (5% MVC). After 3 min of knee extension exercise the cuff was rapidly inflated for 5-10 s for 4 venous occlusions (VO; 70-80 mmHg) and 2 arterial occlusions (AO; 250-300 mmHg) with 45 s of knee-extension exercise between occlusions for the assessment of mBF and $m\dot{V}O_2$, respectively. Zoom panels B and C show [tHb] and [HHb] signals for VO and AO, respectively, during rest. Zoom panels D and E show [tHb] and [HHb] signals for VO and AO, respectively, during exercise with three knee extensions on either side of occlusion. Black arrows denote the inflation and deflation of occlusion and the shaded gray area denotes the linear increase used in the assessment of mBF or $m\dot{V}O_2$

Local Skeletal Muscle Perfusion Change and Tissue Saturation Index

An estimate of relative local skeletal muscle perfusion was calculated as the relative average blood volume ([tHb] signal) for a given period. The [tHb] signal has been said to reflect microvascular blood-volume (Ijichi et al., 2005) which reflects local O_2 diffusing capacity (Groebe & Thews, 1990). Since the [tHb] signal measures absolute

changes from a set baseline, the resting value was set to 0 and the workload values were calculated as μM increases from rest. The tissue saturation index (TSI%) was calculated with manufacturer software using a spatially-resolved spectroscopy approach. The TSI% signal was averaged over the same period used for perfusion analysis.

After resting measurements of mBF and $m\dot{V}O_2$ were taken, the participant's leg was lowered to 90˚ knee-joint angle in preparation for the exercise protocol. The participant then continued to rest to allow the [tHb] signal to stabilize for 30 s to assess resting perfusion and TSI%. Estimated relative perfusion and TSI% were assessed as the average [tHb] and TSI% signal during the 2 s rest period between knee extensions (when the leg was relaxed at 90˚) of the last 8 extensions before the first VO.

Electromyography, Whole Body Oxygen Consumption & Heart Rate

To verify the exercise model elicited the desired metabolic increases, in a separate testing session surface electromyography (EMG), whole body oxygen consumption ($\dot{V}O_2$), and heart rate (HR) were measured in a subset of individuals (N=7). The EMG electrode (Telemyo DTS, Noraxon Inc., Scottsdale, AZ, USA) was placed over the NIRS probe location. To normalize the EMG activity signal prior to beginning the exercise protocol, the participant performed 3 MVCs and the peak forces were averaged and set to 100% activation. Integrated raw EMG signals were analyzed according to standard methods for knee extension exercise (Alkner et al., 2000). To measure $\dot{V}O_2$, a breath-by-breath automatic gas exchange system (Vmax Spectra 29c, Sensormedics Corporation, Yorba Linda, CA, USA) was used, and HR was monitored using a wireless chest strap telemetry system (Polar Electro T31, Kempele, Finland).

Resting and exercise stage protocols were conducted like visits 2-4. However, during exercise after the first three minutes of knee extensions, the leg was not rested as occlusions were not required for assessing parameters. Baseline measures were assessed as the average value for the last minute of the resting period. Exercise parameters were assessed during the fourth minute of exercise. Exercise EMG activity was assessed as the average rectified maximum activity for the last eight contractions for each stage. Exercise

$\dot{V}O_2$ and HR data were expressed as the average value for the last 60 seconds (fourth minute) of each stage.

Statistical Analysis

Statistical analyses were performed using Statistical Package for Social Sciences version 21 (SPSS, Inc., Chicago, Illinois). All data are reported as means with 90% confidence intervals, unless otherwise specified. The NIRS parameters were analyzed to test the effects of intensity and visit order using a two-way repeated measures analysis of variance (ANOVA). Mechanistic inference testing for substantial differences between intensities were calculated from a published spreadsheet using generated p-values (W. G. Hopkins, 2015), with likelihood thresholds of 50% (possible), 75% (likely), 95% (very likely), and 99% (most likely) chance of substantial change. Values for mBF as a function of $m\dot{V}O_2$ were assessed for linearity using linear regression to test goodness of fit as a coefficient of determination (R^2). Likelihoods for correlations using magnitude based inference was used to test individual parameters against exercise intensity and to each other using 95% confidence limits with 0.2 as the threshold for smallest magnitude threshold for differences or change scores (Will G. Hopkins, 2007).

Reliability statistics were calculated with the log transformed raw data using published spreadsheets (W. G. Hopkins, 2015) as described previously (William G. Hopkins et al., 2009). The typical error (i.e. standard error of measurement) defined as $SD/\sqrt{2}$ where *SD* is the standard deviation of the change score for all participants. Test-retest reliability statistics calculated include the intra-class correlation coefficient (ICC), standardized typical error (STE), percentage coefficient of variation (%CV) and percentage of the smallest effect (%SE). The ICC gives visit to visit reproducibility for a given intensity and was calculated as $1\text{-}sd^2/SD_b^2$ where the *sd* is the typical error and SD_b the mean between-participant standard deviation. Thresholds of 0.20 (low), 0.50 (moderate), 0.75 (high), 0.90 (very high), and 0.99 (nearly perfect) reliability for sample populations were used. The STE gives the random error in the calibrated value and is interpreted using thresholds of 0.1 (small), 0.3 (moderate), 0.6 (large), 1 (very large), and

2 (extremely large) (William G. Hopkins et al., 2009). The typical error as a percentage is shown as CV (%). The SE (%) represents the percentage above or below the measured value required for the smallest worthwhile effect given by $0.2 \cdot SD_p$ where the SD_p is the pure between-subject standard deviation calculated as above.

Results

Mean values and inferences for mBF and $m\dot{V}O_2$, relative perfusion, and TSI% are shown in Fig. 2. Mean values for mBF and $m\dot{V}O_2$ were most likely (i.e., 99% chance) substantially greater than resting across all intensities. For both mBF and $m\dot{V}O_2$, mean values for all intensities were substantially greater than the previous intensity except for 30% MVC. Mean mBF correlated linearly with exercise intensity, and was directly proportional to $m\dot{V}O_2$ ($y = 3.75x + 0.5384$; $R2 = 0.8195 - 0.9814$ (Fig. 3A). The mean $m\dot{V}O_2$/mBF ratio was 0.045 at rest and varied from 0.104-0.132 for all exercise stages (Fig. 3B). Mean values for perfusion change from rest at 15-30% MVC were substantially greater to resting, however, only trivial increases to the previous intensity were seen in 10-30% MVC. Mean values for TSI% at 5, 10, and 30% MVC were substantially less than resting. Mean values for EMG, $\dot{V}O_2$, and HR during exercise increased substantially from resting (Fig. 4). For all three parameters, no substantial increase was observed at 10 and 25% MVC from the previous exercise intensity. There was a likely substantial increase in HR at 30% MVC, but not in EMG and $\dot{V}O_2$. All seven parameters were most likely substantially correlated with % MVC and to each other (99.7%-100% likelihood). No visit order effect was observed for all NIRS parameters.

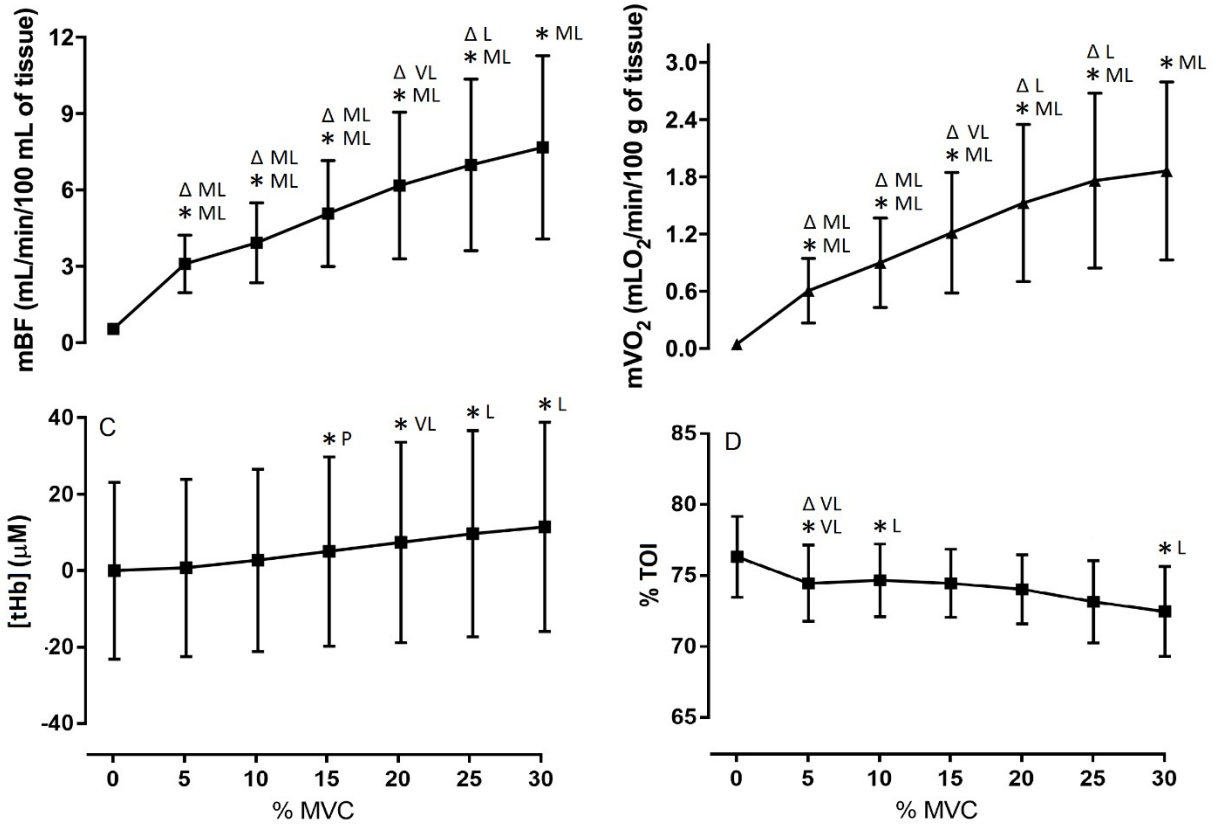

Figure 4.2. The responses of all NIRS parameters over all exercise intensities. to increasing exercise intensity. Panels show (A) mBF, (B) m$\dot{V}O_2$, (C) relative perfusion, and (D) TSI%. Data are means and bars standard deviation. Workloads substantially greater (smallest effect) than resting or the previous workload are denoted with an asterisk (*) or a triangle (Δ), respectively. Statistical likelihoods are given next to the symbol as possible (P, 50-74.9%), likely (L, 75-94.9%), very likely (VL, 95-99.49%) and most likely (ML, 99.5-100%)

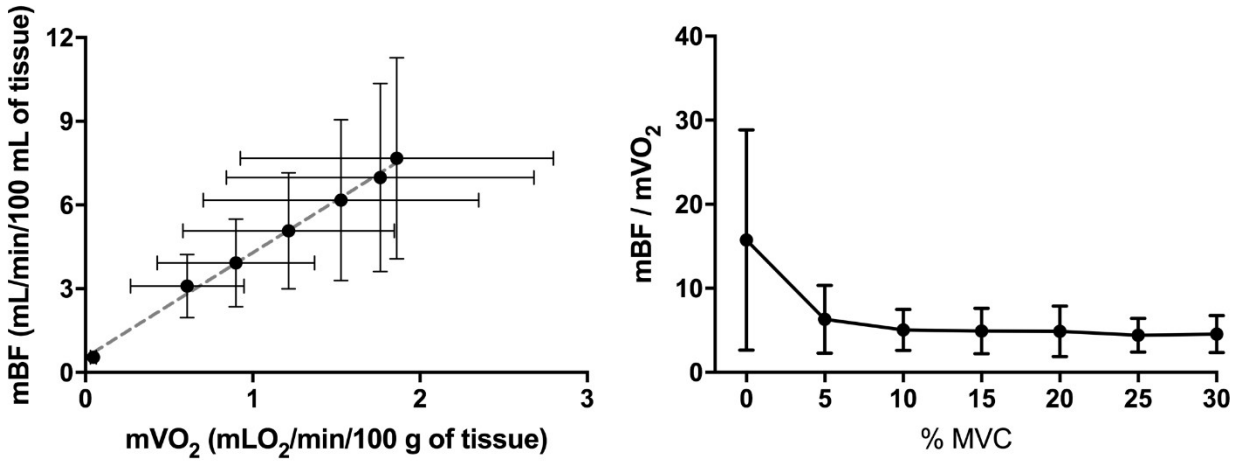

Figure 4.3. The relationship between $m\dot{V}O_2$ and mBF over all exercise intensities. (A) mBF as a function of $m\dot{V}O_2$ with the regression line denoted by the dashed grey line given by the equation $y = 8.071x + 0.5482$; $R^2 = 0.9914$. (B) $m\dot{V}O_2$/mBF ratio as a function of exercise intensity. Data are means and bars standard deviation.

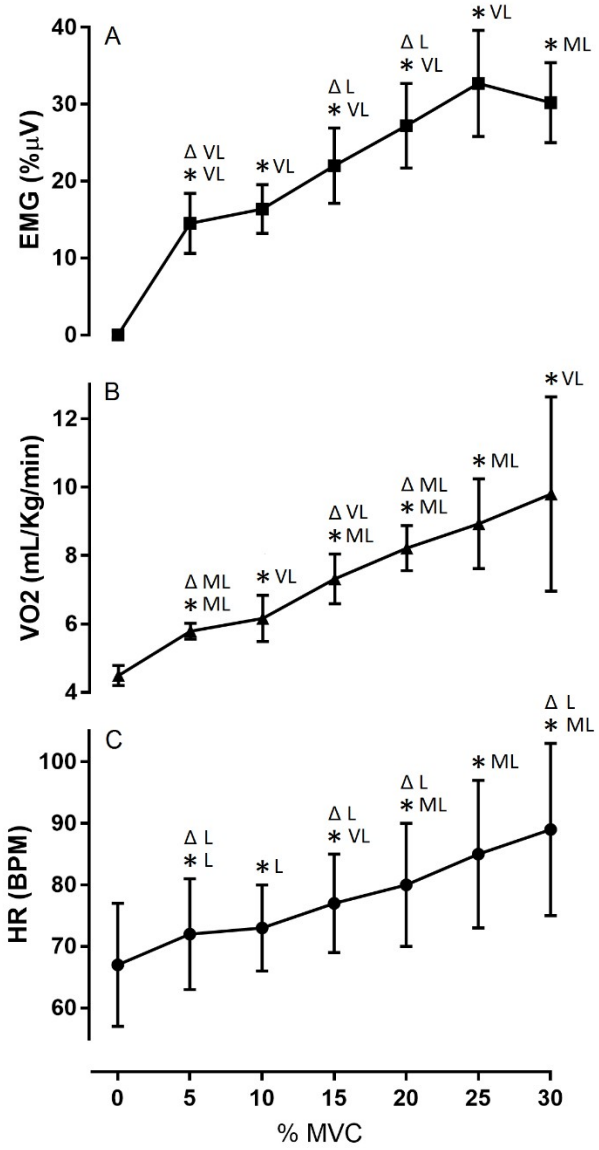

Figure 4.4. Responses of EMG (top), $\dot{V}O_2$ (middle), and HR (bottom) to increasing exercise intensity. Data are means and bars standard deviation. Workloads substantially greater (smallest effect) than resting or the previous workload are denoted with an asterisk (*) or a triangle (Δ), respectively. Chances are given next to symbol as possible (P, 50-74.9%), likely (L, 75-94.9%), very likely (VL, 95-99.49%) and most likely (ML, 99.5-100%)

Reproducibility for all NIRS parameters is shown in Table 2 as statistic value, with upper and lower 90% confidence limits available as supporting information. For

mBF, the ICC indicated moderate reliability (0.69) at 5% MVC, but high reliability at rest and across all other intensities (0.82-0.89) with very high reliability at 25% MVC (0.9). The STE was moderate for rest and all exercise stages (0.35-0.59). It was lowest (best) for 20 and 25% MVC (0.37 and 0.35, respectively) and highest (worst) for 5 % MVC (0.59). The CV varied from 20.2 – 31% and was lowest (best) for 10-25% MVC (20.9-24.8%). The SE varied from 5.5-10.2%. For $m\dot{V}O_2$ the ICC indicated moderate reliability at rest (0.58) and very high reliability across all exercise stages (0.91-0.96). The STE was moderate at rest (0.58) and 5-20% MVC (0.31-0.34), and low (best) for both 25 and 30% MVC (0.22). The CV was 50.4% at rest, 20-22.6% for 5-20% MVC, and 13.5-14.0% for 25-30% MVC. The SE varied from 9.2-13.3% for all exercise stages.

Table 4.2. Reliability of mBF and $m\dot{V}O_2$ for rest and all exercise intensities.

	Rest	5%	10%	15%	20%	25%	30%
				mBF			
ICC	0.83	0.69	0.86	0.82	0.89	0.90	0.80
STE	0.45	0.59	0.41	0.46	0.37	0.35	0.48
CV (%)	14.6	31.0	21.4	24.8	20.9	20.2	30.4
SE (%)	5.5	7.7	8.9	9.0	10.0	10.2	10.1
				$m\dot{V}O_2$			
ICC	0.58	0.92	0.93	0.91	0.91	0.96	0.96
STE	0.68	0.31	0.30	0.34	0.33	0.22	0.22
CV (%)	50.4	20.5	20.0	22.6	24.2	14.0	13.5
SE (%)	9.2	12.3	12.1	12.0	13.3	12.2	11.9
				Relative Perfusion – [tHb]			
ICC	0.98	0.98	0.98	0.98	0.98	0.98	0.98
STE	0.18	0.16	0.17	0.17	0.15	0.17	0.16
CV (%)	4.0	3.7	4.0	4.1	3.8	4.1	3.8
SE (%)	4.5	4.6	4.6	4.7	4.9	4.9	4.9
				%TOI			

ICC	0.71	0.87	0.86	0.75	0.70	0.76	0.78
STE	0.57	0.40	0.41	0.53	0.58	0.53	0.51
CV (%)	2.4	1.6	1.5	2.1	2.3	2.4	2.6
SE (%)	0.7	0.7	0.7	0.6	0.6	0.8	0.9

Abbreviations: ICC, intra-class correlation coefficient; STE, standardized typical error. The STE magnitude thresholds are 0.1, 0.3, 0.6, 1, and 2 for small, moderate, large, very large, and extremely large; %CV, coefficient of variation; %SE, Percentage for smallest effect.

Discussion

The purpose of this study was to determine the reliability of continuous wave NIRS derived estimates of mBF and m$\dot{V}O_2$ in the *vastus lateralis* during short intermittent pauses from dynamic exercise. Using occlusion methodology (i.e. AO and VO) combined with isotonic knee extensions at specific intensities, according to the ICC values, the current study found high to very high reliability from 10-30% MVC, and moderate reliability at 5% MVC. Comparing absolute estimates of mBF and m$\dot{V}O_2$ with previously reported values is difficult due to differences in exercise modality, muscle groups measured, and units used to express values. However, patterns of response in mBF and m$\dot{V}O_2$ to exercise intensity are in agreement with established results (Joyner & Casey, 2015), and the m$\dot{V}O_2$/mBF ratio is also consistent with previous findings (Vogiatzis et al., 2015). Compared to other techniques, NIRS offers reliable, non-invasive application to real-world exercise modalities, and can be used on a wide variety of clinical populations (Paunescu et al., 1999; Rådegran, 1999).

The relationship between mBF and mVO2 was consistent for all exercise intensities and within range of published mBF/m$\dot{V}$O2 ratios of ~5 (Kalliokoski et al., 2005; Richardson et al., 1995; Whipp & Ward, 1982), showing a tight match of mBF to m$\dot{V}O_2$ during steady-state exercise. For both mBF and m$\dot{V}O_2$, no substantial increase was seen from 25-30% MVC, as well as 20-30% MVC for EMG activity and $\dot{V}O_2$. Taken together, the current results suggest that maximal recruitment and/or fatigue developed in

the primary *vastus lateralis* muscle fibers rprompting recruitment of accessory and additional muscle fibers in the quadriceps to sustain contractions (Komi & Tesch, 1979; Vøllestad, 1997). In support, many participants [N=8] appeared to have greater *rectus femoris* use at the higher intensities. Therefore, to obtain more accurate steady state estimates of mBF and $m\dot{V}O_2$ at specific intensities, it is recommended that in future trials, only 2 workloads between 10-25% MVC be tested in succession with adequate rest in between, depending on the population being tested. For example, 15 and 25% MVC may be ideal for physically active to athletic populations, but future trials will be needed to characterize intensities that can be maintained in clinical populations while achieving reproducible results.

Comparing the absolute estimates of mBF to those from other studies is difficult because a) mBF is heterogeneous across the muscle and can vary widely depending on the region measured, b) exercise modality used, and c) the units used to report mBF. Using a similar VO technique with a frequency-domain NIRS device, (Quaresima et al., 2004) estimated blood flow to increase from 0.3-0.5 $mL \cdot min^{-1} \cdot 100\ mL^{-1}$ to 1.4-2.1 $mL \cdot min^{-1} \cdot 100\ mL^{-1}$ across the *vastus lateralis* from rest to maximal isometric exercise. Although the exercise modality differs to the current study, the resting value is within range of the current study and the exercise value for maximal isometric contraction is lower. Comparing indocyanine green injection and ^{133}Xe, (Boushel et al., 2000) measured regional mBF in the calf during incremental plantar-flexion exercise to 9 watts, and found similar mBF values between the techniques concluding that mBF rose from about 2.2 $mL \cdot min^{-1} \cdot 100\ mL^{-1}$ to 15.1 $mL \cdot min^{-1} \cdot 100\ mL^{-1}$. Although these estimates are larger than those reported in the current study, the muscle group and exercise modality differ. However, like the current study, the authors found increases in mBF to be proportional to workload.

Using thermodilution and dynamic knee extension exercise at 60 rpm to peak power, Rådegran et. al. (Rådegran, 1999) found peak knee extensor mBF and $m\dot{V}O_2$ to be $246.2 \pm 24.2\ mL \cdot min^{-1} \cdot 100\ g^{-1}$ and $34.9 \pm 3.7\ mL \cdot min^{-1} \cdot 100\ g^{-1}$, respectively, which is

substantially higher than the current study. However, the exercise modalities differed significantly, in that the current study only went to 30% MVC, allowed for greater rest between contractions, and the force was only exerted at 90˚ rather than throughout extension, which would isolate a lower mass of contracting muscle (Joyner & Casey, 2015). Moreover, the current study measured one region within one knee extensor, the *vastus lateralis*, which has been shown exhibit ~57% mBF heterogeneity and to have ~20% less blood flow than the *vastus intermedius* during knee extension exercise (Rudroff et al., 2014). In the previous study, using positron emission tomography, the authors found mBF in the *vastus lateralis* to be 6.21 ± 1.96 and 9.77 ± 3.82 $mL \cdot min^{-1} \cdot 100\ g^{-1}$ at 2 and 12 min, respectively, of sustained isometric contraction at 25% MVC in young men, which is within range of the current study. In addition, EMG activity was also within range of the current study.

Limitations and Future Direction

Future application of the current protocol should consider a) timing of cuff inflation, b) addition of ECG monitoring and individual blood sampling, and c) concurrent monitoring of additional non-invasive measurements for assessing the entire oxygen cascade. Firstly, since VO can only be inflated between contractions, the resulting tHb slope reflects post-contraction values and not exercise *per se* (Rådegran, 1999). However, immediate post-exercise mBF has been shown to increase in proportion to exercise intensity (Kagaya & Homma, 1997) and reflect the mBF response to exercise (Quaresima et al., 2004). Therefore, the low-pressure occlusion must be rapid (~0.5 s) and inflate immediately upon cessation of exercise. Secondly, the current study was not able to collect ECG or individual hemoglobin concentrations, however it is encouraged as time aligning the VO to cardiac cycles may increase reproducibility and individually sampled hemoglobin concentrations will enhance the accuracy of absolute mBF rates. In addition, synchronizing cuff inflation with ECG trace to occur at the same point within the cardiac cycle may standardize the attenuation effects of the VO on mBF. Lastly, concurrent non-invasive monitoring of additional parameters to assess the entire hemodynamic cascade may prove useful for mechanistic and pathological determinants.

Ensuring high reproducibility of NIRS derived measurements within a single subject is a critical step in the use of NIRS for clinical diagnosis. Our results have characterized reliability for estimating relative changes immediate post exercise mBF and $m\dot{V}O_2$ across a wide range of prevailing arterial inflows and O_2 consumption rates that can be used to estimate sample size and incorporated into future experimental design. Using a standard protocol to compare measurements of mBF and $m\dot{V}O_2$ during exercise in trained, untrained, and diseased populations will enhance our understanding of muscle physiology, mBF regulation, and disease pathogenesis. More research is required to understand the effects of exercise and muscle contraction on: a) the NIR light pathlength, b) changes in blood hemoglobin during exercise and its affect on mBF measures, c) and the contribution of myoglobin to the NIR signal at various exercise stages for the determination of absolute values of mBF and m$\dot{V}$O2. Future research should compare reliability and signal responses of continuous wave NIRS devices to other NIRS technologies, as well as assess the reliability and validity of using occlusions during varying exercise modalities and intensities compared to other leading techniques (Duerschmied et al., 2006; Krix et al., 2005; Partovi et al., 2012; Pollak et al., 2012; Rådegran, 1999) .

Conclusion

In summary, continuous wave NIRS devices can reliably assess mBF and $m\dot{V}O_2$ within the microvasculature of the *vastus lateralis* during intermittent pauses from dynamic exercise in healthy, physically active adults. The relative patterns of response for mBF, and $m\dot{V}O_2$ during incremental exercise and mBF/$m\dot{V}O_2$ ratio agree with other published results using similar methodologies. Using NIRS to assess and characterize local parameters of skeletal muscle hemodynamics and metabolism during rest and exercise opens new research paradigms for the investigation of mBF regulation in health and disease with potential applications in clinical diagnosis and therapeutic assessment.

References

Alkner, B. A., Tesch, P. A., & Berg, H. E. (2000). Quadriceps EMG/force relationship in knee extension and leg press. *Medicine and Science in Sports and Exercise*, *32*(2), 459–463. https://doi.org/10.1097/00005768-200002000-00030

Andersen, P., Adams, R. P., Sjøgaard, G., Thorboe, A., & Saltin, B. (1985). Dynamic knee extension as model for study of isolated exercising muscle in humans. *Journal of Applied Physiology*, *59*(5), 1647–1653. https://doi.org/10.1152/jappl.1985.59.5.1647

Boushel, R., Langberg, H., Olesen, J., Nowak, M., Simonsen, L., Bulow, J., & Kjaer, M. (2000). Regional blood flow during exercise in humans measured by near-infrared spectroscopy and indocyanine green. *Journal of Applied Physiology*, *89*(5), 1868–1878. https://doi.org/10.1152/jappl.2000.89.5.1868

Casavola, C., Paunescu, L. A., Fantini, S., & Gratton, E. (2000). Blood flow and oxygen consumption with near-infrared spectroscopy and venous occlusion: spatial maps and the effect of time and pressure of inflation. *J Biomed Opt*, *5*(3), 269–276. https://doi.org/10.1117/1.429995

Casey, D. P., Curry, T. B., & Joyner, M. J. (2008). Measuring Muscle Blood Flow a Key Link Between Systemic and Regional Metabolism. *Current Opinion in Clinical Nutrition and Metabolic Care*, *11*(5), 580. https://doi.org/10.1097/MCO.0B013E32830B5B34

Chance, B., Dait, M. T., Zhang, C., Hamaoka, T., & Hagerman, F. (1992). Recovery from exercise-induced desaturation in the quadriceps muscles of elite competitive rowers. *American Journal of Physiology - Cell Physiology*, *262*(3 31-3), C766–C775. https://doi.org/10.1152/ajpcell.1992.262.3.c766

Cross, T. J., & Sabapathy, S. (2017). The impact of venous occlusion per se on forearm muscle blood flow: implications for the near-infrared spectroscopy venous occlusion technique. *Clinical Physiology and Functional Imaging*, *37*(3), 293–298. https://doi.org/10.1111/cpf.12301

Duerschmied, D., Olson, L., Olschewski, M., Rossknecht, A., Freund, G., Bode, C., & Hehrlein, C. (2006). Contrast ultrasound perfusion imaging of lower extremities in peripheral arterial disease: A novel diagnostic method. *European Heart Journal*, *27*(3), 310–315. https://doi.org/10.1093/eurheartj/ehi636

Ferrari, M., Muthalib, M., & Quaresima, V. (2011). The use of near-infrared spectroscopy in understanding skeletal muscle physiology: recent developments. *Philosophical Transactions of the Royal Society A: Mathematical, Physical and Engineering Sciences*, *369*(1955), 4577–4590. https://doi.org/10.1098/rsta.2011.0230

Groebe, K., & Thews, G. (1990). Calculated intra- and extracellular PO2 gradients in heavily working red muscle. *American Journal of Physiology-Heart and Circulatory Physiology*, *259*(1), H84–H92. https://doi.org/10.1152/ajpheart.1990.259.1.H84

Hamaoka, T., McCully, K. K., Niwayama, M., & Chance, B. (2011). The use of muscle near-infrared spectroscopy in sport, health and medical sciences: recent developments. *Philosophical Transactions of the Royal Society A: Mathematical, Physical and Engineering Sciences*, *369*(1955), 4591–4604. https://doi.org/10.1098/rsta.2011.0298

Harper, A. J., Ferreira, L. F., Lutjemeier, B. J., Townsend, D. K., & Barstow, T. J. (2006). Human femoral artery and estimated muscle capillary blood flow kinetics following the onset of exercise. *Experimental Physiology*, *91*(4), 661–671. https://doi.org/10.1113/EXPPHYSIOL.2005.032904

Hopkins, W. G. (2015). Spreadsheets for Analysis of Validity and Reliability. *Sportscience*, *19*, 36–45. http://search.ebscohost.com/login.aspx?direct=true&profile=ehost&scope=site&authtype=crawler&jrnl=11749210&AN=124138143&h=B39UQY68DUoNvRvIt7tAAssjUqKAVHNTetEEqp4RCuDd%2BakuTRuJpto7uaBW71ZSyE3PbM3r1RGZWPBgoRwSew%3D%3D&crl=c

Hopkins, Will G. (2007). A spreadsheet for deriving a confidence interval, mechanistic inference and clinical inference from a P value. *Sportscience*, *11*, 16–21. https://go.galegroup.com/ps/i.do?p=AONE&sw=w&u=googlescholar&v=2.1&it=r&id=GALE%7CA189289447&sid=googleScholar&asid=5f628ac6

Hopkins, William G., Marshall, S. W., Batterham, A. M., & Hanin, J. (2009). Progressive statistics for studies in sports medicine and exercise science. *Medicine and Science in Sports and Exercise*, *41*(1), 3–12. https://doi.org/10.1249/MSS.0b013e31818cb278

Ijichi, S., Kusaka, T., Isobe, K., Okubo, K., Kawada, K., Namba, M., Okada, H., Nishida, T., Imai, T., & Itoh, S. (2005). Developmental changes of optical properties in

neonates determined by near-infrared time-resolved spectroscopy. *Pediatric Research*, *58*(3), 568–573. https://doi.org/10.1203/01.PDR.0000175638.98041.0E

Joyner, M. J., & Casey, D. P. (2015). Regulation of Increased Blood Flow (Hyperemia) to Muscles During Exercise: A Hierarchy of Competing Physiological Needs. *Https://Doi.Org/10.1152/Physrev.00035.2013*, *95*(2), 549–601. https://doi.org/10.1152/PHYSREV.00035.2013

Kagaya, A., & Homma, S. (1997). Brachial arterial blood flow during static handgrip exercise of short duration at varying intensities studied by a Doppler ultrasound method. *Acta Physiologica Scandinavica*, *160*(3), 257–265. https://doi.org/10.1046/j.1365-201X.1997.00158.x

Kalliokoski, K. K., Knuuti, J., & Nuutila, P. (2005). Relationship between muscle blood flow and oxygen uptake during exercise in endurance-trained and untrained men. *Journal of Applied Physiology*, *98*(1), 380–383. https://doi.org/10.1152/japplphysiol.01306.2003

Komi, P. V., & Tesch, P. (1979). EMG frequency spectrum, muscle structure, and fatigue during dynamic contractions in man. *European Journal of Applied Physiology and Occupational Physiology*, *42*(1), 41–50. https://doi.org/10.1007/BF00421103

Krix, M., Weber, M. A., Krakowski-Roosen, H., Huttner, H. B., Delorme, S., Kauczor, H. U., & Hildebrandt, W. (2005). Assessment of skeletal muscle perfusion using contrast-enhanced ultrasonography. *Journal of Ultrasound in Medicine*, *24*(4), 431–441. https://doi.org/10.7863/jum.2005.24.4.431

Mancini, D. M., Bolinger, L., Li, H., Kendrick, K., Chance, B., & Wilson, J. R. (1994). Validation of near-infrared spectroscopy in humans. *Journal of Applied Physiology (Bethesda, Md. : 1985)*, *77*(6), 2740–2747. https://doi.org/10.1152/jappl.1994.77.6.2740

Miura, H., McCully, K., Nioka, S., & Chance, B. (2004). Relationship between muscle architectural features and oxygenation status determined by near infrared device. *European Journal of Applied Physiology*, *91*(2–3), 273–278. https://doi.org/10.1007/s00421-003-0964-6

Partovi, S., Karimi, S., Jacobi, B., Schulte, A. C., Aschwanden, M., Zipp, L., Lyo, J. K., Karmonik, C., Müller-Eschner, M., Huegli, R. W., Bongartz, G., & Bilecen, D. (2012). Clinical implications of skeletal muscle blood-oxygenation-level-dependent (BOLD) MRI. In *Magnetic Resonance Materials in Physics, Biology and Medicine*

(Vol. 25, Issue 4, pp. 251–261). Springer. https://doi.org/10.1007/s10334-012-0306-y

Paunescu, L. A., Casavola, C., Franceschini, M.-A., Fantini, S., Winter, L., Kim, J., Wood, D., & Gratton, E. (1999). Calf muscle blood flow and oxygen consumption measured with near-infrared spectroscopy during venous occlusion. *Optical Tomography and Spectroscopy of Tissue III*, *3597*, 317–323. https://doi.org/10.1117/12.356790

Pollak, A. W., Meyer, C. H., Epstein, F. H., Jiji, R. S., Hunter, J. R., Dimaria, J. M., Christopher, J. M., & Kramer, C. M. (2012). Arterial spin labeling mr imaging reproducibly measures peak-exercise calf muscle perfusion: A study in patients with peripheral arterial disease and healthy volunteers. *JACC: Cardiovascular Imaging*, *5*(12), 1224–1230. https://doi.org/10.1016/j.jcmg.2012.03.022

Quaresima, V., Ferrari, M., Franceschini, M. A., Hoimes, M. L., & Fantini, S. (2004). Spatial distribution of vastus lateralis blood flow and oxyhemoglobin saturation measured at the end of isometric quadriceps contraction by multichannel near-infrared spectroscopy. *Journal of Biomedical Optics*, *9*(2), 413. https://doi.org/10.1117/1.1646417

Rådegran, G. (1999). Limb and skeletal muscle blood flow measurements at rest and during exercise in human subjects. *Proceedings of the Nutrition Society*, *58*(4), 887–898. https://doi.org/10.1017/S0029665199001196

Rathbun, S., Heath, J., & Whitsett, T. (n.d.). *Images in vascular medicine The venoarterial reflex*. https://doi.org/10.1177/1358863X08092101

Richardson, R. S., Knight, D. R., Poole, D. C., Kurdak, S. S., Hogan, M. C., Grassi, B., & Wagner, P. D. (1995). Determinants of maximal exercise V̇O2, during single leg knee-extensor exercise in humans. *American Journal of Physiology - Heart and Circulatory Physiology*, *268*(4 37-4). https://doi.org/10.1152/ajpheart.1995.268.4.h1453

Rudroff, T., Weissman, J. A., Bucci, M., Seppänen, M., Kaskinoro, K., Heinonen, I., & Kalliokoski, K. K. (2014). Positron emission tomography detects greater blood flow and less blood flow heterogeneity in the exercising skeletal muscles of old compared with young men during fatiguing contractions. *Journal of Physiology*. https://doi.org/10.1113/jphysiol.2013.264614

Ryan, T. E., Erickson, M. L., Brizendine, J. T., Young, H.-J., & McCully, K. K. (2012). Noninvasive evaluation of skeletal muscle mitochondrial capacity with near-infrared spectroscopy: correcting for blood volume changes. *Journal of Applied Physiology*, *113*(2), 175–183. https://doi.org/10.1152/japplphysiol.00319.2012

Southern, W. M., Ryan, T. E., Reynolds, M. A., & McCully, K. (2014). Reproducibility of near-infrared spectroscopy measurements of oxidative function and postexercise recovery kinetics in the medial gastrocnemius muscle. *Applied Physiology, Nutrition, and Metabolism*, *39*(5), 521–529. https://doi.org/10.1139/apnm-2013-0347

van Beekvelt, M., Colier, W. N. J. M., Wevers, R. O. N. A., Engelen, B. G. M. V. A. N., Wevers, R. A., & Perfor-, B. G. M. V. E. (2001). *Performance of near-infrared spectroscopy in measuring local O 2 consumption and blood flow in skeletal muscle*. 511–519.

Vogiatzis, I., Habazettl, H., Louvaris, Z., Andrianopoulos, V., Wagner, H., Zakynthinos, S., & Wagner, P. D. (2015). A method for assessing heterogeneity of blood flow and metabolism in exercising normal human muscle by near-infrared spectroscopy. *Journal of Applied Physiology*, *118*(6), 783–793. https://doi.org/10.1152/japplphysiol.00458.2014

Vøllestad, N. K. (1997). Measurement of human muscle fatigue. *Journal of Neuroscience Methods*, *74*(2), 219–227. https://doi.org/10.1016/S0165-0270(97)02251-6

Watanabe, K., & Akima, H. (2011). Effect of knee joint angle on neuromuscular activation of the vastus intermedius muscle during isometric contraction. *Scandinavian Journal of Medicine and Science in Sports*, *21*(6), 412–420. https://doi.org/10.1111/j.1600-0838.2011.01347.x

Whipp, B. J., & Ward, S. A. (1982). Cardiopulmonary coupling during exercise. In *Journal of Experimental Biology* (Vol. 100, Issue 1, pp. 175–193). The Company of Biologists. https://doi.org/10.1242/jeb.100.1.175

5 - Skeletal Muscle Microvascular and Respiratory Responses to Exercise in Healthy and T2D Adults: A Comparison and Reproducibility Study of NIRS Technologies

Adam A. Lucero[1], Martin Gram[2], Inge Ramakers[1], Terence Ryan[3], Osvaldo Enriquez[4], James Faulkner[5], Lee Stoner[1,6], David S. Rowlands[1]

[1]*School of Sport, Exercise and Nutrition, Massey University, Auckland, New Zealand*

[2]*Novo Nordisk, Copenhagen, Denmark*

[3]*College of Health and Human Performance, University of Florida, Florida, USA*

[4]*Automation Controls, Applied Medical, California, USA*

[5]*Department of Sport and Exercise, University of Winchester, Winchester, United Kingdom*

[6]*Department of Exercise and Sport Science, University of North Carolina at Chapel Hill, NC, USA*

Running head: Skeletal muscle microvascular blood flow and oxygen kinetics

Correspondence:
Adam Lucero
School of Sport, Exercise, and Nutrition
Massey University
Albany Expressway (SH17), Albany, Auckland 0632
New Zealand
+64 48015799 (63295)
Adamluco1@gmail.com
ORCID: 0000-0002-2743-0209

Abstract

Continuous-wave (cw) near infrared spectroscopy (NIRS) is widely-used in skeletal muscle tissue hemodynamic and respiratory research despite fixed light scattering assumptions. The purpose was to compare reproducibility and technical characteristics of cw-NIRS against a benchmark technology frequency-domain (fd)-NIRS, which permits for intra-individual scattering correction. Muscle blood flow (mBF), oxygen uptake (mVO_2), and perfusion were assessed within 10 healthy (ND) and 10 type-2 diabetic (T2D) men at rest and during knee extensions at 5% and 15% of maximal torque (MVC) on 3 occasions within 10d. In both groups, exercise responses for mBF and $m\dot{V}O_2$ were not substantially different between technology with moderate-high reproducibility (ICC: 0.72-0.98). However, cw-NIRS vs fd-NIRS overestimated perfusion at rest (21 uM; 90%CI 29, 13), 5%MVC (18 uM; 27, 9) and 15%MVC (17 uM; 26, 8) in T2D but not ND. Standardized typical errors during exercise were small-moderate and not clearly different between groups and technology: e.g., 15%MVC mBF, cw-NIRS (ND 0.45, 90%CI 0.35-0.66; T2D 0.49, 0.36-0.67), fd-NIRS (0.35, 0.27-0.51; 0.49, 0.27-0.51); mV̇O2, cw-NIRS (0.24, 0.19-0.36; 0.26, 0.20-0.38), fd-NIRS (0.45, 0.35-0.66; 0.32, 0.25-0.47); perfusion cw-NIRS (0.25, 0.20-0.37; 0.25, 0.19-0.36) and fd-NIRS (0.25, 0.19-0.37; 0.23, 0.18-0.33). Both NIRS technologies were reproducible and parameter estimates were similar apart from cw-NIRS overestimation of perfusion in T2D.

Introduction

Near-infrared spectroscopy (NIRS) is an emerging non-invasive technology capable of assessing the hemodynamic and oxygen-transfer properties of skeletal muscle. This technique relies on principles of traditional spectroscopy yielding concentrations of oxygenated ([O2Hb]), deoxygenated ([HHb]), and total hemoglobin ([tHb] = [O2Hb] + [HHb]) (Yamashita *et al.*, 2013; Stone *et al.*, 2016). A complication with accurate measurement of hemoglobin parameters with NIRS in biological tissues occurs as the speed and direction of the individual photons changes as they transit cellular membranes, organelles, and tissue structures; a phenomenon known as scattering (Rolfe, 2000; Stone *et al.*, 2016). The degree of scattering varies due to muscular structure and make up, and can be altered in cohorts with obesity and metabolic perturbations, such as, those with type-2 diabetes (T2D) due to increased cutaneous adipose tissue thickness (Scheuermann-Freestone et al., 2003), fibrosis (Henninger et al., 2014), intramuscular fat (Henninger et al., 2014), and in situations of different perfusion responsivity such as insulin resistance (Clark, 2008). Additional scattering changes within the skeletal muscle occur during exercise as the area of the muscle cell compresses during contraction and changes in metabolite concentrations combine to change the physical nature of the tissue (L. F. Ferreira et al., 2006). While NIRS based protocols hold promise for investigating aspects of hemodynamics and oxygen kinetics in skeletal muscle of populations with metabolic or microvascular diseases, and during exercise, there is currently limited data specific to these cohorts and physiological state.

Continuous-wave (cw) NIRS, one of the most popular NIRS devices due to versatility, ease of use, and general cost, applies a constant literature-based scattering coefficient - a known limitation that introduces measurement uncertainty (Grassi & Quaresima, 2016b). In cw-NIRS, Hb concentrations are obtained using three literature based constants, differential path-length factor (DPF), h and k which account for scattering (Hammer et al., 2019a) and are set based on measurements conducted in the head, forearm, and calf tissue in men and women (Duncan et al., 1995). The effect of

assuming one set of constants for an entire cohort on local skeletal muscle hemodynamic and respiratory outcomes is not clear, especially in clinical populations. In contrast, a benchmark technology that can accurately measure and correct for inter-individual variation in scattering is frequency-domain (fd-) NIRS (Fantini et al., 1994). Previously we reported acceptable reliability of cw-NIRS combined with rapid venous (VO) and arterial occlusions (AO) for assessing skeletal muscle blood flow (mBF) and oxygen consumption ($m\dot{V}O_2$) response to exercise in healthy individuals (Lucero et al., 2018). In this work, mBF, m$\dot{V}$O2, and perfusion increased from rest to exercise with increasing levels of intensity as expected; however, we were uncertain of the reliability of these measures compared against fd-NIRS. Moreover, characterizing the skeletal muscle NIRS derived in T2D or other metabolically diseased muscle, is required to establish utility of cw-NIRS in these cohorts with known technical complications (e.g., greater subcutaneous body fat) pertaining to reproducible and accurate haemodynamic assessment, which will aid in clinical research interventions.

Therefore, the purpose of this study is to determine the reproducibility and technical characteristics between cw- and fd-NIRS, establish the validity of cw-NIRS during exercise against scattering adjusted fd-NIRS as a criterion instrument, and to define the variation in hemodynamic and respiratory outcomes between healthy and T2D populations at rest and during exercise. Since muscle quality affects degree of light scattering and fd-NIRS can accurately correct for these changes, we hypothesize that cw-NIRS derived [tHb] will vary compared to fd-NIRS, specifically in T2D where muscle quality can vary significantly between individuals.

Methods

Participants

10 young, healthy, physically active men (defined as meeting the daily exercise guidelines according to the American College of Sports Medicine) and 10 sedentary non-insulin dependent men with T2D (HbA1c ≥48 mmol/L, diagnosed minimum 1 y) were recruited into the study (Table 5.1). As the experiment was designed to establish the

reliability of the NIRS devices in ND and T2D populations, the participants were not matched between groups. All participants were excluded if they were a current smoker or have smoked 6 months prior, used β-blockers, injured or had lower limb surgery in the past 4 wk, moderate to severe retinopathy, nephropathy or neuropathy, history of cerebrovascular or cardiovascular diseases. Due to NIRS measurement limitations, participants were also excluded if they had greater than 20 mm of adipose tissue thickness over the NIRS probe region of interest as measured by ultrasound (Van Beekvelt et al., 2001). Ethical approval was obtained from the institutional Human Ethics Committee and all participants were informed of any risks and discomfort associated with the experiments prior to providing written consent.

Table 5.1. Mean values and standard deviations for participant characteristics.

		Age	Height (m)	Weight (kg)	ATT (cm)	VL (cm)	VL Belly (cm)
T2D	Mean	56.3	173.6	91.7	1.82	2.17	3.71
	SD	5.1	6.9	14.4	0.32	4.20	1.39
ND	Mean	22.5	173.2	68.8	0.38	3.14	1.95
	SD	3.40	6.38	10.6	0.12	4.00	0.26

Abbreviations: ATT, adipose tissue thickness; VL, vastus lateralis; VL Belly, distance from skin to the belly of the VL calculated as ATT + 1/2*VL

Experimental procedures

Each participant performed a familiarization trial followed by 3 identical test visits where the participant performed knee-extension exercise (reliability) in a dimly-lit, temperature controlled room (20.5 ˚C, SD 0.8). On the familiarization visit participants

were habituated to the testing protocol and their maximum voluntary contraction (MVC) of the Vastus lateralis in testing position was obtained to calculate the workload for exercise stages. The habituation consisted of several trials where the participant rehearsed the positioning and relaxation of the leg during arterial and venous occlusions. To obtain MVC, participants were seated on an isokinetic dynamometer in the same experimental position (Biodex Medical Systems, Inc. Shirly, NY, USA) reclined to 70° to obtain a 110° hip angle and a 90˚ knee extension angle, which was optimal for experimental measures (Grassi & Quaresima, 2016a). The settings were adjusted so that the axial portion of the knee aligned with the axis of rotation on the dynamometer. The MVC was reported as the maximum of 3 trials.

All experimental tests occurred between 0700-1000 h following an overnight fast, having consumed only water, and refraining from caffeine that morning. Participants were asked to avoid strenuous physical activity and alcohol consumption for 24 s prior to experimentation. At each of the 3 test visits the NIRS parameters mBF, $m\dot{V}O_2$, [tHb] as an index of perfusion, tissue saturation, exercise blood-volume change (ΔEBV) and the m$\dot{V}$O2 recovery rate constant (k) as an index of muscle oxidative capacity were measured using protocols that are described below (See figure 6.1) (Lucero et al., 2018; T. E. Ryan et al., 2012). A rapid-inflation cuff (Hokanson SC 10D, D. E. Hokanson, Inc., Bellevue, WA) was placed as high as possible around the proximal thigh, minimizing patient discomfort and avoiding artefact motion in the NIRS signal. This cuff was connected to a custom-made rapid-inflation device that inflated the cuff to a specific pressure in less than 0.5 s (Lucero et al., 2018). Occlusions for mBF and $m\dot{V}O_2$ estimations occurred in the active leg during brief pauses where the leg was suspended in a 150º knee-joint angle permitting a relaxed muscle length, thereby facilitating blood flow (Miura et al., 2004). The non-working leg was suspended in a 150º knee-joint angle throughout.

Following 20 min of quiet rest, baseline measurements of mBF and $m\dot{V}O_2$ were assessed from the average of 4 VO and 2 AO, respectively. Each occlusion was separated by 45 s of rest with occlusion durations of 15 s and 30 s for VO and AO, respectively

(Southern et al., 2014). The participant then completed 2 stages of progressive intensity (5 and 15% MVC) rhythmic isotonic knee extension exercise (1 extension/4 s) on the dynamometer (Watanabe & Akima, 2011) (Figure 6.1). These intensities were reproducible without inducing fatigue (Lucero et al., 2018). Participants were instructed to contract to full extension and then allow their leg to fall back to the starting position. The participant exercised continuously for 3 min prior to the first occlusion to increase chances of achieving steady state. Participants were instructed to contract to full extension and then allow their leg to fall back to the starting position. Immediately after the contraction phase of the last knee extension for each measurement point, as the leg was falling, the dynamometer was locked to hold the leg in the 150º knee-joint angle and the cuff was inflated for 10 s. Exercise was then resumed for 45 s to maintain steady state before another measurement was collected. Complete occlusion during AO at rest and exercise was verified with Doppler ultrasound in the femoral artery during pilot trials and confirmed during testing by the cessation of the pulsatile motion in the tHb signal. Following the exercise stages, the participant completed two muscle oxygen recovery capacity (MORC) tests which consisted of a brief 15 s bout of light isotonic exercise (16 N·m) followed by 7 min of resting with the active leg having a 150º knee-joint angle during repeated AOs. After finishing the two MORC tests the entire protocol was then repeated in the opposite leg to test the other NIRS device. The starting leg and NIRS device was randomized for the first visit and repeated for the remaining two visits.

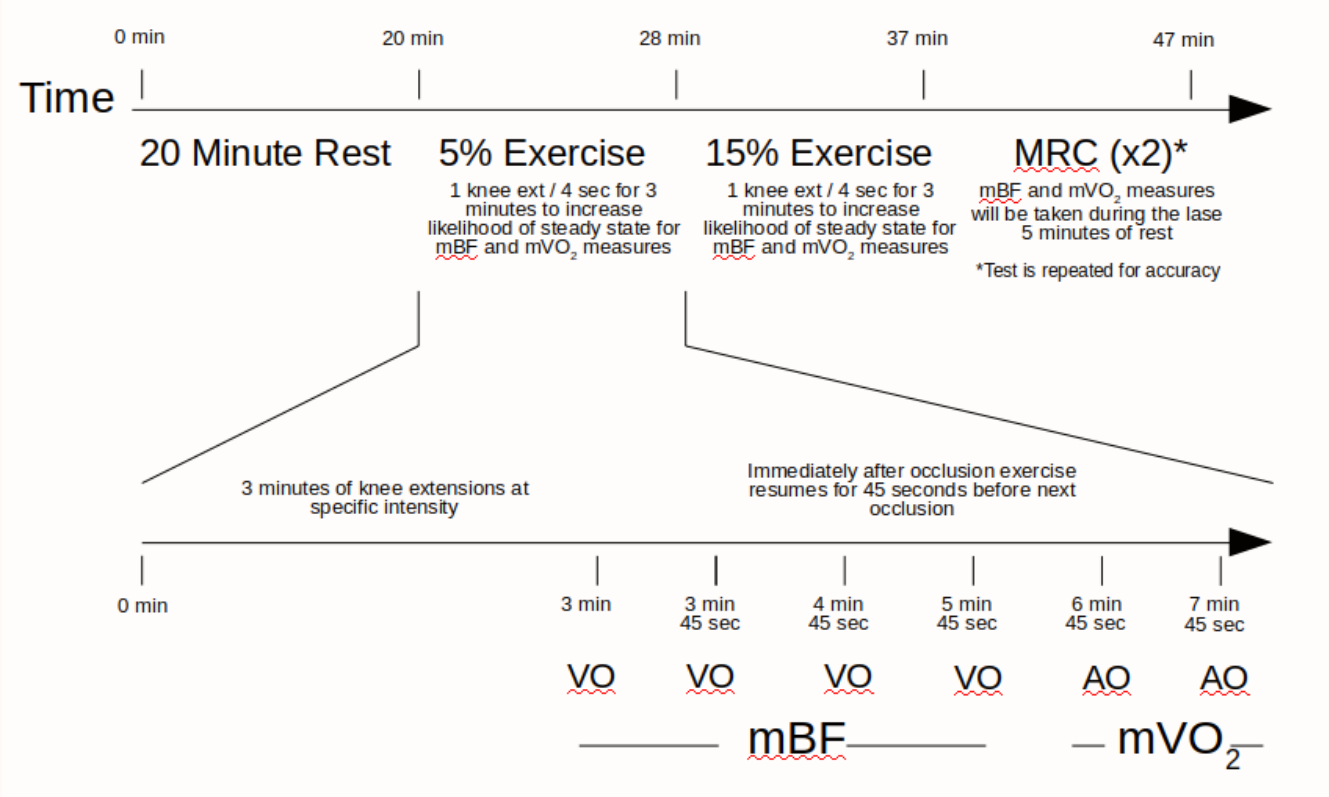

Figure 5.1. Experimental Protocol. The protocol is conducted using one NIRS device on one leg and is repeated on the other leg with the other NIRS device. The expanded portion of the timeline shows the occlusion timing for an example exercise stage. Abbreviations: MORC, Muscle Oxygen Recovery Capacity; VO, venous occlusion; AO, arterial occlusion; mBF, muscle blood flow; mVO2, muscle oxygen consumption.

Near-infrared spectroscopy

Two NIRS devices were used to continuously monitor changes in local concentrations of [O2Hb], [HHb], and [tHb]. One device was placed on the VL of the dominant leg and the other was oppositely placed on the VL of the non-dominant leg. The NIRS devices were randomized. The cw-NIRS device (PortaLite; Artinis Medical Systems BV, Elst, The Netherlands) consists of six light-emitting diodes (760 and 850 nm) from 3 transmission distances of 3.0, 3.5, and 4.0 cm from the detector. A DPF of 4.0, h of 0.00046 nm-1, and k of 1.1 mm-1 were used to correct for scattering, and data were collected at 10 Hz. The cw-NIRS hemoglobin concentration values were calculated from transmitter 2 allowing for a theoretical penetration distance of 1.75 cm. The fd-

NIRS device (Oxiplex TS, ISS Inc., IL) consists of eight light-emitting (690 and 830 nm) diodes from four transmission distances of 2.5, 3.0, 3.5, 4.0 cm from the detector. Unlike the cw-NIRS, all four transmitters on the fd-NIRS are used to determine a best-fit slope of the amplitude of modulation (AC) and phase shift (time of flight) components versus transmitter-detector distance used to continuously determine the degree of scattering, so it can be accurately accounted for to determine hemoglobin concentrations (Fantini et al., 1994). The instrument was calibrated before each measurement by positioning the probe on calibration blocks with known scattering and absorption coefficients. The fd-NIRS calculated hemoglobin concentrations were smoothed using a moving average window of 0.5 s.

For both NIRS devices, the probe was securely adhered using double-sided tape to the skin parallel to the muscle fibers, about two-thirds from the top of the VL over the muscle belly using a custom built guide and verified using US. A custom-made cover shielded the probe from ambient light while allowing it to move with the skin during contractions minimizing changes in contact pressure (T. Hamaoka et al., 2011). The probe position was marked with a pen to ensure that the same position was used for all three trials. The thickness of the VL at the probe location, along with adipose tissue thickness, were determined using B-mode ultrasound (Terason, United Medical Instruments Inc., San Jose, CA).

Local skeletal muscle blood flow

Estimates of mBF were assessed as the [ΔtHb] signal during VO, analyzed using simple linear regression as previously described (Cross & Sabapathy, 2017a; M. van Beekvelt et al., 2001). Briefly, a 3.5 in tourniquet (Hokanson SC 10D, D. E. Hokanson, Inc., Bellevue, WA) was placed as high as possible around the proximal thigh, minimizing patient discomfort and avoiding artefact motion in the NIRS signal. The custom-built tourniquet was rapidly (~0.5 s) inflated to a sub diastolic pressure (60-80 mmHg) to occlude venous outflow without impeding arterial inflow, thus, causing venous volume to increase at a rate proportional to arterial inflow. For both NIRS devices, the

slope of the [tHb] signal during the first cardiac cycle immediately after VO was defined using the pulsatile motion of the [tHb] signal. To determine mBF, the slope of the tHb signal over one cardiac cycle was obtained for 4 VOs, averaged, and converted into units of mL per min per 100 mL of blood (Table 5.2).

Skeletal muscle oxygen consumption

Estimates of m$\dot{V}$O2 from both NIRS devices were calculated as the rate of change in the Hb difference signal ([ΔHbDif] = [ΔHbO2] – [ΔHHb]) during arterial occlusion, analyzed using simple linear regression as previously described (T. E. Ryan et al., 2012). Briefly, the tourniquet was rapidly (~0.5 s) inflated to a supra-systolic pressure (250-300 mmHg) to occlude both venous outflow and arterial inflow, completely arresting blood flow, resulting in an increase of [HHb] and simultaneous decrease in [HbO2] as oxygen is released from hemoglobin and consumed by the surrounding muscle tissue (M. van Beekvelt et al., 2001). After correcting for blood-volume changes (T. E. Ryan et al., 2012), the slope of the [HbDif] signal was converted into milliliters of O_2 per min per 100 grams of tissue (Table 6.2).

Skeletal muscle perfusion index and tissue saturation of oxygen

Local skeletal muscle perfusion index ([tHb]) and tissue saturation were calculated as the relative average blood-volume ([tHb] signal) and tissue saturation, respectively, for a given period. The [tHb] signal has been said to reflect microvascular blood-volume (Ijichi et al., 2005), an indication of local O2 diffusing capacity (Groebe & Thews, 1990). Tissue saturation represents the saturation of oxygen in the blood given as a percentage, calculated as [O_2Hb] / ([O_2Hb] + [HHb]) * 100 using absolute values of [O2Hb] and [HHb]. Due to the limitations of cw-NIRS, oxygen saturation of the tissue (SaO2) must be calculated from estimated measures of absolute O2Hb and HHb using principles of spatially resolved spectroscopy (detailed elsewhere (Suzuki et al., 1999)) and is referred to as tissue saturation index (TSI%), an analogue of SaO2. After resting measurements of mBF and m$\dot{V}O_2$ were taken, the participant's leg was lowered to 90˚ knee-joint angle in preparation for the exercise protocol. The participant then continued

to rest to allow the [tHb] and tissue saturation signals to stabilize for 30 s, which was used for the resting period. During exercise, the average signal values during 2 s rest period (when the leg was relaxed at 90˚) between the last 8 extensions (last 30 s of exercise before occlusions) were averaged.

Skeletal muscle blood-volume change during exercise

Exercise induced blood-volume change was the average change in the [tHb] across the last 8 contraction-relaxation cycles of the knee-extension exercise. To our understanding, this method of determining exercise induced blood-volume change is novel and theoretically justifiable. The force of the muscle contraction causes a rapid increase in the intramuscular pressure, expelling blood from capillaries causing a rapid decrease in the [tHb] signal. During relaxation, intramuscular pressure transiently returns to a level below the venous blood pressure and blood from the capillaries is pulled into and refills the veins until the next contraction. This phenomenon is known as the mechanical muscle pump effect (Tschakovsky et al., 1996). In this context, as stated above, the [tHb] signal reflects microvascular blood-volume and O_2 diffusing capacity. Accordingly, we propose that the range of the [tHb] signal over the contraction-relaxation cycle may be a function of the local muscle pump emptying and refilling capacity at a specific exercise intensity, vasodilatory response, and capillarity.

Muscle oxygen recovery capacity

Muscle oxygen recovery capacity (MORC) was assessed as the $m\dot{V}O_2$ recovery rate constant (k) and reported as a time constant (tc) for mean values, which is equal to the inverse of k (tc = 1/k), detailed elsewhere (T. E. Ryan et al., 2012). Briefly, repeated AOs were done according to a set timing sequence following a brief bout of exercise measuring m$\dot{V}$O2 over a 5-min period to assess recovery. The MORC tests were conducted with the participant in a seated position using knee-extension exercise as the exercise stimulus. The participant performed light, rapid and rhythmic 90˚ isotonic knee extension exercise for 10 s set to 16 N·m with max extension set to 60˚ to obtain maximal VL activation and minimize recovery between contractions increasing m$\dot{V}$O2 while

maintaining muscle oxygen levels above 40% (Adami et al., 2017). Immediately after exercise, the participant was instructed to completely relax while their leg lifted to neutral position for the AOs, the first delivered 8 s after the last contraction. The AO sequence was piloted to optimize mV̇O2 recovery kinetics with minimal disruption to blood flow in the current population and is as follows: AO 1-3: 5s on/10s off, AO 3-6: 6s on/12s off, AO 7-11: 7s on/15s off, AO 12-14: 10s on/30s off, AO 15: 30s on then off. Estimates of mV̇O2 were calculated as the rate of change in the HbDif signal as described earlier. The individual mV̇O2 were plotted as a function of time and fit to a mono-exponential curve (Table 5.2). The recovery rate constant of mV̇O2 after exercise is proportional to the maximal oxidative capacity (Terence E. Ryan et al., 2014) and was assessed the average of two consecutive tests.

Table 5.2. Equations and parameters for mBF and mVO2.

Equation	Calculated Value	Parameter 1	Parameter 2	Parameter 3	Parameter 4
$mBF = [\Delta tHb]/\Delta t \cdot 1/C$ Equation to calculate mBF from the average rate of tHb increase under VO. The molecular mass of hemoglobin (64.458 g·mol-1) and the ratio between hemoglobin and O2 molecules (1:4) were accounted for	mBF Skeletal muscle blood flow in mL·min-1·100 mL-1	$[\Delta tHb]/\Delta t$ Rate of tHb change (slope) during first cardiac cycle under VO	C Hb concentration in the blood, for which we assumed a value of 7.5 and 8.5 mmol·L-1for female and male participants	*N/A*	*N/A*
$m\dot{V}O2 = abs[([\Delta HbDif/\Delta t * ½] \cdot 60)/(10 \cdot 1.04) \cdot 4] \cdot 22.4/1000$ Equation to calculate mVO2 from the average change in HbDiff during AO assuming 22.4 L for the volume of gas (STPD) and 1.04 kg·L-1 for muscle density	$m\dot{V}O2$ Skeletal muscle O2 consumption in MlO2•min-1·100g-1	$\Delta HbDif/\Delta t$ Rate of change in HbDif (slope) under AO. Taking the Hb difference improves signal to noise ratio but	*N/A*	*N/A*	*N/A*

		doubles the rate. Dividing by 2 corrects.			
$y(t) = end - \Delta \cdot e^{-kt}$ Muscle oxygen recovery capacity fit to a mono-exponential curve	*y* relative mV̇O2 during arterial occlusion	*end* mV̇O2 immediately after the cessation of exercise	*Δ* change in mV̇O2 from rest to exercise	*k* fitting rate constant	*t* time
$TE = SD/\sqrt{2}$ Typical Error before standardization	*TE* Typical Error as Standard Error of Measurement	*SD* standard deviation of the change score for all participants	*N/A*	*N/A*	*N/A*
$ICC = 1 - TE^2/SDb^2$ Visit to visit reliability	*ICC* Intra Class Correlation Coefficient	*TE* typical error	*Sdb* mean between-participant standard deviation	*N/A*	*N/A*

Statistics

The precision of the estimate of the between-device difference in hemodynamic outcomes was estimated using two-way repeated measures ANOVA (SPSS 13, Chicago, IL) to obtain two-sided p-values for the pairwise comparisons. The p-values were then used to estimate the magnitude of any differences between devices and associated uncertainty. The reproducibility of the NIRS devices was assessed using the intraclass correlation coefficient (ICC), Cohen *d* smallest standardised difference 0.2 SD, standardized typical error (STE), and coefficient of variation as a percentage (%CV) (Hopkins, et al. 2009) analyzed within a published spreadsheet (Hopkins, 2019). Thresholds for ICC of 0.20 (low), 0.50 (moderate), 0.75 (high), 0.90 (very high), and

0.99 (nearly perfect) reliability for sample populations were used. The STE gives the random error in the calibrated value and is interpreted using thresholds of 0.1 (small), 0.3 (moderate), 0.6 (large), 1 (very large), and 2 (extremely large) (Hopkins *et al.*, 2009).

Uncertainty in the estimates is presented as 90% compatibility limits. Decisions about magnitudes accounting for the uncertainty were based on one-sided interval hypothesis tests, according to which an hypothesis of a given magnitude is rejected if the 90% compatibility interval falls outside that magnitude (Aisbett et al., 2020; Will G Hopkins, 2020). Hypotheses of inferiority (substantial negative) and superiority (substantial positive) were rejected if their respective p values (p– and p+, given by the areas of the sampling distribution of the effect in substantial negative and positive values, respectively) were <0.05; rejection of both hypotheses represents a decisively trivial effect in equivalence testing. If one hypothesis was rejected, the p value for the other hypothesis corresponds to the posterior probability of a substantial true magnitude of the effect in a reference-Bayesian analysis with a minimally informative prior (Will G. Hopkins, 2007) and was interpreted, when >0.25, with the following scale: >0.25, possibly; >0.75, likely; >0.95, very likely; >0.995, most likely (Will G Hopkins, 2020); the probability of a trivial true magnitude (1 – p– – p+) was also interpreted, when >0.25, with the same scale. Probabilities were not interpreted for effects with inadequate precision at the 90% level, defined by failure to reject both hypotheses (p– >0.05 and p+ >0.05). The hypothesis of non-inferiority or non-superiority was rejected if its p value (pN– = 1 – p– or pN+ = 1 – p+) was <0.05, representing a decisively substantial effect in minimum-effects testing: very likely or most likely substantial. Likelihoods were then adjusted for type-1 error by appropriate familywise Bonferroni adjustment.

Results

Descriptive outcome statistics are in Figure 2. To calculate day-to-day reliability of each NIRS device, the ICC value, Typical Error, and %CV were calculated (Table 5.3) with 90% confidence intervals. In assessing the parameter values, two different comparisons are being made. The first of which is comparing the fd- and cw-NIRS

devices in ND and T2D groups, and the second is the same NIRS device between groups, i.e. fd-NIRS in ND to fd-NIRS in T2D. The former comparison assesses the ability of each NIRS device to obtain the same value within an individual, and the latter is assessing between group values within NIRS devices.

Table 5.3. ICC values for all NIRS parameters for non-diabetic (ND) and type 2 diabetic (T2D) groups from frequency-domain (FD) and continuous-wave (CW) NIRS.

Group:	**ND**			**T2D**		
% Max	**Rest**	**5**	**15**	**Rest**	**5**	**15**
	mBf					
FD - ICC	0.39 (0.00, 0.73)	0.83 (0.62, 0.94)	0.91 (0.78, 0.97)	0.21 (0.00, 0.42)	0.91 (0.78, 0.97)	0.81 (0.57, 0.93)
FD - STE	0.81 (0.62, 1.19)	0.46 (0.35, 0.67)	0.35 (0.27, 0.51)	1.01 (0.62, 1.18)	0.34 (0.35, 0.67)	0.49 (0.27, 0.51)
FD - % CV	60.3 (43.8, 99.3)	40.6 (30.0, 64.5)	36.5 (27.1, 57.6)	76.3 (54.7, 129.9)	42.6 (31.4, 68.0)	54.7 (39.9, 89.2)
CW - ICC	0.78 (0.52, 0.91)	0.71 (0.41, 0.89)	0.84 (0.63, 0.94)	0.77 (0.42, 0.89)	0.76 (0.49, 0.91)	0.83 (0.62, 0.93)
CW - STE	0.52 (0.40, 0.75)	0.58 (0.45, 0.85)	0.45 (0.35, 0.66)	0.57 (0.44, 0.84)	0.54 (0.42, 0.79)	0.49 (0.36, 0.67)
CS - % CV	19.4 (14.6, 29.5)	56.2 (41.0, 92.0)	39.6 (29.3, 62.8)	25.3 (19.1, 41.7)	51.6 (37.8, 90.3)	51.5 (37.7, 83.6)
	mV̇O2					
FD - ICC	0.33	0.86	0.84	0.74	0.80	0.92

	(0.00, 0.70)	(0.68, 0.96)	(0.63, 0.94)	(0.45, 0.90)	(0.55, 0.93)	(0.80, 0.97)
FD - STE	0.84 (0.65, 1.23)	0.42 (0.32, 0.61)	0.45 (0.35, 0.66)	0.56 (0.43, 0.82)	0.50 (0.39, 0.73)	0.32 (0.25, 0.47)
FD - % CV	72.6 (52.2, 122.1)	30.4 (22.7, 47.4)	37.3 (27.7, 60.0)	28.6 (21.3, 44.4)	26.6 (19.9, 41.1)	27.3 (20.4, 42.3)
CW - ICC	0.39 (0.00, 0.73)	0.94 (0.85, 0.97)	0.96 (0.89, 0.94)	0.58 (0.21, 0.83)	0.98 (0.94, 0.99)	0.95 (0.87, 0.98)
CW - STE	0.81 (0.62, 1.18)	0.28 (0.22, 0.41)	0.24 (0.19, 0.36)	0.69 (0.53, 1.01)	0.18 (0.14, 0.26)	0.26 (0.20, 0.38)
CW - % CV	53.4 (39.0, 86.9)	22.0 (16.5, 33.7)	18.0 (13.5, 27.3)	60.8 (44.2, 100.4)	18.8 (14.16, 28.6)	29.4 (21.9, 45.7)

Group:	**ND**			**T2D**		
% Max	**Rest**	**5**	**15**	**Rest**	**5**	**15**
	[tHb]					
FD - ICC	0.94 (0.86, 0.98)	0.96 (0.90, 0.98)	0.95 (0.88, 0.98)	0.97 (0.91, 0.99)	0.96 (0.92, 0.99)	0.96 (0.90, 0.99)
FD - STE	0.27 (0.21, 0.40)	0.23 (0.18, 0.33)	0.25 (0.19, 0.37)	0.21 (0.16, 0.31)	0.22 (0.17, 0.32)	0.23 (0.18, 0.33)
FD - % CV	10.5 (8.0, 15.7)	9.4 (7.2, 14.1)	8.6 (6.6, 12.9)	7.1 (5.4, 10.5)	7.6 (5.8, 11.3)	07.5 (5.8, 11.2)
CW - ICC	0.96	0.95	0.95	0.96	0.96	0.96

	(0.90, 0.98)	(0.87, 0.98)	(0.88, 0.98)	(0.88, 0.98)	(0.88, 0.98)	(0.88, 0.98)
CW - STE	0.22 (0.17, 0.32)	0.27 (0.20, 0.39)	0.25 (0.20, 0.37)	0.24 (0.19, 0.35)	0.23 (0.18, 0.34)	0.25 (0.19, 0.36)
CW - % CV	3.5 (2.7, 5.1)	4.1 (3.1, 6.0)	4.0 (3.1, 6.0)	4.9 (3.7, 7.2)	5.2 (3.9, 7.6)	5.1 (3.9, 7.5)
	SaO2/TSI					
FD - ICC	0.75 (0.46, 0.90)	0.92 (0.79, 0.97)	0.90 (0.76, 0.97)	0.70 (0.91, 0.99)	0.87 (0.82, 0.91)	0.89 (0.84, 0.93)
FD - STE	0.55 (0.43, 0.81)	0.33 (0.26, 0.49)	0.36 (0.28, 0.38)	0.60 (0.46, 0.87)	0.40 (0.31, 0.59)	0.38 (0.29, 0.56)
FD - % CV	5.0 (3.8, 7.4)	5.2 (4.0, 7.7)	8.8 (6.7, 13.1)	6.1 (4.6, 9.0)	5.6 (4.3, 8.3)	7.3 (5.6, 10.9)
CW - ICC	0.57 (0.21, 0.83)	0.73 (0.44, 0.90)	0.79 (0.55, 0.93)	0.79 (0.53, 0.92)	0.97 (0.91, 0.99)	0.97 (0.93, 0.99)
CW - STE	0.69 (0.53, 1.01)	0.56 (0.43, 0.82)	0.50 (0.39, 0.74)	0.51 (0.39, 0.74)	0.21 (0.16, 0.31)	0.19 (0.15, 0.28)
CW - % CV	6.7 (5.1, 9.9)	4.5 (3.4, 6.6)	4.3 (3.3, 6.3)	2.5 (1.9, 3.7)	1.4 (1.1, 2.1)	1.9 (1.4, 2.7)
	[tHb] Range					
FD - ICC		0.90 (0.76, 0.97)	0.89 (0.74, 0.96)		0.88 (0.71, 0.95)	0.88 (0.72, 0.96)
FD - STE		0.36 (0.28, 0.53)	0.37 (0.29, 0.55)		0.39 (0.30, 0.57)	0.39 (0.31, 0.57)

FD - % CV		29.5 (22.0, 45.9)	24.7 (18.5, 38.1)		40.6 (30.0, 64.5)	32.4 (24.1, 50.7)
CW - ICC		0.79 (0.53, 0.92)	0.72 (0.42, 0.90)		0.95 (0.87, 0.98)	0.96 (0.89, 0.96)
CW - STE		0.51 (0.39, 0.75)	0.58 (0.44, 0.84)		0.26 (0.20, 0.38)	0.25 (0.19, 0.44)
CW - % CV		35.0 (26.0, 55.0)	42.9 (31.6, 68.5)		20.2 (15.2, 30.8)	19.7 (4.9, 30.1)

The parameters are skeletal muscle blood flow (mBF), oxygen consumption (mV̇O2), total hemoglobin concentration ([tHb]), tissue oxygen saturation (SaO2%/TSI%), and exercise blood-volume change ([tHb] range) at rest, 5% and 15% MVC. Positive and negative error bars denote upper and lower 90% confidence limits, respectively. Thresholds for sample population reliability are 0.20 (low), 0.50 (moderate), 0.75 (high), 0.90 (very high), and 0.99 (nearly perfect).

The parameters are skeletal muscle blood flow (mBF), oxygen consumption (mV̇O2), total hemoglobin concentration ([tHb]), tissue oxygen saturation (SaO2%/TSI%), and exercise blood-volume change ([tHb] range) at rest, 5% and 15% MVC. The magnitude thresholds are 0.1, 0.3, 0.6, 1, and 2 for small, moderate, large, very large, and extremely large. Confidence limits (CL) based on 90% confidence level and expressed as lower CL, upper CL.

Skeletal muscle blood flow and oxygen consumption

For both ND and T2D groups and between NIRS devices, the ICC was high-very high, except for rest and 5% MVC where it was low-moderate (Table 5.3). For both groups, most resting and exercise values for mBF and mV̇O2 between NIRS devices were not substantially different or possibly substantially different. However, likely differences were found in T2D at 5 and 15% MVC for mBF and 5% MVC for $mV̇O_2$. Comparing NIRS devices between groups, there was a likely substantial difference in the

CW NIRS signal at 5% MVC for ND, with possible substantial differences for all other measures except resting which had no substantial difference (See Figure 5.2).

The mBF/m$\dot{V}O_2$ ratios are in Table 5. The ratios for cw-NIRS at rest were almost double to fd-NIRS in ND and ~40% higher in T2D. During exercise, the ratios are closer to the established value of 5 except for cw-NIRS at 5% MVC which is ~6.5 for both groups.

Perfusion index

The ICC value for perfusion index was high to very high for both NIRS devices in both groups (Table 3). Values between FD and CW NIRS were very likely substantially different in ND and most likely substantially different in T2D for rest and exercise. Comparing FD and CW between groups both were likely substantially different. When the perfusion values were normalized to show change from rest, FD and CW NIRS decreased to likely and most likely for ND and T2D, respectively. Between groups, CW NIRS increased to very likely substantially different at 15% MVC with all other comparisons remaining unchanged (See Figure 5.2).

Tissue saturation of oxygen

The ICC value for tissue saturation of O_2 was generally high for FD NIRS and moderate to high for CW NIRS for both groups for TSI% (Table 6.3). Values between FD and CW NIRS were very likely and most likely substantially different in ND and T2D, respectively, for rest and exercise. At rest and 5% MVC FD NIRS was likely substantially different and possibly substantially different at 15% MVC between groups. For rest and exercise CW NIRS was possibly substantially different between groups (Figure 5.2).

Exercise blood-volume change

The ICC values for Exercise blood-volume change between FD and CW NIRS were most likely and possibly substantially different for ND and T2D, respectively, for both 5% and 15% MVC. Between groups, FD NIRS was possibly substantially different for both 5% and 15% MVC and CW NIRS was possibly and likely substantially different for 5% and 15% MVC, respectively (Figure 5.2).

Muscle oxygen recovery capacity (MORC)

The $m\dot{V}O_2$ recovery rate time constant was 31 ± 89 s and 46 ± 142 s for FD NIRS in ND and T2D, respectively. The time constant was 29 ± 103 s and 37 ± 101 s for CW NIRS in ND and T2D, respectively. ICC values were high and low for FD NIRS in ND and T2D, respectively, and low and moderate ICC values for CW NIRS in ND and T2D, respectively. All substantial effects between NIRS devices were trivial.

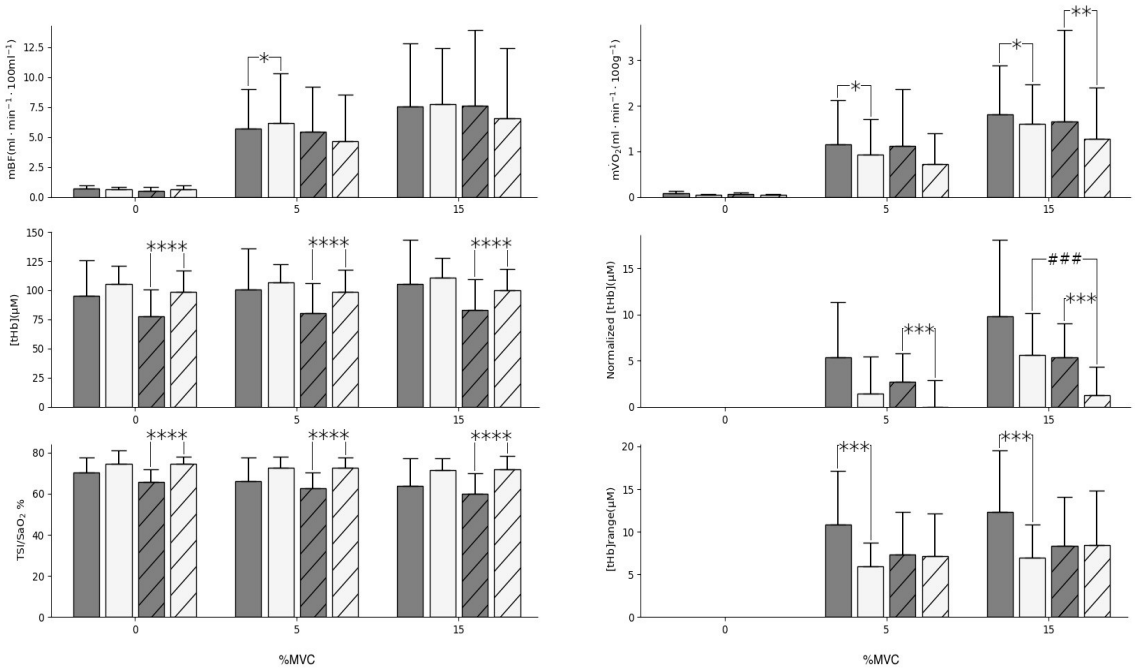

Figure 5.2. Mean values ± standard deviations for all NIRS parameters for non-diabetic (ND; solid) and type 2 diabetic (T2D; hashed) populations from frequency-domain (FD; grey) and continuous-wave (CW; white) NIRS at rest, 5% and 15%. Mean values are staggered for clarity. The parameters are (A) skeletal muscle blood flow (mBF), (B) oxygen consumption (mV̇O2), (C) total hemoglobin concentration ([tHb]), (D) normalized [tHb], (E) tissue oxygen saturation (SaO2%/TSI%) and (F) exercise blood-volume change ([tHb] range). The symbol # denotes substantial differences between T2D and ND groups and * denotes substantial differences within-groups between-technology. Likelihood of substantial difference between values is denoted as #/*, possibly; ##/**, likely; ###/***, very likely; ####/****, most likely.

Table 5.4. The muscle blood flow to oxygen consumption ratio (mBF/m$\dot{V}O_2$) ratio for rest and both exercise intensities for both non-diabetic (ND) and type 2 diabetic (T2D) groups.

	ND			T2D		
	rest	5	15	rest	5	15
FD	9.23	4.91	4.56	8.90	4.93	4.17
CW	17.33	6.37	5.14	13.08	6.59	4.84

Abbreviations: CW, continuous-wave NIRS; FD, frequency-domain NIRS.

Discussion

The primary purpose of the current study was to determine the validity and reproducibility of hemodynamic measures within the skeletal muscle microvascular of healthy and T2D individuals during rest and in response to dynamic exercise when measured with cw-NIRS, compared to fd-NIRS. This comparison is important because cw-NIRS applies constant light scattering correction factors to [Hb] measures, while fd-NIRS measures scattering in real-time to establish accurate [Hb], therefore making it the criterion technology. In addition, we compared parameter values between groups within NIRS devices, assuming fd-NIRS as the criterion, to assess differences between ND and T2D muscle and the effect of applying one set of scattering correction factors to the entire cohort. Using the ICC value to assess reproducibility, for mBF, m$\dot{V}O_2$, and perfusion, both devices were of moderate to high reproducibility during exercise, with lower reproducibility at rest. However, both devices had small to moderate STE and CV% ranging from 19.4% - 76.3%, limiting diagnostic resolution. When comparing ND to T2D, perfusion measures derived from cw-NIRS were underestimated compared to fd-NIRS at rest and during exercise. These results suggest that both NIRS technologies provide for moderately to high reproducibility of mBF and m$\dot{V}O_2$ measures in skeletal muscle research, but suggest measures of perfusion are less precise with cw-NIRS and illuminate the need for more work in investigating best principles for experimental design and analysis approaches and technology selection when considering the use of NIRS as a

tool for measuring skeletal muscle hemodynamics in populations with metabolic health conditions. To the best of our knowledge, this is the first study to assess the validity of cw-NIRS during exercise compared to criterion fd-NIRS, and also the first study to compare devices in an insulin-resistant cohort.

As hypothesized, measures of perfusion, tissue saturation, and exercise induced blood-volume change in T2Ds were substantially different between devices, most likely due to the assumption of constant scattering within the cw-NIRS instead of the measured estimate of real-time scattering provided within the fd-NIRS (Hammer et al., 2019b). Applying a single set of scattering coefficients across all participants within the cw-NIRS does not account for scattering changes due to individual variation in muscle quality and make-up, potentially affecting estimates of [O2Hb], [HHb], and [tHb] (L. F. Ferreira et al., 2006). Calculating [Hb] from literature-based scattering compared to measuring individual scattering-derived [Hb] showed substantial overestimations in [tHb] starting at 21% of peak incremental cycling exercise (L. F. Ferreira et al., 2006) and on the second bout of 6-min heavy leg cycling (Burnley et al., 2002). In fd-NIRS, assuming constant scattering compared with measured, has been shown to significantly overestimate [ΔHb] over time under VO and AO, subsequently increasing the calculated values for mBF and m$\dot{V}$O2 (Hammer et al., 2019b). A particular strength of the current study design was that it directly compared outcomes between cw- and fd-NIRS technologies at rest and during exercise within healthy and diseased cohorts to observe the impact, if any, of the muscle quality and makeup on the NIRS outcomes.

These findings illustrate the importance of accurate measures of the hemoglobin parameters to get actual physiological hemodynamics. For example, decreased perfusion in T2D compared to ND may reflect slower microvascular kinetics (Bauer et al., 2007b) and low capillary density (MÅrin, Per, Björn Andersson, Marcin Krotkiewski, 1994), which is in agreement with the fd- but not the cw-NIRS perfusion measures in the current study limiting the diagnostic potential for cw-NIRS to assess tissue saturation. In addition, cw-NIRS derived change in perfusion from rest to exercise (normalized

perfusion) in T2D (see figure 6.2) and the exercise induced blood-volume change in ND were substantially underestimated compared to fd-NIRS, indicating a decreased sensitivity in cw-NIRS for monitoring changes in perfusion during exercise. Taken together, assumptions used in cw-NIRS appear to be valid for mBF and m$\dot{V}$O2 measures; however, cw-NIRS may not be precise enough to investigate changes in perfusion during exercise.

For mBF and m$\dot{V}$O2 measures, the incremental pattern of change from rest to exercise and from light to moderate workloads was similar for both devices and for both the ND and T2D groups, which was in agreement with our recent report in ND (Lucero et al., 2018) and with other established methodologies to measure mBF like thermodilution using the Fink principle during knee extension exercise (Blomstrand et al., 1997). Moreover, the mBF/m$\dot{V}$O2 ratio during exercise was similar for both devices and both group, and within range of a previous study using NIRS combined with indocyanine green dye flow and fractional tissue oxygen saturation (Vogiatzis et al., 2015). In concurrence, the MORC recovery curve in both groups was within range of previous findings (Southern et al., 2014). Therefore, cw- and fd- NIRS combined with rapid occlusion methodology can be accurately used to assess mBF and m$\dot{V}$O2 responses at rest and to incremental steps of exercise up to 15% MVC and m$\dot{V}$O2 recovery from exercise in both ND and T2D populations.

In empirical research it is important to establish day-to-day reproducibility to validate the methodological utility to render accurate interpretation of experimental results. In the current study, high reproducibility represented by ICC >0.75 for fd and cw-NIRS, in both ND and T2D, were similar to previously established values using cw-NIRS and dynamic knee extension exercise in ND (Lucero et al., 2018); exceptions were the low ICC values for resting mBF in ND and T2D with fd-NIRS compared to cw-NIRS (Table 6.3), which could be due study design differences in using alternative legs and order of rest prior to the first study sampling arm and exercise in the next arm, which would have increased metabolic rate and associated scattering perturbations verified by

lower ICC values in the second test order of the sequence (data not shown). These data confirm the good utility of current protocols for studying skeletal muscle hemodynamic and respiratory response to dynamic exercise, however, appropriate sample size calculations are required to ensure sufficient power.

The current study design contains several limitations. Firstly, each of the two NIRS devices were positioned on opposite legs to provide a practical within-day controlled setting to compare NIRS technologies within participants. The NIRS devices were randomized for leg dominance and starting leg, but it is possible some variability was added to the between-device contrasts, although the within-device reproducibility would be unaffected. Secondly, the groups were not matched for age and BMI. Comparing typical younger healthy to middle-aged diabetic was chosen to show the validity of NIRS in a clinical population and maximize differences in groups for assessing muscle health. However, it is acknowledged that in addition to insulin resistant state, any between-group differences may also be influenced by higher age, generally lower training status, and weekly physical activity duration, although all of these are well-established inherent group characteristics. Thirdly, in the current study, one cardiac cycle for mBF measures was determined using the pulsatile motion of the tHb signal, however, this is not as consistent as using the R_R interval of an ECG overlay. It is recommended that future studies include ECG readings for mBF measures to standardize analysis over the first cardiac cycle as including more than one cardiac cycle may underestimate mBF (Cross & Sabapathy, 2017b). It is also worth noting that since occlusion can only occur between contractions, the resulting [tHb] slope reflects post-contraction values and not exercise *per se* (Rådegran, 1999). However, immediate post-exercise mBF increases in proportion to exercise intensity (Kagaya & Homma, 1997) and reflects the mBF response to exercise (Quaresima et al., 2004). Moreover, NIRS devices are unable to distinguish between hemoglobin and myoglobin, and myoglobin has been said to contribute between 50-70% of NIRS derived [Hb] (Davis & Barstow, 2013). Future research could further delineate the contribution of myoglobin to the NIRS signal at rest and during increasing exercise intensity, and the effect on calculated hemoglobin

values for all NIRS measures. Due to limitations in cw-NIRS, it is helpful that researchers abide by recommendations and report parameters identified by previous research for optimizing validity and reliability, and to be able to compare results between studies (M. Ferrari et al., 2011). Finally, in fd-NIRS measures, a single scattering coefficient was calculated at rest and held constant throughout the experiment. Although it is known that the scattering coefficient changes during exercise (Koga et al., 2007) and as a result of the rapid occlusions (Hammer et al., 2019a), it was assumed constant to isolate the effect of applying a single set of scattering correction factors to all participants as in cw-NIRS. Future research should investigate the effect of applying dynamic scattering on the same NIRS derived metrics and identify the effect of rapid occlusions on scattering and subsequent derived [Hb].

Conclusion

In summary, mBF and mV̇O2 at rest and up to 15% MVC during knee extension exercise derived from cw-NIRS and fd-NIRS are reproducible and demonstrate an intensity-associated pattern in agreement with previous research. In contrast, measures of perfusion index, tissue saturation, and [tHb] range from cw-NIRS were more often substantially different than fd-NIRS, especially in T2D. Based on these findings, assumptions used in cw-NIRS appear to be valid for mBF and m$\dot{V}O_2$ measures. However, care must be taken when interpreting results for perfusion, tissue saturation, and [tHb] range, especially in clinical populations, where we recommend fd-NIRS is used. Overall, both NIRS devices proved to be reproducible and have potential for non-invasive measures of hemodynamic and oxygen uptake kinetics in the skeletal muscle of healthy and T2D individuals.

References

Adami, A., Harry, X., & Rossiter, B. (2017). Principles, insights, and potential pitfalls of the noninvasive determination of muscle oxidative capacity by near-infrared spectroscopy. *Journal of Applied Physiology*, *124*(1), 245–248. https://doi.org/10.1152/japplphysiol.00445.2017

Aisbett, J., Lakens, D., & Sainani, K. (2020). *Magnitude Based Inference in Relation to One-sided Hypotheses Testing Procedures*. https://doi.org/10.31236/OSF.IO/PN9S3

Bauer, T. A., Reusch, J. E. B., Levi, M., & Regensteiner, J. G. (2007). Skeletal Muscle Deoxygenation After the Onset of Moderate Exercise Suggests Slowed Microvascular Blood Flow Kinetics in Type 2 Diabetes. *Diabetes Care*, *30*(11), 2880–2885. https://doi.org/10.2337/DC07-0843

Blomstrand, E., Rådegran, G., & Saltin, B. (1997). Maximum rate of oxygen uptake by human skeletal muscle in relation to maximal activities of enzymes in the Krebs cycle. *Journal of Physiology*, *501*(2), 455–460. https://doi.org/10.1111/j.1469-7793.1997.455bn.x

Burnley, M., Doust, J. H., Ball, D., Jones, A. M., Vanhatalo, A., Poole, D. C., Dimenna, F. J., Bailey, S. J., Physiol, A. J., Integr, R., Physiol, C., Cannon, D. T., White, A. C., Andriano, M. F., Kolkhorst, F. W., Harry, B., Chidnok, W., Barker, A. R., Armstrong, N., & Physiol, J. A. (2002). Effects of prior heavy exercise on VO(2) kinetics during heavy exercise are related to changes in muscle activity. *Journal of Applied Physiology (Bethesda, Md. : 1985)*, *93*(1), 167–174. https://doi.org/10.1152/japplphysiol.01217.2001

Clark, M. G. (2008). Impaired microvascular perfusion: a consequence of vascular dysfunction and a potential cause of insulin resistance in muscle. *AJP: Endocrinology and Metabolism*, *295*(4), E732–E750. https://doi.org/10.1152/ajpendo.90477.2008

Cross, T. J., & Sabapathy, S. (2017a). The impact of venous occlusion per se on forearm muscle blood flow: implications for the near-infrared spectroscopy venous occlusion technique. *Clinical Physiology and Functional Imaging*, *37*(3), 293–298. https://doi.org/10.1111/cpf.12301

Cross, T. J., & Sabapathy, S. (2017b). The impact of venous occlusion per se on forearm muscle blood flow: implications for the near-infrared spectroscopy venous occlusion

technique. *Clinical Physiology and Functional Imaging*, *37*(3), 293–298. https://doi.org/10.1111/cpf.12301

Davis, M. L., & Barstow, T. J. (2013). Estimated contribution of hemoglobin and myoglobin to near infrared spectroscopy. *Respiratory Physiology and Neurobiology*, *186*(2), 180–187. https://doi.org/10.1016/j.resp.2013.01.012

Duncan, A., Meek, J. H., Clemence, M., Elwell, C. E., Tyszczuk, L., Cope, M., & Delpy, D. (1995). Optical pathlength measurements on adult head, calf and forearm and the head of the newborn infant using phase resolved optical spectroscopy. *Physics in Medicine and Biology*, *40*(2), 295–304. https://doi.org/10.1088/0031-9155/40/2/007

Fantini, S., Franceschini, M. A., Fishkin, J. B., Barbieri, B., & Gratton, E. (1994). Quantitative determination of the absorption spectra of chromophores in strongly scattering media: a light-emitting-diode based technique. *Applied Optics*, *33*(22), 5204. https://doi.org/10.1364/AO.33.005204

Ferrari, M., Muthalib, M., & Quaresima, V. (2011). The use of near-infrared spectroscopy in understanding skeletal muscle physiology: recent developments. *Philosophical Transactions of the Royal Society A: Mathematical, Physical and Engineering Sciences*, *369*(1955), 4577–4590. https://doi.org/10.1098/rsta.2011.0230

Ferreira, L. F., Hueber, D. M., & Barstow, T. J. (2006). Effects of assuming constant optical scattering on measurements of muscle oxygenation by near-infrared spectroscopy during exercise. *Journal of Applied Physiology*, *102*(1), 358–367. https://doi.org/10.1152/japplphysiol.00920.2005

Grassi, B., & Quaresima, V. (2016a). Near-infrared spectroscopy and skeletal muscle oxidative function in vivo in health and disease: a review from an exercise physiology perspective. *Journal of Biomedical Optics*, *21*(9), 91313.

Grassi, B., & Quaresima, V. (2016b). <!-- *** Custom HTML *** -->Near-infrared spectroscopy and skeletal muscle oxidative function *in vivo* in health and disease: a review from an exercise physiology perspective. *Journal of Biomedical Optics*, *21*(9), 091313. https://doi.org/10.1117/1.JBO.21.9.091313

Groebe, K., & Thews, G. (1990). Calculated intra- and extracellular PO2 gradients in heavily working red muscle. *American Journal of Physiology-Heart and Circulatory Physiology*, *259*(1), H84–H92. https://doi.org/10.1152/ajpheart.1990.259.1.H84

Hamaoka, T., McCully, K. K., Niwayama, M., & Chance, B. (2011). The use of muscle near-infrared spectroscopy in sport, health and medical sciences: recent developments. *Philosophical Transactions of the Royal Society A: Mathematical, Physical and Engineering Sciences*, *369*(1955), 4591–4604. https://doi.org/10.1098/rsta.2011.0298

Hammer, S. M., Hueber, D. M., Townsend, D. K., Huckaby, L. M., Alexander, A. M., Didier, K. D., & Barstow, T. J. (2019a). Effect of assuming constant tissue scattering on measured tissue oxygenation values during tissue ischemia and vascular reperfusion. *Journal of Applied Physiology*, *127*(1), 22–30. https://doi.org/10.1152/japplphysiol.01138.2018

Hammer, S. M., Hueber, D. M., Townsend, D. K., Huckaby, L. M., Alexander, A. M., Didier, K. D., & Barstow, T. J. (2019b). Effect of assuming constant tissue scattering on measured tissue oxygenation values during tissue ischemia and vascular reperfusion. *Journal of Applied Physiology*, *127*(1), 22–30. https://doi.org/10.1152/japplphysiol.01138.2018

Henninger, A. M. J., Eliasson, B., Jenndahl, L. E., & Hammarstedt, A. (2014). Adipocyte Hypertrophy, Inflammation and Fibrosis Characterize Subcutaneous Adipose Tissue of Healthy, Non-Obese Subjects Predisposed to Type 2 Diabetes. *PLoS ONE*, *9*(8), e105262. https://doi.org/10.1371/journal.pone.0105262

Hopkins, W. G. (2007). A spreadsheet for deriving a confidence interval, mechanistic inference and clinical inference from a P value. *Sportscience*, *11*, 16–21. https://go.galegroup.com/ps/i.do?p=AONE&sw=w&u=googlescholar&v=2.1&it=r&id=GALE%7CA189289447&sid=googleScholar&asid=5f628ac6

Hopkins, W. G. (2020). Magnitude-Based Decisions as Hypothesis Tests. *Sportscience*, *24*.

Ijichi, S., Kusaka, T., Isobe, K., Okubo, K., Kawada, K., Namba, M., Okada, H., Nishida, T., Imai, T., & Itoh, S. (2005). Developmental changes of optical properties in neonates determined by near-infrared time-resolved spectroscopy. *Pediatric Research*, *58*(3), 568–573. https://doi.org/10.1203/01.PDR.0000175638.98041.0E

Kagaya, A., & Homma, S. (1997). Brachial arterial blood flow during static handgrip exercise of short duration at varying intensities studied by a Doppler ultrasound

method. *Acta Physiologica Scandinavica*, *160*(3), 257–265. https://doi.org/10.1046/j.1365-201X.1997.00158.x

Koga, S., Poole, D. C., Ferreira, L. F., Whipp, B. J., Kondo, N., Saitoh, T., Ohmae, E., & Barstow, T. J. (2007). Spatial heterogeneity of quadriceps muscle deoxygenation kinetics during cycle exercise. *Journal of Applied Physiology*, *103*(6), 2049–2056. https://doi.org/10.1152/japplphysiol.00627.2007

Lucero, A. A., Addae, G., Lawrence, W., Neway, B., Credeur, D. P., Faulkner, J., Rowlands, D., & Stoner, L. (2018). Reliability of muscle blood flow and oxygen consumption response from exercise using near-infrared spectroscopy. *Experimental Physiology*, *103*(1), 90–100. https://doi.org/10.1113/EP086537

MÅrin, Per, Björn Andersson, Marcin Krotkiewski, and P. B. (1994). Muscle fiber composition and capillary density in women and men with NIDDM. *Diabetes Care*, *17*(5), 382–386. http://care.diabetesjournals.org/content/17/5/382.short

Miura, H., McCully, K., Nioka, S., & Chance, B. (2004). Relationship between muscle architectural features and oxygenation status determined by near infrared device. *European Journal of Applied Physiology*, *91*(2–3), 273–278. https://doi.org/10.1007/s00421-003-0964-6

Quaresima, V., Ferrari, M., Franceschini, M. A., Hoimes, M. L., & Fantini, S. (2004). Spatial distribution of vastus lateralis blood flow and oxyhemoglobin saturation measured at the end of isometric quadriceps contraction by multichannel near-infrared spectroscopy. *Journal of Biomedical Optics*, *9*(2), 413. https://doi.org/10.1117/1.1646417

Rådegran, G. (1999). Limb and skeletal muscle blood flow measurements at rest and during exercise in human subjects. *Proceedings of the Nutrition Society*, *58*(4), 887–898. https://doi.org/10.1017/S0029665199001196

Ryan, T. E., Erickson, M. L., Brizendine, J. T., Young, H.-J., & McCully, K. K. (2012). Noninvasive evaluation of skeletal muscle mitochondrial capacity with near-infrared spectroscopy: correcting for blood volume changes. *Journal of Applied Physiology*, *113*(2), 175–183. https://doi.org/10.1152/japplphysiol.00319.2012

Ryan, Terence E., Brophy, P., Lin, C.-T., Hickner, R. C., & Neufer, P. D. (2014). Assessment of *in vivo* skeletal muscle mitochondrial respiratory capacity in humans by near-infrared spectroscopy: a comparison with *in situ* measurements. *The Journal of Physiology*, *592*(15), 3231–3241. https://doi.org/10.1113/jphysiol.2014.274456

Scheuermann-Freestone, M., Madsen, P. L., Manners, D., Blamire, A. M., Buckingham, R. E., Styles, P., Radda, G. K., Neubauer, S., & Clarke, K. (2003). Abnormal cardiac and skeletal muscle energy metabolism in patients with type 2 diabetes. *Circulation*, *107*(24), 3040–3046. https://doi.org/10.1161/01.CIR.0000072789.89096.10

Southern, W. M., Ryan, T. E., Reynolds, M. A., & McCully, K. (2014). Reproducibility of near-infrared spectroscopy measurements of oxidative function and postexercise recovery kinetics in the medial gastrocnemius muscle. *Applied Physiology, Nutrition, and Metabolism*, *39*(5), 521–529. https://doi.org/10.1139/apnm-2013-0347

Suzuki, S., Takasaki, S., Ozaki, T., & Kobayashi, Y. (1999). Tissue oxygenation monitor using NIR spatially resolved spectroscopy. In B. Chance, R. R. Alfano, & B. J. Tromberg (Eds.), *Optical Tomography and Spectroscopy of Tissue III* (Vol. 3597, pp. 582–592). International Society for Optics and Photonics. https://doi.org/10.1117/12.356862

Tschakovsky, M. E., Shoemaker, J. K., & Hughson, R. L. (1996). Vasodilation and muscle pump contribution to immediate exercise hyperemia. *The American Journal of Physiology*, *271*(4 Pt 2), H1697-701. https://doi.org/10.1152/ajpheart.1996.271.4.H1697

Van Beekvelt, Borghuis, M. S., Van Engelen, B. G. M., Wevers, R. A., & Colier, W. N. J. M. (2001). Adipose tissue thickness affects in vivo quantitative near-IR spectroscopy in human skeletal muscle. *Clinical Science*, *101*, 21–28. https://pdfs.semanticscholar.org/245c/3c015e19b98384ca48a671593e9a5d0552b5.pdf

van Beekvelt, M., Colier, W. N. J. M., Wevers, R. O. N. A., Engelen, B. G. M. V. A. N., Wevers, R. A., & Perfor-, B. G. M. V. E. (2001). *Performance of near-infrared spectroscopy in measuring local O 2 consumption and blood flow in skeletal muscle*. 511–519.

Vogiatzis, I., Habazettl, H., Louvaris, Z., Andrianopoulos, V., Wagner, H., Zakynthinos, S., & Wagner, P. D. (2015). A method for assessing heterogeneity of blood flow and metabolism in exercising normal human muscle by near-infrared spectroscopy. *Journal of Applied Physiology*, *118*(6), 783–793. https://doi.org/10.1152/japplphysiol.00458.2014

Watanabe, K., & Akima, H. (2011). Effect of knee joint angle on neuromuscular activation of the vastus intermedius muscle during isometric contraction. *Scandinavian Journal of Medicine and Science in Sports*, *21*(6), 412–420. https://doi.org/10.1111/j.1600-0838.2011.01347.x

6 - Deoxygenation kinetics During Ramp Cycle Exercise Correlate to Aerobic and Mitochondrial Capacity

Adam A. Lucero[1], Kim Gaffney[1], Lee Stoner[1,3], James Faulkner[1,2], David S. Rowlands[1].

[1]School of Sport, Exercise and Nutrition, Massey University, Wellington and Auckland, New Zealand, [2]Department of Sport and Exercise, University of Winchester, Winchester, United Kingdom. [4]Department of Exercise and Sport Science, University of North Carolina at Chapel Hill, NC, USA.

Correspondence:

Adam Lucero

School of Sport, Exercise, and Nutrition

Massey University

PO Box 756, Wellington

New Zealand

Adamluco1@gmail.com

ORCID: 0000-0002-2743-0209

Abstract

Recently, near-infrared spectroscopy (NIRS) has been used to measure hemoglobin deoxygenation kinetics during ramp cycle exercise to investigate the dynamics of the coupling between oxygen consumption and delivery in healthy individuals. The purpose of this study was to characterize the deoxygenation kinetics during ramp cycle exercise in a cohort of 24 middle-aged non-insulin dependent sedentary men with type-2 diabetes and to align against oxygen consumption (VO_2), mitochondrial and exercise capacity, and skeletal muscle function. The participants performed incremental ramp cycle exercise to volitional exhaustion while NIRS and systemic VO_2 was measured continuously using breath-by-breath online gas analysis. Skeletal muscle biopsies were performed in the same muscle on the opposite leg of NIRS measures. The NIRS and VO_2 data during incremental exercise were modeled as a double linear function and model parameters associated with other measures using Pearson correlation. Primary phase parameters of deoxygenation kinetics were substantially correlated to peak power and $\dot{V}O_2$max, while secondary phase parameters were strongly correlated to mitochondrial density and COX Activity, but not CS. Combining NIRS with $\dot{V}O_2$ during ramp cycle exercise has potential in investigating skeletal muscle respiratory characteristics and capacity, and exercise tolerance in T2D.

Introduction

Individuals with metabolic diseases, such as, Type 2 Diabetes (T2DM) are known to have impaired microvascular and skeletal muscle respiratory dynamics, which has been associated with reduced glucose disposal and insulin resistance (Sayer et al., 2005). However, individual plasticity is variable and exercise capacity and tolerance limited, relative to healthy individuals. Improving skeletal muscle function and respiration at the microvascular level could benefit from increased understanding of hemodynamic function during exercise and the individual contributions of different systemic components of oxygen delivery and utilization in working muscle.

Recently, near-infrared spectroscopy (NIRS) used during ramp cycle exercise in the *vastus lateralis* has been shown to reflect the arterial-venous oxygen content difference (a-vO_2) (DeLorey et al., 2003; Mancini et al., 1994) across exercise intensities. Combining this with measures of breath-by-breath oxygen consumption provides information on the relationship between microvascular oxygen delivery (DO_2) to oxygen consumption (m$\dot{V}O_2$) (Spencer et al., 2012). These findings demonstrated how the dynamics of DO_2-m$\dot{V}O_2$ behave during incremental exercise to exhaustion, which provides information on microvascular function and limits to tissue oxygenation and associations with muscle respiratory capacity.

Skeletal muscle $\dot{V}O_2$m assessment is done by rearranging the Fick equation (DO_2 = $\dot{V}O_2$m /a-vO_2 where $\dot{V}O_2$m is the systemic oxygen consumption ($\dot{V}O_2$) adjusted to reflect changes in muscle $\dot{V}O_2$ (Murias et al., 2011) and a-vO_2 is the NIRS derived %Δ[HHb]. The temporal profile of %Δ[HHb] to increasing exercise intensity has been modeled and characterized in physically active and sedentary young adults (Boone et al., 2009; Spencer et al., 2012), and compared against older adults (Gravelle et al., 2012). In addition, NIRS has been used in combination with traditional ramp cycle exercise to assess temporal changes in microvascular oxygen extraction within the *vastus lateralis* (VL) (Boone & Bourgois, 2012). Previously we reported that mBF and m$\dot{V}$O2 at rest and

up to 15% MVC during knee extension exercise derived from cw-NIRS is reproducible in T2Ds and demonstrates an intensity-associated pattern in agreement with the literature. The resultant parameters derived from modeling the temporal profile of %Δ[HHb] to increasing exercise intensity from onset to exhaustion has been said to reflect the muscles ability to respond to exercise utilizing aerobic and anaerobic pathways. This test has yet to be done in T2Ds, and has not been evaluated against other markers of aerobic and anaerobic function in skeletal muscle to determine if an individuals aerobic and anaerobic fitness can be assessed from the temporal profile of %Δ[HHb] (Spencer et al., 2012). For example, the profile of %Δ[HHb] plateaus towards exhaustion, which is thought to indicate a slowing of O2 extraction and increased reliance on anaerobic metabolism until an eventual upper limit. The ability of an individual to maintain exercise in this phase is thought to reflect the ability of the mitochondria to continue to create energy despite the low [O_2] in the muscle (Spencer et al., 2012). If this interpretation is correct than we should see correlations between these parameters and other markers of anaerobic and mitochondrial function. Therefore, the purpose of this study was to characterize the parameter estimates for %Δ[HHb] and $\dot{V}O_2$ modeling in T2Ds and correlate with other measures relating to the ability of the active muscles for the metabolism, delivery, and consumption of O_2 to better understand limits to exercise tolerance in T2D.

Methods

Participants

24 middle-aged non-insulin dependent sedentary males with clinically diagnosed T2D via HbA1c >48 mmol/mol (55.8±5.4y, BMI 28.1±3.3, fasting blood glucose 9.4±3.5, HBA) were recruited from local medical centers in Wellington, NZ. Exclusion criteria included smoking or had greater than 12 mm of adipose tissue thickness over the NIRS probe region of interest. The Massey University Human Ethics Committee (13/NTB/69) approved the study and all participants were informed of any risks and discomfort associated with the experiments prior to providing written informed consent.

Participants completed a medical history questionnaire and cleared for participation by a physician following electrocardiogram (ECG) examination at rest and during exercise.

Table 6.1 Mean values and standard deviations for participant characteristics.

	Age	Height (m)	Weight (kg)	ATT (cm)	VL (cm)	VL Belly (cm)
Mean	57.8	174.6	91.9	3.06	2.15	3.90
SD	5.2	7.1	15.5	1.11	0.40	1.31

Abbreviations: ATT, adipose tissue thickness; VL, vastus lateralis; VL Belly, distance from skin to the belly of the VL calculated as ATT + 1/2*VL

Experimental Procedure

Each participant was tested on four different days, the first three being conducted in a dimly-lit, temperature controlled room (20.5˚C, SD 0.8) and the fourth visit was in a hospital with a licensed physician. On visit 1 participants were familiarized with all testing procedures. Cardiac screening via ECG was performed during the familiarization full ramp cycle exercise test. Visit 2 and 3 comprise exercise testing protocols, while visit 4 was conducted in a hospital where participants underwent a muscle biopsy and blood sample for fasted blood [glucose] (FBG). On visit 2 participants underwent a knee extension protocol for assessing resting and exercise perfusion, mBF, m$\dot{V}O_2$, and MORC. On visit 3, participants performed a continuous ramp test protocol to volitional exhaustion on an electronically braked ergometer (VeloTron Racer Mate, Seattle, WA). To measure $\dot{V}O_2$, a breath-by-breath automatic gas exchange system (Vmax Spectra 29c, Sensormedics Corporation, Yorba Linda, CA, USA) was used, and HR was monitored using a wireless chest strap telemetry system (Polar Electro T31, Kempele, Finland). The protocol consisted of a 3 min warm up at 40 W before increasing 1 W every 4 S.

Participants were instructed to keep their hand on the handlebar and maintain a cadence of 70 rpm and the test was terminated when the participant could no longer maintain 60 rpms despite strong verbal encouragement. All visits occurred between the hours of 6-9 am following an overnight fast, having consumed only water, refraining from caffeine and supplement intake that morning. Participants also avoided strenuous physical activity and alcohol for 24 hours prior to experimentation.

Near infrared spectroscopy

Skeletal muscle perfusion, blood flow, and temporal profile of %Δ[HHb] were assessed using a continuous wave NIRS device (PortaLite, Artinis Medical Systems BV, the Netherlands) during knee extension and ramp cycle exercise. This device emitted wavelengths of 760 and 850 nm to detect relative changes in concentrations of oxygenated hemoglobin [O2Hb] and deoxygenated hemoglobin [HHb], respectively, as well as total blood volume ([tHb] = [O_2Hb + HHb]). Both wavelengths were emitted from three transmitters with inter-optode distances of 3.0, 3.5, and 4.0 cm, allowing for theoretical penetration distances of 1.5-2 cm (B. Chance et al., 1992). The [HHb] signal was used for analysis as it has been shown to be related to microvascular oxygen extraction (DeLorey et al., 2003) and less susceptible to skin blood flow than [O_2Hb] (Buono et al., 2005). Photon scattering within the tissue was corrected for using a differential path-length factor of 4.0. Data were collected at 10 Hz (Oxysoft, Artinis Medical Systems BV, the Netherlands). The NIRS probe was securely adhered to the skin parallel to the muscle fibers, approximately two-thirds from the top of the VL over the muscle belly using a custom-made template. The probe location was marked to obtain reproducibility for repeated NIRS testing. A custom-made cover shielded the probe from ambient light while allowing it to move with the skin during contractions minimizing changes in contact pressure (T. Hamaoka et al., 2011). The thickness of the VL at this location, along with adipose tissue thickness, was determined using B-mode ultrasound (Terason, United Medical Instruments Inc., San Jose, CA, USA).

Skeletal muscle biopsy

A muscle biopsy of the VL was taken in the opposite leg from NIRS measures approximately 45 minutes after supine rest under local anesthesia (2% lidocaine) using a 5-mm diameter biopsy needle (Bergstrom). Sterile tubing was attached to the biopsy needle and a syringe was used to apply negative pressure for muscle sample collection. Baseline biopsies were taken about two-thirds from the top of the VL over the muscle belly. Post-intervention biopsies were taken 3 cm above the baseline sample. All biopsies were taken at an approximate depth of 3.5 cm. The biopsied muscle tissue was either flash-frozen using isopentane-liquid nitrogen freezing method and stored at -80˚C for future mitochondrial enzyme analysis or placed in Karnovsky's fix for 2 hours and then stabilized in a buffer solution for electron microscopy. Muscle samples were diluted in cooled lysis buffer (10mM Hepes pH 7.4, 70mM Sucrose, 1mM EDTA, 220mM Mannitol, 0.3 % Brij-35) by 25 x times the sample weight and blended three time with IKA (model) for 20s. Homogenate was placed on an ice shaker and further homogenized by passing it through a 25-gauge syringe 20 times. Homogenate was then centrifuged at 600g for 15 min at 4˚C. The supernatant was removed while the pellet was re-suspended in 25 µL of lysis buffer, further homogenized and re-centrifuged. The combined supernatants were pipetted into 30 µL aliquots and frozen at -80˚C. Protein concentration was measured using a BCA assay kit (Thermo Fisher Scientific).

Cytochrome C Oxidase and Citrate Synthase activity

To assess mitochondrial enzymatic activity, Cytochrome C Oxidase (COX) and Citrate Synthase (CS) were Cytochrome C oxidase activity were measured. The COX enzyme was assessed spectrophotometrically at 25˚ C in a microplate reader (model) by a standard method (Trounce et al., 1996). Cytochrome C absorbs strongly at 550 nm in the reduced state. Briefly, upon oxidation cytochrome C oxidase the absorbance weakens. Thus, the activity of COX is proportional to the decrease in absorbance at 550 nm.

Citrate synthase activity was assessed spectrophotometrically at 25˚ C in a microplate reader by a standard method (Trounce et al., 1996). Briefly, Citrate synthase catalyzes the conversion of oxaloacetate and acetyl-CoA into citrate and thiol-CoA. This reaction is linked in the assay by the reaction of thiol-CoA with 5,5′-Dithiobis(2-nitrobenzoic acid) (DTNB) to form the yellow colored TNB, which can be measured at 412 nm. Thus the activity of citrate synthase is proportional to the increase in the absorbance at 412 nm.

Mitochondrial assessments

Mitochondrial and lipid densities for each component was determined using Image J (version 1.48v, National Institutes of Health, Bethesda, MD) by manually tracing only clearly discernible outlines of SS and IMF mitochondria on electron microscopy images using a graphic tablet (MP1060-HA60, Monoprice, California). A minimum of 10 intermyofibrillar and 10 subsarcolemmal images of a muscle cell were taken for each muscle tissue sample (Morada Camera and Item Soft Imaging System, Philips CM100 TEM).

Data Analysis

Breath-by-breath $\dot{V}O_2$ values were processed using a 15-breath rolling average (Robergs et al., 2010) and interpolated into 1s bins. The [HHb] signal was was averaged into 1s bins and normalized to the total amplitude of the response (%Δ[HHb]), such that 0% represented the steady state value represented as the average of the last 30 seconds of the 40 watt warm-up period and 100% represented the highest average (Δ[HHb]peak) observed during any 20 s of exercise. Subsequently, $\dot{V}O_2$ and [HHb] data was averaged into half-minute increments by using 10 s averages from the 5 s prior to and after the half-minute increment. The %Δ [HHb] data was time aligned to the $\dot{V}O_2$ data by left-shifting the $\dot{V}O_2$ data by 25s to account for the circulatory transit delay between muscle and lung so that changes in active muscle $\dot{V}O_2$ ($\dot{V}O_2$m) were aligned with changes in the

%Δ [HHb] signal (Boone et al., 2009). 25s instead of 20s was chosen to more accurately reflect the current population (Murias et al., 2011).

The %Δ[HHb] as a function of V̇O2 was modeled as a best fit double linear function, the first linear segment (phase b) given as $y = [y1 \cdot (BP – x) + y2 \cdot (x – x1)]/(BP- x1)$ and the second linear segment (phase c) given as $y = [y2 \cdot (x2 – x) + y3 \cdot (x-BP)]/(x2 – BP)$ where x1 and x2 represent the minimum and maximum x (V̇O2) values, respectively; y1 and y3 represent the predicted %Δ[HHb] at x1 and x2, respectively; BP represents the x value at the breakpoint between the two segments; and y2 represents the predicted %Δ[HHb] at BP (Murias et al., 2013). Since phase b and phase c represent light-moderate and moderate-high intensity exercise, the lower and upper bounds of the BP were set to 50 and 80% $\dot{V}O_2$peak, respectively (Okushima et al., 2015; Spencer et al., 2012). The double-linear function was fit using numpy piecewise functions in python (Python Software Foundation. Python Language Reference, version 3.6.2, Anaconda custom).

Statistics

All parameter estimates were compared using Pearson product moment correlation to quantify the relationship using Statistical Package for Social Sciences version 21 (SPSS, Inc., Chicago, Illinois). Intramyocellular lipid, GLUT4, and capillary density data were log-transformed prior to analysis to account for heteroscadasticity. Inferences as to the standardised effect size from Pearson correlation were constructed using published spreadsheets. Correlations were reported with 90% confidence intervals. Least squares linear regression analysis was done on measures of aerobic capacity and primary phase parameters using the least squares method. The threshold for smallest substantial correlation was 0.1 (Will G. Hopkins, 2007). Hypotheses of inferiority (substantial negative) and superiority (substantial positive) were rejected if their respective p values ($p–$ and $p+$, given by the areas of the sampling distribution of the effect in substantial negative and positive values, respectively) were <0.05; rejection of both hypotheses represents a decisively trivial effect in equivalence testing. If one

hypothesis was rejected, the p value for the other hypothesis corresponds to the posterior probability of a substantial true magnitude of the effect in a reference-Bayesian analysis with a minimally informative prior (Will G Hopkins, 2020) and was interpreted, when >0.25, with the following scale: >0.25, possibly; >0.75, likely; >0.95, very likely; >0.995, most likely (Will G. Hopkins, 2007); the probability of a trivial true magnitude (1 – p– – p+) was also interpreted, when >0.25, with the same scale. Probabilities were not interpreted for effects with inadequate precision at the 90% level, defined by failure to reject both hypotheses (p– >0.05 and p+ >0.05). The hypothesis of non-inferiority or non-superiority was rejected if its p value (pN– = 1 – p– or pN+ = 1 – p+) was <0.05, representing a decisively substantial effect in minimum-effects testing: very likely or most likely substantial. Probabilities were then adjusted for type-1 error by appropriate familywise Bonferroni adjustment.

Results

Parameter estimates for the double-linear model are given in Table 2. By design, $\dot{V}O_2$peak, $\dot{V}O_2$peak/kg, and peak power ranged from 1.4 – 4.0 L·min-1, 15.2 – 51.2 L·min-1·kg-1, and 102 – 268 watts, respectively. Data for muscle biopsy and NIRS knee extension measures are in Table 7.3.

Pearson correlation matrix and statistical decisions and inferential outcomes are illustrated within a heat map in Figure 6.3. Primary phase parameters m1 and b1 were moderate to strongly compatible with a substantial association between resting mBF and aerobic capacity measures of $\dot{V}O_2$peak, $\dot{V}O_2$peak/kg, and peak power. The breakpoint transition from phase I to phase II was very likely correlated with mitochondrial density and lipid density, and most likely correlated with capillary-to-fiber ratio. Secondary phase parameters were very likely correlated with mitochondrial density, CS and COX activity. Mitochondrial density was also correlated with $\dot{V}O_2$peak/kg, CS, lipid density, CF Ratio and [tHb] range. Resting mBF was correlated with PP. However, only possible or no

correlation was seen FBG or exercise NIRS measures of mBF, perfusion, blood-volume change, or TSI%.

Linear regression analysis on measures of aerobic capacity and primary phase parameters are illustrated in Figure 4 with the equation of the line and the adjusted R2. The slope of the %Δ[HHb] during the primary phase, m1, was inversely correlated to all three aerobic measures. In contrast, the y-intercept of the primary phase, b1, was positively correlated against all three aerobic measures.

Table 6.2. Parameter estimates for double-linear (%Δ[HHb]) model as a function of systemic VO_2.

m1	b1	m2	b2	BP
98.0 ± 62.0	-89.0 ± 53.1	-35.1 ± 260.0	101.3 ± 360.0	57.6% VO_2m ± 9.6

Values are expressed as means ± SD, derived from each individual. m is the slope of the linear regression and b is the y-intercept of the linear regression for the equation y = mx + b. m1 and m2 are the slopes of the linear regression before and after the %Δ[HHb]-break point, respectively; b1 and b2 are the y-intercept of linear regression before and after the %Δ[HHb]-break point, respectively.

Table 6.3. Outcome parameters derived from skeletal muscle biopsy and NIRS evaluation during knee extension.

Muscle Biopsy Measures					
FBG	**COX**	**CS**	**mito_d**	**lipid_d**	**C/F Ratio**
9.56 (4.58)	0.09 (0.04)	0.10 (0.08)	25329 (11464)	4368 (2798)	0.66 (0.29)

NIRS Measures						
r_[tHb]	**r_TSI**	**r_mBF**	**e_[tHb]**	**[tHb] range**	**e_TSI**	**e_mBF**
53.05 (22.19)	69.08 (22.10)	0.05 (0.03)	50.47 (20.26)	4.22 (3.22)	62.80 (20.16)	0.13 (0.11)

Data are means (SD). Abbreviations and units: FBG, fasting blood glucose (mmol·L-1); COX, Cytochrom C Oxidase activity (µmol·ml -1 ·min -1); CS, Citrate Synthase activity (µmol·ml -1 ·min -1); mito_d, Mitochonrial density (pixels/image x 1000); lipid_d, Lipid density (pixels/image x 1000); C/F Ratio, Capillary to fiber ratio (%); r_[tHb], resting perfusion (µM); r_TSI, Resting tissue saturation index (%); r_mBF, Resting muscle blood flow (mL·min^{-1}·100 mL^{-1}); e_[tHb], Exercise perfusion (µM); [tHb] range, Blood-volume change (µM); e_TSI, Exercise tissue saturation index (%); e_mBF, Exercise muscle blood flow (mL·min^{-1}·100 mL^{-1}).

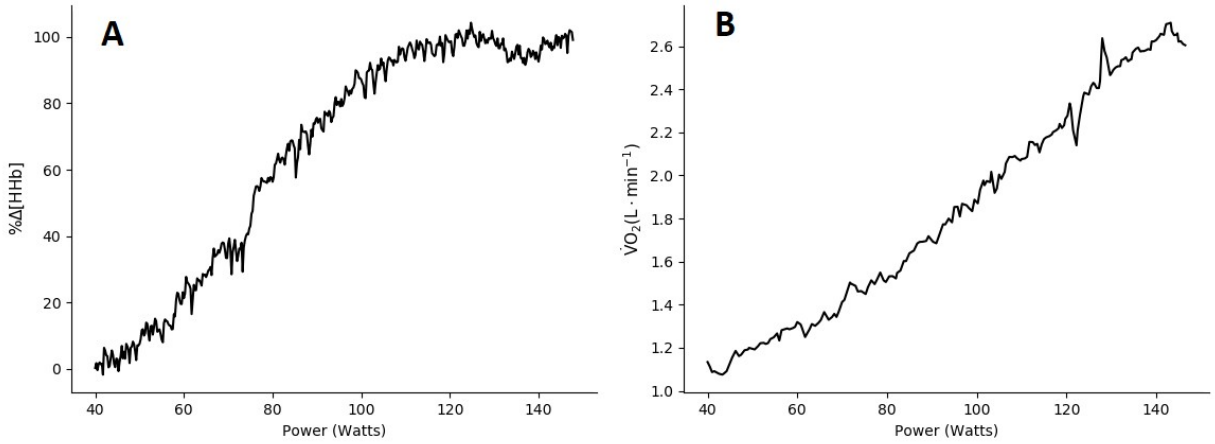

Figure 6.1. Representative plot for an individual of (A) second-by-second normalized

%Δ[HHb] derived from NIRS assessment, and (b) breath-by-breath $\dot{V}O_2$ against absolute external power output during a cycling ramp incremental test.

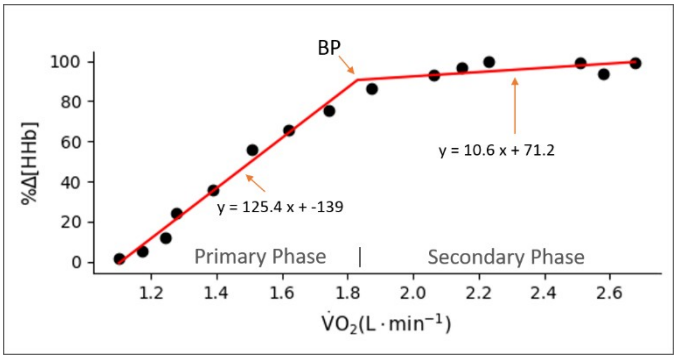

Figure 6.2. Representative profile for O2 extraction (%Δ[HHb]) as a function of systemic $\dot{V}O_2$ for a representative participant. Model fit is a double-linear where the break point (BP) indicates the split of the two segments.

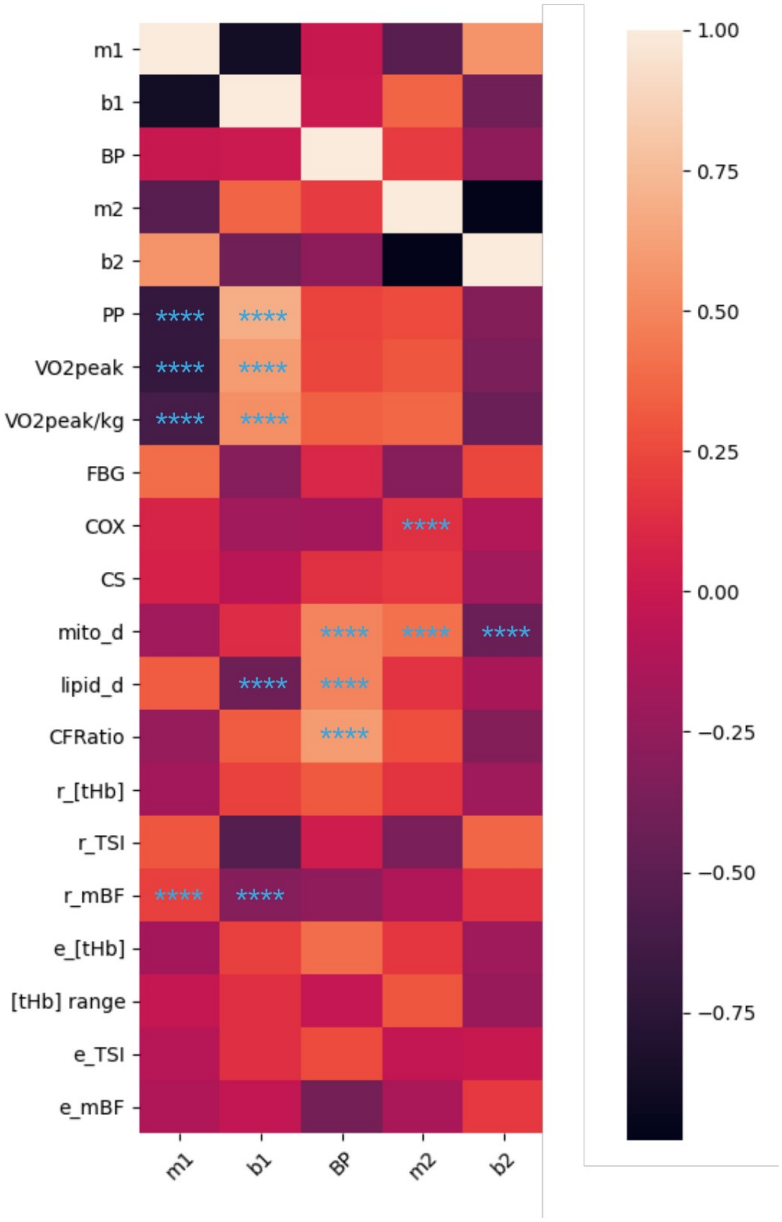

Figure 6.3. Pearson correlation heat map for all parameters. Darker shaded cells indicate a stronger correlation, blue for negative and red for positive, with matching parameters showing dark red in a diagonal (Pearson correlation = 1.0). The threshold for smallest

substantial correlation was 0.1. When the Familywise Bonferroni-adjusted p-value representing the change on the direction of type-1 error was less than the rejection threshold, the alternative hypothesis (opposite hypothesis) was accepted and the probability the effect was more than the smallest important threshold was denoted: * possible p>0.25; ** likely p>0.75; *** very likely p>0.95; **** almost certain p>0.995. After Familywise Bonferroni-adjustment only almost certain correlations remained.

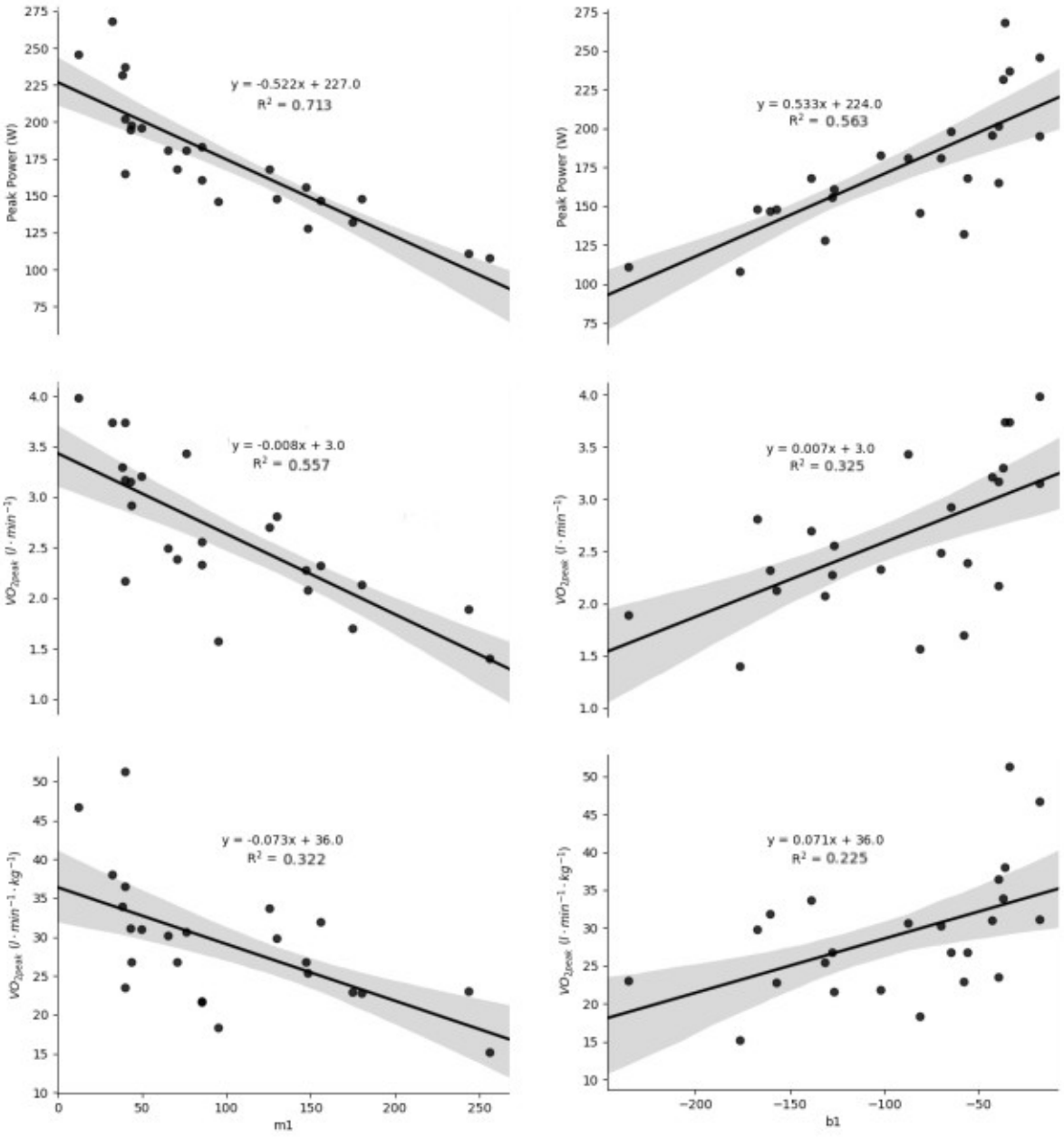

Figure 6.4. Linear regression for aerobic performance measures of peak power (PP), V̇O2peak, and V̇O2peak/kg vs primary component parameters m1 and b1. Grey shaded area is the 90% confidence interval.

Discussion

The present study characterized the parameter estimates for %Δ[HHb] and VO_2 during incremental ramp exercise and modeled them to investigate local adjustments in blood flow to match O_2 delivery and O_2 consumption in T2DM. In agreement with theoretical interpretation of the %Δ[HHb] as a function of $\dot{V}O_2$, the primary phase was positively correlated with measures of aerobic capacity and performance. The breakpoint transitioning the phases were positively correlated with mitochondrial density, lipid density, and capillary-to-fiber ratio. The secondary phase was positively correlated with measures of mitochondrial density and function. Taken together, the data suggest that hemodynamic impairment affecting O_2 delivery was a main determinant of primary phase kinetics as represented by the increase in mitochondrial, lipid, and capillary densities were the main determinant of maintaining primary kinetics. Meanwhile, mitochondrial density and enzyme activity, representing the capacity of the muscle for O_2 extraction, and respiration determined secondary phase kinetics. To our knowledge, interpretation of the %Δ[HHb] signal as it relates to a-vO_2 and local blood flow has been previously interpreted using understood hemodynamic and muscle physiology, but this is the first study to directly correlate the hemodynamic NIRS-derived parameters to criterion measures of skeletal muscle respiratory function.

Correlations between primary phase parameters m1 and b1 with peak power and aerobic capacity indicate that the efficiency of the aerobic systems during submaximal exercise plays a major role in determining the overall endurance exercise capacity. During the primary phase, there is an approximate 1:1 linear increase in %Δ[HHb] relative to $\dot{V}O_2$ indicating an increased reliance on O_2 extraction (aerobic systems) to meet metabolic demand (Spencer, Murias and Paterson, 2012). A higher slope value for m1 indicates O_2 extraction is outpacing O_2 delivery. The degree of reliance on O_2 extraction during this phase has been shown to be increased in older compared to younger

adults (Gravelle *et al.*, 2012) potentially indicating impaired microvascular vasodilation response during exercise. Similarly, in T2D, greater O_2 extraction compared to delivery has been suggested to be an adaptation from reduced vasodilatory response and slowed mBF response (Bauer et al., 2007b; Murias et al., 2010; Wilkerson et al., 2011). In agreement with other studies (Bauer et al., 2007b; Kingwell et al., 2003) the negative correlation between resting mBF and m1 suggests that impaired resting mBF (i.e. capillary resistance) to exercise in T2D is a possible cause of increased reliance on O_2 extraction. Our findings, therefore, agree with di Pampero (di Prampero, 2003) in that O_2 delivery limitations (m1) account for a larger proportion of aerobic capacity than muscle and mitochondrial function. Accordingly, the current data provide new information to relate increased reliance on O_2 extraction during submaximal exercise in T2DMto microvascular hemodynamic and respiratory properties of the skeletal muscle.

Direct measurment if $VO_{2max}$is an important marker of cardiorespiratory fitness that is relegated mainly to a laboratory setting and for healthy and athletic indiciduals, as testing in clinical and sedentery populations may not yield accurate results due to needing a base level of fitness and high intensity exercise may be deleterious to certain populations (Aisbett et al., 2020). For this reason being able to accurately predict VO_{2mac} from submaximal exercise would be a valuable tool for clinical diagnosis and guiding treatment (Aisbett et al., 2020; Akalan et al., 2008). Regression analysis of m1 showed a strong correlation to peak power (PP) and VO_{2max}, yielding the following equations:

eq 6.1: $PP(t) = -0.522*m1 + 227 \quad (R^2 = 0.713)$

eq 6.2: $VO_{2max}(t) = -0.008*m1 + 3.0 \ (R^2 = 0.557)$

In this way combining NIRS with breath-by-breath gas consumption may help to increase the accuracy of submaximal VO_{2max} prediction. Moreover, usine NIRS alone may be prudent in clinical populations where breathing through the breath-by-breath mask may be cumbersome.

The transition from phase 1 kinetics to phase II is denoted by the break point, defined as the % $m\dot{V}O_2$ between the double linear segments. The break point was found to be very likely correlated to mitochondrial density, lipid density, and capillary-to-fiber ratio, but interestingly only had weak correlations with all other parameters. This suggests that the ability to maintain phase I kinetics for a few more moments is highly dependent on both the muscles ability to continually perfuse the muscle with oxygenated blood and having enough mitochondria available for O_2 extraction.

In the secondary phase, there is an abrupt decrease in the %Δ[HHb] despite continual increases in $m\dot{V}O_2$ until eventual exhaustion. This plateauing of %Δ[HHb] indicates a slowing of O_2 extraction and increased reliance on anaerobic metabolism until an eventual upper limit, perhaps due to an upper limit in the capacity for energy production in the active muscle (Spencer, Murias and Paterson, 2012). In the current study, an increased m2 was very likely positively related to COX activity and mitochondrial density, suggesting that in T2D, the rate of O_2 extraction during peak exercise is limited by the enzymatic activity and number of mitochondria. At rest, increased skeletal muscle metabolism associated with increased mitochondria number and function would lead to increased resting energy expenditure, which, similarly to increases in b1, is reflected in the decreased resting TSI%, resting mBF, and FBG. In relation to m2, possible decreases in exercise TSI% and resting mBF may relate to the muscle's increased capacity of O_2 extraction from the blood.

Limitations

Technical considerations in the current study include a) absence of a control group, b) use of continuous wave NIRS, c) use of only one max test to obtain models of [HHb] and VO_2 temporal profiles, and d) assessing only the VL muscle. The current study was designed as a preliminary mechanistic investigation into the temporal profile of %Δ[HHb] during ramp cycle exercise. The lack of a control group in the current study limits comparative inference of the data, however, the substantial correlations that emerged between phase parameters and measures of skeletal muscle respiratory, vascular,

and metabolic function affirms previous interpretation and provides direction for potential avenues of future research in using NIRS as a noninvasive tool for guiding clinical treatment.

The current study used continuous wave NIRS to assess the profile of [HHb] during ramp exercise, which can only assess relative Hb concentration changes and has been shown to be affected by ATT (M. van Beekvelt et al., 2001), skin blood flow (Buono et al., 2005), and exercising muscle (L. F. Ferreira et al., 2006). In the current study, the [HHb] signal from the second transmitter was used since it penetrates closer to the muscle belly (ATT + ½ · VL thickness) for all participants. The temporal profile of [HHb] signal from continuous wave NIRS, different to the [O2Hb] signal, has been shown to not be affected by skin blood flow (Koga et al., 2015). Finally, by normalizing the Δ[HHb] signal limitations of ATT and changing optical properties during exercise are mitigated (Murias et al., 2013).

Compared to similar experimental designs, the current study only used data from one max test to model %Δ[HHb] and $\dot{V}O_2$ profiles instead of ensemble averaging two or more (Boone et al., 2009; Murias et al., 2013). Considering the current population, it was determined that a full familiarization test was needed to allow the participant to become accustomed to using the cycle ergometer during ramp exercise with emphasis placed on cardiac screening to ensure cardiac fitness for exercise. Since measures from the first test (familiarization) were not likely to maintain the required cadence continually until exhaustion affecting the temporal profiles, and adding more than one additional test would start to include exercise effects altering the temporal profile, only one max test following a familiarization test was used.

Local muscle deoxygenation was assessed in the VL, which does not provide a complete assessment of the skeletal muscle blood flow response to exercise. The profile of deoxygenation of the VL is different compared to the *vastus medialis* (VM) or *rectus femoris* (RF) (Chin et al., 2011) and muscle group activation during cycling is heterogeneous and changes in a non-uniform manner with intensity (Green & Patla,

1992). However, the same absolute [HHb] was seen in the VL and RF (Okushima et al., 2015), with no differences (duManoir et al., 2010) or little differences in spatial heterogeneities between quadricep deoxygenation (Koga et al., 2007). Since the VL is important for daily locomotion and general activities and thoroughly activated during the incremental ramp cycle test, it provides a good picture of skeletal muscle kinetics to exercise. Finally, effects of fiber type on the modeling parameters were not assessed and future research should investigate the impact of muscle fiber composition to the relationship of O_2 utilization and delivery.

Future Directions

The current study shows that the primary phase components m1 and b1 are most likely correlated with maximal aerobic measures of VO_2peak, VO2peak/kg, and PP. Further regression analysis shows the effect of magnitude of the primary phase parameters on the aerobic measures. Taken together these data suggest the potential of NIRS to be used as a non-investigative tool to further investigate skeletal muscle impairment and possibly to estimate VO2peak from a submaximal test. This will allow for more accurate estimations of peak aerobic parameters in populations where maximal exercise is ill advised. The break point between primary and secondary components was very likely correlated with mitochondrial, lipid, and capillary densities, suggesting increased ability to deliver and uptake oxygen prolongs phase I kinetics. Secondary phase components m2 and b2 were substantially correlated with COX and mitochondrial density, exhibiting that muscle function at higher exercise outputs is determined by mitochondrial density and number. Furthermore, similar likely correlations were seen in CS and capillary-to-fiber ratio. Future research should investigate how improvements in exercise tolerance through exercise treatment improves muscle structure and function, and explore further how the combinations of variables in the system as a whole contribute to increasing exercise ability.

Conclusion

In conclusion, this study modeled the NIRS %Δ[HHb] signal as a function of $\dot{V}O_2$ to investigate how individual variables of skeletal muscle function contributed to maintaining increasing exercise intensity in the vastus lateralis of sedentary individuals with T2D. Phase 1 parameters were highly correlated with aerobic capacity. The breakpoint between the phases was correlated with mitochondrial, lipid, and capillary densities in the active muscle. Finally, during phase 2, occurring from 50-70% $\dot{V}O_2$peak until exhaustion, the parameters m2 and b2 were substantially correlated with mitochondrial density and efficiency, capillarity, and vascular health. This agrees with previous speculation that the parameters m2 and b2 are related to the muscles ability to continually extract O2 during peak work rates. Combining NIRS with breath-by-breath O2 consumption measures during ramp cycle exercise has potential in investigating systemic barriers glucose disposal and exercise tolerance in T2D and guiding and monitoring treatment options focusing on improved skeletal muscle health, aerobic health, and T2D outcomes.

References

Aisbett, J., Lakens, D., & Sainani, K. (2020). *Magnitude Based Inference in Relation to One-sided Hypotheses Testing Procedures*. https://doi.org/10.31236/osf.io/pn9s3

Akalan, C., Robergs, R. A., & Kravitz, L. (2008). Prediction of VO2max from an individualized submaximal cycle ergometer protocol. *Journal of Exercise Physiology Online*, *11*(2), 1–17. https://eprints.qut.edu.au/96816/

Bauer, T. A., Reusch, J. E. B., Levi, M., & Regensteiner, J. G. (2007). Skeletal Muscle Deoxygenation After the Onset of Moderate Exercise Suggests Slowed Microvascular Blood Flow Kinetics in Type 2 Diabetes. *Diabetes Care*, *30*(11), 2880–2885. https://doi.org/10.2337/DC07-0843

Boone, J., & Bourgois, J. (2012). The oxygen uptake response to incremental ramp exercise: Methodogical and physiological issues. *Sports Medicine*, *42*(6), 511–526. https://doi.org/10.2165/11599690-000000000-00000

Boone, J., Koppo, K., Barstow, T. J., & Bouckaert, J. (2009). Pattern of deoxy[Hb + Mb] during ramp cycle exercise: influence of aerobic fitness status. *European Journal of Applied Physiology*, *105*(6), 851–859. https://doi.org/10.1007/s00421-008-0969-2

Buono, M. J., Miller, P. W., Hom, C., Pozos, R. S., & Kolkhorst, F. W. (2005). Skin Blood Flow Affects In Vivo Near-Infrared Spectroscopy Measurements in Human Skeletal Muscle. *The Japanese Journal of Physiology*, *55*(4), 241–244. https://doi.org/10.2170/jjphysiol.T649

Chance, B., Dait, M. T., Zhang, C., Hamaoka, T., & Hagerman, F. (1992). Recovery from exercise-induced desaturation in the quadriceps muscles of elite competitive rowers. *American Journal of Physiology - Cell Physiology*, *262*(3 31-3), C766–C775. https://doi.org/10.1152/ajpcell.1992.262.3.c766

Chin, L. M. K., Kowalchuk, J. M., Barstow, T. J., Kondo, N., Amano, T., Shiojiri, T., & Koga, S. (2011). The relationship between muscle deoxygenation and activation in different muscles of the quadriceps during cycle ramp exercise. *Journal of Applied Physiology*, *111*(5), 1259–1265. https://doi.org/10.1152/japplphysiol.01216.2010

DeLorey, D. S., Kowalchuk, J. M., & Paterson, D. H. (2003). Relationship between pulmonary O_2 uptake kinetics and muscle deoxygenation during moderate-intensity exercise. *Journal of Applied Physiology*, *95*(1), 113–120. https://doi.org/10.1152/japplphysiol.00956.2002

di Prampero, P. E. (2003). Factors limiting maximal performance in humans. *European Journal of Applied Physiology*, *90*(3–4), 420–429. https://doi.org/10.1007/s00421-003-0926-z

duManoir, G. R., DeLorey, D. S., Kowalchuk, J. M., & Paterson, D. H. (2010). Kinetics of VO2 limb blood flow and regional muscle deoxygenation in young adults during moderate intensity, knee-extension exercise. *European Journal of Applied Physiology*, *108*(3), 607–617. https://doi.org/10.1007/s00421-009-1263-7

Ferreira, L. F., Hueber, D. M., & Barstow, T. J. (2006). Effects of assuming constant optical scattering on measurements of muscle oxygenation by near-infrared spectroscopy during exercise. *Journal of Applied Physiology*, *102*(1), 358–367. https://doi.org/10.1152/japplphysiol.00920.2005

Gravelle, B. M. R., Murias, J. M., Spencer, M. D., Paterson, D. H., & Kowalchuk, J. M. (2012). Adjustments of pulmonary O 2 uptake and muscle deoxygenation during ramp incremental exercise and constant-load moderate-intensity exercise in young and older adults. *Journal of Applied Physiology*, *113*(9), 1466–1475. https://doi.org/10.1152/japplphysiol.00884.2011

Green, H. J., & Patla, A. E. (1992). Maximal aerobic power: neuromuscular and metabolic considerations. *Medicine and Science in Sports and Exercise*, *24*(1), 38–46. http://www.ncbi.nlm.nih.gov/pubmed/1548994

Hamaoka, T., McCully, K. K., Niwayama, M., & Chance, B. (2011). The use of muscle near-infrared spectroscopy in sport, health and medical sciences: recent developments. *Philosophical Transactions of the Royal Society A: Mathematical, Physical and Engineering Sciences*, *369*(1955), 4591–4604. https://doi.org/10.1098/rsta.2011.0298

Hopkins, W. G. (2007). A spreadsheet for deriving a confidence interval, mechanistic inference and clinical inference from a P value. *Sportscience*, *11*, 16–21. https://go.galegroup.com/ps/i.do?p=AONE&sw=w&u=googlescholar&v=2.1&it=r&id=GALE%7CA189289447&sid=googleScholar&asid=5f628ac6

Hopkins, W. G. (2020). Magnitude-Based Decisions as Hypothesis Tests. *Sportscience*, *24*.

Kingwell, B. A., Formosa, M., Muhlmann, M., Bradley, S. J., & McConell, G. K. (2003). Type 2 diabetic individuals have impaired leg blood flow responses to exercise: role

of endothelium-dependent vasodilation. *Diabetes Care*, *26*(3), 899–904. https://doi.org/10.2337/DIACARE.26.3.899

Koga, S., Barstow, T. J., Okushima, D., Rossiter, H. B., Kondo, N., Ohmae, E., & Poole, D. C. (2015). Validation of a high-power, time-resolved, near-infrared spectroscopy system for measurement of superficial and deep muscle deoxygenation during exercise. *Journal of Applied Physiology*, *118*(11), 1435–1442. https://doi.org/10.1152/japplphysiol.01003.2014

Koga, S., Poole, D. C., Ferreira, L. F., Whipp, B. J., Kondo, N., Saitoh, T., Ohmae, E., & Barstow, T. J. (2007). Spatial heterogeneity of quadriceps muscle deoxygenation kinetics during cycle exercise. *Journal of Applied Physiology*, *103*(6), 2049–2056. https://doi.org/10.1152/japplphysiol.00627.2007

Mancini, D. M., Bolinger, L., Li, H., Kendrick, K., Chance, B., & Wilson, J. R. (1994). Validation of near-infrared spectroscopy in humans. *Journal of Applied Physiology (Bethesda, Md. : 1985)*, *77*(6), 2740–2747. https://doi.org/10.1152/jappl.1994.77.6.2740

Murias, J. M., Kowalchuk, J. M., & Paterson, D. H. (2010). Speeding of $\dot{V}o_2$ kinetics with endurance training in old and young men is associated with improved matching of local O_2 delivery to muscle O_2 utilization. *Journal of Applied Physiology*, *108*(4), 913–922. https://doi.org/10.1152/japplphysiol.01355.2009

Murias, J. M., Spencer, M. D., Keir, D. A., & Paterson, D. H. (2013). Systemic and vastus lateralis muscle blood flow and O_2 extraction during ramp incremental cycle exercise. *American Journal of Physiology-Regulatory, Integrative and Comparative Physiology*, *304*(9), R720–R725. https://doi.org/10.1152/ajpregu.00016.2013

Murias, J. M., Spencer, M. D., Kowalchuk, J. M., & Paterson, D. H. (2011). VO2 kinetics parameter estimates Influence of phase I duration on phase II V in older and young adults. *American Journal of Physiology. Regulatory, Integrative and Comparative Physiology*, *301*(1), 218–224. https://doi.org/10.1152/ajpregu.00060.2011.

Okushima, D., Poole, D. C., Rossiter, H. B., Barstow, T. J., Kondo, N., Ohmae, E., & Koga, S. (2015). Muscle deoxygenation in the quadriceps during ramp incremental cycling: Deep vs. superficial heterogeneity. *Journal of Applied Physiology*, *119*(11), 1313–1319. https://doi.org/10.1152/japplphysiol.00574.2015

Robergs, R. A., Dwyer, D., & Astorino, T. (2010). Recommendations for Improved Data Processing from Expired Gas Analysis Indirect Calorimetry. *Sports Medicine*, *40*(2), 95–111. https://doi.org/10.2165/11319670-000000000-00000

Sayer, A. ., Dennison, E., Syddall, H., Gilbody, H., Phillips, D., & Cooper, C. (2005). Type 2 Diabetes, Muscle Strength, and Impaired Physical Function. *Diabetes Care*, *28*(10), 2541–2542. https://doi.org/10.2337/diacare.28.10.2541

Spencer, M. D., Murias, J. M., & Paterson, D. H. (2012). Characterizing the profile of muscle deoxygenation during ramp incremental exercise in young men. *European Journal of Applied Physiology*, *112*(9), 3349–3360. https://doi.org/10.1007/s00421-012-2323-y

Trounce, I. A., Kim, Y. L., Jun, A. S., & Wallace, D. C. (1996). Assessment of mitochondrial oxidative phosphorylation in patient muscle biopsies, lymphoblasts, and transmitochondrial cell lines. *Methods in Enzymology*, *264*, 484–509. https://doi.org/10.1016/s0076-6879(96)64044-0

van Beekvelt, M., Colier, W. N. J. M., Wevers, R. O. N. A., Engelen, B. G. M. V. A. N., Wevers, R. A., & Perfor-, B. G. M. V. E. (2001). *Performance of near-infrared spectroscopy in measuring local O 2 consumption and blood flow in skeletal muscle*. 511–519.

Wilkerson, D. P., Poole, D. C., Jones, A. M., Fulford, J., Mawson, D. M., Ball, C. I., & Shore, A. C. (2011). Older Type 2 diabetic males do not exhibit abnormal pulmonary oxygen uptake and muscle oxygen utilization dynamics during submaximal cycling exercise. *American Journal of Physiology-Regulatory, Integrative and Comparative Physiology*, *300*(3), R685–R692. https://doi.org/10.1152/ajpregu.00479.2010

7 - Conclusion

NIRS is a powerful tool to dynamically assess hemodynamic properties of skeletal muscle at rest and during exercise. Since the first application of NIRS in 1978 to measure tissue oxygenation, various new NIRS technologies, such as, time-resolved spectroscopy, phase modulation (frequency-domain, fd), and continuous wave (cw), have been developed to quantify the NIRS signal as our understanding of near-infrared light travel through human tissue has developed. These technologies offer greater benefits such as faster temporal resolution, increased ease of use, and greater portability. However, each technology has its own set of assumptions that need to be well understood for correct application, data collection, and data interpretation. The majority of NIRS research has been focused on cerebral oxygenation, however, there is a growing interest in using NIRS to assess dynamic changes in skeletal muscle hemodynamic and oxygen-transfer properties. The principles, insights, and potential pitfalls of using NIRS to non-invasively determine tissue oxygenation differ for cerebral and skeletal muscle research, therefore, we have focused only on NIRS use in skeletal muscle. The overall purpose of this thesis was to: 1) experimentally apply understood NIRS principles with skeletal muscle measures to determine optimal materials and methods to obtain accurate, reliable, and repeatable NIRS measures, 2) develop a standardized protocol testing perfusion, blood flow, oxygen consumption, and tissue function in the *vastus lateralis*, 3) test the day-to-day reliability of this protocol in healthy and a clinical population to compare cw- and fd-NIRS technologies and 4) investigate NIRS use to explore the relationship between oxygen delivery and uptake during dynamic exercise testing in adults with T2D.

The general measurement principle of NIRS is the same across technologies and based on the principles of absorption spectroscopy, a technique used to measure the concentration of a molecule dissolved in a homogenous solution. However, with NIRS, two main complications arise: 1) near-infrared light cannot penetrate more than 2-3 cm into the tissue and 2) the medium or “solution” that hemoglobin, the molecule of interest,

is in, is non-homogenous and full of differently shaped cellular structures, fibers, tendons, and tissues with differing refractive indices affecting speed and direction of light travel (scattering), and during different metabolic rates (e.g., rest vs exercise). The various NIRS technologies approach these complications in different ways, leading to variations in accuracy under certain conditions, e.g., due to principles of cw-NIRS, an increase in skin blood flow due to increased skin temperature has been shown to contribute to an increase in the concentration of the O_2Hb signal. These nuances between technologies must be well understood for correct interpretation of NIRS research findings. Moreover, proper, repeatable placement of the probe over the region of interest (ROI) must be standardized for ensuring measurement of desired muscle and intra and inter individual comparison.

In pilot testing we developed standard experimental procedures to address probe placement, probe pressure on tissue being measured during dynamic movement, blocking out of ambient light, and standard resting and exercise procedures to illicit incremental exercise response on the muscle. In addition, we tested the rapid-cuff placement in relation to the NIRS probe to minimize artefact motion due to rapid arterial and venous occlusions delivered from the custom-built rapid inflation device. Finally, various analysis methods were trialed to reduce signal-to-noise ratio and increase accuracy of final results based on findings from the literature (see chapter 2).

One observation noted during the contraction-relaxation cycle was that the tHb signal decreased during contraction while blood is forced out and increased during relaxation when blood is allowed to return. The Δ[tHb] can be related to the volume of blood displaced during the contraction-relaxation cycle, and increased with physical fitness, indicating a better ability of trained individuals to continuously expel deoxygenated blood and replenish with oxygenated during exercise. Future research should further investigate the correlation of the NIRS signal during contraction-relaxation cycle and its relationship with the dynamics of the muscle pump, microvascular volume capacity, cardiovascular dynamics, and their relationship to exercise tolerance.

The purpose of the first study (chapter 4) was to combine several established NIRS protocols and methods that evaluate skeletal muscle perfusion, microvascular blood flow, oxygen consumption, muscle oxygen respiratory capacity (MORC), and the dynamic balance of oxygen delivery and consumption during incremental exercise, when using cw-NIRS. Moreover, this research was expanded upon to include a novel approach to assay mBF, $m\dot{V}O_2$, and perfusion during exercise. To achieve this, all of these protocols and methods were combined into one standard protocol that could be used at rest and during exercise at specific workloads to investigate the relationship between these parameters in healthy individuals and how they are affected by disease. In doing this, the order of tests and spacing between measurements needed to be considered so that the action of one did not alter the results of another. Firstly, since resting measures required 20 minutes of rest and the NIRS needed a minimum of 10 minutes of collection prior to measurement collection (M. van Beekvelt et al., 2001), the NIRS was placed first and collection started during resting measures. A spacing of 45 seconds between occlusions was followed, as suggested by beekvelt (M. C. P. Van Beekvelt et al., 2002) to allow for a return to basal metabolic rates. Since, to our knowledge, there was no research on using occlusion methodology during dynamic exercise, an exercise period of three minutes prior to measurements was determined as a good balance between achieving steady-state (Lutjemeier et al., 2005) without introducing fatigue. One complication of using occlusion methodology during exercise is that the occlusion can only be inflated between contractions and the participant must be fully relaxed during occlusion, therefore the resulting NIRS signal slope reflects post-contraction values and not exercise per se (Rådegran, 2017). However, immediate post-exercise mBF and $m\dot{V}O_2$ increases in proportion to exercise intensity (Kagaya & Homma, 1997) and reflects the response to exercise (Quaresima et al., 2004). Due to this cessation of activity, the participant was required to continue to exercise to again achieve steady-state levels, and the same 45s period used between resting occlusions was found to be adequate for achieving reproducible, repeatable occlusion measures. In concurrence with previous research (Cross & Sabapathy, 2017a; M. van Beekvelt et al., 2001), a minimum of 4 venous

occlusions and 2 arterial occlusions were conducted at each stage, with the averaged used to increase the mean signal to noise ratio while minimizing participant discomfort and overall experiment duration. Finally, the MORC test was placed after the exercise stages as this measure needed to be repeated and was more reproducible and tolerable to participants when the muscle was primed (Terence E Ryan et al., 2013). This protocol allowed for the reproducible assessment of mBF, mVO_2, perfusion, and MORC using cw-NIRS at rest and during exercise in young, healthy individuals. The profile of mBF and mVO2 from rest to increasing exercise intensity was found to reflect research using other non-NIRS methodology (Kalliokoski et al., 2005; Richardson et al., 1995; Whipp & Ward, 1982) and future research can use these patterns of increase to investigate pathophysiology in metabolically diseased populations.

After achieving reproducible results using cw-NIRS in a young, healthy cohort, in the second study (Chapter 5), we sought to again establish this reproducibility in healthy and a clinical cohort (T2D) when compared against the benchmark NIRS technology, fd-NIRS. In addition, since fd-NIRS accounted for individual scattering of NIR light while cw-NIRS assumes a single constant correction factor, the effect of this assumption on measurement outcomes could be evaluated. It was found that both NIRS devices were reproducible in both cohorts and measures of mBF and mVO_2 were in agreement with previous research (Kalliokoski et al., 2005; Richardson et al., 1995; Whipp & Ward, 1982). An interesting finding of this study was that in T2Ds, the estimated absolute [tHb] derived from cw-NIRS using equations of spatially-resolved spectroscopy was overestimated compared to the actual absolute [tHb] obtained from the fd-NIRS, and the magnitude of this overestimation decreased with increasing exercise intensity, indicating that the cw-NIRS was not sensitive enough to accurately track changes in perfusion from rest to exercise in T2Ds. However, substantial differences were not seen in healthy individuals for the assessed exercise intensities. This same pattern was observed when normalizing perfusion to resting levels, and in tissue saturation of oxygen. Moreover, in the exercise induced blood-volume change, fd-NIRS was substantially larger than cw-NIRS for both exercise stages in healthy individuals, reaffirming this conclusion. The

decrease in cw-NIRS sensitivity to changes in [tHb] during exercise may be due to cw-NIRS software applying a literature-based scattering correction factor derived from a group of healthy individuals. Previous research has shown changing properties of adipose and skeletal muscle layer, as would be the case in the quality of skeletal muscle between healthy and clinical populations, can have a significant impact on scattering and its properties (L. F. Ferreira et al., 2006; Franceschini et al., 1999). In agreement, the degree of scattering in T2D was significantly higher than in ND. In addition to investigating the effect of individual differences in scattering on [Hb] measures, future research should compare the results of applying dynamic scattering to further identify the effect of scattering on NIRS derived measures during exercise, and the contribution of muscle quality to changes in scattering.

The third and final study explored using NIRS to assess the relationship of microvascular blood flow to O_2 delivery during incremental cycle exercise. The temporal profile of %Δ[HHb] as a function of $\dot{V}O_2$ was modeled as a best fit double linear function representing the $\dot{V}O_2$/a-vO_2 coupling response to incremental exercise. To meet the increasing energetic demand, the primary phase is thought to be reliant on oxygen extraction and the secondary phase increasingly on anaerobic metabolism (Spencer et al., 2012). In concurrence, the study found primary phase parameters highly correlated with peak power and $\dot{V}O_2$ peak while secondary phase parameters were highly correlated with lipid density, mitochondrial density, and mitochondrial COX activity. Future research should further investigate the correlation of the primary phase slope to peak power and $\dot{V}O_{2max}$ as a potential way to estimate peak power and $\dot{V}O_2$max during submaximal exercise, and as a tool for identifying interventions that may improve muscle respiratory capacity of people with T2D. In addition, the test could be useful in clinical populations where testing to exhaustion is ill advised and potentially inaccurate.

General Limitations & Recommendations

While NIRS is a promising technology for non-invasive skeletal muscle research, a number of limitations exist:

1. Although NIRS benefits in its non-invasiveness compared to traditional methodology for measuring blood flow such as thermodilution or ultrasound microbubbles, NIRS use during exercise introduces complexity and limitations that need to be well understood to obtain accurate results.

2. The use of venous occlusion to obtain a blood flow measurement must be of sufficient pressure to collapse the veins to stop blood outflow but not too high to impede blood inflow. Using occlusions means that exercise must cease in order to take a measurement, while techniques such as thermodilution and microbubbles can be done during exercise. In order to obtain accurate exercise induced blood flow measures with venous occlusions, timing is critical and the participant must be trained so that the occlusion is applied immediately after exercise with the participant in a resting position; failure to provide adequate familiarisation sessions would accentuate this methodological feature.

3. It is recommended to time align ECG measures to standardize the blood flow measurement over the duration of the first cardiac cycle under occlusion to prevent underestimation and standardize the window of measurement.

4. As opposed to traditional methods, NIRS $m\dot{V}O_2$ measurements require rapid AO, which can impact upon subsequent measures of perfusion and mBF. The rapid occlusions may also be uncomfortable for the participant, in which case familiarization and training is required so that the participant can fully relax the muscles prior to contraction to minimize artefact motion in the NIRS measures. his was minimized by using 3-second incremental ‘priming’ occlusions that start well below the occlusion pressure and incrementally increase ~10-15 mmHg until about 20-40 mmHg above the occlusion pressure. Conducting the arterial occlusions after the venous occlusions is suggested as it is still unknown if the arterial occlusion has long term effects that will alter the vessel mechanics. As mentioned previously, the rapid inflation of the cuff can be a surprise to the participant causing involuntary spasms or contractions that affect the NIRS signal.

Priming above the occlusion pressure will set an upper threshold of expectation for the participant that we found significantly cut down on involuntary spasms. As long as the pressure from successive occlusions did not exceed this pressure then the occlusion was normalized to the participant.

5. The NIRS probe measures [Hb] changes directly underneath the probe as the light penetrates into the muscle tissue on its way to the detector. Firstly, the probe must be placed parallel to the muscle fibers and ideally positioned over only one muscle to avoid measurements across multiple muscle groups. Secondly, the probe must be placed in the exact same spot trial-to-trial and any derivation in positioning could impact on reliability (Buchheit et al., 2011). Therefore, it is recommended that careful attention to probe placement and replacement trial to trial is attained and standardized to achieve repeatability. Additionally, consideration of the possible effects of changes in subcutaneous to muscle thicknesses following diet or exercise intervention on probe placement and measurement depth should be made.

6. Using occlusion methodology with NIRS during exercise requires special consideration of the probe placement, repeated placement, and participant tolerance. To measure activity of a specific muscle being heavily recruited during exercise, the exercise method, position of NIRS probe, and participant tolerance to exercise load and occlusion must all be considered. Initially, following the lead of other protocols, I piloted supine rest with resistance bands and a foot pedal to provide specific exercise intensity to the vastus lateralis. However, I found the position awkward for conducting rapid occlusions on the leg and difficult to control the exercise intensity for day to day comparisons and found VL activation in this position highly variable. Using EMG electrodes, I measured activation of the rectus femoris, vastus lateralis, and calf muscles during supine foot press and seated knee extensions. I found that the rectus femoris and calf muscle were more heavily used during supine foot press and that the VL could be more specifically

targeted using isotonic knee extensions on the biodex. Moreover, participants seemed to prefer the seated position vs supine since the entire protocol was 50-60 min long. Under supine conditions, the participant experienced more involuntary twitches that caused significant spikes in the NIRS signal (artefact motion), affecting the time series data. In a seated position, however, the participant felt more comfortable and aware of their surroundings, and being able to see the occlusion cuff during inflation cut down on the involuntary twitches. Therefore for the purposes of the current experiment the seated position was superior to the supine position, and suggest that the participant be slightly reclined (~110 degrees) and to suspend the participants legs behind the ankle in a natural elevation so that the knee rests naturally slightly above the edge of the seat. This position encouraged a natural relaxed state from the participant for the entirety of the session and prevented occluding or pinching of blood vessels that would affect the NIRS measures. However, the lack of reproducible results in the MORC test in the current thesis suggests a supine position may be preferred for this test.

7. Adipose tissue thickness is known to affect the NIRS signal as the more adipose tissue between the probe and the skeletal muscle tissue, the less NIRS light that penetrates the actual muscle tissue measuring skeletal muscle hemodynamic and metabolic properties. This is further complicated by long-term interventions where the adipose tissue thickness could potentially change from baseline to post measures. Correction curves for adipose tissue thickness have been proposed (Soller et al., 2005) but exactly how to correct for adipose tissue thickness is still being debated and varies by NIRS device (Franceschini et al., 1999; Koga et al., 2015; Pirovano et al., 2021). It is recommended to measure adipose tissue thickness using ultrasound or similar technology for reference.

8. Because much research with NIRS is focused on cerebral microvascular perfusion, a lot of procedures relating to skeletal muscle research require additional tools for obtaining clear measurements. Conditions such as ambient

light can affect the NIRS signal, and under static conditions a standard black cloth can be used to block out light, under dynamic exercise conditions it is recommended to use a cover that will allow the probe to move freely with the skin as the muscle underneath contracts.

9. Technicalities of analysis are still debated and vary highly with NIRS technology and device. For example, from the fd-NIRS device, [Hb] can be calculated using the AC or DC signal. The difference between the calculated [Hb] between these signals is similar but can vary depending on change in scattering. Both signals are currently used in NIRS research, and when to use one signal over the other is not clear (Fantini et al., 1994). In the current research I used the AC signal as it showed to be more reproducible at lower intensities. In addition, for the cw-NIRS device constants of h, k, and DPF can be changed altering the calculated [Hb] and although most research maintains the same constants for the entire cohort, it is arguable that choosing parameters based on individual criteria may yield more accurate NIRS derived [Hb]. Future research should compare the reliability of fd-NIRS derived outcomes using both the AC and DC signal and constant versus dynamic scattering assumptions during exercise.

10. Because the degree of scattering is highly variable even within the same person, a physiological calibration of the NIRS signal must be done to allow for inter-individual and day-to-day comparisons. This physiological calibration requires a 3-5 minute arterial ischaemic occlusion resulting in the complete disappearance of HbO_2/MbO_2 and maximum HHb/HMb in the tissue being measured and the reactive hyperemia upon release of the occlusion will reach maximum HbO_2/MbO_2 and minimum HHb/HMb, which cis used to normalize the NIRS signal to physiological zero and 100. Because of the stress and discomfort caused by the ischaemic occlusion, through pilot testing I discovered it best to do it after the blood flow measures were taken to prevent impairment or influence. Other NIRS technologies do not require this calibration, which should be strongly

considered when deciding which NIRS device to use, especially in clinical populations where it would be intolerable if not harmful. To obtain skeletal muscle blood flow and oxygen consumption measures, rapid venous and arterial occlusions, respectively, are used. We found that the cuff must be placed at least 2 cm upstream of the NIRS probe cover to avoid probe movement due to occlusion induced skin deformation.

11. It is recommended to test and optimise the reproducibility of the occlusion technology and methodology prior to conducting actual trials.

12. Finally, it is recommended to reduce the number of measures taken in one testing session to increase reproducibility. Conducting too many workloads or attempting to take too many different measures in a single testing session can induce fatigue in the participant affecting day-to-day reproducibility.

Conclusion

Continuous-wave (cw) NIRS has become the most popular form of NIRS for skeletal muscle research as it has a high temporal resolution, is relatively inexpensive, portable, and easy to use. The primary findings of this thesis and conclusions were that: 1) continuous wave NIRS devices can reliably assess mBF and $m\dot{V}O_2$ within the microvasculature of the *vastus lateralis* during intermittent pauses from dynamic exercise in healthy, physically active adults. 2) The relative patterns of response for mBF, and $m\dot{V}O_2$ during incremental exercise and mBF/$m\dot{V}O_2$ ratio agree with other published results using similar methodologies validating the NIRS approach. 3) mBF and $m\dot{V}O_2$ measures taken at rest and up to 15% MVC during knee extension exercise derived from cw-NIRS was comparable and reproducible in healthy and T2Ds when compared to benchmark fd-NIRS. In contrast, measures of perfusion index, tissue saturation, and [tHb] range from cw-NIRS were more often substantially different than fd-NIRS, especially in T2D. 4) cw-NIRS can also be used during continuous ramp cycle exercise to investigate the coupling between oxygen delivery and consumption and mitochondrial characteristics during incremental exercise in T2Ds. Moreover, NIRS has potential to be

used with or without breath-by-breath O_2 monitoring to submaximally estimate VO_{2max}. This provides an experimental framework for the study of exercise and other interventions on skeletal muscle respiratory dynamics in insulin resistant populations.

Overall, both NIRS devices proved to be reproducible and have potential for non-invasive measures of hemodynamic and oxygen uptake kinetics in the skeletal muscle of healthy and T2D individuals. The use of NIRS technology in skeletal muscle research combined with exercise offers exciting research opportunities to investigate the dynamics of skeletal muscle hemodynamic and respiratory responses to stressors, however, a thorough understanding of the principles of NIRS and various NIRS technologies is still required for accurate analysis and therefore much work remains before NIRS can be used in a clinical setting.

References

Buchheit, M., Ufland, P., Haydar, B., Laursen, P. B., & Ahmaidi, S. (2011). Reproducibility and sensitivity of muscle reoxygenation and oxygen uptake recovery kinetics following running exercise in the field. *Clinical Physiology and Functional Imaging*, *31*(5), 337–346. https://doi.org/10.1111/j.1475-097X.2011.01020.x

Cross, T. J., & Sabapathy, S. (2017). The impact of venous occlusion per se on forearm muscle blood flow: implications for the near-infrared spectroscopy venous occlusion technique. *Clinical Physiology and Functional Imaging*, *37*(3), 293–298. https://doi.org/10.1111/cpf.12301

Fantini, S., Franceschini, M. A., Fishkin, J. B., Barbieri, B., & Gratton, E. (1994). Quantitative determination of the absorption spectra of chromophores in strongly scattering media: a light-emitting-diode based technique. *Applied Optics*, *33*(22), 5204. https://doi.org/10.1364/AO.33.005204

Ferreira, L. F., Hueber, D. M., & Barstow, T. J. (2006). Effects of assuming constant optical scattering on measurements of muscle oxygenation by near-infrared spectroscopy during exercise. *Journal of Applied Physiology*, *102*(1), 358–367. https://doi.org/10.1152/japplphysiol.00920.2005

Franceschini, M. A., Gratton, E., Hueber, D. M., & Fantini, S. (1999). Near-Infrared Absorption and Scattering Spectra of Tissues in Vivo. *Breast Tumors/Techniques*, *3597*(526), 526–531. https://doi.org/10.1117/12.356854

Kagaya, A., & Homma, S. (1997). Brachial arterial blood flow during static handgrip exercise of short duration at varying intensities studied by a Doppler ultrasound method. *Acta Physiologica Scandinavica*, *160*(3), 257–265. https://doi.org/10.1046/j.1365-201X.1997.00158.x

Kalliokoski, K. K., Knuuti, J., & Nuutila, P. (2005). Relationship between muscle blood flow and oxygen uptake during exercise in endurance-trained and untrained men. *Journal of Applied Physiology*, *98*(1), 380–383. https://doi.org/10.1152/japplphysiol.01306.2003

Koga, S., Barstow, T. J., Okushima, D., Rossiter, H. B., Kondo, N., Ohmae, E., & Poole, D. C. (2015). Validation of a high-power, time-resolved, near-infrared spectroscopy system for measurement of superficial and deep muscle deoxygenation during

exercise. *Journal of Applied Physiology*, *118*(11), 1435–1442. https://doi.org/10.1152/japplphysiol.01003.2014

Lutjemeier, B. J., Miura, A., Scheuermann, B. W., Koga, S., Townsend, D. K., & Barstow, T. J. (2005). Muscle contraction-blood flow interactions during upright knee extension exercise in humans Muscle contraction-blood flow interactions during upright knee ex- tension exercise in humans. *J Appl Physiol*, *98*, 1575–1583. https://doi.org/10.1152/japplphysiol.00219

Pirovano, I., Porcelli, S., Re, R., Spinelli, L., Contini, D., Marzorati, M., & Torricelli, A. (2021). Effect of adipose tissue thickness and tissue optical properties on the differential pathlength factor estimation for NIRS studies on human skeletal muscle. *Biomedical Optics Express*, *12*(1), 571. https://doi.org/10.1364/boe.412447

Quaresima, V., Ferrari, M., Franceschini, M. A., Hoimes, M. L., & Fantini, S. (2004). Spatial distribution of vastus lateralis blood flow and oxyhemoglobin saturation measured at the end of isometric quadriceps contraction by multichannel near-infrared spectroscopy. *Journal of Biomedical Optics*, *9*(2), 413. https://doi.org/10.1117/1.1646417

Rådegran, G. (2017). Limb and skeletal muscle blood flow measurements at rest and during exercise in human subjects. *Proceedings of the Nutrition Society*, *58*, 887–898. https://doi.org/10.1017/S0029665199001196

Richardson, R. S., Knight, D. R., Poole, D. C., Kurdak, S. S., Hogan, M. C., Grassi, B., & Wagner, P. D. (1995). Determinants of maximal exercise V̇O2, during single leg knee-extensor exercise in humans. *American Journal of Physiology - Heart and Circulatory Physiology*, *268*(4 37-4). https://doi.org/10.1152/ajpheart.1995.268.4.h1453

Ryan, T. E., Southern, W. M., Reynolds, M. A., & McCully, K. K. (2013). A cross-validation of near-infrared spectroscopy measurements of skeletal muscle oxidative capacity with phosphorus magnetic resonance spectroscopy. *Journal of Applied Physiology*, *115*(12), 1757–1766. https://doi.org/10.1152/japplphysiol.00835.2013

Soller, B. R., Landry, M. R., Soyemi, O. O., & Yang, Y. (2005). Influence of a fat layer on the near infrared spectra of human muscle: quantitative analysis based on two-layered Monte Carlo simulations and phantom experiments. *Optics Express, Vol. 13, Issue 5, Pp. 1570-1579*, *13*(5), 1570–1579. https://doi.org/10.1364/OPEX.13.001570

Spencer, M. D., Murias, J. M., & Paterson, D. H. (2012). Characterizing the profile of muscle deoxygenation during ramp incremental exercise in young men. *European Journal of Applied Physiology*, *112*(9), 3349–3360. https://doi.org/10.1007/s00421-012-2323-y

Van Beekvelt, M. C. P., Van Engelen, B. G. M., Wevers, R. A., & Colier, W. N. J. M. (2002). In vivo quantitative near-infrared spectroscopy in skeletal muscle during incremental isometric handgrip exercise. *Clinical Physiology and Functional Imaging*, *22*(3), 210–217. https://doi.org/10.1046/j.1475-097X.2002.00420.x

van Beekvelt, M., Colier, W. N. J. M., Wevers, R. O. N. A., Engelen, B. G. M. V. A. N., Wevers, R. A., & Perfor-, B. G. M. V. E. (2001). *Performance of near-infrared spectroscopy in measuring local O 2 consumption and blood flow in skeletal muscle*. 511–519.

Whipp, B. J., & Ward, S. A. (1982). Cardiopulmonary coupling during exercise. In *Journal of Experimental Biology* (Vol. 100, Issue 1, pp. 175–193). The Company of Biologists. https://doi.org/10.1242/jeb.100.1.175

Appendix

A – Ethics

Human Ethics Application

FOR APPROVAL OF PROPOSED RESEARCH/TEACHING/EVALUATION

INVOLVING HUMAN PARTICIPANTS

(All applications are to be typed and presented using language that is free from jargon and comprehensible to lay people)

SECTION A

1 Project Title Reproducibility of two different near infrared spectroscopy devices for investigating skeletal muscle of Type 2 diabetics

Projected start date for data collection 15 Oct 2015 **Projected end date** 15 March 2016

(In no case will approval be given if recruitment and/or data collection has already begun).

2 Applicant Details *(Select the appropriate box and complete details)*

ACADEMIC STAFF APPLICATION (excluding staff who are also students)

Full Name of Staff Applicant/s Martin Gram

School/Department/Institute Massey University, School of Sport and Exercise

Campus *(mark one only)* **Albany** [ ] **Palmerston North** [ ] **Wellington** [X]

Telephone *+64 0221692343* **Email Address** m.gram@massey.ac.nz

STUDENT APPLICATION

Full Name of Student Applicant

Employer (if applicable)

Telephone **Email Address**

Postal Address .....

Full Name of Supervisor(s) .....

School/Department/Institute .....

Campus *(mark one only)* **Albany** ☐ **Palmerston North** ☐ **Wellington** ☐

Telephone **Email Address**

GENERAL STAFF APPLICATION

Full Name of Applicant .....

Section .....

Campus *(mark one only)* **Albany** ☐ **Palmerston North** ☐ **Wellington** ☐

Telephone ..... **Email Address** .....

Full Name of Line Manager .....

Section .....

Telephone ..... **Email Address** .....

---

3 Type of Project *(provide detail as appropriate)*

Staff Research/Evaluation:		**Student Research:**		**If other, please specify:**
Academic Staff	**X**	**Specify Qualification**		
General Staff		**Specify Credit Value of Research**		
Evaluation		**(e.g. 30, 60, 90, 120, 240, 360)**		

---

4 Summary of Project

Please outline in no more than 200 words in lay language why you have chosen this project, what you intend to do and the methods you will use.

(Note: All the information provided in the application is potentially available if a request is made under the Official Information Act. In the event that a request is made, the University, in the first instance, would endeavour to satisfy that request by providing this summary. Please ensure that the language used is comprehensible to all.)

The development and progression of Type 2 Diabetes Mellitus (T2DM) has been linked to mitochondrial dysfunction. Poor mitochondrial function will impair substrate metabolism, including metabolism of glucose. Near-infrared spectroscopy (NIRS) is a non-invasive, portable and practical tool which allows real-time assessment of skeletal muscle oxygen consumption (mVO2), blood flow (BF), mitochondrial function, and total muscle oxidative capacity in a specific region/muscle of interest. We have developed and optimized these measures on a continuous wave NIRS device (*PortaLite, Artinis Medical Systems BV, the*

Netherlands) in a young, healthy population (ICC: 0.72-0.96). Continuous wave devices are popular due to being cheap, portable, and easy to use. However, the assumptions made using these devices may not always be valid, especially in clinical populations. Frequency domain NIRS devices on the other hand (*Oxiplex ISS, Inc., Champaign Il)* allow for more precise measurements but are significantly more expensive and technical than continuous wave devices. The primary purpose of this study is therefore to test the reproducibility of NIRS measurements on patients with T2DM. The secondary purpose of this study is to compare the frequency domain NIRS measurements to continuous wave NIRS measurements to assess the validity of assumptions made using continuous wave devices in T2DM.

---

5 **List the Attachments to your Application**, e.g. Completed "Screening Questionnaire to Determine the Approval Procedure" (compulsory), Information Sheet/s *(indicate how many*), Translated copies of Information Sheet/s, Consent Form/s *(indicate of how many),* Translated copies of Consent Form/s, Transcriber Confidentiality Agreement, Confidentiality Agreement *(for persons other than the researcher / participants who have access to project data)*, Authority for Release of Tape Transcripts, Advertisement, Health Checklist, Questionnaire, Interview Schedule, Evidence of Consultation, Letter requesting access to an institution, Letter requesting approval for use of database, Other *(please specify)*.

Health Screening Form
Participant Information Sheet
Participant Consent Form
Recruitment Letter to Nurses-GPs
Screening Questionnaire 2015

Applications that are incomplete or lacking the appropriate signatures will not be processed. This will mean delays for the project.

Please refer to the Human Ethics website (http://humanethics.massey.ac.nz) for details of where to submit your application and the number of copies required.

SECTION B: PROJECT INFORMATION

General

6	**I/We wish the protocol to be heard in a closed meeting (Part II).**	**Yes**		**No**	X

(If yes, state the reason in a covering letter.)

7	**Does this project have any links to previously submitted MUHEC or HDEC application(s)?**	**Yes**		**No**	X

If yes, list the MUHEC or HDEC application number/s (if assigned) and relationship/s.

8	**Is approval from other Ethics Committees being sought for the project?**	**Yes**		**No**	X

If yes, list the other Ethics Committees.

9	**For staff research, is the applicant the only researcher?**	**Yes**		**No**	X

If no, list the names and addresses of all members of the research team.

Adam Lucero a.lucero@massey.ac.nz

Project Details

10 State concisely the aims of the project.

The aim of this project is to determine the between-day reproducibility of two NIRS devices (ISS, Oxiplex and PortaLite, Artinis Medical systems) in skeletal muscle of T2DM patients. This data will permit comparisons against data we have collected in a healthy population, and enable us to determine the viability of these measurements in T2DM.

11 Give a brief background to the project to place it in perspective and to allow the project's significance to be assessed. *(No more than 200 words in lay language)*

The primary site of glucose disposal is skeletal muscle. The ability for skeletal muscle to clear glucose is dependent on the oxidative capacity (the ability to convert glucose to energy) of the muscle. In turn, muscle oxidative capacity is dependent on oxygen delivery (microvascular blood flow) and muscle mitochondrial function. Mitochondria, which are inside of skeletal muscle cells, are the engines which convert glucose to energy. Mitochondrial dysfunction has been shown to be a hallmark feature of Type 2 Diabetes (T2DM). NIRS measurements have the potential to non-invasively determine mitochondrial function and muscle blood flow. However, the reproducibility of these measures has not been determined in muscle of T2DM. This knowledge will aid future investigations of muscle function in diabetic populations.

12 Outline the research procedures to be used, including approach/procedures for collecting data. Use a flow chart if necessary.

Partipants:

15 male participants with diagnosed T2DM will be recruited

Inclusion criteria: age 40-65 years, stable weight, BMI < 40, HbA1c > 48 mmol/mol, not requiring insulin therapy, have been diagnosed for a minimum of 1 year.

Exclusion criteria: Physically active defined as having achieved a minimum of 150 minutes of moderate to vigorous intensity exercise each week over the past 6 months. (American College of Sports Medicine and American Diabetes Association guidelines). Current smoker or have smoked 6 months prior, use of β-blockers, have injured or had lower limb surgery in the past 4 weeks, moderate to severe retinopathy, nephropathy or neuropathy, history of cerebrovascular or cardiovascular diseases.

Recruitment

Participants will be recruited by contacting medical centers.

Study design:

The study will be performed over a 15 day period. Participants will come in to the lab at Massey University Sport & Exercise Laboratory, Wellington on four occasions. For each visit we will ask participants to report to the laboratory between 7 and 11 am, in the fasting state and having refrained from caffeine and alcohol 12 hours prior. Participants will be asked to refrain from taking their normal medication until after the testing session. Once testing is completed participants will be provided with water and a breakfast bar. The first visit will include screening, familiarization, consent as well as determination of 1RM in a Biodex dynamometer, assessment of adipose tissue thickness and muscle diameter over the vastus lateralis muscle by ultrasound. The remaining three experimental visits will take place within 10 non-consecutive days. The tests on visit 2 - 4 will be identical (Figure 1), apart from a finger-prick blood sample taken on visit 2. Each session is expected to take approximately 90 min. Two NIRS devices (ISS, Oxiplex and Portalite, Artinis Medical systems) will be used. The reproducibility protocol will be done on one leg with one NIRS device and then immediately after the protocol will be repeated on the other leg with the other NIRS device. The order of the devices will be randomized according to dominant, non-dominant leg (Figure 2).

Figure 1. Experimental Design.

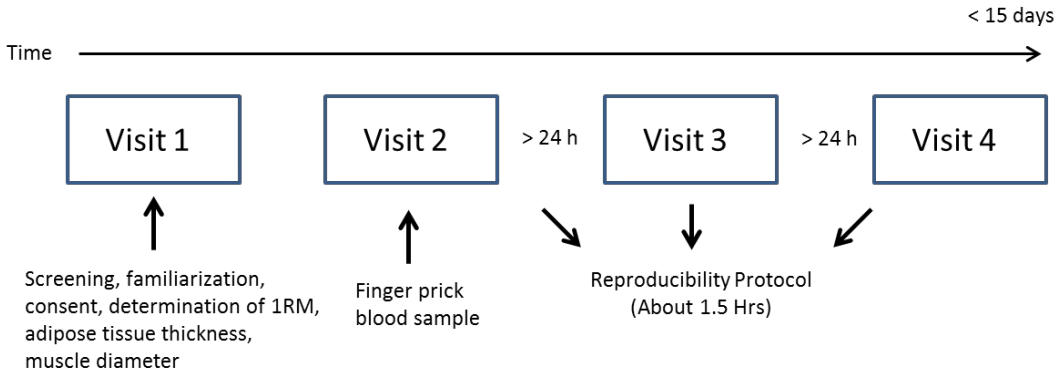

Figure 2. Reproducibility Protocol to be repeated on visit 2, 3 and 4.**

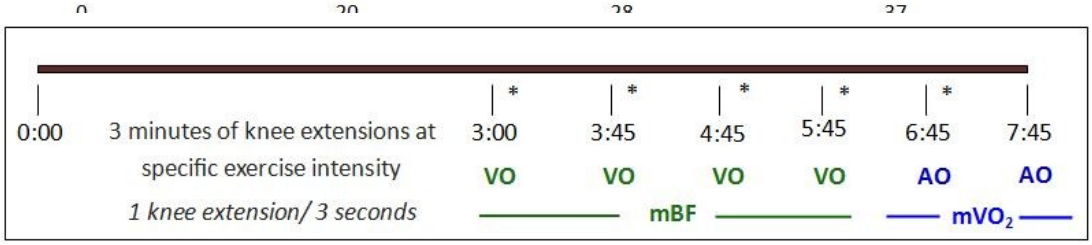

VO = venous occlusion—participant rested leg while tourniquet [rapidly] inflated to 70 mmHg for 15 s.

mBF = assessed as the mean rate of linear increase in total haemoglobin (O2Hb + HHb) during occlusions.

AO = arterial occlusion—participant rested leg while tourniquet [rapidly] inflated to 250 mmHg for 10 s.

mVO_2= assessed as the mean rate of linear increase in deoxyhaemoglobin (HHb) during occlusions.

*Immediately following occlusion participant will continue knee extensions for 45 seconds to maintain steady state.

****This figure shows the protocol using the first NIRS device on one leg. The protocol is immediately repeated on the second leg using the other NIRS device.**

Measures

Determination of leg strength – 1 repetition maximum (1RM)

1 RM will be measured in a Biodex dynamometer. Participants will be placed in a seat and secured with belts to minimize movement. The knee is positioned in a 90° angle and fixed. After a short warmup consisting of 2–3 submaximal trials, each participant will perform 3 isometric knee extensions at maximal voluntary effort with an interval of approximately 1 min between repetitions. The subjects will be verbally encouraged throughout the repetitions, and the best result is used.

Blood Glucose and haemoglobin concentration

During visit 2, a finger prick sample will be taken while the participant is resting and used to measure fasting blood glucose using a portable analyser and haematocrit using a benchtop centrifuge to spin the blood in a capillary tube. The blood will be immediately disposed of.

Ultrasound

Duplex Doppler ultrasound (Terason T3200) equipped with a linear array transducer will be used to measure adipose tissue thickness and muscle thickness by placing the ultrasound probe on the belly of the vastus lateralis over the NIRS probe location

Near Infra-Red Spectroscopy (NIRS)

Microvascular blood flow, muscle oxygen consumption and mitochondrial respiratory capacity will be estimated using a two-wavelength (760 and 850 nm) continuous wave NIRS device (*PortaLite, Artinis Medical Systems*) as well as a frequency-domain NIRS device (*Oxiplex ISS, Inc., Champaign Il*). The two wavelengths correspond to the absorption wavelengths of oxyhemoglobin (O_2Hb) and deoxyhemoglobin (HHb). The probe will be attached to the skin overlying the vastus lateralis. A blood pressure cuff will be placed upstream (thigh) from the NIRS placement site.

Microvascular Blood Flow

Microvascular blood flow (mBF) will be assessed by inflating a blood pressure cuff to a sub-diastolic pressure (venous occlusion (VO); ~ 70 mmHg) for 10 seconds. Microvascular flow is assessed as the rate of linear increase in total haemoglobin (O_2Hb + HHb) during occlusion. This will be repeated 4-5 times at rest and following knee extension exercise at 5 and 15% of 1 RM. These work intensities have been chosen because they will likely be able to be maintained by the T2D cohort and we have shown them to be highly reproducible in a young healthy population.

Muscle Oxygen Uptake

Muscle oxygen consumption (mVO_2) will be assessed by inflating a blood pressure cuff to a supra-systolic pressure (arterial occlusion (AO); ~250 mmHg) for 10 seconds. Muscle oxygen consumption is assessed as the rate of linear increase in deoxygenated haemoglobin (HHb) during occlusion. This will be repeated 2-3 times at rest and following knee extension exercise at 5 and 15% of 1 RM.

Mitochondrial Capacity:

Mitochondrial capacity will be estimated using the arterial occlusion method. Mitochondrial capacity will be estimated from mVO_2 recovery kinetics by repeatedly measuring mVO_2 with arterial occlusions (10 seconds) following 15 seconds of exercise. Exercise will consist of rapid leg presses in a Biodex dynamometer as resistance. The repeated mVO_2 data will be fit to a mono-exponential curve and the time constant (Tc) calculated as a measure of muscle mitochondrial function.

13 Where will the project be conducted? Include information about the physical location/setting.

All testing will take place in the sport and exercise laboratory at Massey University, Wellington.

14 If the study is based overseas:

i) Specify which countries are involved;

ii) Outline how overseas country requirements (if any) have been complied with;

iii) Have the University's Policy & Procedures for Course Related Student Travel Overseas been met? *(Note: Overseas travel undertaken by students – refer to item 5.10 in the document "Additional Information" on the MUHEC website.)*

N/A

15 Describe the experience of the researcher and/or supervisor to undertake this type of project?

Adam Lucero is a PhD student at School of Sport and Exercise. His PhD studies are focused on non-invasive measurements of mitochondrial function and exercise capacity in T2DM. Data from this study will be used as a part of his PhD studies.

Dr Martin Gram (Research Officer, School of Sport and Exercise) will supervise this project. Dr Gram has previously undertaken a human intervention study focusing on the effects of physical inactivity (immobilization) on mitochondrial function in older adults and therefore has experience working with frail individuals.

16 Describe the process that has been used to discuss and analyse the ethical issues present in this project.

Massey University's Code of Ethical Conduct for Research, Teaching and Evaluations involving Human Participants has been critically analysed to ensure that the research study is undertaken within the appropriate guidelines and research policies of the University. During visit 1 to the laboratory, participants will be screened for eligibility using the Health Screening Form (Appendix A).

Participants

17 Describe the intended participants.

Male sedentary participants aged 40-65 years with diagnosed T2DM

18 How many participants will be involved?

15

What is the reason for selecting this number?

Our main statistical aim is to estimate variances for the outcome variables to enable calculation of reproducibility statistics so that power calculations can be conducted for subsequent studies. A sample size of 10 was estimated using magnitude based inference (Hopkins, 2009), where the smallest worthwhile change in mitochondrial function was 10% (corresponds to a CV of 8%). We are over-sampling to account for the unknown variance of using T2DM.

(Where relevant, attach a copy of the Statistical Justification to the application form)

19 **Describe how potential participants will be identified and recruited?**

Through medical centres

20	**Does the project involve recruitment through advertising?**	**Yes**		**No**	x

(If yes, attach a copy of the advertisement to the application form)

21	**Does the project require permission of an organisation (e.g. an educational institution, an academic unit of Massey University or a business) to access participants or information?**	**Yes**	x	**No**	

If yes: i) list the organisation(s)

Brooklyn Medical

Capital Care Health

City Medical

Courtenay Medical

Hataitai Medical

Island Bay Medical

Kelburn Medical

Kilbirnie Medical

Miramar Medical

Newtown Medical

newtown union house service.. Pacific Health Medical Centre

Peninsula Medical

Port Nicholson medical

Te Aro Health

The Terrace Medical

Brooklyn Central Health

City GPs

Seatoun Medical

Johnsonville Medical Centre

Karori Medical Centre, Main Surgery

Khandallah Medical Centre

Newlands Medical Centre

Ngaio Medical Centre

Northland Village Surgery

Onslow Medical Centre

Tawa Medical Centre

ii) attach a copy of the draft request letter(s) to the application form, e.g. letter to Board of Trustees, PVC, HoD/I/S, CEO etc (include this in your list of attachments (Q5).

(Note that some educational institutions may require the researcher to submit a Police Security Clearance.)

See appendix D

22 Who will make the initial approach to potential participants?

The medical centres will make the initial approach to potential participants and bring to their attention that the study exists. Interested participants will contact Dr Martin Gram. He will supply the potential participant with the full study information via email (Participant Information Sheet and Consent Form).

23 Describe criteria (if used) to select participants from the pool of potential participants.

The first 15 participants aged 40-65 years with diagnosed T2DM satisfying the inclusion/exclusion criteria, and who will be available for all testing sessions will be selected to participate in the study.

Inclusion criteria: age 40-65 years, stable weight, BMI < 40, HbA1c > 48 mmol/mol, not requiring insulin therapy, have been diagnosed for a minimum of 1 year.

Exclusion criteria: Physically active defined as having achieved a minimum of 150 minutes of moderate to vigorous intensity exercise each week over the past 6 months. (American College of Sports Medicine and American Diabetes Association guidelines). Current smoker or have smoked 6 months prior, use of β-blockers, have injured or had lower limb surgery in the past 4 weeks, moderate to severe retinopathy, nephropathy or neuropathy, history of cerebrovascular or cardiovascular diseases.

24 How much time will participants have to give to the project?

4 mornings, < 90 minutes per morning.

Data Collection

25 Does the project include the use of participant questionnaire/s? **Yes** [x] **No** [ ]

(If yes, attach a copy of the Questionnaire/s to the application form and include this in your list of attachments (Q5))

If yes: i) indicate whether the participants will be anonymous (i.e. their identity unknown to the researcher). **Yes** [ ] **No** [x]

ii) describe how the questionnaire will be distributed and collected.

(If distributing electronically through Massey IT, attach a copy of the draft request letter to the Associate Director Service Delivery, Information Technology Services to the application form. Include this in your list of attachments (Q5) – refer to the policy on "Research Use of IT Infrastructure").

(Note: All requests for IT related aspects of ethics committee approvals can be directed through the IT service desk in the first instance – the request will be registered and on a response timeline, with the Associate Director dealing with the request).

A Health Screening Form (appendix A) will be completed by each participant prior to the experimental protocol and collected by Dr Martin Gram upon completion. In addition, Dr Martin Gram will ask for permission from the participant to receive a medical history from the participants own GP. This is to ensure medications and medical history is accurate as certain medications and conditions can affect study outcomes and from experience in previous studies some participants are not aware of all of the medications they are on. The medical information is strictly confidential and will be kept in a locked file cabinet in Dr. Martin Grams office. Information will only be shared with other project researchers if necessary to decide eligibility.

26	**Does the project involve observation of participants? If yes, please describe.**	**Yes**		**No**	x
27	**Does the project include the use of focus group/s?**	**Yes**		**No**	x

(If yes, attach a copy of the Confidentiality Agreement for the focus group to the application form)

If yes, describe the location of the focus group and time length, including whether it will be in work time. *(If the latter, ensure the researcher asks permission for this from the employer).*

28	**Does the project include the use of participant interview/s?**	**Yes**		**No**	x

(If yes, attach a copy of the Interview Questions/Schedule to the application form)

If yes, describe the location of the interview and time length, including whether it will be in work time. *(If the latter, ensure the researcher asks permission for this from the employer)*

29	**Does the project involve sound recording?**	**Yes**		**No**	x
30	**Does the project involve image recording, e.g. photo or video?**	**Yes**		**No**	x

If yes, please describe. *(If agreement for recording is optional for participation, ensure there is explicit consent on the Consent Form)*

31	**If recording is used, will the record be transcribed?**	**Yes**		**No**	x

If yes, state who will do the transcribing.

(If not the researcher, a Transcriber's Confidentiality Agreement is required – attach a copy to the application form. Normally, transcripts of interviews should be provided to participants for editing, therefore an Authority For the Release of Tape Transcripts is required – attach a copy to the application form. However, if the researcher considers that the right of the participant to edit is inappropriate, a justification should be provided below.)

32	**Does the project involve any other method of data collection not covered in Qs 25-31?**	**Yes**		**No**	x

If yes, describe the method used.

33	**Does the project require permission to access databases?**	**Yes**		**No**	x

(If yes, attach a copy of the draft request letter/s to the application form. Include this in your list of attachments (Q5). Note: If you wish to access the Massey University student database, written permission from Director, National Student Relations should be attached.)

34 Who will carry out the data collection?

Adam Lucero and Martin Gram

SECTION C: BENEFITS / RISK OF HARM (Refer Code Section 3, Para 10)

35 What are the possible benefits (if any) of the project to individual participants, groups, communities and institutions?

There will be no direct benefits from the proposed study. The principal benefit of this study is contributing to research which will potentially be of considerable benefit to aid future investigations of muscle function in diabetic populations

36 What discomfort (physical, psychological, social), incapacity or other risk of harm are individual participants likely to experience as a result of participation?

There will be some discomfort associated with the required physical effort in the performance tests but the equipment used in this study will result in no significant risks to the subjects. The Doppler Ultrasound and NIRS devices are considered safe as no reported adverse events have occurred with commercial units. There is a slight discomfort associated with the arterial occlusion; however, our cuff ischemia protocols have been well tolerated in previous studies at Massey in both healthy individuals and patients with T2DM. To ensure participants can tolerate discomfort from arterial occlusion, all testing procedures are demonstrated on the participant during familiarisation and can opt out at any time. Arterial occlusion has little potential to damage blood vessels in either young healthy adults or in T2DM patients. For instance flow mediated dilation (FMD) includes a 5 minute arterial occlusion and is the standard test used to assess the health of the endothelium. A PubMed database search (18-11-2013) reveals 5,598 publications, 526 of which have used diabetic populations. This is an example of a publication looking at a high-risk cohort:

Szwejkowski BR, Gandy SJ, Rekhraj S, Houston JG, Lang CC, Morris AD, George J, Struthers AD. Allopurinol Reduces Left Ventricular Mass In Patients With Type 2 Diabetes And Left Ventricular Hypertrophy. J Am Coll Cardiol. 2013 Aug 15. pii: S0735-1097(13)03888-6. doi: 10.1016/j.jacc.2013.07.074. [Epub ahead of print]

In addition, we have experienced no adverse effects using the same occlusion protocols in our recent study with 26 T2DM patients with the same eligibility criteria (HDEC application titled "Can Amino Acids in combination with Exercise Training Improve Glycaemic Control and Cardiovascular Health in Type-2 Diabetics?"

There is a slight discomfort associated with morning fasting; however, it is a common practice in diabetes research to standardize measurements. To counteract this discomfort we will be providing participants with a breakfast bar immediately following testing.

The exercise protocol is low-intensity, though as with any exercise protocol, a slight risk of injury is associated. While the risk of harm is minimal, there is some risk of muscle or tendon strains and risk of a sudden cardiac event as is the case with any physical activity. This risk is noted in the information sheet.

Finger prick blood samples can in principle cause infection but we use gloves and disinfect the area where the blood is drawn before accessing blood.

Contact with GP to access information with regards to current medication and medical history will only be made with consent of participant.

37 Describe the strategies you will use to deal with any of the situations identified in Q36.

Both researchers are trained in first aid and basic life support and both researchers have taken a course in phlebotomy and cannulation. In addition, there is access to an AED within 30 meters of the lab. The researchers will also have a mobile phone available and lab phone available should the support of emergency services become necessary. Non-serious injuries will be recorded in incident documentation and the participant asked to see their GP for assessment and treatment as required. All testing sessions will be carefully monitored throughout the respective protocols.

38 **What is the risk of harm (if any) of the project to the researcher?**

No additional risk to that normally experienced at the workplace

39 **Describe the strategies you will use to deal with any of the situations identified in Q38.**

Ensuring a first aid trained personnel is also present during testing. Dr Martin Gram and PhD student Adam Lucero has completed a comprehensive first aid course.

40 **What discomfort (physical, psychological, social) incapacity or other risk of harm are groups/communities and institutions likely to experience as a result of this research?**

None

41 **Describe the strategies you will use to deal with any of the situations identified in Q40.**

N/A

42 **Is ethnicity data being collected as part of the project?** **Yes** [ ] **No** [X]

If yes, please describe how the data will be used.

(Note that harm can be done through an analysis based on insufficient sample or sub-set numbers).

43 **If participants are children/students in a pre-school/school/tertiary setting, describe the arrangements you will make for children/students who are present but not taking part in the research**.

(Note that no child/student should be disadvantaged through the research)

N/A

SECTION D: INFORMED & VOLUNTARY CONSENT (Refer Code Section 3, Para 11)

44 **By whom and how, will information about the research be given to potential participants?**

Interested participants (from medical centres) will contact Dr Martin Gram. He will supply the potential participant with the study information via email (Participant Information Sheet and Consent Form). After the potential participant have read the information and remains interested Dr Martin Gram will invite the potential participant to a screening. At this screening the study information will be given orally and the potential participant will have the chance to ask questions. If the potential participant is still interested he will sign the consent form. At this time Dr Martin Gram will ask for permission from the participant to receive a medical history from the participants own GP (stated in the consent form as a YES/NO question). This is to ensure medications and medical history is accurate as certain medications and conditions can affect study outcomes. The information asked for is detailed in Appendix B "Participant Information Sheet", in Appendix C "Participant Consent Form" and in Appendix D "Recruitment letter to nurses-GPs". If the potential participant chooses not to provide access to this information through his own GP he will still be able to join the study.

45 **Will consent to participate be given in writing?** **Yes** [X] **No** [ ]

(Attach copies of Consent Form/s to the application form)

If no, justify the use of oral consent.

46	**Will participants include persons under the age of 16?**	**Yes**		**No**	X
	If yes: i) indicate the age group and competency for giving consent.				
	ii) indicate if the researcher will be obtaining the consent of parent(s)/caregiver(s).	**Yes**		**No**	X

(Note that parental/caregiver consent for school-based research may be required by the school even when children are competent. Ensure Information Sheets and Consent Forms are in a style and language appropriate for the age group.)

47	**Will participants include persons whose capacity to give informed consent may be compromised?**	**Yes**		**No**	X

If yes, describe the consent process you will use.

48	**Will the participants be proficient in English?**	**Yes**	X	**No**	

If no, all documentation for participants (Information Sheets/Consent Forms/Questionnaire etc) must be translated into the participants' first-language.

(Attach copies of the translated Information Sheet/Consent Form etc to the application form)

SECTION E: PRIVACY/CONFIDENTIALITY ISSUES (Refer Code Section 3, Para 12)

49	**Will any information be obtained from any source other than the participant?**	**Yes**	X	**No**	

If yes, describe how and from whom.

Contact with GP to access information with regards to current medication and medical history for purposes of determining eligibility to participate will only be made with consent of participant.

50	**Will any information that identifies participants be given to any person outside the research team?**	**Yes**		**No**	X

If yes, indicate why and how.

51	**Will the participants be anonymous (i.e. their identity unknown to the researcher?)**	**Yes**		**No**	X

If no, explain how confidentiality of the participants' identities will be maintained in the treatment and use of the data.

All data collected will be identified by a code known only to the primary investigator. No participant's name will appear on any record, and all research data will be securely stored

52	**Will an institution (e.g. school) to which participants belong be named or be able to be identified?**	**Yes**		**No**	X

If yes, explain how you have made the institution aware of this?

53 **Outline how and where:**

i) the data will be stored, and

(Pay particular attention to identifiable data, e.g. tapes, videos and images)

The data will be used only for the purposes of this project. Only the investigators of the study will have access to personal information and this will be kept secure and strictly confidential. Participants will be identified only by a study identification number. All raw data will be locked in a filing cabinet immediately after an exercise test, located in Dr Gram's office (3C09) on the Massey University's Wellington campus. This data will not be taken out of the office. Results of this project may be published or presented at conferences or seminars. No individual will be able to be identified.

ii) Consent Forms will be stored.

(Note that Consent Forms should be stored separately from data)

Consent forms will be stored separate from other data in a locked cabinet in the secure/locked office of Dr. Gram (3CO9) on the Massey University premises at the Wellington campus

54 **i) Who will have access to the data/Consent Forms?**

Dr Gram

ii) How will the data/Consent Forms be protected from unauthorised access?

They are kept in a locked cabinet to which only Dr. Gram has a key.

55 **How long will the data from the study be kept, who will be responsible for its safe keeping and eventual disposal? (Note that health information relating to an identifiable individual must be retained for at least 10 years, or in the case of a child, 10 years from the age of 16).**

(For student research the Massey University HOD Institute/School/Section / Supervisor / or nominee should be responsible for the eventual disposal of data. Note that although destruction is the most common form of disposal, at times, transfer of data to an official archive may be appropriate. Refer to the Code, Section 4, Para 24.)

All data will be retained in secure storage for 10 years, after which it will be destroyed.

SECTION F: DECEPTION (Refer Code Section 3, Para 13)

56	**Is deception involved at any stage of the project?**	**Yes**		**No**	X

If yes, justify its use and describe the debriefing procedures.

SECTION G: CONFLICT OF ROLE/INTEREST (Refer Code Section 3, Para 14)

57	**Is the project to be funded or supported in any way, e.g. supply of products for testing?**	**Yes**		**No**	X

If yes: i) state the source of funding or support:

Massey Academic Unit
Massey University (e.g. MURF, SIF)
External Organisation (provide name and detail of funding/support)

ii) does the source of the funding present any conflict of interest with regard to the research topic?

iii) identify any potential conflict of interest due to the source of funding and explain how this will be managed?

58	**Does the researcher/s have a financial interest in the outcome of the project?**	**Yes**		**No**	X

If yes, explain how the conflict of interest situation will be dealt with.

59 Describe any professional or other relationship between the researcher and the participants? (e.g. employer, employee, work colleague, lecturer/student, practitioner/patient, researcher/family member). Indicate how any resulting conflict of role will be dealt with.

No conflict of interest is foreseen between researcher and participant. Contact details of the researchers will be made available to subjects in the event they have any questions.

SECTION H: COMPENSATION TO PARTICIPANTS (Refer Code Section 4, Para 23)

60	**Will any payments, koha or other form of compensation or acknowledgement be given to participants?**	**Yes**		**No**	X

If yes, describe what, how and why.

(Note that compensation (if provided) should be given to all participants and not constitute an inducement. Details of any compensation provided must be included in the Information Sheet.)

SECTION I: TREATY OF WAITANGI (Refer Code Section 2)

61	**Are Maori the primary focus of the project?**	**Yes**		**No**	X

If yes: Answer Q62 – 65

If no, outline: i) what Maori involvement there may be, and

Subjects involved in the study may be of Māori decent but their involvement will be the same as all other participants.

ii) how this will be managed.

The participant's ethnicity will not be identified, so it should be a non-factor as all participants who agree to the study are treated equally.

62	**Is the researcher competent in te reo Maori and tikanga Maori?**	**Yes**		**No**	X

If no, outline the processes in place for the provision of cultural advice.

Input or assistance for cultural advice is available through Dr Nick Roskruge, Kai Arahi Maori for the College of Sciences, as needed (see attached letter)

63 Identify the group/s with whom consultation has taken place or is planned and describe the consultation process.

(Where consultation has already taken place, attach a copy of the supporting documentation to the application form, e.g. a letter from an iwi authority)

N/A

64 Describe any ongoing involvement of the group/s consulted in the project.

N/A

65 Describe how information resulting from the project will be shared with the group/s consulted?

N/A

SECTION J: CULTURAL ISSUES (Refer Code Section 3, Para 15)

66 What ethnic or social group/s (other than Maori) does the project involve?

Selection for the study will be voluntary rather than based on ethnicity and ethnicity data will not be recorded.

67	**Are there any aspects of the project that might raise specific cultural issues?**	**Yes**		**No**	X

If yes, explain. Otherwise, proceed to Section K.

68	**Does the researcher speak the language of the target population?**	**Yes**		**No**	

If no, specify how communication with participants will be managed.

69 **Describe the cultural competence of the researcher for carrying out the project.**

(Note that where the researcher is not a member of the cultural group being researched, a cultural advisor may be necessary)

70 **Identify the group/s with whom consultation has taken place or is planned.**

(Where consultation has already taken place, attach a copy of the supporting documentation to the application form)

71 **Describe any ongoing involvement of the group/s consulted in the project.**

72 **Describe how information resulting from the project will be shared with the group/s consulted.**

73 **If the research is to be conducted overseas, describe the arrangements you will make for local participants to express concerns regarding the research.**

SECTION K: SHARING RESEARCH FINDINGS (Refer Code Section 4, Para 26)

74 **Describe how information resulting from the project will be shared with participants and disseminated in other forums, e.g. peer review, publications, and conferences.**

(Note that receipt of a summary is one of the participant rights)

The findings will likely be disseminated at a conference. The data will also be used to compile a manuscript for publication, which will be shared with the participants. Participants will also receive a summary of findings in a report at the conclusion of the study. This report will also contain individual results and reference values from a healthy cohort previously tested. Using this information we will be able to provide individual feedback and advice.

SECTION L: INVASIVE PROCEDURES/PHYSIOLOGICAL TESTS (Refer Code Section 4, Para 21)

75	**Does the project involve the collection of tissue, blood, other body fluids; physiological tests or the use of hazardous substances, procedures or equipment?**	**Yes**	X	**No**	

If yes, are the procedures to be used governed by Standard Operating Procedure(s)? If so, please name the SOP(s). If not, identify the procedure(s) and describe how you will minimise the risks associated with the procedure(s)?

We will use the School of Sport and Exercise SOP for blood collection and disposal. In short, during visit 2, blood will be sampled from a finger-prick. While wearing gloves, the operator will clean the finger with an alcohol wipe, allow time for the alcohol to evaporate off, and the finger prick will be done by using a single use sterile Lancing device (Accu-Chek Safe-T-Pro Plus). The first drop of blood will be wiped away using a sterile swap (Propax) to allow for collection of a clean sample. Blood is then collected in a heparinized capillary tube and centrifuged at 2000 RPM for 2 minutes. Pressure is applied to the sampling area to stop the bleeding and a bandage applied.

76	**Does the project involve the use of radiation (x-ray, CT scan or bone densitometry (DEXA))?**	**Yes**		**No**	X
	If yes, has the Massey Licensee been contacted and consulted?	**Yes**		**No**	

(A copy of the supporting documentation must be provided with the ethics application, i.e. relevant SOP, participant dose assessment calculation sheet and approval of the dose assessment from the relevant authority). NOTE: See "Additional Information for Researchers" (Item 4.2) document for further detail.

(If yes to Q75 and/or Q76, complete Section L; otherwise proceed to Section M)

77 **Describe the material to be taken and the method used to obtain it. Include information about the training of those taking the samples and the safety of all persons involved. If blood is taken, specify the volume and number of collections.**

A single drop of blood will be taken from the fingertip using a prick to determine blood glucose concentration. The same prick will then be used to fill a capillary tube (60-100 μL) to determine haemoglobin concentration. This will be done only once, during visit 2. Both investigators have certification in phlebotomy and cannulation and first aid.

78	**Will the material be stored?**	**Yes**		**No**	X

If yes, describe how, where and for how long.

79 **Describe how the material will be disposed of (either after the research is completed or at the end of the storage period).**

(Note that the wishes of relevant cultural groups must be taken into account)

Biohazard containers

80	**Will material collected for another purpose (e.g. diagnostic use) be used?**	**Yes**		**No**	X
	If yes, did the donors give permission for use of their samples in this project? *(Attach evidence of this to the application form).*	**Yes**		**No**	

If no, describe how consent will be obtained. Where the samples have been anonymised and consent cannot be obtained, provide justification for the use of these samples.

N/A

81	**Will any samples be imported into New Zealand?**	**Yes**		**No**	X

If yes, provide evidence of permission of the donors for their material to be used in this research.

82	**Will any samples go out of New Zealand?**	**Yes**		**No**	X

If yes, state where.

(Note this information must be included in the Information Sheet)

83 **Describe any physiological tests/procedures that will be used.**

The physiological tests used are outlined in Q12.

84	**Will participants be given a health-screening test prior to participation?** *(If yes, attach a copy of the health checklist)*	**Yes**	X	**No**	

See Appendix A

Reminder: Attach the completed Screening Questionnaire and other attachments listed in Q5

SECTION M: DECLARATION (*Complete appropriate box)*

ACADEMIC STAFF RESEARCH
Declaration for Academic Staff Applicant

I have read the Code of Ethical Conduct for Research, Teaching and Evaluations involving Human Participants. I understand my obligations and the rights of the participants. I agree to undertake the research as set out in the Code of Ethical Conduct for Research, Teaching and Evaluations involving Human Participants. My Head of Department/School/Institute knows that I am undertaking this research. The information contained in this application is to the very best of my knowledge accurate and not misleading.

Staff Applicant's Signature ..... Date: .....

STUDENT RESEARCH
Declaration for Student Applicant

I have read the Code of Ethical Conduct for Research, Teaching and Evaluations involving Human Participants and discussed the ethical analysis with my Supervisor. I understand my obligations and the rights of the participants. I agree to undertake the research as set out in the Code of Ethical Conduct for Research, Teaching and Evaluations involving Human Participants.

The information contained in this application is to the very best of my knowledge accurate and not misleading.

Student Applicant's Signature ..... Date: .....

Declaration for Supervisor

I have assisted the student in the ethical analysis of this project. As supervisor of this research I will ensure that the research is carried out according to the Code of Ethical Conduct for Research, Teaching and Evaluations involving Human Participants.

Supervisor's Signature ..... Date: .....

Print Name .....

GENERAL STAFF RESEARCH/EVALUATIONS
Declaration for General Staff Applicant

I have read the Code of Ethical Conduct for Research, Teaching and Evaluations involving Human Participants and discussed the ethical analysis with my Line Manager. I understand my obligations and the rights of the participants. I agree to undertake the research as set out in the Code of Ethical Conduct for Research, Teaching and Evaluations involving Human Participants. The information contained in this application is to the very best of my knowledge accurate and not misleading.

General Staff Applicant's Signature ..... Date: .....

Declaration for Line Manager

I declare that to the best of my knowledge, this application complies with the Code of Ethical Conduct for Research, Teaching and Evaluations involving Human Participants and that I have approved its content and agreed that it can be submitted.

Line Manager's Signature ..... Date: .....

Print Name .....

TEACHING PROGRAMME
Declaration for Paper Controller

I have read the Code of Ethical Conduct for Research, Teaching and Evaluations involving Human Participants. I understand my obligations and the rights of the participants. I agree to undertake the teaching programme as set out in the Code of Ethical Conduct for Research, Teaching and Evaluations involving Human Participants. My Head of Department/School/Institute knows that I am undertaking this teaching programme. The information contained in this application is to the very best of my knowledge accurate and not misleading.

Paper Controller's Signature ..... Date: .....

Declaration for Head of Department/School/Institute

I declare that to the best of my knowledge, this application complies with the Code of Ethical Conduct for Research, Teaching and Evaluations involving Human Participants and that I have approved its content and agreed that it can be submitted.

Head of Dept/School/Inst Signature ..... Date: .....

Print Name .....

B – Participation Sheet

MASSEY UNIVERSITY
TE KUNENGA KI PŪREHUROA
UNIVERSITY OF NEW ZEALAND

School of Sport and Exercise
Massey University
PO Box 765
Wellington 6140
New Zealand

Reproducibility of two different near infrared spectroscopy devices for investigating skeletal muscle of Type 2 diabetics

INFORMATION FOR PARTICIPANTS

Thank you for showing an interest in this study. Please read everything below before deciding if you want to take part. This information sheet will tell you a little more about the study and what we would like you to do.

The research is being conducted by PhD student Adam Lucero from Massey University, School of Sport and Exercise and supervised by Dr Martin Gram. This research will act as part of Adam Lucero's PhD and will be pilot data for upcoming intervention studies.

Why is this research important?

The ability of your muscles to use oxygen is influenced by the health of your mitochondria (mitochondrial function). Mitochondria are inside your muscle cells, and are responsible for using the delivered oxygen to produce energy. The development and progression of Type 2 Diabetes Mellitus (T2DM) has been linked to poor function of mitochondria and delivery of blood to the muscles. This will impair the ability of mitochondria to break down glucose which leads to elevated blood glucose levels.

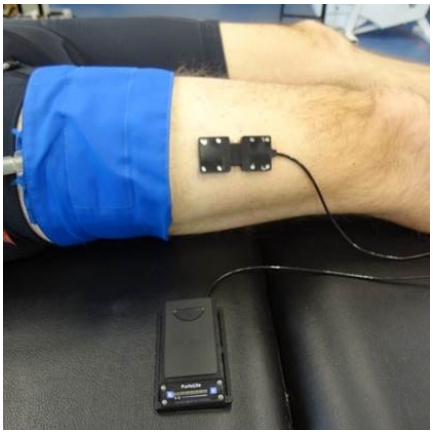

Until recently it was very complicated to measure mitochondrial function, which typically involved taking a muscle biopsy (cutting out a small piece of muscle). Fortunately, the method of non-invasive near-infrared spectroscopy (NIRS) has been developed (Figure 1). This protocol enables simple and non-invasive measurements. However, it is currently not known whether these devices can reliably make measurements on people with T2DM. Furthermore, we will be using two different NIRS devices to compare the reliability of the different technologies.

Figure 1 showing NIRS setup

Who can take part in this study?

We are seeking a total of 15 men who:

Have had type-2 diabetes for at least one year
Do not require insulin
Are aged 40-70
Have a body mass index (BMI) < 40 and a stable weight

You cannot take part in this study if:

You participate in more than three sessions of structured exercise equaling to 150 minutes of moderate-vigorous exercise per week

You use Beta-blockers

You have moderate to severe retinopathy, nephropathy or neuropathy or a history of cardiovascular disease

You have injured or had lower limb surgery in the past 4 weeks

You are currently or have been a smoker in the last 6 months

What will I be asked to do if I take part?

You will be asked to provide a medical history and information about current medications according to the above criteria. We use this information to determine your eligibility in this study. This information can be provided through your GP with your permission.
You will be required to make 4 visits to the Massey University Sport & Exercise Laboratory in Wellington. Please see Figure 2.
Each visit can be scheduled between 7 and 11 am
Each visit will last approximately 90 minutes.
On visit 1, you will be familiarized with all test protocols.
For visits 2, 3 and 4 you will also be asked to come fasted, having not had anything to eat or drink except water for the previous 12 hours. Once testing is completed you will be provided with a breakfast bar.
On visit 2 we will take a finger prick blood sample
You will be asked to refrain from taking morning medications. Bring any medications with you to testing sessions so you can take them upon completion of testing.
We will ask you to not change your way of life and just do everything as you would normally do.

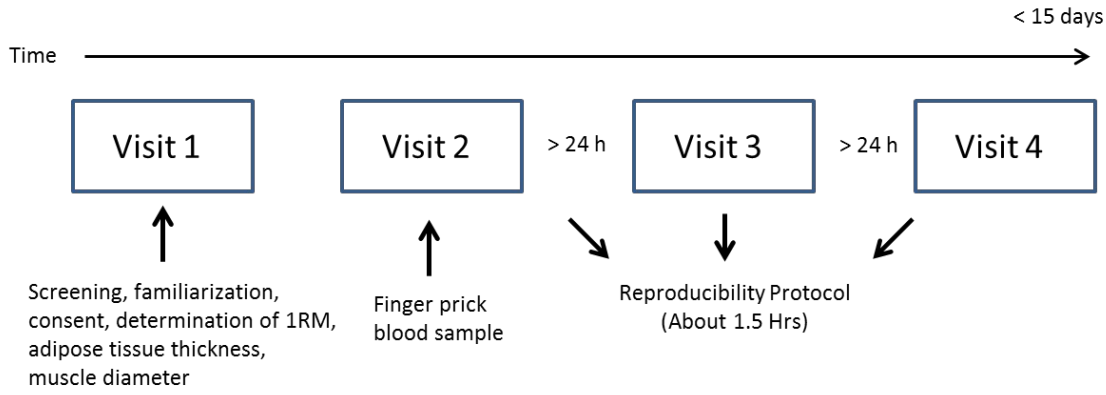

Figure 2. Experimental design.

Visit 1 (screening): Consent, Familiarisation, ultrasound and 1 RM.

You will complete a health screening questionnaire and consent form.
You will be familiarized with the near infrared spectroscopy (NIRS) test protocols and equipment.
We will measure your leg fat tissue thickness and muscle diameter with ultrasound
Lastly, we will ask you to perform three maximal knee extensions to measure your 1 repetition maximum (1 RM).
To be able to perform the measurements we will ask you to wear sport gear (shorts, shirt and shoes).

Visit 2, 3 and 4: NIRS reproducibility

During visit 2, 3 and 4 muscle measurements with the NIRS will be taken on both legs with two different NIRS devices.
On visit 2 we will take a finger prick blood sample to measure blood glucose and haemoglobin concentration.

Measures

Near Infra-Red Spectroscopy (NIRS)

NIRS is a device which uses light to measure concentrations of oxygenated and deoxygenated haemoglobin. We can use this device to measure blood flow through the smaller vessels within muscle as well as how much oxygen the muscle is taking up. The NIRS unit will be placed on your quadriceps muscle. A blood pressure cuff will be placed around your upper thigh (above the NIRS device – please see Figure 1).

Microvascular Blood Flow and Mitochondrial Capacity:

Resting microvascular blood flow and muscle oxygen consumption (mVO2) will be assessed by inflating the blood pressure cuff five times for 10-30 seconds while you sit in a relaxed position. You will then be asked to perform exercise in the form of leg kicks using a leg kicking machine as

resistance at 5 and 15% of 1RM. During these leg kicks the blood pressure cuff will be inflated five times for 10-30 seconds at each exercise intensity. Finally, you will be asked to perform rapid leg kicks for 15 seconds followed by 12-15 brief (5 – 10 seconds) blood pressure cuff inflations while you sit relaxed in order to measure maximal muscle oxygen consumption. All measurements will then be taken on the opposite leg using the second NIRS device.

Ultrasound

A commercial ultrasound device will be used to look at the size of your quadriceps muscle and the thickness of adipose tissue (fat) covering your quadriceps by imaging the belly of your quadriceps.

What will happen to this information?

The data will be used only for the purposes of this project and no individual will be identified. Only the investigators of the study will have access to personal information and this will be kept secure and strictly confidential. Participants will be identified only by a study identification number. Results of this project may be published or presented at conferences or seminars, and disseminated in scientific research journals. No individual will be able to be identified. At the end of the study you will receive a brief report summarizing the main findings of the project as well as feedback on your individual results via post or e-mail.

Are any of the Procedures Harmful or Painful?

There is a small discomfort associated with the inflation of the blood pressure cuff that quickly dissipates. To ensure you are comfortable with the arterial occlusion, all testing procedures are demonstrated during the familiarisation and you can opt out at any time. Arterial occlusion has little potential to damage blood vessels in either young healthy adults or in T2DM patients. We have experienced no adverse effects using the same occlusion protocols in our recent study with 26 T2DM patients.

As with any physical exercise, there is a small increase in the chance of muscle or tendon strains. You can voluntarily stop at any time point if you feel you cannot do more, or if you experience considerable discomfort.

Participant's Rights

You are under no obligation to accept this invitation. If you decide to participate, you have the right to:

decline to answer any particular question;

withdraw from the study at any time;

ask any questions about the study at any time during participation;

provide information on the understanding that your name will not be used,

be given access to a summary of the project findings when it is concluded.

Who may I contact for further information?

For any questions, please feel free to contact:

Dr Martin Gram

m.gram@massey.ac.nz; 0221692343

School of Sport and Exercise

Massey University

Private Bag 756

Wellington

Thank you for considering participating in this study!

Committee Approval Statement

This project has been reviewed and approved by the Massey University Human Ethics Committee: Southern A, Application 15/64. If you have any concerns about the conduct of this research, please contact Mr Jeremy Hubbard, Chair, Massey University Human Ethics Committee: Southern A, telephone 04 801 5799 x 63487, email humanethicsoutha@massey.ac.nz.

Compensation for Injury

If physical injury results from your participation in this study, you should visit a treatment provider to make a claim to ACC as soon as possible. ACC cover and entitlements are not automatic and your claim will be assessed by ACC in accordance with the Accident Compensation Act 2001. If your claim is accepted, ACC must inform you of your entitlements, and must help you access those entitlements. Entitlements may include, but not be limited to, treatment costs, travel costs for rehabilitation, loss of earnings, and/or lump sum for permanent impairment. Compensation for mental trauma may also be included, but only if this is incurred as a result of physical injury.

If your ACC claim is not accepted you should immediately contact the researcher. The researcher will initiate processes to ensure you receive compensation equivalent to that to which you would have been entitled had ACC accepted your claim.

C – Participant Consent Form

Reproducibility of two different near infrared spectroscopy devices for investigating skeletal muscle of Type 2 diabetics

PARTICIPANT CONSENT FORM – INDIVIDUAL

I have read the Information Sheet and have had the details of the study explained to me. My questions have been answered to my satisfaction, and I understand that I may ask further questions at any time.

I agree to provide access to information about the following three points from my general practitioner to the research staff. The information will be treated strictly confidential. This information will help us determine your eligibility in this study. If you decide not to provide us with this information you can still participate in the study.

Recent HbA1c
Current medication (type and dosage)
History of retinopathy, nephropathy, neuropathy and cardiovascular disease

Yes	No

I agree to participate in this study under the conditions set out in the Information Sheet.

Signature: ..... **Date:** .....

Full Name - printed .....

D – Recruitment Letter to Nurses

For enquires:

Dr. Martin Gram

Massey University Wellington

Tel: +6449793167

Cell: 0221692343

Email: m.gram@massey.ac.nz

Massey University Type-2 Diabetes Studies

Dear Doctor, Nurse

The Massey University College of Health has developed a novel non-invasive Near Infrared Spectroscopy (NIRS) method to determine mitochondrial function and blood flow in skeletal muscle. We have begun to validate this method in a healthy population but we have reason to believe that these values might be different in a diabetic population due to potential dysfunction of mitochondria and capillarity in type 2 diabetes. We are currently looking for T2D volunteers to participate in a short and non-invasive reproducibility study that will be of significant value to future investigations of muscle function in diabetic populations.

The research is being conducted by PhD student Adam Lucero from Massey University, School of Sport and Exercise and supervised by Dr Martin Gram. This research will act as part of Adam Lucero's PhD and will be pilot data for upcoming intervention studies.

We are seeking to recruit 15 patients who meet the following study criteria:

Inclusion criteria:

2. Male aged 40-65
3. Diagnosed type-2 diabetic for at least one year and not requiring insulin therapy
4. HbA1c > 48 mmol/mol
5. BMI < 40
6. A stable weight
7. Over the past 6 months have not achieved a minimum of 150 minutes of moderate to vigorous intensity exercise each week. (American College of Sports Medicine and American Diabetes Association guidelines)

Exclusion criteria:

- Use of Beta-blockers
- Moderate to severe retinopathy, nephropathy or neuropathy or a history of cardiovascular disease
- Injured or had lower limb surgery in the past 4 weeks
- Current smoking or a history of smoking in the last 6 months

Study Design:

The study duration will be approximately 15 days and encompasses 4 visits in total – three of them in a fasting state. The first visit will include familiarization, screening, consent, determination of maximum leg strength (1RM), and leg adipose tissue thickness and muscle diameter.

The remaining three experimental visits will occur within 10 non-consecutive days. The tests on the three visits are identical and consists of short (10-30 sec) venous (70mmHg) and arterial (250mmHg) occlusions that will be performed during rest and at two different exercise intensities (5% and 15% or 1RM) with two different NIRS devices in order to measure reproducibility of muscle oxygen consumption and blood flow. In addition, on the second visit we will take a finger prick blood sample to analyse fasting blood glucose and haemoglobin concentration.

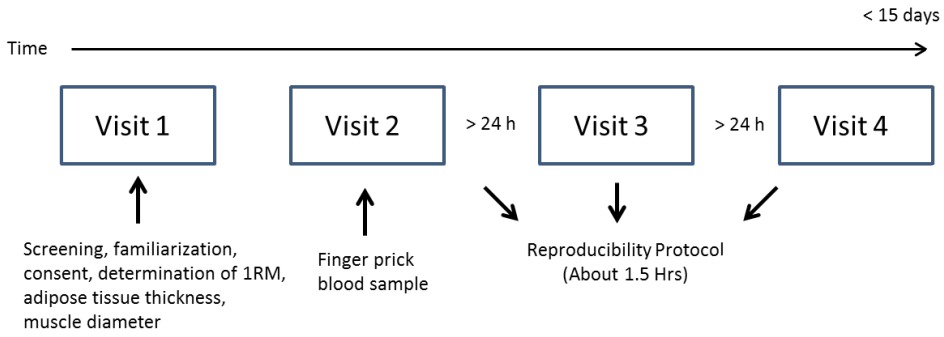

What is involved from the practice?

For practice staff to identify potential participants according to the inclusion and exclusion criteria outlined above and invite them to contact us for further information about the study.

Once consent has been obtained from potential participants, to share patient health information with the research team. This information enables us to determine the eligibility of the participant and consists of:

Recent HbA1c

Current medication (type and dosage)

History of retinopathy, nephropathy, neuropathy and cardiovascular disease

Who to contact for more information

The point of contact for this study is Dr. Martin Gram, a Research Officer at Massey University

I look forward to your involvement in this project.

Yours sincerely

Dr. Martin Gram

This project has been reviewed and approved by the Massey University Human Ethics Committee: Southern A, Application 15/64. If you have any concerns about the conduct of this research, please contact Mr Jeremy Hubbard, Chair, Massey University Human Ethics Committee: Southern A, telephone 04 801 5799 x 63487, email humanethicsoutha@massey.ac.nz.

E – Screening Questionnaire

Massey University
Te Kunenga ki Pūrehuroa

SCREENING QUESTIONNAIRE
TO DETERMINE THE APPROVAL PROCEDURE

(Part A and Part B of this questionnaire must both be completed)

Name:
Project Title:

This questionnaire should be completed following, or as part of, the discussion of ethical issues.

Part A

The statements below are being used to determine the risk of your project causing physical or psychological harm to participants and whether the nature of the harm is minimal and no more than is normally encountered in daily life. The degree of risk will then be used to determine the appropriate approval procedure.

If you are in any doubt you are encouraged to submit an application to one of the University's ethics committees.

Does your Project involve any of the following?
(Please answer all questions. Please circle either YES or NO for each question)

Risk of Harm

1.	Situations in which the researcher may be at risk of harm.	YES NO
2	Use of questionnaire or interview, whether or not it is anonymous which might reasonably be expected to cause discomfort, embarrassment, or psychological or spiritual harm to the participants.	YES NO
3.	Processes that are potentially disadvantageous to a person or group, such as the collection of information which may expose the person/group to discrimination.	YES NO
4.	Collection of information of illegal behaviour(s) gained during the research which could place the participants at risk of criminal or civil liability or be damaging to their financial standing, employability, professional or personal relationships.	YES NO
5.	Collection of blood, body fluid, tissue samples, or other samples.	YES NO
6.	Any form of exercise regime, physical examination, deprivation (e.g. sleep, dietary).	YES NO
7.	The administration of any form of drug, medicine (other than in the course of standard medical procedure), placebo.	YES NO
8.	Physical pain, beyond mild discomfort.	YES NO
9.	Any Massey University teaching which involves the participation of Massey University students for the demonstration of procedures or phenomena which have a potential for harm.	YES NO

Informed and Voluntary Consent

10. Participants whose identity is known to the researcher giving oral consent rather than written consent (if participants are anonymous you may answer No).	YES NO
11. Participants who are unable to give informed consent.	YES NO
12. Research on your own students/pupils.	YES NO
13. The participation of children (seven (7) years old or younger).	YES NO
14. The participation of children under sixteen (16) years old where active parental consent is not being sought.	YES NO
15. Participants who are in a dependent situation, such as those who are under custodial care, or residents of a hospital, nursing home or prison or patients highly dependent on medical care.	YES NO
16. Participants who are vulnerable.	YES NO
17. The use of previously collected identifiable personal information or research data for which there was no explicit consent for this research.	YES NO
18. The use of previously collected biological samples for which there was no explicit consent for this research.	YES NO

Privacy/Confidentiality Issue

19. Any evaluation of organisational services or practices where information of a personal nature may be collected and where participants or the organisation may be identified.	YES NO

Deception

20. Deception of the participants, including concealment and covert observations.	YES NO

Conflict of Interest

21. Conflict of interest situation for the researcher (e.g. is the researcher also the lecturer/teacher/treatment-provider/colleague or employer of the research participants or is there any other power relationship between the researcher and research participants?)	YES NO

Compensation to Participants

22. Payments or other financial inducements (other than reasonable reimbursement of travel expenses or time) to participants.	YES NO

Procedural

23. A requirement by an outside organisation (e.g. a funding organisation or a journal in which you wish to publish) for Massey University Human Ethics Committee approval.	YES NO

Part B

FOR PROPOSED HEALTH AND DISABILITY RESEARCH ONLY

Not all health and disability research requires review by a Health and Disability Ethics Committee (HDEC).

Your study is likely to require HDEC review if it involves:

- **human participants recruited in their capacity as:**
  - **consumers of health or disability support services; or**
  - **relatives or caregivers of such consumers; or**
  - **volunteers in clinical trials; or**
- **human tissue; or**
- **health information.**

In order to establish whether or not HDEC review is required: (i) read the Massey University Digest of the HDEC Scope of Review standard operating procedure; (ii) work through the 'Does your study require HDEC review?' flowchart; and (iii) answer Question 24 below.

If you are still unsure whether your project requires HDEC approval, please email the Ministry of Health for advice (hdecs@moh.govt.nz) and keep a copy of the response for your records.

24. Is HDEC review required for this study?	YES NO

Select the appropriate procedure to be used (choose one option):

If you answer **YES** to any of the questions 1 to 23 (Part A) and **NO** to Q24 in Part B	If you answer **YES** to question 24 (Part B)	If you answer **NO** to all of the questions in Parts A and B*
↓	↓	↓
Prepare an application using the MUHEC Application Pack	**Prepare an application using the Health & Disability Ethics Committee Application Form**	**Prepare a Low Risk Notification** ** Note- researchers who are new to the University, new to research with human participants or have significant other reasons, are welcome to send in a full MUHEC application, even if the Screening Questionnaire questions have all been answered "no".*
↓	↓	↓

GO BACK TO APPROVAL PROCEDURES, STEP 4, AND DOWNLOAD THE INFORMATION REQUIRED.

http://www.massey.ac.nz/massey/research/research-ethics/human-ethics/forms-and-procedures.cfm

F – Statement of Contribution: DRC – 16

DRC 16

MASSEY UNIVERSITY
TE KUNENGA KI PŪREHUROA
UNIVERSITY OF NEW ZEALAND

GRADUATE RESEARCH SCHOOL

STATEMENT OF CONTRIBUTION
DOCTORATE WITH PUBLICATIONS/MANUSCRIPTS

We, the candidate and the candidate's Primary Supervisor, certify that all co-authors have consented to their work being included in the thesis and they have accepted the candidate's contribution as indicated below in the *Statement of Originality*.

Name of candidate:	Adam Lucero
Name/title of Primary Supervisor:	Dr. David S. Rowlands
In which chapter is the manuscript /published work:	4

Please select one of the following three options:

☑ The manuscript/published work is published or in press

- Please provide the full reference of the Research Output:
Lucero, A. A., Addae, G., Lawrence, W., Neway, B., Credeur, D. P., Faulkner, J., ... & Stoner, L. (2018). Reliability of muscle blood flow and oxygen consumption response from exercise using near infrared spectroscopy. Experimental physiology, 103(1), 90-100.

☐ The manuscript is currently under review for publication – please indicate:

- The name of the journal:
Experimental Physiology

- The percentage of the manuscript/published work that was contributed by the candidate: 80

- Describe the contribution that the candidate has made to the manuscript/published work:
The candidate piloted and developed the protocol, wrote the ethics with help from supervisors, recruited participants, supervised collection of data, analyzed all data, and wrote the majority of the manuscript.

☐ It is intended that the manuscript will be published, but it has not yet been submitted to a journal

Candidate's Signature:	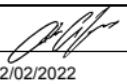
Date:	02/02/2022
Primary Supervisor's Signature:	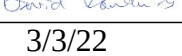
Date:	3/3/22

This form should appear at the end of each thesis chapter/section/appendix submitted as a manuscript/ publication or collected as an appendix at the end of the thesis.

GRS Version 5 – 13 December 2019
DRC 19/09/10

G – Example custom Python code for fd-NIRS and Analysis

```
# ------------------------------------------------------------ #
""" Accompanying variable and functions for ISS analysis version 3.2 """
# Revision History
# Developer:            Version:   Date:        Notes:
# Adam A. Lucero        3.0.0      05/06/2017   LC and ISS data files
# Adam A. Lucero        3.1.0      05/06/2017   Bug fixes and perfusion fix
# Adam A. Lucero        3.1.1      05/06/2017   Occlusion marker fix
# ------------------------------------------------------------ # Import
statements
import numpy as np
from pandas import Series, DataFrame
import pandas as pd
import matplotlib.pyplot as plt
from scipy import stats
from scipy.optimize import curve_fit
import ctypes
import pickle
# ------------------- # Variables
wavlen = {1:692, 2:834} # Wavelengths used (nm)
extHHb_wl1 = 4.5821 # extinction coefficient of HHb at 692 nm (cm^-1*mM^-1)
extO2Hb_wl1 = 0.9556 # extinction coefficient of O2Hb at 692 nm (cm^-1*mM^-1)
extH2O_wl1 = 1.01e-07 # extinction coefficient of H2O at 692 nm (cm^-1*mM^-1)
extHHb_wl2 = 1.7891 # extinction coefficient of HHb at 834 nm (cm^-1*mM^-1)
extO2Hb_wl2 = 2.3671 # extinction coefficient of O2Hb at 834 nm (cm^-1*mM^-1)
extH2O_wl2 = 6.06e-07 # extinction coefficient H2O at 834 nm (cm^-1*mM^-1)
corrCoefH2O = 55508.0 # H2O extinction conversion factor (mM)
percH2O = 0.7 #Percentage of H2O for absorption correction
v = 22600000000 # speed of light (cm/s)
F = 110000000 # Modulation frequency (Hz/2*pi)
HbSrce = ['Hb_csAC', 'Hb_csDC', 'Hb_AC', 'Hb_DC'] # Source of Hb signal
HbSig = ['HHb', 'HbDif', 'cHHb', 'cHbDif'] # Hb Signal for AO analysis
voName = {0: 'VO1', 1: 'VO2', 2: 'VO3', 3: 'VO4', 4: 'VO5', 5: 'VO6', 6: 'VO7',
7: 'VO8', 8: 'VO9', 9: 'V10'}
aoName = {0: 'AO1', 1: 'AO2', 2: 'AO3', 3: 'AO4', 4: 'AO5', 5: 'AO6', 6: 'AO7',
7: 'AO8', 8: 'A09', 9: 'A10',
          10: 'AO11', 11: 'AO12', 12: 'AO13', 13: 'AO14', 14: 'AO15', 15:
'AO16', 16: 'AO17', 17: 'AO18', 18: 'AO19',
          19: 'AO20'}
# ------------------- # Equation Functions
def radPhase(df):
    """ Takes phase signal in degrees/cm and converts to the absolute value in
radians/cm """
    Sp = abs(df['SlopePh']) * (np.pi / 180)
    Sp.columns = [['radSlopePh'] * 2, ['wl1', 'wl2']]
    df = pd.concat([df, Sp], axis=1)
    return df

def scatMan_AC(df, Ph_slope, AC_slope):
    """ Calculates AC & Phase scattering for a given df """
    ua = ((np.pi * F) / v) * ((df[Ph_slope] / df[AC_slope]) - (df[AC_slope] /
df[Ph_slope]))
    us = ((df[AC_slope] ** 2 - df[Ph_slope] ** 2))/(3 * ua) - ua
    us.columns = [['AC scat'] * 2, ['wl1', 'wl2']]
    return us

def scatMan_DC(df, Ph_slope, DC_slope):
```

```
    """ Calculates DC & Phase scattering for a given df """
    ua = -((np.pi * F) / v) * (df[DC_slope] / df[Ph_slope]) * \
            ((df[Ph_slope] ** 2 / df[DC_slope] ** 2) + 1) ** (-1 / 2)
    us = (df[DC_slope] ** 2/(3*ua)) - ua
    us.columns = [['DC scat'] * 2, ['wl1', 'wl2']]
    return us

def ua_ACscat(scat, Sac, Sp):
    ua = ((-scat + np.sqrt(scat ** 2 + 4 * ((Sac ** 2 - Sp **2)/3)))/2)
    ua['wl1'] = ua['wl1'] - (extH2O_wl1 * corrCoefH2O * percH2O)
    ua['wl2'] = ua['wl2'] - (extH2O_wl1 * corrCoefH2O * percH2O)
    return ua

def ua_DCscat(scat, Sdc):
    ua = (-scat + np.sqrt(scat ** 2 + 4 * ((Sdc ** 2)/3)))/2
    ua['wl1'] = ua['wl1'] - (extH2O_wl1 * corrCoefH2O * percH2O)
    ua['wl2'] = ua['wl2'] - (extH2O_wl1 * corrCoefH2O * percH2O)
    return ua

def Hb_sigs(uacn_wl1, uacn_wl2, title):
    O2Hb = 1000 * ((uacn_wl1 * extHHb_wl2) - (uacn_wl2 *
extHHb_wl1))/((extO2Hb_wl1 * extHHb_wl2) - (extO2Hb_wl2 * extHHb_wl1))
    HHb =  1000 * ((uacn_wl2 * extO2Hb_wl1) - (uacn_wl1 *
extO2Hb_wl2))/((extO2Hb_wl1 * extHHb_wl2) - (extO2Hb_wl2 * extHHb_wl1))
    tHb = O2Hb + HHb
    SaO2 = 100 * O2Hb/tHb
    Hb = pd.concat([O2Hb, HHb, tHb, SaO2], axis=1)
    Hb.columns = [[title]*4, ['O2Hb', 'HHb', 'tHb', 'SaO2']]
    return Hb

def hbdif(df, HbSrce):
    """Calculates HbDif and adds to DataFrame"""
    HbDif = df.xs('O2Hb', axis=1, level=1) - df.xs('HHb', axis=1, level=1)
    HbDif.columns = [ HbSrce, ['HbDif'] * len(HbSrce)]
    dat = [df, HbDif]
    df = pd.concat(dat, axis=1)
    return df

def chb(df, HbSrce):
    """Calculates corrected Hb signals"""
    beta = df.xs('O2Hb', axis=1, level=1) / df.xs('tHb', axis=1, level=1)
    beta.columns = [HbSrce, ['beta'] * len(HbSrce)]
    dat1 = [df, beta]
    df = pd.concat(dat1, axis=1)
    cO2Hb = df.xs('O2Hb', axis=1, level=1) - df.xs('tHb', axis=1, level=1) * (1
- df.xs('beta', axis=1, level=1))
    cHHb = df.xs('HHb', axis=1, level=1) - (df.xs('tHb', 1, 1) * df.xs('beta',
1, 1))
    cO2Hb.columns = [HbSrce, ['cO2Hb'] * len(HbSrce)]
    cHHb.columns = [HbSrce, ['cHHb'] * len(HbSrce)]
    dat2 = [df, cO2Hb, cHHb]
    df = pd.concat(dat2, axis=1)
    cHbDif = df.xs('cO2Hb', axis=1, level=1) - df.xs('cHHb', axis=1, level=1)
    cHbDif.columns = [HbSrce, ['cHbDif'] * len(HbSrce)]
    dat3 = [df, cHbDif]
    df = pd.concat(dat3, axis=1)
    return df

def fitFunc(t, A, B, k):
```

```
    """ Curve fitting function """
    return A - B*np.exp(-k*t)

# ------------------- # Plotting Functions
def pickpoint(df, num, reset=False):
    """
    Collects x-axis value from user clicks
    Parameters
    ----------
    df: DataFrame
    num: number of points to pick
    reset: if True, resets first and last points to equal df size if out of
bounds.
           Default = False
    """
    points = plt.ginput(num, timeout=0)
    points = np.array(points)
    points = points[:, 0]
    points = np.trunc(points)
    if reset == True:
        if points[0] < 0:
            points[0] = 0
        else:
            points[0] = points[0]
        if points[-1] > len(df)-1:
            points[-1] = len(df)-1
        else:
            points[-1] = points[-1]
    else: pass
    plt.close()
    return points

def stage_dfs(df, num_stages, points, seg=1):
    """ Puts stage DataFrame segments into a list """
    stages = []
    if seg == 1:
        for i in range(num_stages):
            y = df.ix[points[i]:points[i+1]]
            stages.append(y)
        return stages
    elif seg == 2:
        for i in np.arange(1, num_stages+1):
            y = df.ix[points[(i*2-1)-1]:points[(i*2)-1]]
            stages.append(y)
        return stages

def antpoint(x, y, adj=0.10):
    """Annotate data with consecutive numbers"""
    i = x.tolist()
    j = y.tolist()
    n = list(range(len(y)))
    for k, HbSrcet in enumerate(n):
        plt.annotate(HbSrcet, (i[k], j[k]+adj))

def Mbox(title, text, style):
    """ Creates a message box """
    result = ctypes.windll.user32.MessageBoxW(0, text, title, style)
    return result
```

```
def hPlotter(df, ylist, label, title, ylabel, xlabel, colors=False):
    if colors == False:
        plt.plot(df[ylist])
    else:
        for i in range(len(ylist)):
            plt.plot(df[ylist[i]], colors[i])
    plt.legend(label, loc='best')
    plt.title(title)
    plt.xlabel(xlabel)
    plt.ylabel(ylabel)


def _plot(x, mph, mpd, threshold, edge, valley, ax, ind):
    """Plot results of the detect_peaks function, see its help.
    __author__ = "Marcos Duarte, https://github.com/demotu/BMC"
    __version__ = "1.0.4"
    __license__ = "MIT"
    """
    try:
        import matplotlib.pyplot as plt
    except ImportError:
        print('matplotlib is not available.')
    else:
        if ax is None:
            _, ax = plt.subplots(1, 1, figsize=(8, 4))

        ax.plot(x, 'b', lw=1)
        if ind.size:
            label = 'valley' if valley else 'peak'
            label = label + 's' if ind.size > 1 else label
            ax.plot(ind, x[ind], '+', mfc=None, mec='r', mew=2, ms=8,
                    label='%d %s' % (ind.size, label))
            ax.legend(loc='best', framealpha=.5, numpoints=1)
        ax.set_xlim(-.02 * x.size, x.size * 1.02 - 1)
        ymin, ymax = x[np.isfinite(x)].min(), x[np.isfinite(x)].max()
        yrange = ymax - ymin if ymax > ymin else 1
        ax.set_ylim(ymin - 0.1 * yrange, ymax + 0.1 * yrange)
        ax.set_xlabel('Data #', fontsize=14)
        ax.set_ylabel('Amplitude', fontsize=14)
        mode = 'Valley detection' if valley else 'Peak detection'
        ax.set_title("%s (mph=%s, mpd=%d, threshold=%s, edge='%s')"
                     % (mode, str(mph), mpd, str(threshold), edge))
        # plt.grid()
        plt.show()

def detect_peaks(x, mph=None, mpd=1, threshold=0, edge='rising',
                 kpsh=False, valley=False, show=False, ax=None):
    """Detect peaks in data based on their amplitude and other features.
    __author__ = "Marcos Duarte, https://github.com/demotu/BMC"
    __version__ = "1.0.4"
    __license__ = "MIT"


    Parameters
    ----------
    x : 1D array_like
        data.
    mph : {None, number}, optional (default = None)
        detect peaks that are greater than minimum peak height.
```

```
    mpd : positive integer, optional (default = 1)
        detect peaks that are at least separated by minimum peak distance (in
        number of data).
    threshold : positive number, optional (default = 0)
        detect peaks (valleys) that are greater (smaller) than `threshold`
        in relation to their immediate neighbors.
    edge : {None, 'rising', 'falling', 'both'}, optional (default = 'rising')
        for a flat peak, keep only the rising edge ('rising'), only the
        falling edge ('falling'), both edges ('both'), or don't detect a
        flat peak (None).
    kpsh : bool, optional (default = False)
        keep peaks with same height even if they are closer than `mpd`.
    valley : bool, optional (default = False)
        if True (1), detect valleys (local minima) instead of peaks.
    show : bool, optional (default = False)
        if True (1), plot data in matplotlib figure.
    ax : a matplotlib.axes.Axes instance, optional (default = None).

    Returns
    -------
    ind : 1D array_like
        indeces of the peaks in `x`.

    Notes
    -----
    The detection of valleys instead of peaks is performed internally by simply
    negating the data: `ind_valleys = detect_peaks(-x)`

    The function can handle NaN's

    See this IPython Notebook [1]_.

    References
    ----------
    .. [1]
http://nbviewer.ipython.org/github/demotu/BMC/blob/master/notebooks/
DetectPeaks.ipynb

    Examples
    --------
    """

    x = np.atleast_1d(x).astype('float64')
    if x.size < 3:
        return np.array([], dtype=int)
    if valley:
        x = -x
    # find indices of all peaks
    dx = x[1:] - x[:-1]
    # handle NaN's
    indnan = np.where(np.isnan(x))[0]
    if indnan.size:
        x[indnan] = np.inf
        dx[np.where(np.isnan(dx))[0]] = np.inf
    ine, ire, ife = np.array([[], [], []], dtype=int)
    if not edge:
        ine = np.where((np.hstack((dx, 0)) < 0) & (np.hstack((0, dx)) > 0))[0]
    else:
        if edge.lower() in ['rising', 'both']:
```

```
            ire = np.where((np.hstack((dx, 0)) <= 0) & (np.hstack((0, dx)) >
0))[0]
        if edge.lower() in ['falling', 'both']:
            ife = np.where((np.hstack((dx, 0)) < 0) & (np.hstack((0, dx)) >=
0))[0]
    ind = np.unique(np.hstack((ine, ire, ife)))
    # handle NaN's
    if ind.size and indnan.size:
        # NaN's and values close to NaN's cannot be peaks
        ind = ind[np.in1d(ind, np.unique(np.hstack((indnan, indnan - 1, indnan
+ 1))), invert=True)]
    # first and last values of x cannot be peaks
    if ind.size and ind[0] == 0:
        ind = ind[1:]
    if ind.size and ind[-1] == x.size - 1:
        ind = ind[:-1]
    # remove peaks < minimum peak height
    if ind.size and mph is not None:
        ind = ind[x[ind] >= mph]
    # remove peaks - neighbors < threshold
    if ind.size and threshold > 0:
        dx = np.min(np.vstack([x[ind] - x[ind - 1], x[ind] - x[ind + 1]]),
axis=0)
        ind = np.delete(ind, np.where(dx < threshold)[0])
    # detect small peaks closer than minimum peak distance
    if ind.size and mpd > 1:
        ind = ind[np.argsort(x[ind])][::-1]  # sort ind by peak height
        idel = np.zeros(ind.size, dtype=bool)
        for i in range(ind.size):
            if not idel[i]:
                # keep peaks with the same height if kpsh is True
                idel = idel | (ind >= ind[i] - mpd) & (ind <= ind[i] + mpd) \
                              & (x[ind[i]] > x[ind] if kpsh else True)
                idel[i] = 0  # Keep current peak
        # remove the small peaks and sort back the indices by their occurrence
        ind = np.sort(ind[~idel])

    if show:
        if indnan.size:
            x[indnan] = np.nan
        if valley:
            x = -x
        _plot(x, mph, mpd, threshold, edge, valley, ax, ind)

    return ind

def normalize(y):
    norm = (y - min(y)) / (max(y) - min(y))
    return norm

# ------------------- # LabChart fxs
def lc_dat(fp, fn, Hz, startmk=1, addpts=0):
    """ Read in LC data and create start """
    lc_names = ['time', 'ECG', 'Occlusion', 'Marker']
    lc_skip = ['NaN', 'Interval=', 'ExcelDateTime=', 'TimeFormat=',
'DateFormat=', 'ChannelTitle=', 'Range=']
    lc_dat = pd.read_table(fp + fn, header=None, na_values=lc_skip,
names=lc_names, skip_blank_lines=True,
                           low_memory=False, skiprows=[0,1,2,3,4,5],
```

```
usecols=[0,1,2,3])
     lc_dat = DataFrame(lc_dat)
     marker = lc_dat.dropna().index.values
     start = marker[startmk - 1] - addpts
     lc_dat.drop(['Marker'], axis=1, inplace=True)
     lc_dat.columns = [['LC']*3, ['time', 'ECG', 'Occlusion']]
     lc_dat = lc_dat.loc[start:]
     marker = marker - lc_dat.index.values[0]
     lc_dat.loc[:, ('LC', 'time')] = (lc_dat['LC', 'time'].values - lc_dat['LC',
'time'].iloc[0])
     #lc_ind = (lc_dat['LC', 'time'].values - lc_dat['LC', 'time'].iloc[0])*Hz
     #lc_ind = lc_ind.astype(int)
     #lc_dat.set_index((lc_dat.index.values - lc_dat.index.values[0]),
inplace=True)
     return lc_dat, marker

 def iss_dat(fp, fn, startmk=1):
     """ Read in ISS data and create start """
     iss_dat = pd.read_table(fp + fn, header=None, skiprows=[0, 1, 2],
low_memory=False,
                             usecols=[0, 1, 2, 3, 4, 5, 6, 7, 8])
     iss_dat.columns = ([['LC'] * 3 + ['SlopeAC'] * 2 + ['SlopeDC'] * 2 +
['SlopePh'] * 2,
                         ['infl', 'defl', 'marker'] + ['wl1', 'wl2'] * 3])
     marker = iss_dat[iss_dat['LC', 'marker'] > 0].index.values
     iss_start = marker[startmk - 1]
     iss_dat.drop(['marker'], axis=1, level=1, inplace=True)
     iss_dat['LC', 'infl'] = 0
     iss_dat['LC', 'defl'] = 0
     #iss_dat = iss_dat.loc[start:]
     #iss_dat.set_index((iss_dat.index.values - iss_dat.index.values66[0]),
inplace=True)
     return iss_dat, marker, iss_start

 def timealign(lc_dat, iss_dat, iss_start, mph=2.5):
     lc_dat.set_index((np.arange(iss_start, (iss_start + len(lc_dat)))),
inplace=True)
     df = iss_dat.join(lc_dat).bfill()
     infl = detect_peaks(df['LC', 'Occlusion'], mph=mph, threshold=0.05,
show=True)
     defl = detect_peaks(df['LC', 'Occlusion'], mph=0.3, threshold=0.05)
     defl = [x for x in defl if x not in infl]
     df.loc[infl, ('LC', 'infl')] = 1
     df.loc[defl, ('LC', 'defl')] = 1
     return df

 def markers(df, dat, perc=0.1, onesig=False, x0=False):
     infl = df['LC', 'infl'].copy()
     defl = df['LC', 'defl'].copy()
     if onesig == True:
         mx = dat.max()
         mn = dat.min()
     else:
         mx = max(dat.max())
         mn = min(dat.min())
     infl.loc[infl == 1] = mx + (mx * perc)
     infl.loc[infl == 0] = mn - (mn * perc)
     defl.loc[defl == 1] = mx + (mx * perc)
     defl.loc[defl == 0] = mn - (mn * perc)
```

```
    if x0 == True:
        plt.plot(np.array(range(len(infl))), infl, ls='solid', color='magenta',
label='inflate', linewidth=0.7)
        plt.plot(np.array(range(len(defl))), defl, ls='--', color='lightpink',
label='deflate', linewidth=0.7)
    else:
        plt.plot(infl, ls='solid', color='magenta', label='inflate',
linewidth=0.7)
        plt.plot(defl, ls='--', color='lightpink', label='deflate',
linewidth=0.7)

def ecgnormnpeak(df, mpd):
    ecg = df['LC', 'ECG'].copy()
    ecg = normalize(ecg)
    mph = (max(ecg)-min(ecg))*0.5
    r_peak = detect_peaks(ecg, mph=mph, mpd=mpd)
    return ecg, r_peak

# ------------------- # Analysis fxs
def proc_scat(df, rolWin, proc=1):
    r_ACscat = scatMan_AC(df, 'radSlopePh', 'SlopeAC')
    r_DCscat = scatMan_DC(df, 'radSlopePh', 'SlopeDC')
    scat = pd.concat([r_ACscat, r_DCscat], axis=1)
    if proc == 1:
        scat = scat.mean()
    elif proc == 2:
        scat = scat.rolling(rolWin).mean().bfill()
    elif proc == 3:
        scat = scat
    return scat

def hbdif_sigs(df, numVO, numAO):
    """ Calculates HbDiff and corrected HbDiff signals """
    for i in range(numVO, numVO + numAO):
        df[i] = hbdif(df[i], HbSrce)
        df[i] = chb(df[i], HbSrce)
    return df

def hbsigcalc(df, scatdf, rolWin):
    """ Calculates Hb signals for AC and DC sources """
    corrAC_ua = ua_ACscat(scatdf['AC scat'], df['SlopeAC'], df['radSlopePh'])
    corrDC_ua = ua_DCscat(scatdf['DC scat'], df['SlopeDC'])
    Hb_AC = Hb_sigs(corrAC_ua['wl1'], corrAC_ua['wl2'], 'Hb_AC')
    Hb_AC = Hb_AC.rolling(rolWin).mean().bfill()
    Hb_DC = Hb_sigs(corrDC_ua['wl1'], corrDC_ua['wl2'], 'Hb_DC')
    Hb_DC = Hb_DC.rolling(rolWin).mean().bfill()
    hbdf = pd.concat([Hb_AC, Hb_DC], axis=1)
    return hbdf

def restScat(df, rolWin):
    """ User select resting data for resting us calculations """
    df = radPhase(df)
    instr = 'Select Resting Segment for Constant Scattering'
    fig = plt.figure(2, figsize=(14, 8))
    hPlotter(df, ['SlopeDC'], ['wl1', 'wl2'], instr, 'Slope DC', 'Sample')
    rest = pickpoint(df, 2)
    r_dat = stage_dfs(df, 1, rest)
    constScat = proc_scat(r_dat[0], rolWin, proc=1)
    hbdf = hbsigcalc(df, constScat, rolWin)
```

```
    hbdf.rename(columns={'Hb_AC':'Hb_csAC', 'Hb_DC':'Hb_csDC'}, inplace=True)
    df = pd.concat([df, hbdf], axis=1)
    scat = DataFrame(constScat, columns=[['rest'], ['rest']]).T
    return df, scat

def occ_name(occName, numOcc, numRepeat=1):
    occIndex = []
    for i in range(numOcc):
        x = [occName[i]] * numRepeat
        occIndex.extend(x)
    return occIndex

def datSeg(df, source, numVO, numAO=0, exP=0, instr=1, LC=False):
    """ Plots data for segment selection """
    if instr == 1:
        title = 'pick start/end of each stage'
    elif instr == 2:
        title = 'pick st of ' + str(numVO) + 'x VO and ' + str(numAO) + 'x AO
and 2 x perf segs'
    elif instr == 3:
        title = 'pick st of ' + str(numVO) + 'x VO and ' + str(numAO) + 'x AO'
    elif instr == 4:
        title = 'pick start/end of each MI test'
    else: instr = instr
    fig = plt.figure(1, figsize=(14, 8))
    hPlotter(df[source], ['O2Hb', 'HHb', 'tHb'], ['O2Hb', 'HHb', 'tHb'], title,
'[Hb] (uM)', 'Sample',
             colors=['r', 'b', 'lawngreen'])
    if LC == True:
        markers(df, df[source].loc[:,('O2Hb', 'HHb', 'tHb')])
    else: pass
    points = pickpoint(df['Hb_csAC'], (numVO + numAO + exP))
    return points

def rOccSeg(df, points, Hz, sec=17):
    """ Puts VOs into a list and calculates resting perfusion """
    rOccs = []
    for i in range(len(points) - 5):
        x = df.ix[points[i]:points[i] + sec * Hz]
        rOccs.append(x)
    y = df.ix[points[-5]:points[-5] + sec * Hz * 2]
    rOccs.append(y)
    return rOccs

def occSeg(df, points, Hz, sec=15):
    """ Puts VOs and perfusion segment into a list"""
    occs = []
    for i in range(len(points)):
        x = df.ix[points[i]:points[i] + sec * Hz]
        occs.append(x)
    perfSeg = df.ix[points[0]-45*Hz:points[0]]
    return occs, perfSeg

def perfusion(df, rolWin):
    """ Calculates perfusion for a given data segment """
    avgScat = proc_scat(df, rolWin, proc=2)
    hbdf = hbsigcalc(df, avgScat, rolWin)
    df = pd.concat([df, hbdf], axis=1)
    tHb = df.xs('tHb', axis=1, level=1).mean()
```

```
    SaO2 = df.xs('SaO2', axis=1, level=1).mean()
    perf = pd.concat([tHb, SaO2], axis=1)
    return perf

def r_perfusion(df, points, rolWin):
    """ Calculates resting perfusion """
    r = df.ix[points[-4]:points[-3]]
    bf = df.ix[points[-2]:points[-1]]
    r_p = perfusion(r, rolWin)
    bf_p = perfusion(bf, rolWin)
    perf = pd.concat([r_p, bf_p], axis=1)
    perf = DataFrame(perf)
    perf.columns = [['rest']*4,['perf', 'SaO2', 'r_t[Hb]', 'r_SaO2']]
    perf = perf.T
    print(perf)
    return perf

def caprange_calc(df, stage, Hz, mpd=3.8, delmax=[], delmin=[]):
    sigdat = pd.concat([df['Hb_csAC', 'tHb'], df['Hb_csDC', 'tHb'],
df['Hb_csAC', 'SaO2'], df['Hb_csDC', 'SaO2']],
                       axis=1)
    cols = ['Hb_csAC', 'Hb_csDC']
    capDat = []
    for i in cols:
        cap = caprange(sigdat, i, Hz, mpd, delmax, delmin)
        capDat.append(cap)
    plt.title('Select 8x st/end between-kick perfusion segments for ' +
str(cols))
    result = Mbox('Continue?', 'Are max and min points correct?', 4)
    if result == 7:
        plt.close()
    if result == 6:
        points = pickpoint(df, 16, reset=False)
        points = np.array(points, dtype=int)
        perfSegs = []
        for i in np.arange(1, 9):
            y = sigdat.ix[points[(i * 2 - 1) - 1]:points[(i * 2) - 1]]
            perfSegs.append(y)
        segs = pd.concat(perfSegs)
        perf = DataFrame.mean(segs)
        capDat[0].append(perf[0])
        capDat[0].append(perf[2])
        capDat[1].append(perf[1])
        capDat[1].append(perf[3])
        capdf = DataFrame(capDat, index=cols, columns=['Max', 'Min', 'Range',
'Perf', 'SaO2'])
        capdf.columns = ([[stage] * 5, ['Max', 'Min', 'Range', 'Perf',
'SaO2']])
        capdf = capdf.T
        print(capdf)
        return capdf, points

def caprange_calc_rol(df, rolWin, stage, Hz, points, mpd=3.8, delmax=[],
delmin=[]):
    exPerfScat = proc_scat(df, rolWin, proc=2)
    exHb = hbsigcalc(df, exPerfScat, rolWin)
    exHb = pd.concat([df, exHb], axis=1)
    sigdat = pd.concat([exHb['Hb_AC', 'tHb'], exHb['Hb_DC', 'tHb'],
exHb['Hb_AC', 'SaO2'], exHb['Hb_DC', 'SaO2']],
```

```
                      axis=1)
    cols = ['Hb_AC', 'Hb_DC']
    capDat = []
    for i in cols:
        cap = caprange(sigdat, i, Hz, mpd, delmax, delmin)
        capDat.append(cap)
    plt.title('Are Max and Mins correct?')
    result = Mbox('Continue?', 'Are max and min points correct?', 4)
    if result == 7:
        plt.close()
    if result == 6:
        plt.close()
        perfSegs = []
        for i in np.arange(1, 9):
            y = sigdat.ix[points[(i * 2 - 1) - 1]:points[(i * 2) - 1]]
            perfSegs.append(y)
        segs = pd.concat(perfSegs)
        perf = DataFrame.mean(segs)
        capDat[0].append(perf[0])
        capDat[0].append(perf[2])
        capDat[1].append(perf[1])
        capDat[1].append(perf[3])
        capdf = DataFrame(capDat, index=cols, columns=['Max', 'Min', 'Range',
'Perf', 'SaO2'])
        capdf.columns = ([[stage] * 5, ['Max', 'Min', 'Range', 'Perf',
'SaO2']])
        capdf = capdf.T
        print(capdf)
        return capdf

def caprange(df, source, Hz, mpd, delmax, delmin):
    """Detects maximum and minimum of signal and annotates on plot,
    calculates tHb range and averages exercise perfusion segments"""
    maxs = detect_peaks(df[source, 'tHb'], mpd=mpd*Hz)
    mins = detect_peaks(df[source, 'tHb'], mpd=mpd*Hz, valley=True)
    maxz = np.delete(maxs, delmax)
    minz = np.delete(mins, delmin)
    max = df.iloc[maxz][source, 'tHb'].mean()
    min = df.iloc[minz][source, 'tHb'].mean()
    range = max - min
    cap = [max, min, range]
    plt.figure(4, figsize=(14, 10))
    plt.plot(df[source, 'tHb'])
    plt.plot(df[source, 'tHb'].iloc[maxz], ls='None', marker='D', color='b')
    plt.plot(df[source, 'tHb'].iloc[minz], ls='None', marker='o', color='r')
    antpoint(df.iloc[maxs].index.values, df[source, 'tHb'].iloc[maxs])
    antpoint(df.iloc[mins].index.values, df[source, 'tHb'].iloc[mins])
    plt.show(block=False)
    return cap

def pickOccScat(df, points, numVO, numAO, occDflist, rolWin):
    """ Calculates scattering for user selected segments """
    occScatRol = proc_scat(df, rolWin, proc=2)
    y = occScatRol['DC scat', 'wl1'].iloc[0] + (occScatRol['DC scat',
'wl2'].iloc[0] - occScatRol['DC scat', 'wl1'].iloc[0])/2
    a = np.empty(len(points))
    a.fill(y)
    plt.figure(3, figsize=(14, 10))
    plt.plot(points, a, ls='', marker='+')
```

```
    title = 'Pick st of ' + str(numVO) + 'x VO and ' + str(numAO) + 'x AO'
    hPlotter(occScatRol, ['DC scat'], ['Chosen Occs', 'wl1', 'wl2'], title, 'ua
(1/cm)', 'Sample')
    occSegs = pickpoint(df['Hb_csDC'], (numVO + numAO)*2)
    occScatdfs = stage_dfs(df, (numVO + numAO), occSegs, seg=2)
    scats = []
    for i in range(len(occScatdfs)):
        occScat = proc_scat(occScatdfs[i], rolWin, proc=1)
        scats.append(occScat)
    Hb_dfs = []
    for i in range(len(occScatdfs)):
        HbDf = hbsigcalc(occDflist[i], scats[i], rolWin)
        Hb_const = occDflist[i].drop(['SlopeAC', 'SlopeDC', 'SlopePh',
'radSlopePh'], axis=1, level=0)
        HbDf = pd.concat([Hb_const, HbDf], axis=1)
        Hb_dfs.append(HbDf)
    voIndex = occ_name(voName, numVO)
    aoIndex = occ_name(aoName, numAO)
    scats = DataFrame(scats, index=voIndex + aoIndex)
    return Hb_dfs, scats

def occ_scat(df, occ_df, numOcc, rolWin):
    scats = []
    Hb_dfs = []
    for i in range(numOcc):
        occScat = proc_scat(occ_df[i], rolWin)
        occHb = hbsigcalc(df[i], occScat, rolWin)
        Hb_const = df[i].drop(['SlopeAC', 'SlopeDC', 'SlopePh', 'radSlopePh'],
axis=1, level=0)
        HbDf = pd.concat([Hb_const, occHb], axis=1)
        scats.append(occScat)
        Hb_dfs.append(HbDf)
    Hb_dfs = hbdif_sigs(Hb_dfs, 0, numOcc)
    return Hb_dfs, scats

def pickVoccslp(occlist, stage, source, Hz, rolWin, numVO=4, mpd=25, LC=False):
    """ User selects segments for VO and AO slope analysis """
    if LC == True:
        ecg, r_peak = [], []
        for i in range(numVO):
            e, r = ecgnormnpeak(occlist[i], mpd=mpd)
            ecg.append(e)
            r_peak.append(r)
        vo_plt = [(0, 0), (0, 1), (3, 0), (3, 1)]
        ecg_plt = [(2, 0), (2, 1), (5, 0), (5, 1)]
        plt.figure(figsize=(14, 10))
        for i in range(numVO):
            plt.subplot2grid((6, 2), vo_plt[i], rowspan=2)
            plt.plot(occlist[i][source, 'tHb'], 'g', label=['VO' + str(i+1)])
            markers(occlist[i], occlist[i][source, 'tHb'], perc= 0.001,
onesig=True)
            plt.legend(loc='lower right')
        for i in range(numVO):
            plt.subplot2grid((6, 2), ecg_plt[i], rowspan=1)
            plt.plot(ecg[i], 'r')
            markers(occlist[i], ecg[i], perc= 0.03, onesig=True)
            plt.plot(ecg[i].iloc[r_peak[i]], ls='None', marker='+', color='b')
            antpoint(ecg[i].iloc[r_peak[i]].index, ecg[i].iloc[r_peak[i]],
adj=0.05)
```

```
        plt.tight_layout()
        plt.show()
        plt.pause(0.001)
        rpks = input('Input first four r peaks for VOs')
        rpks = [x.strip() for x in rpks.split(',')]
        rpks = np.array(rpks, dtype=int)
        plt.close()
        z = [0, 4, 8, 12]
        ccs = []
        for i in range(numVO):
            for j in range(4):
                x = r_peak[i][rpks[z[i]+j]]
                ccs.append(x)
    else:
        plt.figure(3, figsize=(14, 10))
        for i in range(numVO):
            plt.plot(np.arange(len(occlist[i])), occlist[i][source, 'tHb'],
label=['VO' + str(i+1)])
        plt.legend(loc='lower right')
        plt.title('Pick start of cardiac cycles 1-4 for ' + str(numVO) + 'x
VO')
        ccs = pickpoint(occlist[0], numVO*4)
    ccs = np.array(ccs, dtype=int)
    ccslist = []
    HbOccDat = []
    vo = list(range(0, numVO*4, 4))
    for p in np.arange(numVO):
        j = vo[p]
        z = occlist[p].iloc[ccs[j] - 1:ccs[j + 3] - 1]
        HbOccDat.append(z)
    Hb_dfs, occScat = occ_scat(occlist[:numVO], HbOccDat, len(HbOccDat),
rolWin)
    for p in np.arange(numVO):
        j = vo[p]
        HbDat = Hb_dfs[p].xs('tHb', axis=1, level=1)
        for i in np.arange(3):
            y = HbDat.iloc[ccs[j+i]-1:ccs[j+i+1]-1]
            for t in HbSrce:
                q, *b = stats.linregress(y.index.values / Hz, y[t].values)
                ccslist.append(q)
        z = HbDat.iloc[ccs[j]-1:ccs[j+3]-1]
        for u in HbSrce:
            w, *b = stats.linregress(z.index.values / Hz, z[u].values)
            ccslist.append(w)
    ccslist = np.reshape(ccslist, (numVO*4, len(HbSrce)))
    voIndex = occ_name(voName, numVO, 4)
    voslps = DataFrame(ccslist, index=[[stage] * numVO*4, voIndex, ['cc1',
'cc2', 'cc3', 'cc1:3'] * numVO],
                       columns=HbSrce)
    occScat = DataFrame(occScat, index=[[stage]*numVO, occ_name(voName,
numVO)])
    print(voslps)
    return voslps, occScat

 def pickAoccslp(occlist, stage, source, sig, Hz, rolWin, numVO=4, numAO=2,
LC=False):
    """ Calculates linear regression through given signals for user selected
data segments """
    plt.figure(2, figsize=(14, 10))
```

```
    for i in range(numVO, numVO + numAO):
        plt.plot(np.arange(len(occlist[i])), occlist[i][source, sig],
label=['AO' + str(i-numVO+1)])
        if LC == True:
            markers(occlist[i], occlist[i][source, sig], onesig=True, x0=True,
perc = 0.001)
        else:
            pass
    plt.legend(loc='lower right')
    plt.title('Pick st/end of ' + str(numAO) + 'x AO')
    aos = pickpoint(occlist[numVO], numAO*2)
    aos = np.array(aos, dtype=int)
    aolist = []
    HbOccDat = []
    for j in range(numAO):
        a = occlist[numVO + j].iloc[aos[((j+1) * 2 - 1)-1]:aos[((j+1) * 2)-1]]
        HbOccDat.append(a)
    Hb_dfs, occScat = occ_scat(occlist[numVO:numVO+numAO], HbOccDat, numAO,
rolWin)
    for j in range(numAO):
        a = Hb_dfs[j].iloc[aos[((j+1) * 2 - 1)-1]:aos[((j+1) * 2)-1]]
        for p in HbSrce:
            HbDat = a.xs(p, axis=1, level=0)
            for s in HbSig:
                q, *b = stats.linregress(HbDat.index.values / Hz, HbDat[s])
                aolist.append(q)
    aolist = np.reshape(aolist, (numAO * len(HbSig), len(HbSrce)))
    aoslps = []
    for i in range(numAO):
        j = i*len(HbSrce)
        y = aolist[j:j+len(HbSig)].T
        aoslps.extend(y)
    aoIndex = occ_name(aoName, numAO, len(HbSig))
    aoslps = DataFrame(aoslps, index=[[stage] * numAO * len(HbSig), aoIndex,
HbSig * numAO],
                                       columns=HbSrce)
    occScat = DataFrame(occScat, index=[[stage] * numAO, occ_name(aoName,
numAO)])
    print(aoslps)
    return aoslps, occScat

def mito_occ(df, source, numAO, LC=False):
    plt.figure(3, figsize=(14, 10))
    colors = ['r', 'b']
    hPlotter(df[source], ['O2Hb', 'HHb'], ['O2Hb', 'HHb'], 'MI test', '[Hb]
(uM)', 'Sample', colors=colors)
    plt.tight_layout()
    if LC == True:
        markers(df, df[source].loc[:,('O2Hb', 'HHb')])
    else:
        pass
    MIPts = pickpoint(df, numAO * 2)
    return MIPts

def mitoslopes(df, points, stage, Hz, rolWin):
    """ Calculates and plots MI occ slopes """
    numAO = len(points) // 2
    MI_dfs = [df] * numAO
    MI_scatDfs = stage_dfs(df, numAO, points, seg=2)
```

```
    Hb_dfs, MIscat = occ_scat(MI_dfs, MI_scatDfs, numAO, rolWin)
    ao_dfs = []
    for i in range(numAO):
        y = Hb_dfs[i].ix[points[((i+1)*2-1)-1]:points[((i+1)*2)-1]]
        ao_dfs.append(y)
    aolist = []
    time = []
    for i in HbSig:
        for k in range(numAO):
            t = ao_dfs[k].index.values / Hz
            x = t.mean()
            time.append(x)
            for j in HbSrce:
                q, *b = stats.linregress(t, ao_dfs[k][j, i])
                aolist.append(q)
    timeList = []
    for i in range(0, numAO * len(HbSig), numAO):
        x = time[i:i + numAO] - time[i]
        timeList.extend(x)
    timeList = np.round(timeList, 2)
    aolist = np.reshape(aolist, (numAO * len(HbSig), len(HbSrce)))
    aoIndex = occ_name(aoName, numAO)
    HbIndex = occ_name(HbSig, len(HbSig), numAO)
    aoslps = DataFrame(aolist, index=[HbIndex, timeList], columns=HbSrce)
    MIscat = DataFrame(MIscat, index=[[stage]*len(aoIndex), aoIndex])
    return aoslps, MIscat

def plot_mi(slps, test):
    """ Plots MI slopes for all Hb Sigs and all Hb sources """
    plt.figure(3, figsize=(14, 8))
    plt.suptitle(test + ' slopes')
    plt.xlabel('time (s)')
    ax1 = plt.subplot(2, 2, 1)
    ax1.plot(slps.loc[HbSig[0]], marker='o')
    ax1.legend(HbSrce, loc='upper right')
    plt.ylabel(HbSig[0])
    plt.xlabel('time (s)')
    antpoint(slps.loc[HbSig[0]].index.values, slps.loc[HbSig[0],
HbSrce[3]].values)
    ax2 = plt.subplot(2, 2, 2)
    ax2.plot(slps.loc[HbSig[1]], marker='o')
    ax2.legend(HbSrce, loc='lower right')
    plt.ylabel(HbSig[1])
    plt.xlabel('time (s)')
    antpoint(slps.loc[HbSig[0]].index.values, slps.loc[HbSig[1],
HbSrce[3]].values)
    ax3 = plt.subplot(2, 2, 3)
    ax3.plot(slps.loc[HbSig[2]], marker='o')
    ax3.legend(HbSrce, loc='upper right')
    plt.ylabel(HbSig[2])
    plt.xlabel('time (s)')
    antpoint(slps.loc[HbSig[0]].index.values, slps.loc[HbSig[2],
HbSrce[3]].values)
    ax4 = plt.subplot(2, 2, 4)
    ax4.plot(slps.loc[HbSig[3]], marker='o')
    ax4.legend(HbSrce, loc='lower right')
    plt.ylabel(HbSig[3])
    plt.xlabel('time (s)')
    antpoint(slps.loc[HbSig[0]].index.values, slps.loc[HbSig[3],
```

```
HbSrce[3]].values)

 def curvefit(slps, sig, srce, fileName, test):
     """ Fits slope points to fitFunc and prints graph """
     time, slopes = slps.loc[sig].index.values, slps.loc[sig, srce].values
     fitParams, fitCovs = curve_fit(fitFunc, time, slopes, p0=np.random.rand(1,
3))
     A, B, k, tc = fitParams[0], fitParams[1], fitParams[2], 1/fitParams[2]
     y = fitFunc(tc, A, B, k)
     x = np.linspace(0, time[-1], 200)
     y_mod = fitFunc(x, A, B, k)
     plt.plot(time, slopes, marker='o', color='b', label=sig)
     plt.plot(x, y_mod, 'r--', label='$f(t) = %.3f$ - %.3f e^(-%.3f t)' %
(A,B,k))
     plt.annotate('tc=' + str(round(tc, 2)) + '(s)', size=15, xy=(tc, y),
xytext=(tc + 50, y),
                  arrowprops=dict(arrowstyle="->", connectionstyle="arc3",
facecolor='black'))
     plt.legend(loc='lower right')
     plt.title(test)
     plt.xlabel('time (s)')
     plt.ylabel('mVO2(slope)')
     plt.savefig(fileName + '_' + sig + '_' + srce + '_' + test + '.png')
     return fitParams, fitCovs

 def curvefit_srce(slps, srce, fileName, test):
     """ Fits slope points to fitFunc and prints graph """
     time = slps.loc['HHb'].index.values
     HHb, HbDif, cHHb, cHbDif = slps.loc['HHb', srce].values, slps.loc['HbDif',
srce].values, \
                                slps.loc['cHHb', srce].values,
slps.loc['cHbDif', srce].values
     x = np.linspace(0, time[-1], 200)
     fP, SD = [], []
     A, B, k, tc = [], [], [], []
     y, y_mod = [], []
     for i in [HHb, HbDif, cHHb, cHbDif]:
         popt, pcov = curve_fit(fitFunc, time, i, bounds=([-np.inf, -np.inf,
0.005], [np.inf, np.inf, 0.067]))
         A_var, B_var, k_var = popt
         tc_var = 1/k_var
         y_var = fitFunc(tc_var, A_var, B_var, k_var)
         y_mod_var = fitFunc(x, A_var, B_var, k_var)
         fP.append([A_var, B_var, k_var, tc_var])
         SD.append(np.sqrt(np.diag(pcov)))
         A.append(A_var)
         B.append(B_var)
         k.append(k_var)
         tc.append(tc_var)
         y.append(y_var)
         y_mod.append(y_mod_var)
     # Figure
     fig = plt.figure(3, figsize=(12, 8))
     fig.suptitle(srce + ' ' + test)
     # Ax 1
     ax1 = plt.subplot(2, 2, 1)
     ax1.plot(time, HHb, marker='o', color='b', label='HHb')
     ax1.plot(x, y_mod[0], 'r--', label='$f(t) = %.3f$ - %.3f e^(-%.3f t)' %
(A[0],B[0],k[0]))
```

```
    ax1.annotate('tc=' + str(round(tc[0], 2)) + '(s)', size=15, xy=(tc[0],
y[0]), xytext=(tc[0] + 50, y[0]),
                 arrowprops=dict(arrowstyle="->", connectionstyle="arc3",
facecolor='black'))
    ax1.legend(loc='upper right')
    plt.xlabel('time (s)')
    plt.ylabel('HHb mVO2(slope)')
    # Ax 2
    ax2 = plt.subplot(2, 2, 2)
    ax2.plot(time, HbDif, marker='o', color='b', label='HbDif')
    ax2.plot(x, y_mod[1], 'r--', label='$f(t) = %.3f$ - %.3f e^(-%.3f t)' %
(A[1],B[1],k[1]))
    ax2.annotate('tc=' + str(round(tc[1], 2)) + '(s)', size=15, xy=(tc[1],
y[1]), xytext=(tc[1] + 50, y[1]),
                 arrowprops=dict(arrowstyle="->", connectionstyle="arc3",
facecolor='black'))
    ax2.legend(loc='lower right')
    plt.xlabel('time (s)')
    plt.ylabel('mVO2(slope)')
    # Ax 3
    ax3 = plt.subplot(2, 2, 3)
    ax3.plot(time, cHHb, marker='o', color='b', label='cHHb')
    ax3.plot(x, y_mod[2], 'r--', label='$f(t) = %.3f$ - %.3f e^(-%.3f t)' %
(A[2],B[2],k[2]))
    ax3.annotate('tc=' + str(round(tc[2], 2)) + '(s)', size=15, xy=(tc[2],
y[2]), xytext=(tc[2] + 50, y[2]),
                 arrowprops=dict(arrowstyle="->", connectionstyle="arc3",
facecolor='black'))
    ax3.legend(loc='upper right')
    plt.xlabel('time (s)')
    plt.ylabel('mVO2(slope)')
    # Ax 4
    ax4 = plt.subplot(2, 2, 4)
    ax4.plot(time, cHbDif, marker='o', color='b', label='cHbDif')
    ax4.plot(x, y_mod[3], 'r--', label='$f(t) = %.3f$ - %.3f e^(-%.3f t)' %
(A[3],B[3],k[3]))
    ax4.annotate('tc=' + str(round(tc[3], 2)) + '(s)', size=15, xy=(tc[3],
y[3]), xytext=(tc[3] + 50, y[3]),
                 arrowprops=dict(arrowstyle="->", connectionstyle="arc3",
facecolor='black'))
    ax4.legend(loc='lower right')
    plt.xlabel('time (s)')
    plt.ylabel('mVO2(slope)')
    plt.savefig(fileName + '_' + srce + '_' + test + '.png')
    fP = DataFrame(fP, index=[[test + '_' + srce]*len(HbSig), HbSig],
columns=['A', 'B', 'k', 'tc'])
    SD = DataFrame(SD, index=[[test + '_' + 'SD']*len(HbSig), HbSig],
columns=['A', 'B', 'k'])
    return fP, SD
```

H – Occlusion Device

Parts List

Occlusion Device

Description	Quantity	Price
REG 1/4 SENS .02-.5BAR 0-10LSEC MAX	1	359.00
REG 1/4 0.3-3.5BAR	1	53.00
FILT PURE 1/4 PACKAGED UNIT TRANS MAN	1	131.50
BRKT 07 R24 ADJ CW NUT	1	12.80
BRKT 07 FILT WALL	1	10.70
TEE SWI SIDE 10-1/4 PNEUFIT	2	51.80
CONN RED 10STEM-6TUBE PNEUFIT	2	24.60
PLUG 1/4 BR ENOTS	1	1.75
SILENCER 1/4 PLAS	2	20.20
ADAPT STR 10MM-1/4 BSP PAR PNE	1	9.60
COIL 12 DC 48 SER LED LOW 1.8W	2	102
ELBOW ADAPT 4MM-MS PT PHEUFIT	1	7.78
NIP HEX ¼ BRASS ENOTS	1	10.80
5.3 ¼ APB SOL SOL W EXT PIL	1	355.96
ELBOW SWI 4 – ¼ PHEUFIT	1	10.60
TERMINAL PCB SCREW 2 WAY BLU	3	4.50
RELAY REED DIL 14 5VDC 500R SPST N/O	2	5.90
PCB EXP MINI 130X45MM 2X20X16=2X320HOLES	1	5.90
TERMINAL LINE SKT SCREW 3 WAY	2	9.00
TERMINAL LINE SKT SCREW 2WAY	1	2.90
HEADER PLUG PCB VRT 8WAY	1	4.90
18 GAUGE WIRE – 2 M	1	2.00
SPDT CNTR OFF SPRNG RTN BOTH SIDES	1	5.90
FREETRONICS ELEVEN (ARDUINO COMPATIBLE)	1	49.90
12 V AC 500 MA PLUGPACK	1	22.90
HOKANSON CUFF	1	?
OTHER HARDWARE		20

Total: 1,295.89

Prototype

Version 1

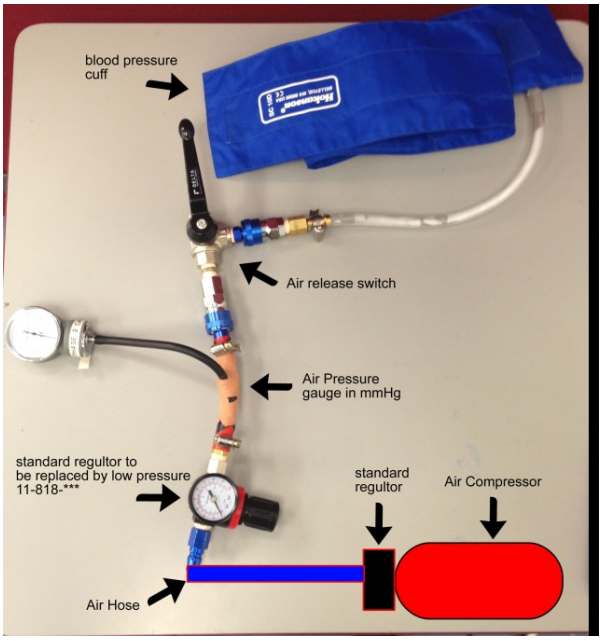

Version 2